
EXTRACTION AND FORMULATION OF PLANT SUBSTANCES

Dissertation

Zur Erlangung des Grades
Doktor der Naturwissenschaften (Dr. rer. Nat.)
der Fakultät für Chemie und Pharmazie
Universität Regensburg



vorgelegt von

Pierre DEGOT

Bains-Les-Bains, Januar 2022

Promotionsausschuss

- | | |
|---------------------|--|
| 1. Gutachter | Prof. Dr. Werner Kunz, Institut für Physikalische und Theoretische Chemie, Universität Regensburg (Deutschland) |
| 2. Gutachter | Prof. Dr. Jörg Heilmann, Lehrstuhl für Pharmazeutische Biologie, Universität Regensburg (Deutschland) |
| 3. Prüfer | Prof. Dr. Joachim Wegener, Institut für analytische Chemie, Chemo- und Biosensoren, Universität Regensburg (Deutschland) |
| Vorsitzender | Prof. Dr. Oliver Tepner |

Promotionsgesuch eingereicht am: 09.02.2022

Diese Doktorarbeit entstand in der Zeit von Mai 2018 bis Juli 2021 am Institut für Physikalische und Theoretische Chemie der Universität Regensburg unter der Betreuung von Prof. Dr. Werner Kunz.

Acknowledgments

An dieser Stelle möchte mich bei all denen bedanken, die mich während der Anfertigung dieser Doktorarbeit unterstützt haben.

Allen voran danke ich Herrn Prof. Dr. Werner Kunz und Herrn Prof. Dr. Jörg Heilmann, die mich während der gesamten Arbeit hervorragend betreut haben und die mir es ermöglichten, an diesem überaus interessanten Themen zu forschen.

Außerdem möchte ich mich bei Herrn Dr. Marcel Flemming und Herrn Dr. Didier Touraud für die gute Zusammenarbeit und die zahlreichen Ideen danken.

Ebenfalls bedanke ich mich bei Christoph, Clara, Josephine, Diana, Lea, Christin, Clément und Verena, die mich im Rahmen ihrer Forschungsarbeiten im Labor unterstützt haben. Besonderer Dank geht an Verena für die gute und tolle Zusammenarbeit während ihrer Masterarbeit.

Ebenfalls bedanke ich mich bei den Mitarbeitern des Lehrstuhls für Physikalische Chemie an der Universität Regensburg für die schöne Zeit, die tolle Arbeitszeit im Labor und auch die wissenschaftliche Hilfe während meiner Arbeit. Besonderer herzlicher Dank an meine Bürokollegen.

Bei den Mitgliedern des Lehrstuhls für Chemie und Pharmazie an der Universität Regensburg möchte ich mich namentlich bedanken. Danke, dass ihr mir so herzlich aufgenommen haben und für die tolle Unterstützung, während ich bei euch gearbeitet habe. Besonderer Dank geht an Gabi, für die Einarbeitung bei der Zellkultur, Julia für die Unterstützung und Zusammenarbeit bei der Bakterienkultur und Tom, Sebastian, Katrin und Miri für die Unterstützung bei der HPLC.

List of abbreviations

AA	Anisaldehyde reagent
ACN	Acetonitrile
BuOH	1-Butanol
<i>C. longa</i>	<i>Curcuma longa</i>
DCM	Dichloromethane
DiA	Diacetin
DLS	Dynamic light scattering
DMEM	Dulbecco's modified eagle medium
DMSO	Dimethyl sulfoxide
<i>E. coli</i>	<i>Escherichia coli</i>
ECBM	Endothelial cell growth supplement
ECGM	Endothelial cell growth medium
ECGS	Endothelial cell growth supplement
EDTA	Ethylenediaminetetraacetic acid
EtOAc	Ethyl acetate
EtOH	Ethanol
FACS	Fluorescence-activated cell sorting
FBS	Fetal bovine serum
FSC	Forward scatter
HPLC	High-performance liquid chromatography
ICAM-1	Intercellular adhesion molecule-1
IFN-γ	Interferon- γ
IKK	I- κ B-kinase-komplex
IL-1	Interleukin-1
JAK	Janus kinase
LB	Lysogeny broth
LC-MS	Liquid chromatography-mass spectroscopy
LPS	Lipopolysaccharide
MEM	Minimum essential medium
MeOH	Methanol
MIC	Minimum inhibitory concentration
MTT	3-(4,5-Dimethylthiazol-2-yl)-2,5-diphenyltetrazoliumbromide
N	Natural product reagent
NaSal	Sodium salicylate
NEA	Non-essential amino acid
NF-κB	Nuclear factor kappa B
NIK	NF- κ B induced kinase
NMR	Nuclear magnetic resonance

NP	Normal phase chromatography
PBS	Phosphate buffer saline
PCA	Pyroglutamic acid
RP-18	Reverse phase chromatography endcapped with C18 chains
<i>S. aureus</i>	Staphylococcus aureus
SDS	Sodium dodecyl sulfate
SFME	Surfactant-free microemulsion
SGS	Silica gel column
SSC	Side scatter
STAT	Signal transducers and activators of transcription
SXS	Sodium xylene sulfate
TLC	Thin layer chromatography
TNF-α	Tumour necrosis factor α
TRAF	Tumour necrosis receptor associated factor
TriA	Triacetin
V	Vanillin reagent
θ	Angle
wt%	Weight percent

Abstract

The aim of this thesis was to investigate the extraction of potential valuable nutraceuticals from different rhizomes: *Iris germanica* L. and *Curcuma longa*. On the one hand, three different curcuminoids (curcumin, dimethoxy-, and bisdemethoxycurcumin) from *Curcuma longa* were extracted. On the other hand, extraction and isolation of isoflavones and benzophenones of *Iris germanica* L. were performed. Most of the isolated compounds from *Iris germanica* L. were tested for their potential anti-inflammatory and antibacterial abilities.

First, curcuminoids were successively extracted from *Curcuma longa* using a green, sustainable, biodegradable and food-approved surfactant-free microemulsion (SFME) consisting of water, ethanol (EtOH) and triacetin (TriA) exhibiting high extraction yields (15.28 mg curcuminoids per g *Curcuma longa*). The best yield was achieved by the usage of a SFME consisting of 40/24/36 H₂O/EtOH/TriA (wt%). The maximum of solubility of curcumin was investigated in the binary mixture EtOH/TriA via UV measurements. The binary mixture EtOH/TriA (40/60 in wt%) turned out to be the best one for the solubilisation of curcumin. The structuring of the SFME was previously investigated with DLS and conductivity measurements. It was also found and demonstrated that the addition of water to the binary mixture of EtOH/TriA was responsible for the structuring of the SFME and for the high extraction yield. Indeed, bisdemethoxycurcumin, one of the curcuminoids, is the most “polar” curcuminoid and therefore, the most sensitive to water. Compared to the binary mixture EtOH/TriA (40/60 in wt%), the extraction yield of demethoxycurcumin and especially bisdemethoxycurcumin could be increased by 14 % and 32 % respectively.

Recycling and up-concentration of the SFME with curcuminoids was attempted. Therefore, the SFME was re-used to perform several extraction cycles and to concentrate the curcuminoids in the SFME. One of the goals of this study was to solubilise the curcuminoids in an aqueous solution. Therefore, different purification methods (hydro distillation, vacuum distillation and freeze-drying) were used to remove the essential oils of *Curcuma longa* and to enhance the relative purity of the extract. Purification of the extract was achieved by freeze-drying the rhizome of *Curcuma longa*, as it leads to high relative purity of the extract (about 94%) through repetitive lyophilisation cycles and did not destroy the curcuminoids before extraction. Using an appropriate composition of the SFME (50/32.5/17.5 H₂O/EtOH/TriA in wt%), dilution of the curcuminoids extract solution with water and stabilisation against day light and precipitation were achieved.

The extraction efficiencies of the curcuminoids were further enhanced using different additives, which were solubilised in the water phase of the SFME. Meglumine has been found to be the best additive while using pyroglutamic acid (PCA) as pH regulator of the SFME and as hydrotrope for curcumin. Using meglumine with and without PCA, high extraction efficiencies of the curcuminoids were achieved: 17.3 mg curcuminoids per g *Curcuma longa* using a SFME (15/34/51 H₂O/EtOH/TriA in wt%) at pH 9 containing 5 wt% meglumine neutralised with PCA in pure water and 18.3 mg curcuminoids per g *Curcuma longa* using a SFME (5/38/57 H₂O/EtOH/TriA in weight percent) at pH 11.5 containing 15 wt% meglumine without PCA in pure water. A simple water extraction (water containing 15 wt% of meglumine) achieved the best extraction efficiency for bisdemethoxycurcumin (3.46 ± 0.62 mg per g *Curcuma longa*).

Further, another SFME consisting of water, sodium salicylate (NaSal) and ethyl acetate (EtOAc) was investigated concerning its capacity to solubilize, stabilize and separate the three curcuminoids. The extraction efficiency of one curcuminoid could be enhanced using different SFME compositions: H₂O/NaSal/EtOAc 17/12/71 and 7/13/80 (in wt%) for respectively bisdemethoxy- and demethoxycurcumin and the pure EtOAc for curcumin. The presence of NaSal in the SFME enhanced the stability of curcumin and the other two curcuminoids in solution, because of its antioxidant and UV absorbing properties.

In the second part of this thesis, isoflavones and benzophenones were successively extracted and isolated from the rhizomes and the roots of *Iris germanica* L. by chromatographic methods (silica gel column followed by high-performance liquid chromatography (HPLC) and semi preparative HPLC). Using NMR and LC-MS data, structures of eleven isolated compounds were revealed. Some of the isolated compounds were tested as potential anti-inflammatory agents but had unexpected pro-inflammatory properties, of which the rhizome extract showed the highest pro-inflammatory activity. The isolates and the extracts were also tested as potential antibacterial agents. None of the extracts nor isolates were active against the bacterium *S. aureus*. Only the iris butter (the essential oil of orris) showed a potent antibacterial activity, certainly due to the presence of irones. The iris butter showed also an antibacterial activity against the bacterium *E. coli*.

Table of Contents

1	General introduction	2
2	General information	4
2.1	Extraction techniques	4
2.1.1	Solid-liquid extraction.....	4
2.1.1.1	Maceration	4
2.1.1.2	Soxhlet	5
2.1.2	Liquid-liquid extraction.....	5
2.1.3	Hydro distillation	5
2.1.4	Green extraction.....	5
2.2	Isolation and identification techniques	6
2.2.1	Thin layer chromatography	6
2.2.2	Derivatisation reagents for the thin layer chromatography	7
2.2.2.1	Anisaldehyde reagent	7
2.2.2.2	Natural product reagent.....	7
2.2.2.3	Vanillin reagent.....	8
2.2.3	Column chromatography.....	8
2.2.4	High-performance liquid chromatography.....	9
2.2.5	Optical density measurement	9
2.3	Dynamic light scattering	10
2.4	Surfactant-free microemulsions	11
2.5	NMR and NOESY	12
2.5.1	NMR.....	12
2.5.2	NOESY	12
3	Green and sustainable extraction of curcuminoids from the rhizome of <i>Curcuma longa</i>	13
3.1	Introduction.....	13
3.2	Material and methods	18
3.2.1	Material	18
3.2.2	Methods.....	20
3.2.2.1	H ₂ O/EtOH/TriA and H ₂ O/EtOH/DiA	20
3.2.2.1.1	Ternary phase diagram.....	20
3.2.2.1.2	Dynamic light scattering	20
3.2.2.1.3	Conductivity measurement	21

3.2.2.1.4	Solubility measurements	21
3.2.2.1.5	Stability of curcumin in binary solvent mixtures	21
3.2.2.1.6	Curcuminoid content of different <i>C. longa</i> powders	21
3.2.2.1.7	Extraction procedure with <i>C. longa</i> from Wagner	22
3.2.2.1.8	High-Performance-Liquid-Chromatography method	22
3.2.2.1.9	Determination of the curcuminoid content	22
3.2.2.1.10	Determination of the best ratio <i>C. longa</i> to extraction mixture	23
3.2.2.1.11	Extraction procedure	23
3.2.2.1.12	Extraction and enrichment procedure	23
3.2.2.1.13	Distillation	24
3.2.2.1.14	Vacuum distillation	24
3.2.2.1.15	Lyophilisation	24
3.2.2.1.16	Water solubility and stability of the extracts	25
3.2.2.2	(Meglumine/PCA/H ₂ O)/EtOH/TriA	25
3.2.2.2.1	Solubility of curcumin in water with different additives	25
3.2.2.2.2	Stability of curcumin in water with different additives	25
3.2.2.2.3	Nuclear magnetic resonance experiment	26
3.2.2.2.4	Ternary phase diagram	26
3.2.2.2.5	Determination of the pKa of meglumine	26
3.2.2.2.6	Dynamic light scattering	26
3.2.2.2.7	Solubility of curcumin	26
3.2.2.2.8	Selective precipitation of the curcuminoids by varying the pH	27
3.2.2.2.9	Stability of curcumin in the ternary phase diagram	27
3.2.2.2.10	High-Performance-Liquid-Chromatography method	27
3.2.2.2.11	Extraction procedure	27
3.2.2.3	H ₂ O/NaSal/EtOAc	28
3.2.2.3.1	Ternary phase diagram	28
3.2.2.3.2	Solubility measurement	28
3.2.2.3.3	High-Performance-Liquid-Chromatography method	28
3.2.2.3.4	Determination of the best ratio <i>C. longa</i> to extraction mixture	28
3.2.2.3.5	Extraction procedure	29

3.2.2.3.6	Stability of curcumin in the ternary system	29
3.2.2.3.7	Determination of the oxygen content.....	29
3.2.2.3.8	Determination of the curcuminoids' partition coefficient.....	29
3.2.2.3.9	Interfacial tension.....	30
3.2.2.3.10	Precipitation of curcumin.....	30
3.3	Results and discussion	31
3.3.1	H ₂ O/EtOH/TriA and H ₂ O/DiA/TriA.....	31
3.3.1.1	Phase diagrams and structuring	31
3.3.1.2	Solubility, stability and extraction of curcumin from different <i>C. longa</i> powder.....	34
3.3.1.3	Extraction, improvement of concentration, purity and stability.....	39
3.3.1.4	Overview.....	52
3.3.2	(Meglumine/PCA/H ₂ O)/EtOH/TriA.....	53
3.3.2.1	Solubility and stability of curcumin in water with different additives	53
3.3.2.2	Solubility, stability and extraction of curcumin with meglumine and PCA as additive in water in the SFME extraction system.....	61
3.3.3	Conclusion of the curcuminoids extraction from <i>C. longa</i> with the ternary systems H ₂ O/EtOH/TriA (with and without additives in the water phase) and H ₂ O/DiA/TriA	85
3.3.4	H ₂ O/NaSal/EtOAc.....	87
3.3.4.1	Ternary phase diagram and solubility measurement.....	87
3.3.4.2	Extraction and stability of the curcuminoids.....	90
3.3.4.3	Precipitation and separation of the curcuminoids.....	97
3.3.5	Conclusion and outlook of the extraction of the curcuminoids from <i>C. longa</i> using a ternary mixture of H ₂ O/NaSal/EtOAc.....	100
4	Phytochemical and pharmacological <i>in vitro</i> investigation of rhizomes and roots of <i>Iris germanica</i> L. growing in Bavaria.....	102
4.1	Introduction.....	102
4.1.1	<i>Iris germanica</i> L. in the history	102
4.1.2	Genus <i>Iris</i>	102
4.1.3	Subgenus <i>Iris</i>	103
4.1.4	<i>Iris germanica</i> L.....	104
4.1.5	Phytochemical composition and medicinal use of <i>Iris germanica</i> L.....	105
4.1.5.1	Irones and fatty acids	106
4.1.5.2	Flavonoids and isoflavonoids.....	107
4.1.5.3	Xanthonoids and benzophenones	108

4.1.6	HeLa, SK-Mel-28 and HMEC-1 cells	109
4.1.6.1	HeLa and SK-MEL-28	109
4.1.6.2	HMEC-1	109
4.1.7	MTT assay.....	109
4.1.8	Inflammatory processes and the role of the ICAM-1 molecule.....	110
4.1.8.1	Adhesion molecules	110
4.1.8.2	Transduction pathway of the production of ICAM-1	112
4.1.9	Antimicrobial assay: <i>Escherichia coli</i> and <i>Staphylococcus aureus</i>	113
4.1.10	Goal of the investigation, cell biological tests and antimicrobial assays	115
4.2	Material and methods.....	116
4.2.1	Material and chemicals	116
4.2.2	Methods	124
4.2.2.1	Harvest and processing	124
4.2.2.2	Aging process	124
4.2.2.3	Distillation	124
4.2.2.4	Extraction process.....	124
4.2.2.5	TLC comparison	128
4.2.2.6	Cell culture, cytotoxicity and MTT assay.....	129
4.2.2.6.1	Cytotoxicity of several extracts on HeLA and SK-MEL-28	129
4.2.2.6.2	Production of medium for cell culture.....	129
4.2.2.6.3	Defrosting of the cells.....	130
4.2.2.6.4	Medium change	130
4.2.2.6.5	Splitting of the cells.....	130
4.2.2.6.6	Cell counting	130
4.2.2.6.7	Processing of the studied extract solutions	131
4.2.2.6.8	MTT assay.....	131
4.2.2.7	Isolation process	132
4.2.2.7.1	Chromatographic methods	132
4.2.2.7.2	Isolated compounds from 18I4A (EtOAc extract of the fresh (=unaltered) rhizomes) 133	
4.2.2.7.3	Isolated compounds from 19IA (EtOAc extract of the fresh roots)	136
4.2.2.8	ICAM assay with HMEC-1 cells.....	138

4.2.2.8.1	Collagen and production of medium.....	138
4.2.2.8.2	Defrosting.....	138
4.2.2.8.3	Splitting.....	139
4.2.2.8.4	Cell counting.....	139
4.2.2.8.5	Processing of the studied extracts and isolates.....	139
4.2.2.8.6	MTT assay.....	139
4.2.2.8.7	ICAM assay.....	140
4.2.2.9	Antimicrobial assays.....	141
4.2.2.9.1	Defrosting and cultivation of <i>S. aureus</i> and <i>E. coli</i>	141
4.2.2.9.2	Determination of the colony-forming unit.....	142
4.2.2.9.3	Broth dilution method.....	142
4.2.2.9.4	Agar diffusion.....	142
4.2.2.10	Statistical analysis.....	143
4.3	Results and discussion.....	144
4.3.1	Yield and TLC comparison of the different extracts.....	144
4.3.2	Cytotoxicity on HeLa and SK-MEL-28 cells.....	161
4.3.3	Isoflavonoids and a phenone in the EtOAc extract 18I4A from the fresh rhizomes of <i>Iris germanica</i> L.....	163
4.3.3.1	Isolation of the compounds 1 , 5 and 6 (three isoflavonoids).....	163
4.3.3.2	Isolation of the compounds 2 (phenone), 3 and 4 (two isoflavonoids).....	168
4.3.3.3	Structure elucidation.....	171
4.3.4	Isoflavonoids and benzophenones in the EtOAc extract 19IA from the fresh roots of <i>Iris germanica</i> L.....	179
4.3.4.1	Isolation of compound 7 (benzophenone).....	179
4.3.4.2	Isolation of compounds 3 (irigenin), 8 (benzophenone), 9 and 10 (two isoflavonoids) from fraction F4.....	181
4.3.4.3	Structure elucidation.....	183
4.3.5	Comparison of the phytochemical profile of roots and rhizomes.....	190
4.3.6	MTT and ICAM-1 assays.....	193
4.3.7	Antimicrobial assay.....	199
4.3.8	Utilisation of the roots and rhizomes as raw material for isolation of isoflavones and benzophenones.....	206
4.4	Conclusion.....	207

5	References.....	209
6	Appendix	228
6.1	Compositions used for the DLS experiment with H ₂ O/EtOH or DiA/TriA	228
6.2	Calibration curves of the three curcuminoids.....	228
6.3	Compositions used for the extraction procedure with H ₂ O/EtOH or DiA/TriA.....	229
6.4	Second calibration curves of the three curcuminoids	229
6.5	Compositions for the extraction experiments with meglumine	230
6.6	Compositions for the stability of curcumin in the phase diagram with meglumine with and without PCA	231
6.7	Compositions for all experiments in the ternary phase diagram H ₂ O/NaSal/EtOAc.....	231
6.8	Curcuminoid extraction yields	233
6.9	Preliminary test for the enrichment procedure.....	233
6.10	Detailed curcuminoid content after each extraction cycle.....	234
6.11	Average loss of extraction system after each extraction cycle.....	235
6.12	Detailed curcuminoid content after different purification processes	235
6.13	Pictures of the precipitate after dilution of the extract solution with water	237
6.14	Kinetic measurement	238
6.15	Detailed ¹ H-NMR spectra of curcumin and meglumine.....	239
6.16	ROESY meglumine/curcumin 1/2.....	241
6.17	Determination of the pK _a of meglumine.....	242
6.18	Viscosity measurement.....	243
6.19	Precipitation of curcumin.....	244
6.20	Precipitation of curcumin and bisdemethoxycurcumin.....	244
6.21	Total of curcuminoids extracted with different additives in water [71].....	245
6.22	Detailed curcuminoid extraction efficiencies for the SFME H ₂ O/NaSal/EtOAc	247
6.23	Free energy of extraction and excess chemical potential.....	248
6.24	DOSY and SAXS experiments.....	248
6.25	GC-MS chromatograms.....	250
6.26	TLC plates of 18I1, 18I2, and 18I3	251
6.27	TLC plates of the comparison between 18I4B, 18I5B and 18I6B	254
6.28	Comparison between BuOH-extracts and 18I9.....	254
6.29	19IA and 19IH.....	255
6.30	Comparison DCM-extracts and 19IH.....	257
6.31	GC-MC of 20IH.....	258
6.32	Cytotoxicity of the BuOH-extracts on HeLa and SK-MEL-28 cells	259

6.33	Overview of the 25 fractions obtained from the elution of 18I4A.....	260
6.34	Z3 and 18I9	261
6.35	F4_18I4A and Z2	262
6.36	F4F1_19IA and Z2_18I4A.....	263
6.37	WST-1.....	264
6.38	PMA	265
7	Eidesstattliche Erklärung	266

1 General introduction

Extraction was performed and studied for centuries by humankind. Anyone who has ever made a cup of tea or coffee has performed an extraction. The compounds responsible for the flavour and colour of the tea are extracted from the ground material into the added hot water. Humankind have been using plants for curing illness for millennia, because plants contain compounds possessing specific therapeutic activities. But the use of plants directly can cause undesirable side effects and the dosage of active substances is complicated. Therefore, the extraction of such beneficial target compounds is of great interest in the domain of the chemistry of natural substances and therapeutic chemistry. Thus, different extraction and isolation techniques, such as liquid-solid extraction or high-performance liquid chromatography, are performed to obtain the desired active compounds. Having the pure target compound, pharmacological and phytochemical tests can reveal the biological and therapeutic activity of the isolated compounds. Other domains, in which extraction is essential, are the food and fragrance industry. Especially in the fragrance industry, where different parts of a plant are extracted or additionally treated to obtain the desired fragrance. The most common extraction technique is the hydro distillation.

The use of natural colouring agents in the food industry is growing every year because of the growing consumer's concern for safety and health of food formulations. Thus, the food industry is keen on finding alternatives to the common synthetic dyes, such as tartrazin. Natural colouring agents offer an alternative to synthetic dyes. Dyes are mostly used as powders or have to be formulated to be incorporated in food. Here again, because of the current growing consumers' demand on natural, organic, and sustainable food formulations, the food industry needs to find alternative extraction techniques to replace the commonly used non-sustainable solvents, which are toxic for the human body and harmful to the environment. Nowadays, it is necessary to expand, modify, and reinvent the traditional extraction techniques in order to protect the consumer and the environment. For this purpose, the twelve principles of green chemistry, developed and published by P. Anastas and J. C. Warner in 1998, and the six principles of green extraction, developed and published by F. Chemat in 2012, are focused on reducing the environmental and health impacts and are of interest for the food and fragrance industry.

The aim of this work is first to extract a very popular natural colouring agent, curcumin, from *Curcuma Longa* with a green, bio-based, and sustainable solvent systems, which could be directly used in the food industry. Moreover, the aim is to investigate other solvent systems to extract and isolate

curcumin, by for example pH-dependent precipitation, or other solvent systems, which could be used in the pharmaceutical industry. Secondly, the aim was to explore the composition of the roots and rhizomes of *Iris germanica* L. and further to look into its biological and therapeutic activity. Indeed, many compounds from the rhizome of *Iris germanica* L. are already well known in the literature. On the contrary, the roots alone are less studied. Moreover, *Iris germanica* L. is used since centuries as alternative medicine in Asia and especially in India. Therefore, the potential anti-inflammatory and antibacterial properties of *Iris germanica* L. and of the different isolated compounds were investigated.

2 General information

2.1 Extraction techniques

Extraction is the first procedure to separate the desired natural molecules or groups of molecules from the raw materials. Sample preparation is a crucial step to perform solvent or steam extraction. The plant material often has to be washed first, then dried and finally ground before the extraction process [1]. These and several other steps are performed to obtain a homogenous plant material and to increase the contact area between the plant material and the extraction solvent or solvent mixture to achieve better extraction yield [2]. In this thesis, several different extraction techniques have been used: the solid-liquid (more specifically maceration and Soxhlet), liquid-liquid and steam extraction.

2.1.1 Solid-liquid extraction

Solid-liquid extraction (also known as solvent extraction) involves the separation of the constituents of a solid material (plant) by contact with a liquid. Every constituent (solute) of the plant has a different affinity for different solvents. This preference depends mainly on the polarity of the solvent and the solutes. Generally, non-polar solutes are dissolved by non-polar solvents, whereas polar solutes are dissolved by polar solvents [3]. This equilibrium is reflected by the partition coefficient K , the quotient of the activity of the solute in the respective phase, as described in equation 1:

$$K = \frac{a_{\text{solute in the phase 1}}}{a_{\text{solute in the phase 2}}} \quad (1)$$

It can be categorised into non-exhaustive (maceration) and exhaustive (Soxhlet) solid-liquid extraction processes. The difference will be explained in the following.

2.1.1.1 Maceration

In the maceration process, the plant material stays in contact with the solvent at room temperature for several hours under agitation or not. The process can be repeated three or more times to ensure a good extraction efficiency. The agitation is provided to enhance the surface contact between the solvent and the plant material, more precisely to increase the mass transfer of the solutes from the matrix (plant material) to the solvent. Sometimes to further enhance the extraction efficiency, the temperature can be increased. However, heating should be avoided to prevent the decomposition of thermosensitive molecules. The choice of solvent is also crucial in the maceration process. It should be selective for the target molecule and if possible, as volatile as necessary in order to be removable by evaporation. After the maceration process, the plant material can be obtained by filtration in order to

perform successive extraction with fresh solvent. The solvent is removed from the extract by evaporation or drying [1,2,4].

2.1.1.2 Soxhlet

Soxhlet extraction was developed approximately 150 years ago [5]. The Soxhlet apparatus is a closed solvent circuit. The raw material is placed in a thimble and the solvent in the flask. Through refluxing and condensing, the solvent percolates the raw material and is rinsed back into the flask. The raw material is then extracted multiple times with fresh solvent. The advantages of the Soxhlet extraction are that only few amounts of the solvent are needed and it is hardly time consuming compared to maceration [6]. The disadvantage is that thermosensitive molecules can be degraded during the extraction process, because the solvent in the flask is always at its boiling temperature.

2.1.2 Liquid-liquid extraction

The liquid-liquid extraction can be performed analogously to the solid-liquid extraction. The partition coefficient of the solutes is the key parameter. Liquids involved are usually water (polar solvent) and an inorganic solvent (non-polar). The transfer of one or more solutes from one liquid phase to the other, generally from water to the inorganic solvent, is driven by the chemical potential. The solvent-rich product is called the extract, and the residual solvent from which solutes have been removed is called the raffinate. Liquid-liquid extractions are performed in a separatory funnel in the laboratory scale. [1,6,7]

2.1.3 Hydro distillation

Hydro distillation has been used in the manufacture and extraction of essential oils for centuries [8]. The etymology of the word attests to its traditional use. Indeed, “hydro” comes from Greek and signifies “water” and “distillation” from Latin “*distillare*”, meaning to drip. The raw material is placed in a flask with water, which is heated to boil. The high temperature destroys the plant matrix whereby the essential oil, which is not miscible with water at room temperature, is released. The oil forms a low boiling azeotrope with water, passes through a condenser, where it is separated by density difference into water and the essential oil phase. The duration of the distillation depends on the raw material, its preparation and on the nature of the essential oil. However, it is a time and energy consuming procedure to obtain the essential oil. Thermosensitive molecules can also be extracted using hydro distillation, because they are substantially less exposed to high temperature in comparison to Soxhlet.

2.1.4 Green extraction

The concept of green extraction was developed by F. Chemat et al. in 2012 on the basis of green chemistry, which was developed by P. Anastas and J. C. Warner in 1998 [9,10]. It is focused on reducing

environmental and health impacts of extraction processes. Six principles were listed as a guideline as follows:

Principle 1: Innovation by selection and use of varieties of renewable plant resources.

Principle 2: Use of alternative solvents, principally water or bio-based solvents.

Principle 3: Reduction of energy consumption by energy recovery, using innovative technologies.

Principle 4: Production of coproducts instead of waste to include in the bio- and agro-refining industry.

Principle 5: Reduce unit operations and flavour safe, robust, and controlled processes.

Principle 6: Aim for a non-denatured biodegradable extract without contaminants.

Nowadays, because of the growing consumers' awareness of safety and health aspects of manufactured products, especially in food and cosmetic industry, industry has to change or partially adapt its extraction processes to match the consumers' perception and demand. Most of the solvents currently used in the industry are derived from crude oil, which is toxic for the human body and non-degradable. Currently used solvents are often flammable, volatile, and responsible for the greenhouse effect and pollution. The use of alternative, green and bio-based solvents is a major challenge for the industry. Extraction of natural products is applied in almost every production process in the cosmetic, pharmaceutical, and food industry. Nowadays, the focus is set on protecting both the environment and the consumers.

2.2 Isolation and identification techniques

2.2.1 Thin layer chromatography

Thin layer chromatography (TLC) works with two phases, one stationary phase, the plate, and one mobile, the solvent flowing on the plate. The two phases interact differently with the target molecules which should be isolated. The stationary phase is held in place while the mobile phase moves through the plate [11]. If the stationary phase is polar (e.g. SiO_2), the chromatography is termed normal-phase chromatography (NP). On the contrary, a non-polar stationary phase (alkane-sidechain attached to the silanol on the plate, C_{18} for example) is referred to as a reversed-phase chromatography (RP-18). Commonly, TLC uses an aluminium plate coated with the stationary phase, silica gel (NP) or C_{18} modified silica gel (RP-18). A drop of the extract solution is placed on the bottom of the aluminium plate, then the plate is placed in a chamber in contact with the mobile phase and is eluted. The TLC is a mandatory step to develop suitable mobile phases for column chromatography, as it can show how an extract will behave during column chromatography.

The mobile phase can be defined by the eluent strength, an empirical value of solvent. High values of eluent strength can be assigned to polar solvents, whereas low values to non-polar solvents. The eluent strength of a solvent mixture can be evaluated with equation 2, where ϵ^0 is the eluent strength of the solvent mixture, ϵ_i^0 the eluent strength of the pure solvent i and v_i the volume fraction of solvent i :

$$\epsilon^0 = \sum_i v_i \times \epsilon_i^0 \quad (2)$$

Another empirical value used to define the elution efficacy of the mobile phase is the retention time R_f of a compound i . It is used for comparing and identifying compounds or families of molecules. The R_f value of a solute is defined as the distance d_{solute} travelled by the molecule divided by the distance d_{solvent} travelled by the solvent or solvent mixture, as shown in equation 3:

$$R_f = \frac{d_{\text{solute}}}{d_{\text{solvent}}} \quad (3)$$

Theoretically, to have a good separation the R_f values should be between 0.2 and 0.6.

2.2.2 Derivatisation reagents for the thin layer chromatography

2.2.2.1 Anisaldehyde reagent

Anisaldehyde reagent (AA) is a universal reagent to visualize natural oxidisable molecules such as phenols, glycosides, antioxidants, steroids, essential oils, terpenes, and carbohydrates. Compounds, which appear to be colourless on the TLC plate, can be visualised on the TLC plate by the anisaldehyde reagent. The reagent is sensitive to most functional groups except to alkenes, alkynes, and aromatic molecules (without other functional groups). The solution of anisaldehyde reagent is sprayed on the TLC plate, which is then heated for 2-10 min to 105-110°C. Depending on the molecule, different colours are produced upon heating, making the anisaldehyde reagent an excellent visualisation method for examining oxidizable compounds on TLC plates.

2.2.2.2 Natural product reagent

Natural product reagent (N) is an analytical reagent for the determination of flavonoids, isoflavonoids and vegetable acids by compound dependent colour changes due to complex formation with the reagent. Natural product reagent contains the active reagent diphenylboryloxyethylamin, which reacts with free hydroxy groups as described in Figure 1.

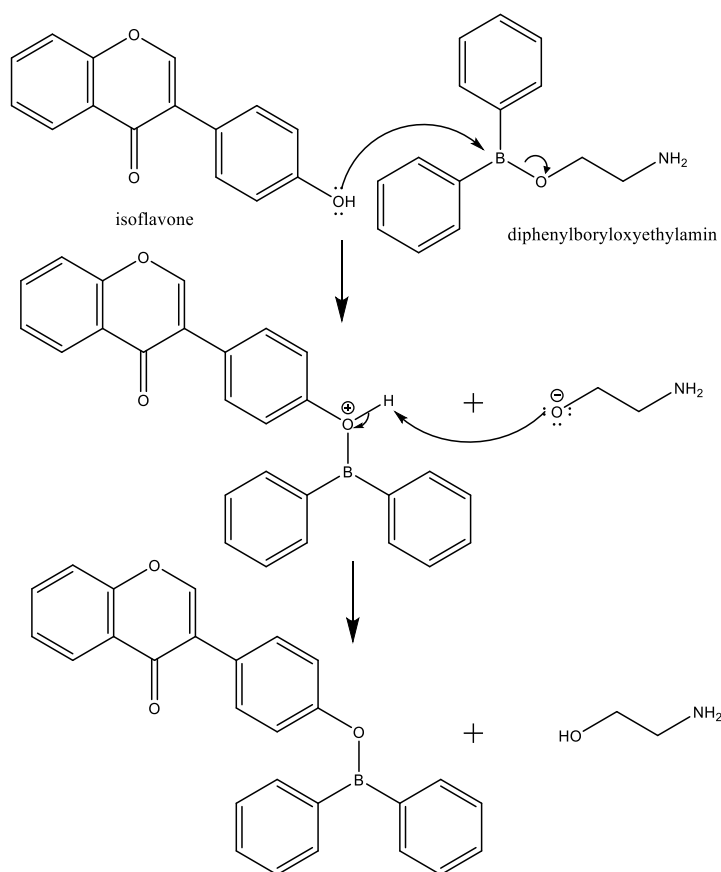


Figure 1: Mechanism of reaction of diphenylboryloxyethylamin with isoflavonoids.

Therefore, the TLC plate is heated to 100°C to accelerate the formation of the flavonoids-diphenylboron complex and then sprayed with natural product reagent. After about 15 minutes intensive fluorescence will occur depending on the structure of the molecule under 254 and 366 nm. Molecules with one hydroxy group will appear yellow, molecules with two hydroxy groups orange yellow and molecules with three hydroxy groups green.

2.2.2.3 Vanillin reagent

Just as anisaldehyde, the vanillin reagent (V) is used to detect oxidisable compounds and a universal reagent. The reagent is used for the detection of steroids, higher alcohols, phenols and essential oils. Two different solutions, one with vanillin and one with sulfuric acid, are sprayed on the TLC plate. Then it is heated for 3-5 min until colouration occurs.

2.2.3 Column chromatography

Column chromatography is widely used in a chemistry lab to separate molecules from an extract solution. It is based on different adsorption of the molecules to the adsorbent, the stationary phase. In most of the case, the adsorbent is silica gel, which is packed in a glass column. A glass frit at the end of the column holds the stationary phase in place. The eluent and the extract are then added on top

of the glass column to pass through the column by gravity. The molecules are percolating through the column with different speed rates (related to the different R_f values of the thin layer chromatography), allowing them to be collected in different fractions. The main advantage of a silica gel column is the low cost and disposability of the stationary phase used.

2.2.4 High-performance liquid chromatography

High-performance liquid chromatography (HPLC) is a very important separation method in chemistry. It is used to analyse and even isolate (with a preparative HPLC) molecules from a plant extract. The separation principle is based on the distribution of the molecules in the sample between a mobile phase (the eluent) and a stationary phase (adsorbent in the column). An HPLC is composed of several units: pumps, autosampler, UV detector. The autosampler is responsible for the injection of the sample onto the column. The pumps are responsible for keeping the mobile phase afloat through the column. The pumps can be operated with two different elution modes: isocratic, where the composition of the eluent does not change during the measurement, and gradient mode, where the composition of the eluent is varying. The presence molecules can be monitored by a UV detection system, either with one or more wavelengths, but other detection systems exists, such as refractive index detectors or evaporative light scattering detectors [12]. A good separation is achieved when the peaks are entirely separated in the chromatogram. The time taken for a molecule to travel through the column to the detector is known as its retention time. The retention time is characteristic for each molecule in the sample. Qualitative information on the molecule is provided with the retention time and the UV-spectra, whereas quantitative information is given by the peak area [13,14]. The choice of the eluent, gradient conditions, and column depends on the nature of the sample's components. The commonly used solvents are methanol (MeOH), acetonitrile (ACN), water, and isopropanol, sometimes with some additives like acetic acid, phosphoric acid or trifluoroacetic acid (TFA) to assure complete protonation of the target molecules and to prevent the detection of several peaks due to the presence of one molecule with different charges. Different columns are available for HPLC: in most of the cases people are working with a RP-18 or NP column. But other types of columns such as phenyl, diphenyl, diol or chiral columns exist, too. The choice of the packaging material of the column is strongly depending on the structure of the molecules in the sample. A preparative HPLC is composed of the same units as a classic HPLC, just a fraction collector is added after the UV-detector in order to collect the separated compounds.

2.2.5 Optical density measurement

Optical spectroscopy is a method widely used in research for the study of molecules, as well as production and quality control [15,16]. The basis for optical spectroscopy is the interaction of light with

the sample. It is based on the transmission of light or other electromagnetic radiation through matter. The emission and absorption depend on the wavelength of the radiation. When light passes through a sample, certain wavelengths can be absorbed resulting in colouration when the absorption is located between 400 and 800 nm. The remaining light, which is not absorbed, can be recorded as a function of wavelength by a suitable detector, generating a UV/Vis spectrum, which is characteristic of the analysed sample. For quantification purposes the wavelength of highest absorption (λ_{\max}) is of importance. When starting a measurement, a blank is taken (only the solvent without the sample) to subtract the solvent absorption. Then the sample is irradiated by light with an intensity I_0 . The detector measures the remaining light intensity I after passing through the sample and the absorbance A is then calculated, as described in equation 4. The ratio between I_0 and I is called the transmittance.

$$A = \text{Log} \left(\frac{I_0}{I} \right) = \text{Log}(T) \quad (4)$$

The Lambert-Beer's Law finally links the measured absorbance A to the concentration c of the sample, as described in equation 5, where ϵ is the molar extinction coefficient and L the illuminated layer thickness:

$$A = \epsilon \times L \times c \quad (5)$$

2.3 Dynamic light scattering

If light hits matter, light can be absorbed (cf. Optical density measurement, section 2.2.5) or scattered. Light scattering is used to study the presence and size of colloids, aggregates, micelles, or macromolecules in solutions. The dynamic light scattering (DLS) technique measures Brownian motion and correlates it to the particles' size. The Brownian motion is the random movement of particles suspended in a medium, the solvent. The larger the particle is, the slower the Brownian motion. The sample is illuminated by a laser beam and the intensity of fluctuations of the scattered light due to the Brownian motion of the particles is detected at a scattering angle Θ by a detector. The detection of scattered light is the result of destructive and constructive phases. The autocorrelator correlates this intensity fluctuations over time and an intensity correlation function $G_2(\tau)$ can be generated, as described in the equation 6. It describes the Brownian motion of the particles in the sample and is expressed as an integral over the product of intensities at time t and delayed time $(t+\tau)$, where τ is the lag time [17].

$$G_2(\tau) = \langle I(t).I(t + \tau) \rangle \quad (5)$$

For most of the cases, the correlation function is an exponentially decaying function of the time delay τ (monodisperse particle size). By fitting this correlation function, a translational diffusion coefficient can be extrapolated and then with the use of the Stokes-Einstein equation the hydrodynamic radius

can be calculated. The hydrodynamic radius is the radius of a hypothetical sphere diffusing at the same rate as a particle. DLS measurements were proven to be useful to examine and characterize surfactant-free microemulsions (SFME) [18,19].

2.4 Surfactant-free microemulsions

An emulsion is a mixture of two immiscible liquids, commonly water and an oil, where no apparent phase separation but a turbidity is observed. Two types of emulsions are distinguished: oil in water (O/W) and water in oil (W/O). One phase is dispersed as droplets in the other outer phase, the continuous phase. The size of the droplets characterizes the name of the emulsion: if the droplet size is between 0.1 and 10 μm , it is spoken of a macroemulsion. If the droplet size is under 100-200 nm, a microemulsion is present. Macroemulsions are only kinetically stable. Over time a macroemulsion will revert back to their separate phases. On the contrary, microemulsions are thermodynamically stable. A microemulsion is considered as a one-phasic and isotropic solution containing water, oil, and a surfactant. Its formation is spontaneous and does not require any input of energy, in contrast to emulsions. Surfactant-free microemulsions (SFMEs) are a special case of microemulsion as they consist, like emulsions, of two immiscible liquids, an aqueous phase (often water), an organic phase (oil), and a third component called “co-solvent”. SFMEs, as indicated in the name, are without surfactant [19,20]. The “co-solvent”, sometimes called amphi-solvent, is an amphiphilic molecule and partially or completely miscible with the aqueous and organic phase. The role of the “co-solvent” is to enhance the solubility of the organic phase in the aqueous phase, e.g. to reduce the miscibility gap between them.

SFMEs are widely studied in the literature. One example of SFMEs is the ternary mixture composed of water, ethanol (EtOH), and octanol [21–24]. In this ternary system, Zemb et al. have examined the pre-Ouzo and Ouzo effect in this SFME [19]. They observed scattering signals in the monophasic region inducing a structuring in the domain near to the phase separation border. The effect behind the formation of this structuring was named pre-Ouzo [25]. The name takes its origin in the Ouzo effect, which can be observed in emulsions. The Ouzo effect describes a spontaneous emulsification, happening during the addition of water to a binary mixture of octanol/EtOH. The same effect appears with the beverage Ouzo, a drink containing EtOH and anethole, which turns turbid (milky) upon the addition of water while being still stable against macroscopic phase separation into two layers. SFMEs are of great importance in the industry as the absence of surfactant is a big advantage. Indeed, the use of surfactants leads to several problems: irritating taste, not always bio-degradable, poisoning of the aquatic life if their waste ends up in the groundwater, skin irritation, influence on enzymes, or accumulation in the body.

2.5 NMR and NOESY

2.5.1 NMR

Nuclear Magnetic Resonance (NMR) spectroscopy is used in research and quality control as analytical technique for determining the content and purity of sample or for structure elucidation [26–28]. NMR is based on a simple principle: all nuclei have a spin and are electrically charged. When placed in a magnetic field, nuclei absorb electromagnetic radiation and an energy transfer takes place from base energy to a higher energy level. When the spin returns to its base level, the corresponding emitted energy is measured and processed in order to obtain an NMR spectrum of the concerned nuclei. A signal in the NMR spectrum is referred to as a resonance. The frequency of a signal is known as its chemical shift. The chemical shift is defined by the resonant frequency of a nucleus relative to a standard in a magnetic field and depends of the nucleus' chemical environment. It gives information about the composition of atomic groups within the molecule and adjacent atoms. The signal intensity is used to determine proportions of different compounds in a mixture.

2.5.2 NOESY

^1H - ^1H NOESY (**N**uclear **O**verhauser **E**ffect **S**pectroscop**Y**) is a 2-D NMR experiment. It uses the **N**uclear **O**verhauser **E**ffect (NOE) to provide information about which proton resonances are from protons which are close together in space. The basic pulse sequence consists of three 90° pulses. The pulse sequence is shown in Figure 2.

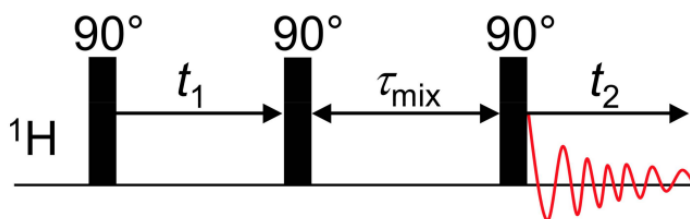


Figure 2: Schematic representation of the three pulses sequence [29].

A first excitation 90° ^1H pulse creates transverse spin magnetisation. The spins precess during a defined waiting time t_1 . A second 90° ^1H pulse creates a longitudinal magnetisation, where magnetisation transfer via cross-relaxation takes place during a defined mixing time t_m . The mixing time t_m should be between half t_1 and t_1 to ensure good sensitivity. A third 90° pulse creates transverse spin magnetisation from the remaining longitudinal magnetisation and acquisition takes place during a defined time t_2 . The NOESY spectrum is generated by a Fourier transformation, which contains cross-peaks when magnetisation transfer has occurred during the mixing time t_m . In this thesis, NOESY spectra were measured for structure elucidation, especially for isoflavones and benzophenones.

are natural phenols, which constitute about 0.1 to 6 % of the dried turmeric [30,31]. There are many different curcuminoids, which can be found in *C. Longa* the three most famous are: curcumin (curcumin I), demethoxycurcumin (curcumin II), and bisdemethoxycurcumin (curcumin III) [32–34]. They can be distinguished from each other by the number of methoxy groups on the aromatic ring, as shown in Figure 4.

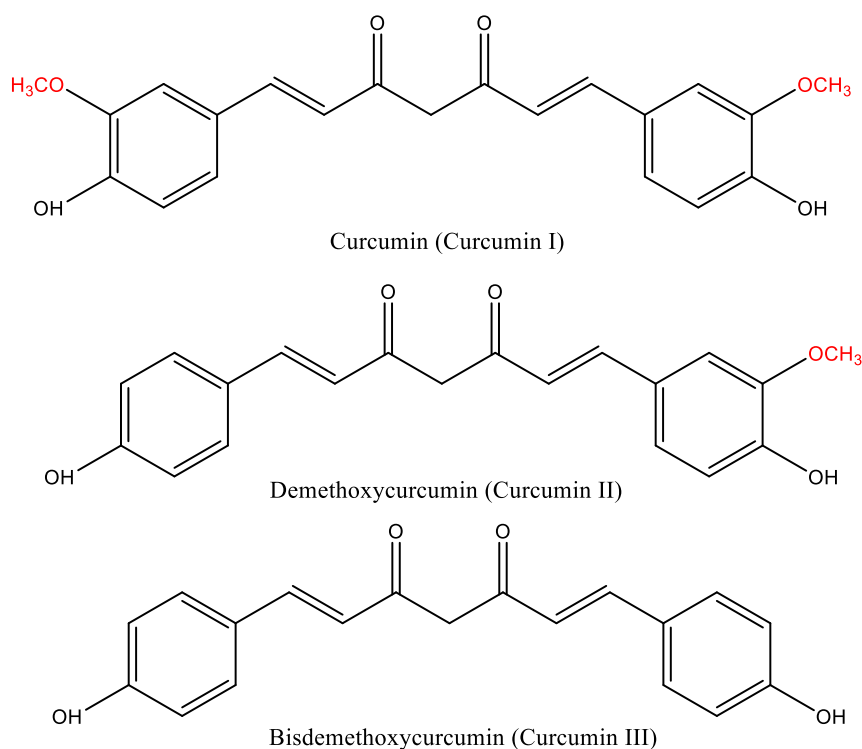


Figure 4: Structure of curcumin (top), demethoxycurcumin (middle) and bisdemethoxycurcumin (bottom).

The term curcumin, in general, can be used to represent all curcuminoids found in *C. longa*. The curcuminoids are non-toxic to humans and insoluble in water at physiological or acidic pH, slightly soluble in water at alkaline pH, and highly soluble in oil and non-sustainable solvents such as acetone or MeOH [35,36]. *C. longa* has been used for centuries worldwide, particularly in Asia and especially in India, as a culinary spice and colouring agent, food preservative, and antioxidant in the food industry and as an anti-inflammatory, therapeutic agent or dietary supplement in the pharmaceutical industry [37–42]. Besides the curcuminoids, other phytochemicals and essential oils (0.1 to 2% of the dried turmeric) can be found in *C. longa* [43–46].

Nowadays, various extraction methods and solvents are found in the literature. The most common extraction methods are Soxhlet, ultrasonic, solvent, microwave, or supercritical carbon dioxide extraction [47–50]. Conventionally, non-sustainable and toxic solvents are used, such as MeOH, acetone, and petroleum ether. They have to be removed after the extraction. One of the first

challenges for the industry is the replacement of these extraction solvents by harmless, green, and bio-based solvents [9]. Indeed, due to the growing current consumers' perception of the safety and health of food formulations, the development and extraction of natural dyes is more and more important for the food industry [51–54]. The use of synthetic dyes, such as tartrazine (E102, Figure 5), one of the most popular synthetic azo-dyes (because of its low price, high solubility in water, stability against UV-light and oxidative stress, and the small necessary amount to colour the food), does not match with the consumers' perception anymore (tartrazine can be responsible for allergic reactions and hyperactivity in children) [53]. However, tartrazine is still permitted in the food industry (reference daily intake <7.5 mg/kg body weight [51]), but the food formulations, which contain tartrazine, have to carry a warning label: “May have an adverse effect on activity and attention in children”.

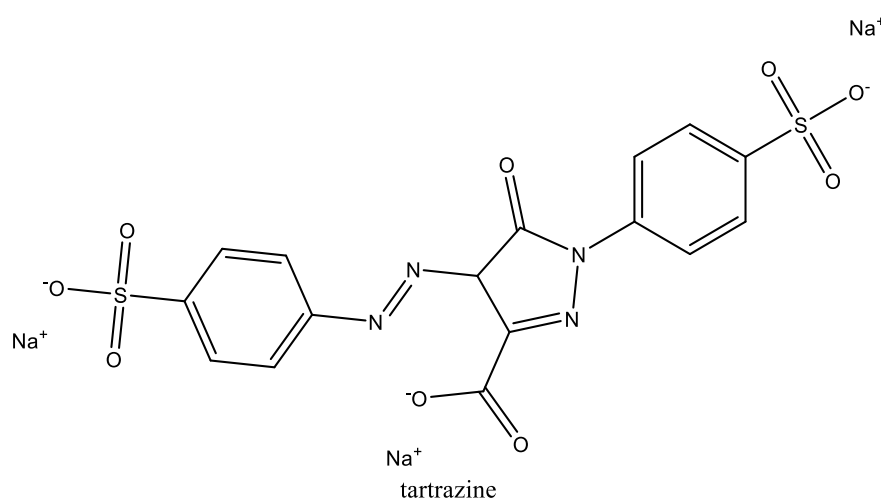


Figure 5: Structure of tartrazine.

Curcuminoids are among the potential natural dyes that are an excellent alternative to tartrazine. They are basically non-toxic and biodegradable [35]. Nevertheless, the poor water solubility is a drag to its extraction and use in the food industry. In the industry, the curcuminoids are extracted with EtOH or aqueous EtOH solutions (it is the most popular sustainable alternative). To obtain a powder, they are recrystallised from the aqueous EtOH solution. Before extraction and recrystallisation, the essential oils present in the turmeric rhizomes need to be removed [55]. To remove them, toxic and volatile solvents such as hexane or pentane are used. Curcumin is then obtained from unflavoured *C. longa*. Many studies have shown that supercritical carbon dioxide could be an alternative to unflavour the turmeric [55,56]. In the literature, the binary mixture EtOH/H₂O (80/20 in volume or weight) is commonly used as a reference, but the extraction yield of the curcuminoids remains low and needs, therefore, further optimisation. Another way to extract the curcuminoids from *C. longa* is the use of hydrotropes. A hydrotrope is a small amphiphilic molecule and highly soluble in water [57]. The

difference compared to a surfactant is the non-polar part, which is much smaller than the hydrophobic part of a surfactant. Hence, hydrotropes cannot build defined structures such as micelles or liquid crystals in water. Often, they form aggregates in water in the presence of a hydrophobic compound, which allows the latter to be dissolved in an aqueous phase [58]. The concentration which is needed to dissolve a hydrophobic compound in water is called the minimum hydrotropic concentration (MHC). Different types of hydrotrope exist: non-ionic ones such as EtOH, urea, or nicotinamide and ionic ones such as sodium salicylate (NaSal), sodium xylene sulfonate (SXS), or sodium benzoate. In the literature, different hydrotropes (NaSal, SXS or sodium cumene sulfonate for example) have been used to solubilize and extract the curcuminoids by Dandekar et al [59]. However, the used hydrotropes are petroleum-based, non-green, and exhibit low extraction efficiencies as compared to the standard solvent extraction. In this thesis, a mixture of water, EtOH, and triacetin (TriA) has been used as an extraction system and compared with Soxhlet, the common green extraction mixture EtOH/H₂O, and other solvents. TriA is a triglyceride and is widely used in the food industry as a food additive, solvent, or humectant (E1518). The advantage of the mixture of water, EtOH, and TriA is the fact that the mixture is entirely green, bio-based, and sustainable [60]. Therefore, it could be a promising alternative for the extraction of the curcuminoids from *C. longa*. Another ternary mixture consisting of NaSal, water, and ethyl acetate (EtOAc) will also be used as an extraction medium [61]. NaSal is not food-approved but it is used a preservative in the cosmetic, pharmaceutical, and also the food industry, unless it is ingested.

After the extraction, the second challenge of using curcuminoids is their stability as powder or in solutions. The major problems with the curcuminoids are their instability against UV-light, alkaline and physiological pH, oxidation, and temperature [35,36,62–65]. Elevated temperatures degrade the curcuminoids, which is also a problem for their extraction [66]. Indeed, before extraction, the rhizomes of *C. longa* get unflavoured and one of the commonly used methods to extract essential oils is the hydro distillation. But this method is not used to obtain unflavoured turmeric because the curcuminoids get strongly degraded during the process. In alkaline and physiological solutions, the hydroxide catalyses the degradation of the curcuminoids. Several different products can be formed during the degradation of the curcuminoids, such as vanillin, acetone, ferulic acid, hexahydrocurcumin, or bicyclopentadione. One of the main mechanisms of degradation of curcumin is the autoxidation with the help of dissolved oxygen. Indeed, the role of oxygen radicals on the degradation of the curcuminoids is well known in the literature and has been studied over decades [35,63,67]. Moreover, curcuminoids are also known for being antioxidants [68–70]. This means that the curcuminoids react preferably with oxygen species. Antioxidants are food additives in the cosmetic, pharmaceutical, or

food industry and used to prevent the oxidation of the formulation caused by oxygen. In this study, the stability of curcumin against UV-light in the different extract medium has been studied. Moreover, the role of NaSal, a charged hydrotrope as antioxidant and potential stabiliser for the curcuminoids will be investigated more deeply. The addition of different additives such as meglumine (solubilizer) and pyroglutamic acid (PCA, hydrotrope) to the extraction medium has been explored for the extraction and stabilisation of the curcuminoids [71]. Meglumine, N-methyl glucamine, is a sugar-based, biodegradable pharmaceutical excipient. Meglumine is well known and widely used in the pharmaceutical industry to improve the solubility of poorly water-soluble drugs in water [72–74]. It is already used to solubilize antimonate (treatment against Leishmaniasis), gadoteric acid (contrast agent for magnetic resonance imaging), or ioxaglic acid (contrast agent for angiography) [75–78]. PCA is a small amphiphilic molecule, which is present in the human skin and could be used as hydrotrope for the extraction of the curcuminoids. It is a non-essential nutrient and is biosynthesised by the body [79,80]. The difference between the other used hydrotropes in the literature and PCA is that PCA is allowed in the food, cosmetic, and pharmaceutical industries.

3.2 Material and methods

3.2.1 Material

All used chemicals and materials are summarised in Table 1 and Table 2.

Table 1: Listing of all used chemicals.

Chemicals			
Name	Purity	Description/Grade	Company (city, country)
Curcumin	> 97%	synthetic phytochemical	TCI (Eschborn, Germany)
Demethoxycurcumin	≥ 98%	synthetic phytochemical	Merck (Darmstadt, Germany)
Bisdemethoxycurcumin	> 98%	synthetic phytochemical	Merck (Darmstadt, Germany)
Curcuma longa	n.a.	turmeric powder	Kwizda (Linz, Austria)
Curcuma longa	n.a.	turmeric powder	Wagner Gewürze GmbH (Schwäbisch Gmünd, Germany)
Curcuma longa	n.a.	turmeric powder	Schuhbeck's Gewürze GmbH (München, Germany)
Curcuma longa	n.a.	turmeric powder	Sonnentor (Sprögnitz, Austria)
Curcuma longa	n.a.	turmeric powder	Lebensbaum GmbH (Overath, Germany)
Sodium salicylate (NaSal)	> 99.5%	white powder	Merck (Darmstadt, Germany)
Meglumine	> 99%	ReagentPlus®	Merck (Darmstadt, Germany)
Pyroglutamic acid (PCA)	> 99%	white powder	Merck (Darmstadt, Germany)
D-Glucamine	> 97%	white powder	TCI (Eschborn, Germany)
D-(+)-Glucosamine hydrochloride	> 98%	white powder	TCI (Eschborn, Germany)
Sodium hydroxide (NaOH)	≥ 98%	pro analysi (p.a.), pellets	Merck (Darmstadt, Germany)
NaOH	n.a.	1mol/L	Carl ROTH (Karlsruhe, Germany)
Sodium Bromide NaBr	n.a.	extra pure	Merck (Darmstadt, Germany)
Hydrochloric acid (HCl)	n.a.	1mol/L, Titripur®	Merck (Darmstadt, Germany)
Ethanolamine	n.a.	for synthesis	Merck (Darmstadt, Germany)
Diethanolamine	≥ 98%		Merck (Darmstadt, Germany)

Triethanolamine	n.a.	p.a.	Merck (Darmstadt, Germany)
Triacetin (TriA)	99%	food grade, FCC	Merck (Darmstadt, Germany)
Diacetin (DiA)			
Ethanol (EtOH)	≥ 99.8%	p.a., Rotipuran®	Merck (Darmstadt, Germany) or Carl ROTH (Karlsruhe, Germany)
Acetone	≥ 99.5%	p.a.	Merck (Darmstadt, Germany)
Acetonitrile	n.a.	HPLC grade, LiChrosolv®	Merck (Darmstadt, Germany)
Acetic acid	≥ 99.8%	p.a.	Merck (Darmstadt, Germany)
Ethyl acetate (EtOAc)	≥ 99.8%	analytical reagent grade	Thermo Fisher Scientific (Steingrund, Germany)
Toluene	≥ 99.8%	analytical reagent grade	Thermo Fisher Scientific (Steingrund, Germany)
Methanol (MeOH)	n.a.	HPLC grade, LiChrosolv®	Merck (Darmstadt, Germany)
Sulfuric acid 95-97%	95-97%	p.a.	Merck (Darmstadt, Germany)
Anisaldehyde (AA)	≥ 97.5%	FCC, Kosher	Merck (Darmstadt, Germany)
Anisaldehyde reagent (AA reagent)	n.a.	AA: 0.5 mL acetic acid: 10 mL MeOH: 85 mL sulfuric acid: 5 mL	n.a.
Dimethylsulfoxide-d ₆	99.8%	NMR solvent	Deutero (Kastellaun, Germany)
D ₂ O	99.96%	NMR solvent	Deutero (Kastellaun, Germany)
Water	millipore	Milli-Q purification system	Merck Millipore (Billerica, MA USA)

Table 2: Listing of all used materials.

Materials		
Name	Description	Company
Cellulose filter	grade 1289, diameter 240mm, 84 g/m ²	Sartorius (Göttingen, Germany)
Syringe filter 0.2	0.2 µm PTFE or CA Membrane, diameter 13 or 25mm	VWR international (Ismaning, Germany)
Syringe filter 0.45	0.45 µm PTFE or CA Membrane, diameter 25 mm	VWR international (Ismaning, Germany)
Silica gel plate	TLC silica gel 60 F ₂₅₄ 20x20 cm	Merck (Darmstadt, Germany)
Centrifuge tube	50 mL, PP, 20 000 g, Conical-Bottom, sterile or not	VWR international (Ismaning, Germany)
GC-HPLC vials	brown glass 1.5 mL ND9 with screw caps	Carl ROTH (Karlsruhe, Germany)
DC Chamber	twin through chamber for 100 x 100 mm plates	Camag (MuttENZ, Switzerland)
NMR tubes	NMR tubes borosilicate length 8 inch	Deutero (Kastellaun, Germany)
Tube for DLS	Tube, culture, disposable, 10x75mm, borosilicate	Corning Incorporated (New York, USA)
Pipette tips	10, 100, 200, and 1000 µL	VWR international (Ismaning, Germany)

3.2.2 Methods

3.2.2.1 H₂O/EtOH/TriA and H₂O/EtOH/DiA

3.2.2.1.1 Ternary phase diagram

The different ternary phase diagrams were recorded at 25°C. 3 g samples of a binary mixture (EtOH/TriA, EtOH/H₂O and EtOH/DiA ranging from 100/0 to 0/100 with a step of 10 in weight percent) with a defined composition were prepared. The third component (H₂O, TriA, and DiA respectively) was then added dropwise to the binary mixture until a change in phase behavior occurred (the solution became turbid or clear). The samples were mixed manually or with a vortex if needed. The needed amount of the third component was recorded to obtain the miscibility gap and, therefore, the desired ternary phase diagram.

3.2.2.1.2 Dynamic light scattering

DLS measurements were performed at 25°C with an ALV/CGS-3 goniometer with an ALV/LSE-5004 correlator. The solutions (for the compositions see Table S 1 of the Appendix) were measured in

borosilicate glass tubes. To remove dust and impurities, the tubes were cleaned with acetone (in a distillation apparatus) and the solutions were filtered with 0.2 µm syringe filters before the measurement. All solutions were recorded for 300s.

3.2.2.1.3 Conductivity measurement

Conductivity measurements were carried out with a low-frequency WTW inoLab Cond730 conductivity meter, connected with a WTW TetraCon325 electrode (Weilheim, Germany) at $25.0 \pm 0.2^\circ\text{C}$ (thermostatic measuring cell) under constant stirring at 500 rpm. 20 g of samples (EtOH, DiA, binary mixture EtOH/TriA, and DiA/TriA) containing 0.2 wt% of NaBr (to ensure a sufficient amount of charge for the conductivity) were filled into the measuring cell. The samples were successively diluted with pure water and the related conductivity was noted.

3.2.2.1.4 Solubility measurements

Optical density measurements were carried out via UV/Vis, using a Lamda 18 UV/Vis spectrometer by Perkin Elmer (Waltham, USA) at 422 nm. The examined solutions (5 g of each sample) were saturated with curcumin under constant stirring (750 rpm) at room temperature to find the optimum in the binary mixtures (EtOH/TriA and EtOH/DiA going from 100/0 to 0/100 with a step of 10). After that, the saturated solutions were filtered (syringe filter PTFE 0.2 µm) and analysed via UV/Vis. Then, water was added to this optimum binary mixture and the maximum solubility of curcumin was examined again. Before the measurements, all of the samples were adequately diluted 1000-fold with acetone (extinction coefficient $0.138 \text{ L}\cdot\text{g}^{-1}\cdot\text{cm}^{-1}$). A calibration curve in acetone was done with curcumin (maximum absorbance at 422 nm (Y) against the concentration in g/L (X), $Y = 0.138 * X$, $R^2 = 0.9997$).

3.2.2.1.5 Stability of curcumin in binary solvent mixtures

Binary mixtures (EtOH/TriA 40/60 and DiA/TriA 60/40 in weight) were saturated with curcumin (under constant stirring (750 ppm) for one hour) and the stability of curcumin at daylight, in darkness, and in darkness at 8°C was carried out via UV/Vis measurements, as described in section 3.2.2.1.4. The stability of curcumin in the binary mixture of EtOH and TriA stored in a brown and blue glass bottle was also investigated via UV/Vis.

3.2.2.1.6 Curcuminoid content of different *C. longa* powders

2 g of *C. longa* was extracted using a Soxhlet apparatus with 50-60 mL of acetone. Turmeric powders from different brands were used: Wagner, Schuhbeck, Sonnentor, and Lebensbaum. After the extraction (extraction time of about five hours), the presence of curcuminoids in the extract solutions was tested via TLC. A defined sample volume of 4 µL was spotted using a glass syringe of 100 µL (Hamilton, Switzerland) and a Linomat 5 from CAMAG (Berlin, Germany), on a TLC plate (silica gel). Then, the TLC plate was eluted with a mixture of toluene and acetic acid (40/10, v/v). Derivatisation of

the TLC plate was carried out with anisaldehyde reagent (AA reagent). Pictures were taken before and after derivatisation.

3.2.2.1.7 Extraction procedure with *C. longa* from Wagner

C. longa (Wagner) was extracted in centrifuge tube with different extraction mixture compositions (EtOH/TriA, H₂O/EtOH/TriA, DiA/TriA, and H₂O/DiA/TriA) under constant stirring at room temperature for one hour. The weight ratio of *C. longa* to extraction mixture of 1 to 5 was used for the extraction. The extract solutions were then centrifuged (4200 g for 10 min), filtered (EtOH/TriA system with 0.2 µm syringe filter, DiA/TriA system with 0.45 µm) and the curcuminoid extraction efficiency was measured via UV/Vis.

3.2.2.1.8 High-Performance-Liquid-Chromatography method

The curcuminoid content of the extract solutions was analysed by HPLC using the following HPLC system: Waters HPLC system with two Waters 515 HPLC pumps, Waters 717 autosampler, Waters 2487 UV/Vis detector, ACE Equivalence 3 C18-Column (110Å, 3 µm, 150x2.1 mm) and Empower® as software. Table 3 summarizes the used gradient method and the different parameters of the HPLC. Each sample was made in triplicate and eluted three times. Three calibration curves of the curcuminoids (curcumin, demethoxycurcumin, and bisdemethoxycurcumin) were recorded in the concentration range of 0.04 to 0.2 mg/mL, as shown in Figure S 1 of the Appendix. The same gradient method and parameters, as described in Table 3, were used.

Table 3: Parameter and gradient method used for the HPLC system.

Parameters		Gradient method		
		Solvent A	Solvent B	Time (min)
Temperature	40 °C	60-40	40-60	0-17
Flow	0.4 mL/min	40-0	60-100	17-18
Injection volume	10 µL	0	100	18-24
Solvent A	H ₂ O with 0.3 % of acetic acid	0-60	100-40	24-25
Solvent B	Acetonitrile	60	40	25-32

3.2.2.1.9 Determination of the curcuminoid content

2 g of *C. longa* (Kwizda) was extracted using a Soxhlet apparatus with 50-60 mL of acetone. After the extraction process, the extract solution was filtered using cellulose filter, put in a volumetric flask, topped off with acetonitrile, diluted 50-fold, and finally eluted by HPLC (average of three runs), as

described in section 3.2.2.1.8. The Soxhlet extraction was done in triplicates and the curcuminoid content was then determined using the calibration curves (Figure S 1 of the Appendix).

3.2.2.1.10 Determination of the best ratio *C. longa* to extraction mixture

4 g of *C. longa* (Kwizda) was extracted at different weight ratios *C. longa* to binary mixture EtOH/TriA 40/60 (w/w) under constant stirring for one hour at room temperature in a centrifuge tube. Different weight ratios from 1:2 to 1:7 (*C. longa* to EtOH/TriA) were investigated. After that, all the extract solutions were centrifuged (4200 g for 10 min), filtered with cellulose filters, put in volumetric flasks, topped off with acetonitrile, diluted 25-fold, filtered through 0.2 µm syringe filters into HPLC glass bottles, and finally eluted by HPLC. All the samples were eluted three times through the HPLC and made in triplicates. The curcuminoid content of each extract solution was determined using the calibration curves (Figure S 1 of the Appendix).

3.2.2.1.11 Extraction procedure

The same extraction procedure, as described before in section 3.2.2.1.10, was used with a constant weight ratio *C. longa* to extraction mixture of 1:4. Therefore, 4 g of *C. longa* was extracted with 16 g of extraction mixture. Different extraction mixtures were investigated (see Table S 2 of the Appendix). The same procedure, as described before in section 3.2.2.1.10, was used to determine the curcuminoid content of all extract solutions. All samples were made in triplicates.

3.2.2.1.12 Extraction and enrichment procedure

The same extraction, as described in section 3.2.2.1.10, was used with two different weight ratios *C. longa* to extraction mixture: 1:16 and 1:24. Therefore, 2 g of *C. longa* was extracted with respectively 32 g and 48 g of different extraction mixture compositions. The same extraction mixture compositions of EtOH/TriA and H₂O/EtOH/TriA (see Table S 2 of the Appendix) were investigated. After the extraction, the extract solutions were centrifuged (4200 g for 10 min), the supernatant was collected and 2 g of fresh *C. longa* was added again (one cycle). After several cycles (2, 3 and 4), the curcuminoid content was determined, as described in section 3.2.2.1.10. All samples were made in triplicates. After each cycle and for all extract solutions with the two different weight ratios, the amount of solvent loss was also determined.

A preliminary test was done via UV/Vis with *C. longa* (Wagner). 2 g of *C. longa* was extracted with 32 g of the binary mixture EtOH/TriA 60/40 in weight (ratio *C. longa* to extraction mixture of 1 to 16) with the same extraction procedure as described above. Before all measurements, the samples were adequately diluted with acetone.

3.2.2.1.13 Distillation

C. longa (Kwizda) was distilled using a Clevenger apparatus for two hours (1 g of *C. longa* for 8.5 g of water). Then, a binary mixture of EtOH/TriA (40/60, w/w) was added to the distillation flask to start the extraction (composition of the extraction mixture after addition of the binary mixture: H₂O/EtOH/TriA 40/24/36 in weight). Then, the same extraction and analytical procedures, as described in section 3.2.2.1.10, were used to determine the curcuminoid content (weight ratio *C. longa* to extraction mixture: 1:20). Moreover, the purity of the extract solution (approximation based on area percent by HPLC: area of the three curcuminoid peaks divided by the area of all the peaks) was also determined. A reference extraction with the same weight ratio (1:20) but without distillation was also done for comparison. All samples were made in triplicates.

3.2.2.1.14 Vacuum distillation

C. longa (Kwizda) was distilled under vacuum three times at 30°C using a water bath (1 g of *C. longa* for 10 g of water). To this purpose, *C. longa* was put with water in a 50 mL flask connected to a reflux condenser, a 100 mL flask (for the distillate) and a vacuum oil pump. After each distillation cycle (three in total), half of the initial amount of water in the distillation flask was accumulated as distillate in the 100 mL flask. The collected water as distillate was replaced in the distillation flask by the corresponding mass of fresh water. After three times, a binary mixture of EtOH/TriA (40/60 and 65/35, w/w both) was added to the distillation flask to start the extraction procedure (compositions of the extraction mixture after addition of the binary mixture: H₂O/EtOH/TriA 40/24/36 and H₂O/EtOH/TriA 50/32.5/17.5 in weight). After that, the same extraction and analytical procedures, as described in section 3.2.2.1.10, were used to determine the curcuminoid content (weight ratio *C. longa* to extraction mixture: 1:26.5). Moreover, the purity of the extract solutions, as described in section 3.2.2.1.13, was also determined. All samples were made in triplicates.

3.2.2.1.15 Lyophilisation

2 g of *C. longa* (Kwizda) with 30-35 mL of water in a centrifuge tube was freeze-dried several times (3-6 times). After each freeze-drying cycle, approximately the same initial amount of water was added to the 2 g of dried *C. longa*. After 3, 4, 5 and 6 cycles of freeze-drying, the 2 g of dried *C. longa* were extracted, using the same extraction procedure as described in section 3.2.2.1.10, with two different ternary extraction mixtures (H₂O/EtOH/TriA 40/24/36 and H₂O/EtOH/TriA 50/32.5/17.5 in weight) with a weight ratio *C. longa* to ternary extraction mixture of 1:8. The same analytical procedure, as described in section 3.2.2.1.10, was used to determine the curcuminoid content. Moreover, the purity of the extract solutions after each cycle, as described in section 3.2.2.1.13, was also determined. All samples were made in triplicates.

3.2.2.1.16 Water solubility and stability of the extracts

0.1 mL of purified curcuminoid extract (via lyophilisation (4, 5 and 6 times, cf. 3.2.2.1.15)) were diluted in 10 mL of water. The half of the diluted curcuminoid extract was stored at daylight and room temperature and the other half in darkness at room temperature. Photos were taken after 3, 14 and 30 days to investigate the colour stability of the diluted extracts. The colour stability of the purified curcuminoid extracts were also investigated by the same way.

3.2.2.2 (Meglumine/PCA/H₂O)/EtOH/TriA

3.2.2.2.1 Solubility of curcumin in water with different additives

18 g of a sample containing 5 wt% meglumine in water was divided in 6 identical samples of 3 g. Curcumin was added (150 mg) to all the samples. After 10, 20, 30, 40, 50 and 60 minutes, one sample was filtered (0.45 µm CA) and measured via UV/Vis (2000-fold in acetone).

The maximum solubility of curcumin was investigated as described in section 3.2.2.1.4. Different additives (triethanolamine, diethanolamine, ethanolamine, D-glucamine, meglumine, D-(+)-glucosamine (at pH 11 and 12, adjusted with NaOH tablets) and NaOH) were solubilised in water at different weight concentrations (1, 3, 5, 7, 10 and 15 wt%). For NaOH, the pH of the water was adjusted to 11.5. Before measurement, the solutions were adequately diluted with acetone (2000-fold for meglumine and D-(+)-glucosamine at pH 11 and 12, 5000-fold for ethanolamine, 1000-fold for diethanolamine and D-glucamine, 100-fold for triethanolamine and NaOH). All the measurements were made in duplicate.

For the hydrotropic curve, different amounts of PCA, NaSal, or EtOH were solubilised in water (3 g samples). Then, the solutions were saturated with curcumin overnight at room temperature. After the solubilisation process, the solutions were filtered (0.2 µm syringe filter) and the maximum solubility of curcumin was investigated via UV/Vis measurements. The solutions were diluted with acetone before measurement (500-fold for PCA and NaSal and 1000-fold for EtOH)

3.2.2.2.2 Stability of curcumin in water with different additives

The stability of solutions containing 15 wt% of additives (same as described above in section 3.2.2.2.1, only the additives were tested and not the different hydrotropes) were investigated under constant lighting (30 W corresponding to 150 W halogen lamp). The stability was investigated via UV/Vis measurements with the same dilutions in acetone as described previously. All the measurements were made in duplicate. The pH of the solution after saturation with curcumin was measured using a VWR phenomenal 211 electrode connected to a VWR phenomenal instrument (pH 1000 L).

3.2.2.2.3 Nuclear magnetic resonance experiment

Heteronuclear Multiple Bond Correlation (HMBC) experiments were conducted using a Bruker Avance III HD-400 NMR-spectrometer (Billerica, MA, USA) operating at 400 MHz. Two identical samples (34 wt% of PCA in 66 wt% of water) at two different pH (1.3 and 10.2) were measured. The first sample with an initial pH of 1.3 (without any additives). The pH value 10.2 of the second sample was adjusted using NaOH tablets. Approximately, 0.8 mL of the samples was filled in the NMR tube. The sample at pH 10.2 was measured with an insert containing D₂O so that D₂O is not in contact with the sample.

Different mole ratios of curcumin to meglumine (1/4, 1/3, 1/2, 1/1, 2/1, 3/1 and 4/1) were investigated via NMR (¹H-NMR). Curcumin and meglumine were solubilised in DMSO-d₆. Curcumin and meglumine alone were also measured as references. Rotating frame Overhauser Enhancement Spectroscopy (ROESY) experiments were also done with the ratio curcumin to meglumine 2 to 1.

3.2.2.2.4 Ternary phase diagram

Meglumine was solubilised in water at different weight concentration (5 and 15 wt% of meglumine in respectively 95 and 85 wt% of water) and the desired pH was then adjusted with PCA. The different phase diagrams were recorded at room temperature at different pH values (7,9, 11.3 and 11.5) for both weight concentrations of meglumine in water. At pH 7, one more concentration of meglumine was investigated (20 wt% of meglumine in 80 wt% of water). The pH was adjusted for the water that was used to record the phase diagrams. The same procedure, as described in section 3.2.2.1.1, was used to obtain the different phase diagram.

3.2.2.2.5 Determination of the pKa of meglumine

1.76 g of meglumine was dissolved in 10.1 g of water (solution at 15 wt% of meglumine) and titrated with a 0.5 M HCL solution. During the titration, the pH was recording using a VWR phenomenal 211 electrode connected to a VWR phenomenal instrument (pH 1000 L).

3.2.2.2.6 Dynamic light scattering

The same method as described in section 3.2.2.1.2 was used. The following samples were measured over the time: TriA/EtOH/(H₂O containing 15 wt% of meglumine, pH 11.5) 36/24/40, TriA/EtOH/(H₂O containing 5 wt% of meglumine, pH 11.3) 36/24/40 and TriA/EtOH/(H₂O containing 5 wt% of meglumine, pH 9 (addition of PCA)) 36/24/40 (w/w/w).

3.2.2.2.7 Solubility of curcumin

The same method as described in section 3.2.2.1.4 was used. The addition of meglumine with or without PCA to the water was carried out as described in section 3.2.2.2.4. All the samples were made in duplicates. Before measurements, all samples were diluted with acetone.

3.2.2.2.8 Selective precipitation of the curcuminoids by varying the pH

The pH-driven precipitation of curcumin and bisdemethoxycurcumin was investigated. Therefore, meglumine was dissolved in water (5 wt%), then the solution was saturated with curcumin or bisdemethoxycurcumin and filtered (40 mL sample). 1 mL of a HCL solution at 0.5 mol/l was added to the solution. The pH was then measured and 1 mL of solution was taken and put in a centrifuge tube. In total 14 mL of HCl were added and 14 mL were taken and put into 14 centrifuge tubes. After that, all the centrifuge tubes were centrifuged (4200 g for 10 min).

The pH of the ternary solution H₂O/EtOH/TriA (40/24/36 in weight) with 15 wt% and 5 wt% meglumine as concentration in pure water were investigated over the time with and without saturation of curcumin.

3.2.2.2.9 Stability of curcumin in the ternary phase diagram

Solubility measurements were carried out as described in section 3.2.2.1.5 over time. In Table S 4 of the Appendix are given the investigated compositions. Before the measurement all the solutions were diluted 5000-fold with acetone.

3.2.2.2.10 High-Performance-Liquid-Chromatography method

The same HPLC system was used as described in section 3.2.2.1.8, but with a new ACE Equivalence 3 C18-column (110Å, 3 µm, 150x2.1 mm). Since the column changed, the calibration curves have been repeated as described in section 3.2.2.1.8. The used parameter and gradient method are given in Table 4. The curcuminoid calibration curves are shown in Figure S 2 of the Appendix.

Table 4: New parameter and gradient method used for the HPLC system.

Parameters		Gradient method		
		Solvent A	Solvent B	Time (min)
Temperature	40 °C	60-40	40-60	0-17
Flow	0.4 mL/min	40-0	60-100	17-18
Injection volume	5 µL	0	100	18-24
Solvent A	H ₂ O with 0.3 % of acetic acid	0-60	100-40	24-25
Solvent B	Acetonitrile	60	40	25-32

3.2.2.2.11 Extraction procedure

The same extraction method was used as described in section 3.2.2.1.11. 4 g of *C. longa* (Kwizda) was extracted with 16 g of extraction mixtures (for the compositions see Table S 3 of the Appendix). The same analytical method as described in section 3.2.2.1.11 was used with the only difference, that the

volumetric flask was topped off with a mixture of acetonitrile/water. The curcuminoid content of the extract solutions was determined using the calibration curves (Figure S 2 of the Appendix).

A water extraction with only meglumine as additive was carried out. Meglumine was solubilised in water at different weight concentration (5 and 15 wt% of meglumine in respectively 95 and 85 wt% of water). 4 g of *C. longa* (Kwizda) was extracted with 16 g of these two extractions mixtures in centrifuge tubes (one hour at room temperature under constant stirring). After the extraction, about 20-25 mL of an 1M HCL solution was added to the extraction medium. After centrifugation (4200 g for 10 min), the supernatant was removed and the precipitate was extracted again with acetonitrile. After centrifugation, the extract solution was topped off with acetonitrile in a volumetric flask and eluted by HPLC, as described in section 3.2.2.2.10. The curcuminoid content and the purity, as described in section 3.2.2.1.13, of the extract solutions were determined.

3.2.2.3 *H₂O/NaSal/EtOAc*

3.2.2.3.1 Ternary phase diagram

To obtain the miscibility gap of the phase diagram *H₂O/NaSal/EtOAc*, the same method as described in section 3.2.2.1.1 was used.

3.2.2.3.2 Solubility measurement

The same method has been used as described in section 3.2.2.1.4. The solutions (for composition see Table S 5 of the Appendix) were saturated with curcumin in the monophasic region of the ternary compositions to determine the solubility map of curcumin.

3.2.2.3.3 High-Performance-Liquid-Chromatography method

The same method as described in section 3.2.2.2.10 has been used to determine the curcuminoid content of the extract solutions.

3.2.2.3.4 Determination of the best ratio *C. longa* to extraction mixture

The composition of the critical point was used to determine the best ratio *C. longa* to extraction mixture. Therefore, 1 g of *C. longa* (Kwizda) was extracted with different weight ratios: 1:2 to 1:6 with a step of 1, 1:10, 1:15 and 1:20 (*C. longa* : extraction mixture, w : w) under constant stirring for one hour at room temperature in centrifuge tubes. The extracts solutions were then centrifuged (4200 g for 10 min), the supernatant was filtered into 10 mL (ratios 1:2 to 1:6 and 1:10) or 25 mL (ratios 1:15 and 1:20) volumetric flask using cellulose filters, topped off with acetonitrile (ratios 1:2 to 1:6) or acetonitrile/water 90/10 (w/w) (ratios 1:10, 1:15 and 1:20), diluted 25-fold with acetonitrile, filtered through 0.2 µm syringe filters into HPLC glass bottles, and finally eluted by HPLC. All samples were

eluted three times and made in triplicates. The curcuminoid content was determined using the calibration curves of the curcuminoids (Figure S 2 of the Appendix).

3.2.2.3.5 Extraction procedure

The same extraction and analytical procedures as described before in section 3.2.2.3.4 were used with a constant ratio *C. longa* to extraction mixtures of 1 to 10. Different extraction mixtures were investigated (see Table S 5 of the Appendix).

3.2.2.3.6 Stability of curcumin in the ternary system

Stability measurement were carried out via UV/Vis as described in section 3.2.2.1.5. The different solutions (for compositions see Table S 5 of the Appendix) were saturated with curcumin, then filtered (0.2 µm syringe filter) and store at daylight only. The optical density was measured over the time.

3.2.2.3.7 Determination of the oxygen content

Measurements of the dissolved oxygen were carried out using a TPS Aqua-D oxygen-meter connected to a TPS ED1 electrode (Brisbane, Australia) at $25 \pm 1^\circ\text{C}$. 10 g of the samples (for compositions see Table S 5 of the Appendix) were prepared and the measurements were carried out after a two-point calibration against air and a solution of 2 g sodium sulfite in 100 mL water under constant stirring. Values were taken after 5 minutes to ensure equilibration.

3.2.2.3.8 Determination of the curcuminoids' partition coefficient

The same HPLC method as described in section 3.2.2.2.10 was used to determine the partition coefficient of the three curcuminoids. Three 6 g samples with the composition of the critical point ($\text{H}_2\text{O}/\text{NaSal}/\text{EtOAc}$ 17/12/71 in weight) were prepared in centrifuge tubes, and 1 wt% of curcumin was dissolved in every sample. After homogenisation, different amounts of water were added to the samples (1 g, 2 g, and 3 g of water respectively) to obtain a phase separation. After centrifugation (4200 g for 10 min), the two phases were separated and put into 10 mL volumetric flasks. Two different dilutions were used for the two phases: 25-fold for the oil-rich phase and 2- to 3-fold for the water-rich phase. All the phases were then analysed by HPLC as described in section 3.2.2.3.3.

The same procedure described above was used with an extract solution (0.6 g of *C. longa* (Kwizda) was extracted with an extraction mixture with the critical point composition). In this case, the water-rich sample was not diluted before the HPLC measurements.

The partition coefficient of the curcumin and curcuminoids was determined as the logarithm of the ratio between the concentration of curcumin or cucuminoids in the oil-rich phase and the concentration of curcumin or cucuminoids in the water-rich phase.

3.2.2.3.9 Interfacial tension

The interfacial tension measurements were performed by Asmae El Maangar in Marcoule (France, ICSM, university of Montpellier, CEA, CNRS, ENSCM). The method was described in the paper El Maangar et al. [61] and will be described here again. A Krüss Spinning Drop tensiometer has been used to measure the interfacial tensions γ between the aqueous and organic-rich phases. The aqueous phase was used as the outer phase and the organic phase as the droplet. The measurements (duplicate, mean of two oil droplets) were carried out at 4000 to 8000 rpm. The data were collected only in this rotation speed range and only if the resulting interfacial tension had a constant value. Density data, which have been made in the previous work of El Manngar et al. [81]de are needed to obtain the interfacial tension.

3.2.2.3.10 Precipitation of curcumin

500 mg of curcumin was dissolved in 20 g of a ternary mixture at the critical point composition. After that, 10 g of water (half of the weight of the ternary mixture) was added to the sample to force phase separation. Overnight, a solid precipitate appeared at the interface. The obtained solid was isolated (Buchner filtration), washed three times with water and finally analysed via NMR. The oil-rich phase was evaporated with a rotary evaporator and the solid precipitate resulting from the solvent evaporation analysed. The sample was made in triplicate to give a standard deviation.

An enrichment procedure, as described in section 3.2.2.1.12, has been used. 2 g of *C. longa* (Kwizda) was extracted with the above ternary mixture (critical point composition) for one hour under constant stirring at room temperature. The extract solution was centrifuged, the supernatant collected and 2 g of fresh *C. longa* (Kwizda) added to the supernatant. The enrichment procedure was performed 5 times. After that, the final supernatant was filtered (cellulose filter paper) into centrifuge tubes and water was added (50% of the solution weight). The solution was centrifuged (10 min, 20 400 g), filtered (0.2 μm syringe filter), and the precipitate was analysed via HPLC.

3.3 Results and discussion

3.3.1 H₂O/EtOH/TriA and H₂O/DiA/TriA

3.3.1.1 Phase diagrams and structuring

TriA, DiA and EtOH were chosen as investigated solvents because of their edibility, low toxicity, sustainability, and miscibility. The idea was to combine an edible oil (TriA) with different edible co-solvents (EtOH and DiA) in water to develop a green, sustainable, and edible ternary mixture, which could be used for the extraction of curcuminoids from *C. longa*. TriA is slightly miscible with water, DiA and EtOH are completely miscible with water and TriA. The ternary mixtures H₂O/EtOH/TriA and H₂O/DiA/TriA have been investigated, focusing on their mixing behaviour and their possible structuring as SFME (TriA plays the role of the oil phase and EtOH and DiA as co-solvent). The two obtained phase diagrams and the different solvent mixtures used to investigate the maximum solubility of curcumin and the extraction of the curcuminoids from *C. longa* are described in Figure 6.

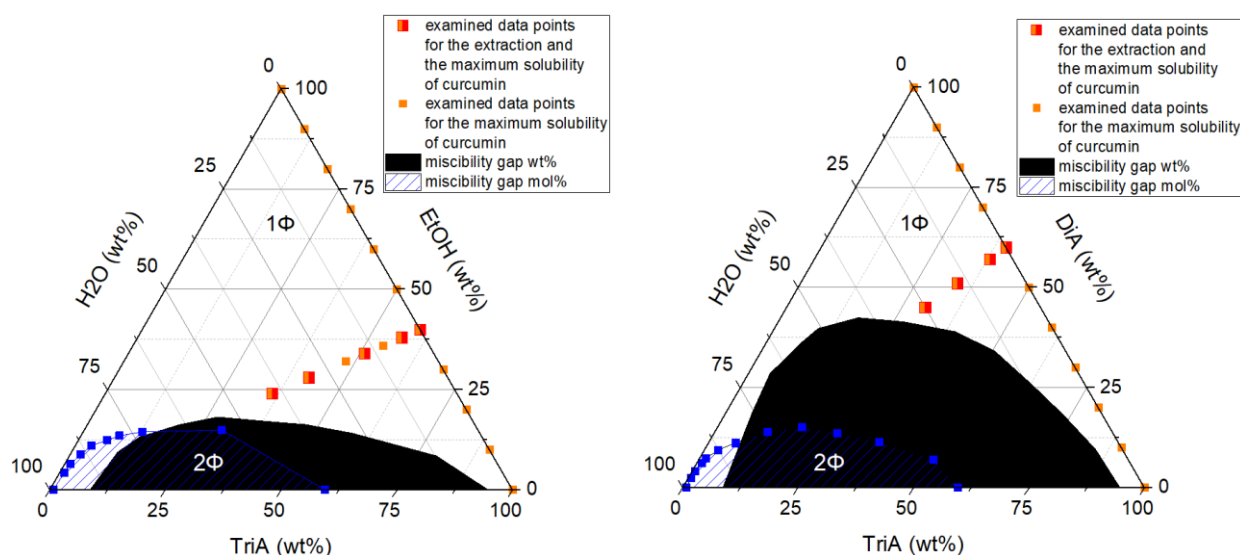


Figure 6: Ternary phase diagram of the systems (left) H₂O/EtOH/TriA and (right) H₂O/DiA/TriA in wt% (black) and mol% (blue square) containing the examined data points for the determination of the maximum of solubility of curcumin (orange square) and of the curcuminoid extraction efficiency from *C. longa*.

The ternary system with DiA showed a bigger miscibility gap (two phasic region, dark area in the phase diagram) than the ternary mixture with EtOH in weight ratio. The ternary mixture with EtOH made it preferable for further investigation because more water could be solubilised in TriA. However, the miscibility gaps were of comparably smaller size and covered almost the same area for both co-solvents in mole. Therefore, EtOH and DiA can be presumed as equally potent. The phase diagram with DiA instead of EtOH as co-solvent has been investigated too, as alternative for people with eating restrictions. Since the obtained phase diagrams showed a similar behaviour as common phase

diagrams between water, oil and hydrotrope, the possible structuring of the systems was investigated via DLS measurements. Indeed, DLS was performed to confirm or not the presence of SFME.

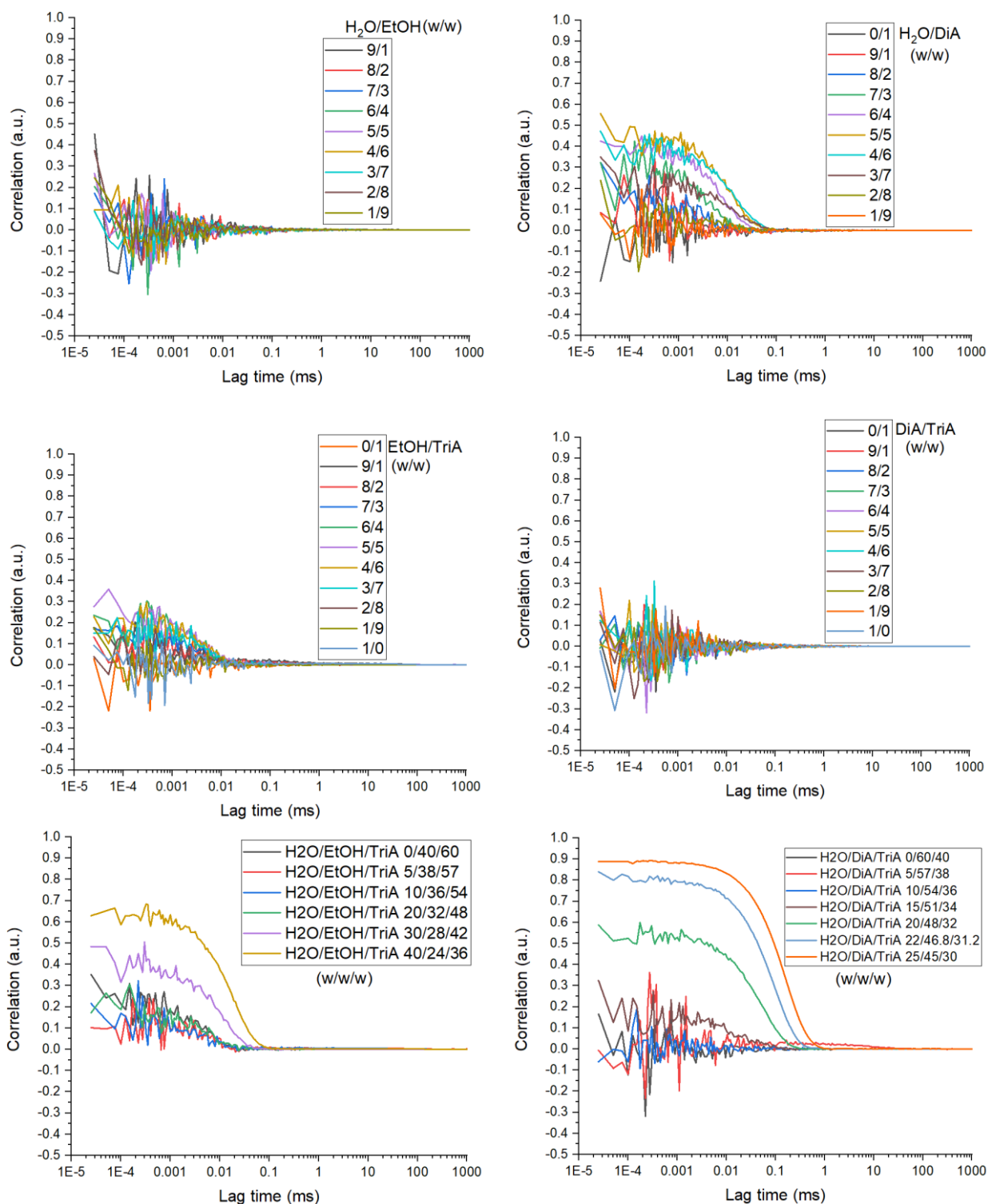


Figure 7: DLS measurements of the investigated binary mixtures water and co-solvents ($H_2O/EtOH$ on the top left; H_2O/DiA on the top right), co-solvents and TriA ($EtOH/TriA$ in the middle left; $DiA/TriA$ in the middle right), and ternary mixtures ($H_2O/EtOH/TriA$ on the bottom left; $H_2O/DiA/TriA$ on the bottom right). All the investigated compositions are given in weight ratio [82]. The data concerning the binary mixture $H_2O/EtOH$ were provided by Buchecker T. and Krickl S. et al. [83].

The DLS measurements are shown in Figure 7. The different binary mixtures water/co-solvent and co-solvent/TriA were investigated. As can be seen in Figure 7, the binary systems with water showed a different behaviour. The H₂O/EtOH did not show pronounced correlation functions. It was already known that this binary mixture did not show any peculiarities via DLS because of the mixtures' high diffusion coefficients. Indeed, these cause too rapid fluctuations and, therefore, were not detectable with DLS. On the contrary, the binary mixture H₂O/DiA did show some correlation functions, more or less pronounced following the weight ratio. The most pronounced correlation functions were found between 40 wt% and 60 wt% of DiA in the binary mixture. It was the sign of fluctuating structures in these binary mixtures, which are more pronounced and defined than in the binary mixture H₂O/EtOH. Regarding the binary mixtures of co-solvent/TriA, only a slight increase of the correlation function in the case of the binary mixture EtOH/TriA (50/50 in weight) has been detected, but only to a small extent. However, it did not give an indication of structuring. No correlation functions were detected with the binary mixtures DiA/TriA. After the behaviour of the different binary mixtures, the behaviour of the ternary mixtures was investigated with the two systems. The compositions EtOH/TriA 40/60 and DiA/TriA 60/40 have been chosen to be examined upon addition of water (these compositions were chosen because of the maximum solubility of curcumin, see section 3.3.1.2). The more water was added to the systems, the more defined and pronounced correlation functions appeared. This finding indicated the spontaneous formation of a SFME upon addition of water for the two systems. Moreover, bigger structures are created because of the decrease of the correlation function at later lag time for both systems. The closer was the composition of the SFME to the miscibility gap, the bigger were the formed structures. The structuring was more pronounced with the system containing DiA as co-solvent than EtOH. To further examine and to prove the structuring and the formation of SFME, conductivity measurements were performed. The conductivity measurements are shown in Figure 8. They gave information about the structuring of a system through a charge carrier's mobility (NaBr). Since NaBr was not soluble in DiA and TriA, a little bit of water was added to perform the measurement and ensure charge mobility (which is the reason why the curves do not start by 0).

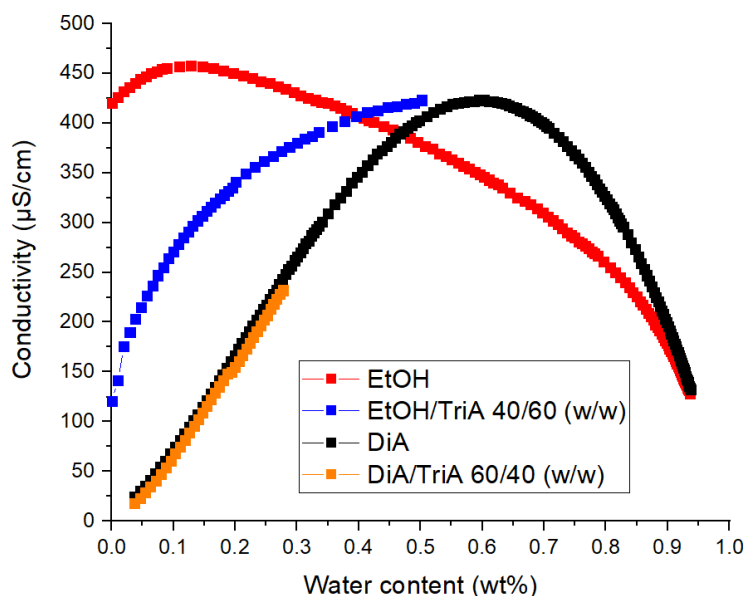


Figure 8: Conductivity curves obtained with addition of water to EtOH (red square), DiA (black square), EtOH/TriA 40/60 in weight (blue square) and DiA/TriA 60/40 in weight (orange square) [82].

As can be seen in Figure 8, all the curves showed an increase in conductivity at low water content. The same behaviour was observed for the pure co-solvents: the conductivity increased until a maximum followed by a decrease of conductivity due to a dilution of the charge. For EtOH, a small increase with low water content was noted until the charges were diluted too much (after around 10 wt% of water). This slight increase was due to the enhanced ion dissociation and the high electrophoretic mobility in the aqueous media [83]. For DiA, a larger increase was noted, which would indicate an association between TriA and DiA. If the binary mixtures are compared to the pure co-solvent, different behaviours are obtained. For EtOH/TriA, a strong increase of the conductivity was observed. This indicated that TriA was responsible for the structuring of the mixture and the formation of the SFME. The curve was stopped at around 50 wt% of water because of the miscibility gap. Indeed, with more water, the solution became turbid. On the contrary, for DiA/TriA, the same increase was also observed for pure DiA. It indicated that TriA did not contribute to the structuring since DiA alone was capable of structuring. For the same reason as before, the curve was stopped around 30 wt% of water.

3.3.1.2 Solubility, stability and extraction of curcumin from different *C. longa* powder

First, the ability of the binary mixtures of co-solvent/TriA and the SFMEs to solubilize curcumin was investigated. The results are shown in Figure 9. As can be seen, the binary mixture EtOH/TriA showed a remarkable solubilizing synergy. Indeed, the maximum solubility could be increased 3-fold in a binary mixture EtOH/TriA 60/40 (w/w) compared to pure TriA and 6-fold compared to EtOH. In contrast, no strong solubilizing synergy was observed in the binary mixture DiA/TriA. Therefore, and for viscosity reasons also, the binary mixtures EtOH/TriA 60/40 and DiA/TriA 40/60 were chosen as the optimum

binary compositions and were studied further. Indeed, the maximum solubility of curcumin was investigated upon addition of water to those optimum binary compositions. The same trend, as expected, was obtained for both SFMEs: the maximum of solubility of curcumin decreased upon the addition of water. This was not surprising because curcumin is a hydrophobic compound and therefore not soluble in water. However, in the SFME with DiA, it was found that the maximum solubility of curcumin first increased (upon addition of 5 wt% of water) and then decreased as expected. All these results gave the idea that extraction should be performed to see if the water addition to a binary mixture of EtOH/TriA or DiA/TriA has an influence on the curcuminoids extraction efficiencies.

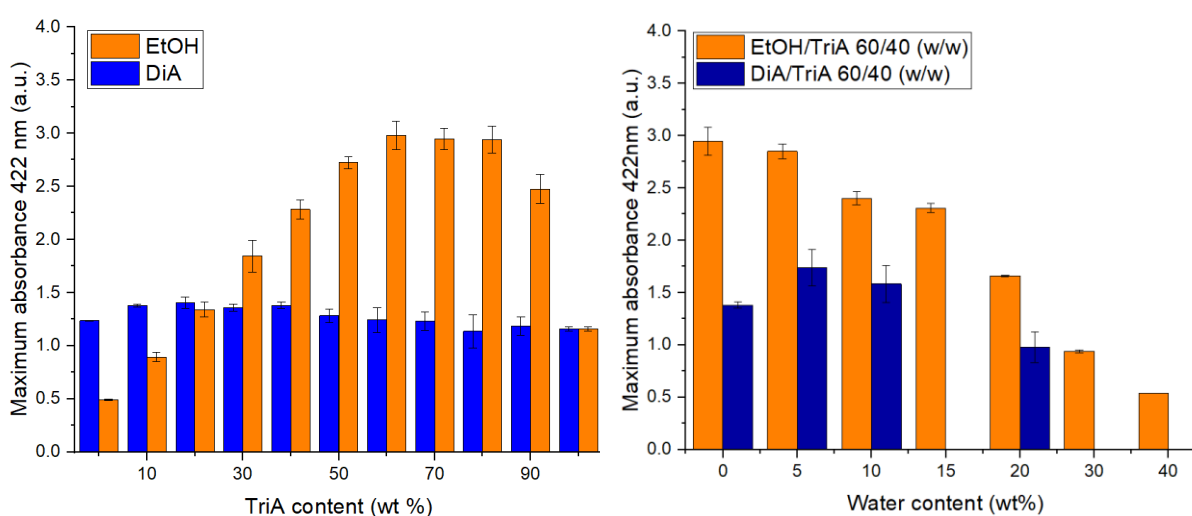


Figure 9: Determination of the maximum solubility of curcumin in the binary mixtures of EtOH/TriA (orange barres, on the left) and DiA/TriA (blue barres, on the left) and in the SFME H₂O/EtOH/TriA (orange barres, on the right, starting from a weight ratio of 40/60 EtOH/TriA) and the SFME H₂O/DiA/TriA (blue barres, on the right, starting from a weight ratio of 60/40 DiA/TriA). Upon addition of water, the weight ratio co-solvent/TriA stays constant at 40/60 and 60/40 for respectively EtOH/TriA and DiA/TriA [60].

First, different *C. longa* powders from the supermarket were tested regarding their curcumin content. Therefore, the different *C. longa* powders were extracted using a Soxhlet apparatus und the curcumin content was determined using UV/Vis. Information about the different powders are given in Table 5. The determination of the curcumin content via Soxhlet and UV/Vis gave acceptable results in comparison with the curcumin content provided by the suppliers. Only the curcumin content of the *C. longa* powder from Wagner was below the indicated curcumin content. All the determined curcumin contents were closed to the minimum curcumin content given by the suppliers. It can be explained by the fact that curcumin and the curcuminoids, in general, are temperature sensitive. Indeed, the extraction time with Soxhlet was several hours (5-8 hours) and the extracted curcuminoids were always in contact with boiling acetone (temperature above 60°C). Therefore, they could be degraded during the extraction time.

Table 5: Information concerning the different *C. longa* powders.

Label	Curcumin content (wt%) (determine by UV/Vis)	Price per Kg (€)	Origin of the rhizome	Curcumin content (wt%) (given by the suppliers)
Lebensbaum	4.2	49.8	India	3-6
Sonnentor	3.1	99.8	Tanzania	3-4
Schuhbeck	1.9	82.0	India	1.5-2.2
Wagner	1.2	29.9	India	1.5-2.2

Moreover, TLC was used to provide information about the constitution of the obtained extracts. Since the chemical composition of the rhizome is strongly depending on the growing conditions (weather, soil, environment, etc ...), it was useful to compare the different *C. longa* powders and to know if different constituents as the curcuminoids could be extracted during the Soxhlet extraction or not. The TLC plates are shown in Figure 10.

As can be seen, the four different extracts showed six different spots, the same for each brand. The lower three spots (the yellow ones on the picture with visible light after derivatisation with AA on the bottom at the left) were the curcuminoids: bisdemethoxycurcumin, demethoxycurcumin and curcumin (starting from the bottom). The three other spots were probably essential oils. This will be proved later in section 3.3.1.3. Regarding the curcumin content, the differences between the *C. longa* powders were visible on the TLC plates. Indeed, the intensity of the curcuminoid spots increased from the left to the right. This result was in accordance with the determined curcumin content by Soxhlet and UV/Vis. Considering the price of the different *C. longa* powders, the brand Wagner was chosen for conducting the first extraction experiments. The same binary and SFME compositions as in Figure 9 (on the right) were investigated to extract the curcuminoids. The results are shown in Figure 11.

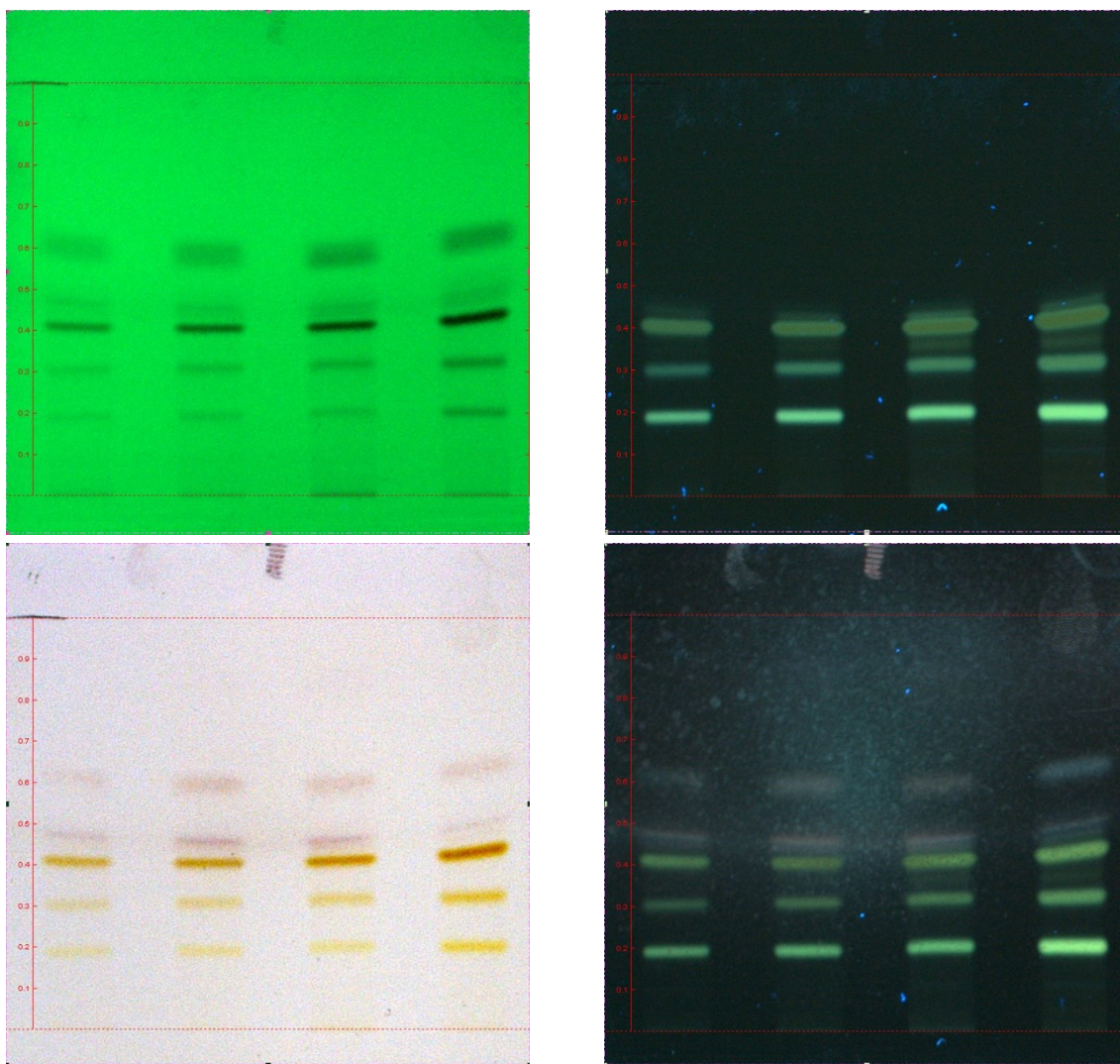


Figure 10: TLC plates of the different *C. longa* powders: Wagner, Schuhbeck, Sonnentor, and Lebensbaum (from the left to the right) before derivatisation (top) and after derivatisation with AA (bottom). The plate is irradiated with light at 254nm (top, on the left), white light (bottom, on the left), and with light at 365 nm (bottom and top, on the right) [82].

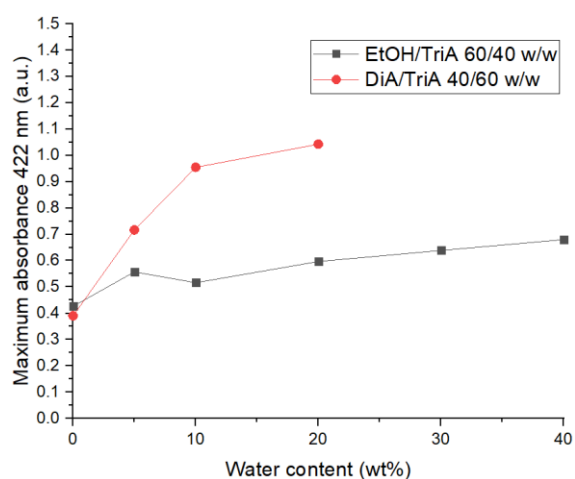


Figure 11: Maximum absorbance after extraction depending on the water content of the extraction mixtures for both SFMEs ($H_2O/DiA/TriA$ (red circle) and $H_2O/EtOH/TriA$ (dark square)). The ratio co-solvent/TriA remain constant for the different SFME compositions [82].

One hour extraction time was determined to be enough for the extraction of the curcuminoids from *C. longa*. As depicted in Figure 11, the amount of extracted curcuminoids increased with the water content of the SFME. The composition of the extraction mixtures, more specifically the SFME, had a strong influence on the extraction efficiencies of the curcuminoids. It was not possible with UV/Vis to distinguish the three different curcuminoids. Therefore, the extraction was further investigated using HPLC (to obtain the different extraction efficiencies of the three different curcuminoids) and with one batch of *C. longa* powder (10 Kg were bought by Kwizda) to avoid standard deviation due to the rhizome composition. Before that, the stability of curcumin in the binary mixture co-solvent/TriA was investigated to have an idea about the instability of curcumin at visible light in the extraction mixture. Moreover, knowing the ability of the binary mixtures to stabilize curcumin was of interest concerning the extraction time. Indeed, if curcumin was degraded in one hour, it was not necessary to investigate the extraction efficiency. Furthermore, the storage life is of high importance for product formulations. Different conditions were tested: room temperature and daylight, room temperature and darkness, 8°C and darkness, room temperature and dark bottle and room temperature and blue bottle. The two found optimum binary mixtures of EtOH/TriA and DiA/TriA for the maximum solubility of curcumin were investigated. The results are shown in Figure 12.

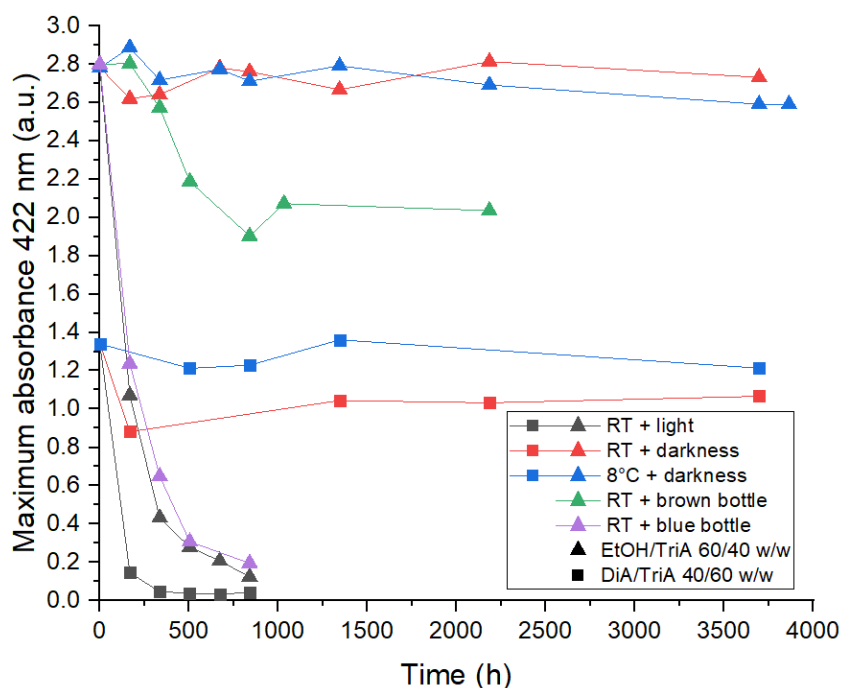


Figure 12: Stability measurements of curcumin in the binary mixtures of EtOH/TriA (triangle up) and DiA/TriA (square) under different conditions: room temperature and light (dark colour), room temperature and darkness (red colour), 8°C and darkness (blue colour), room temperature and blue bottle (purple colour), and room temperature and brown bottle (green colour).

It is well known that curcumin is photolabile [62,84] and, therefore, will be degraded very quickly under daylight conditions. As can be seen, it was evident that the two binary mixtures did not stabilise curcumin under daylight conditions, as the maximum absorbance decreased exponentially. In contrast, the samples stored in the dark and in the fridge had a much better stability. Indeed, almost no curcumin was degraded over several months. These results confirmed the low photostability of curcumin. But this was not a problem for the extraction process (samples stirred one hour at room temperature). Moreover, the difference between room temperature and 8 °C did not have an influence on the degradation of curcumin if the samples are stored in the darkness, as the maximum absorbance of these samples are rather constant (for both binary mixtures). It was not surprising, because the degradation of curcumin is an auto-degradation process activated by light [63]. It is also well known that oxygen plays a role in the degradation process of curcumin. Here, the samples were stored at normal air atmosphere and no oxygen was removed. Oxygen had only an influence in combination with light. This aspect will be analysed deeper and better in one of the following ternary phase diagrams (H₂O/NaSal/EtOAc, see section 3.3.4.2). Since curcumin was strongly degraded under daylight conditions, the packaging of a formulation containing curcumin (as a solid or in solution) is of great importance. Therefore, the influence of two different coloured glass bottles (brown and blue) on the degradation of curcumin was investigated only with the binary mixture EtOH/TriA. As can be seen in Figure 12, the same results were obtained as described above: the brown glass bottle provided a better protection of curcumin than the blue one, as the brown one covers a broader spectral area than the blue one. An oversaturation of the sample could explain the little decrease of the maximum absorbance at the beginning.

3.3.1.3 *Extraction, improvement of concentration, purity and stability*

In the following sections of this thesis, the same batch of *C. longa* powder from Kwizda (Linz, Austria) was used for all experiments. First, the best weight ratio of *C. longa* to extraction mixture was determined using the binary mixture EtOH/TriA 40/60 (in weight). This result was then used as a basis for all investigated SFME compositions with EtOH and DiA as co-solvents and extraction solvents. Then, the influence of water and the hence formed SFME on the extraction efficiencies of the curcuminoids was investigated by HPLC. The results are shown in Figure 13 and Figure 14. The detailed extraction yields are given in Figure S 6 of the Appendix. A total of 17.13 mg curcuminoids per gram *C. longa* was obtained by the Soxhlet extraction. This determined amount is undervalued because the curcuminoids are degraded by the impact of heat [42,64]. During the Soxhlet extraction process (several hours), the curcuminoids were solubilised in boiling acetone (temperature above 60°C). Indeed, as can be seen in Figure 13 and Table S 6 of the Appendix, the amount of bisdemethoxycurcumin extracted with a weight

ratio *C. longa* to binary extraction mixture (EtOH/TriA 60/40 in weight) of 1:4, 1:5, 1:6 and 1:7 was above the amount of bisdemethoxycurcumin extracted by Soxhlet. The weight ratio 1:6 was found to be the optimum for the extraction of the curcuminoids from *C. longa*. However, only a slight increase of the extraction yield of 7% is achieved in comparison with the weight ratio 1:4. Therefore, the ratio 1:4 was chosen to perform the further extractions. Indeed, the ratio 1:4 was the best ratio regarding the green and sustainable aspect: less waste of extraction mixture and a good extraction efficiency.

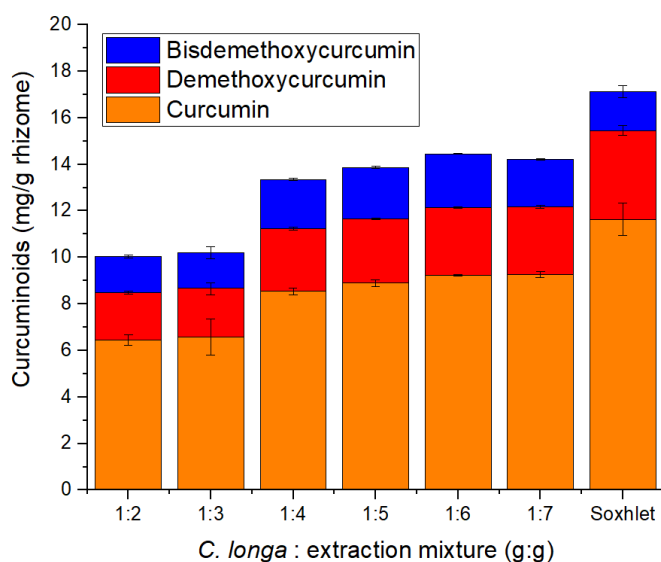


Figure 13: Curcuminoid yields in mg curcuminoids per g *C. longa* for varying *C. longa* to binary EtOH/TriA extraction mixture weight ratios. The used extraction mixture was the binary mixture EtOH/TriA 60/40 (in weight). The Soxhlet results are also given as reference [60].

The influence of water and, therefore, of the structuring of the extraction mixture (SFMEs) on the curcuminoid extraction efficiencies was then investigated with the ratio 1:4. As can be seen in Figure 14, the addition of water to the binary mixtures of co-solvent/TriA led to an increase of the extraction efficiencies of the curcuminoids for the two investigated systems. The result with Soxhlet was used as reference, as shown in Table S 6 of the Appendix. The highest extraction efficiencies for curcumin and demethoxycurcumin were given by Soxhlet. As mentioned before, the result for bisdemethoxycurcumin was undervalued and once again, it was the case here. Moreover, the lowest extraction efficiencies for bisdemethoxycurcumin are provided by the solvents alone and Soxhlet.

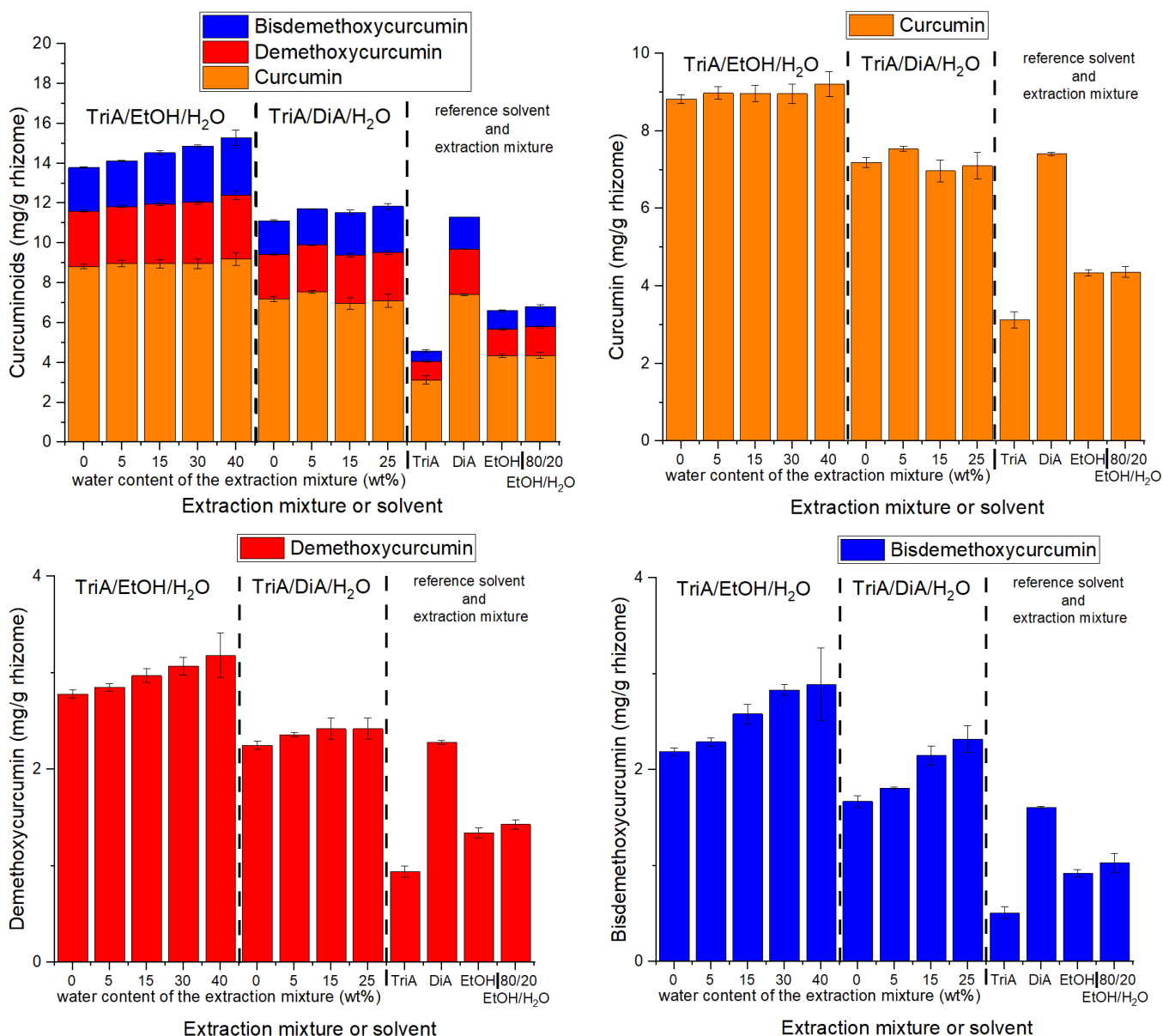


Figure 14: Overview of the curcuminoid extraction efficiencies (in mg curcuminoids per g *C. longa*) for the different extraction mixtures with a varying water content and solvents (top) and overview of the single extraction efficiencies of curcumin (second from the top), demethoxycurcumin (third from the top) and bisdemethoxycurcumin (bottom) for the different extraction mixtures with a varying water content and solvents (in mg per g *C. longa*).

First, the total of curcuminoids extracted (graph on the top at the left of Figure 14) will be compared. The system H₂O/EtOH/TriA showed the highest increase of the total curcuminoid content. The system H₂O/DiA/TriA also showed an increase of the total curcuminoid content but to a lesser extent than with the system with EtOH as co-solvent. The difference between the two systems was due to various reasons: as shown in Figure 9, the maximum solubility of curcumin was higher in the system containing EtOH as co-solvent and secondly the viscosity of the extraction mixtures and SFMEs containing DiA was much higher than those with EtOH. Surprisingly, DiA as extraction solvent alone showed a good extraction efficiency compared to the binary mixture DiA/TriA and the SFMEs containing DiA as co-

solvent. On the contrary, EtOH and TriA as extraction solvent alone showed really bad extraction efficiencies in comparison with the binary mixture EtOH/TriA and the SFMEs containing EtOH as co-solvent. Moreover, the EtOH/H₂O 80/20 (in weight) mixture was investigated as reference. Indeed, this mixture is used in the literature and also in the industry to extract the curcuminoids from *C. longa*. This mixture showed the same extraction efficiencies as the other solvent alone except DiA. Surprisingly, the best extraction mixture was the SFME containing EtOH as co-solvent and 40 wt% of water (i.e. H₂O/EtOH/TriA 40/24/36 in weight per cent), although the curcuminoids are not water soluble. It was also the most structured SFME, according to Figure 7. The addition of water helped to swell the rhizomes and to open the plant matrix, so that the extraction efficiencies of the curcuminoids increased. It was also the case for the extraction with EtOH and EtOH/H₂O 80/20 (in weight) as extraction solvent or mixture. Now the different curcuminoid extraction efficiencies will be compared: the addition of water had almost no influence on the extraction of curcumin. On the contrary, it had an influence on the extraction of demethoxycurcumin and even more on the extraction of bisdemethoxycurcumin. The increase of the total curcuminoid extraction efficiency was almost exclusively due to bisdemethoxycurcumin and demethoxycurcumin. Indeed, bisdemethoxycurcumin has been found to be the most polar and “water-soluble” curcuminoid. This was demonstrated using COSMO-RS calculations [71]. For that reason, the addition of a polar solvent like water to the binary mixtures EtOH/TriA and DiA/TriA increased the extraction efficiency of bisdemethoxycurcumin and to a small extent of demethoxycurcumin. All these results proved that the extraction was not solely dependent on the solubility of curcumin in the extraction mixture, but was driven by various other factors, such as viscosity, ability of the solvent to penetrate the plant matrix, desorption of the target molecule, the mass transfer of the latter from the plant matrix to the extraction solvent or mixture. However, the solubility efficiency of a solvent or a mixture of solvents gave a first and necessary idea prior to extraction experiments.

The two developed SFMEs (H₂O/EtOH/TriA and H₂O/DiA/TriA) were able to extract the curcuminoids from *C. longa*. Moreover, the two different SFMEs were food-approved, green, and edible. Indeed, regarding the six principles of green extraction, as explained by Chemat et al. [9], the two SFMEs could be classified as green and biocompatible extraction systems. The six principles were described in this thesis in 2.1.4 and are applicable for the two developed SFME extraction systems.

C. longa has been used as raw material, a renewable plant resource and therefore is conformed with the first principle. Concerning the second principle, all used solvents were food-approved, non-toxic, and biodegradable. Moreover, water was used partly as extraction solvent and the best extraction SFME contained 40 wt% of water. EtOH is a commonly used solvent and TriA is a triglyceride and is

already used as an additive in the food industry. They were responsible for the formation of the SFME and for the good extraction and solubilisation of the curcuminoids. To extract the curcuminoids, the maceration method at room temperature under constant stirring was performed for one hour, so that the energy consumption remains very low. Indeed, no need to heat or to stir for a long time to obtain very good curcuminoid extraction results, which agree with the third and fifth principle. The fact that the developed SFMEs were food-approved was the big advantage of this extraction procedure. Indeed, there was no need to remove the solvents (high energy consuming) as the SFMEs were food-agreed and edible. The only produced waste was the remaining plant material *C. longa* which is renewable. It can be used as a bio-compost and is bio-degradable (fourth principle). Lastly, the only “contaminants” of the extract were the essential oils. They are coextracted, but are non-toxic and edible too. If they are not desired, they can be removed upstream. This aspect will be investigated in the following as well as the ability to enrich the SFMEs by reusing the SFME extraction system with fresh *C. longa*.

The SFME with EtOH as co-solvent has been chosen to study the enrichment of the SFME extraction system for different reasons: it was the best solubilizing SFME and the SFME with the lower viscosity, so that the SFME extraction system should be more workable. To be sure that the enrichment procedure worked, a preliminary test was carried out with the cheap *C. longa* powder from Wagner, which was monitored via UV/Vis as proof of concept. The results are shown in Figure S 3 of the Appendix. The linear increase of the maximum absorbance proved that the extract solutions can be enriched in curcuminoids. Thus, to exploit the full potential of the EtOH-based SFME, cycle extractions were made along the same dilution line as previously investigated. Two different weight ratios *C. longa* to SFME extraction system were investigated: 1 to 16 and 1 to 24. A saturation of the SFMEs with higher water content should be reached with the smaller weight ratio, which should be not the case with the higher one. The reuse of the SFME extraction system strengthened the fact that the SFME extraction system should be classified as a green and biocompatible one, according to the six principles of the green extraction [9]. The results are shown in Figure 15 and Figure 16, as well as the detailed total of the curcuminoids in the binary or SFME extraction systems in Table S 7 of the Appendix and the average loss of binary or SFME extraction solution after each extraction cycle in Table S 8 of the Appendix, for both weight ratios 1:16 and 1:24

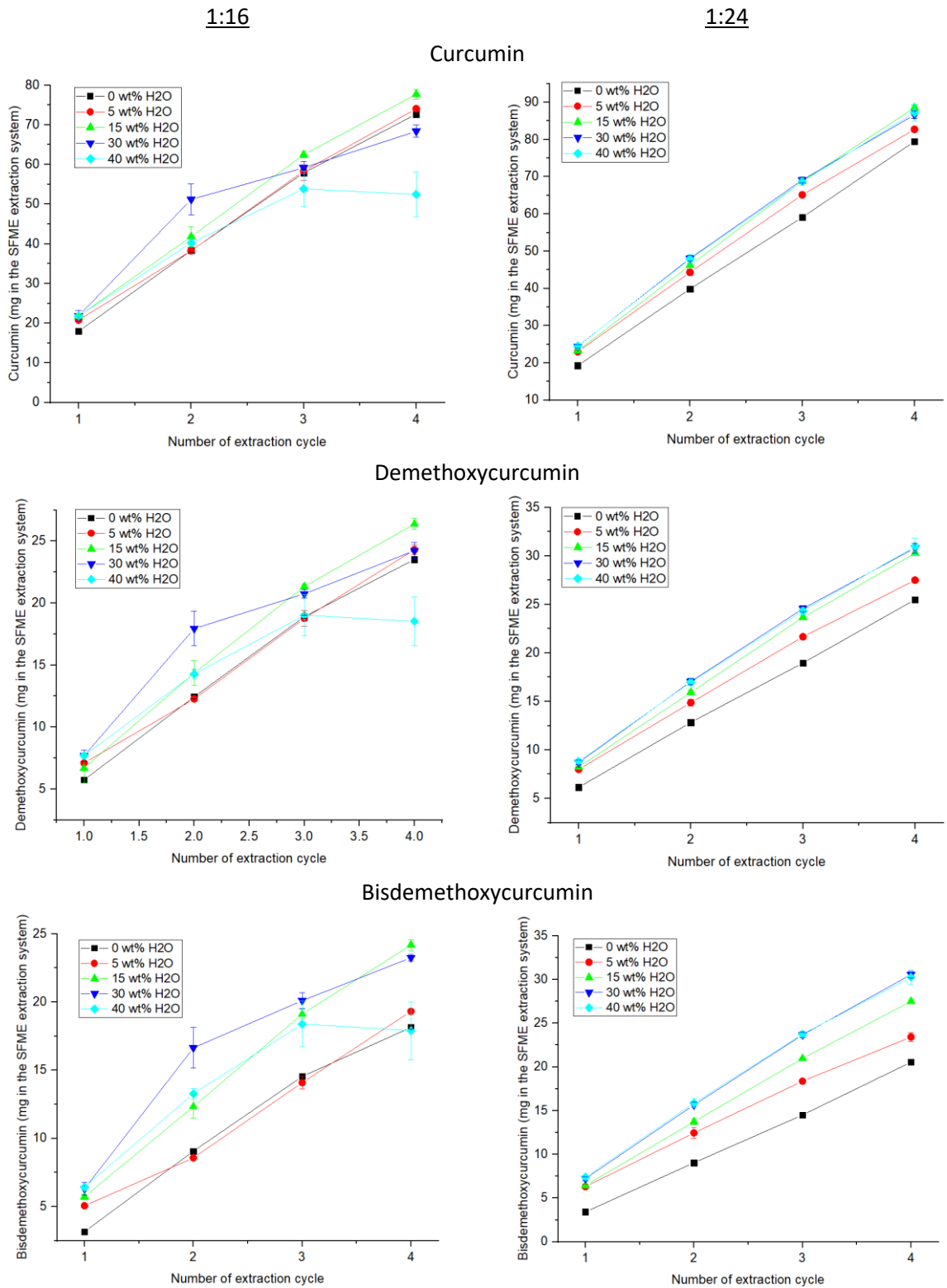


Figure 16: Overview of the extraction cycles for different binary and SFME extraction mixtures with varying water content at two different weight ratios 1:16 (on the left) and 1:24 (on the right) for the single component curcumin (top), demethoxycurcumin (middle), and bisdemethoxycurcumin (bottom) as mg single component in the binary or SFME extraction system [85].

It was possible to enrich the binary or SFME extraction system in curcuminoids for both ratios to a certain extent. If the total of curcuminoids in the binary or SFME extraction system of both ratios (Figure 15, on the top) are compared, some noticeable differences can be seen. With the ratio 1:16, the standard deviations were larger than with the ratio 1:24. Many reasons were responsible for this: the loss of extraction volume, agitation problems (due to the loss of the extraction volume), and saturation of the binary or SFME extraction system. Indeed, final saturation of the curcuminoids in the SFME containing 40 wt% of water was detected with the ratio 1:16. On the contrary, no saturation was detected with the ratio 1:24. For both ratios, the curcuminoid content was increased almost linearly, as long as no saturation occurs. The water had a strong influence on the curcuminoid extraction efficiencies, especially with the ratio 1:24. Indeed, the addition of a small amount of water (5 wt%) to the binary mixture EtOH/TriA 60/40 in weight had a big influence on the curcuminoid content in the SFME extraction system, since the gap between the binary curve (black curve, Figure 16 on the right) and the SFME extraction system curves (red, green, dark blue, and turquoise curves, Figure 16 on the right) increased with the polarity and “water-solubility” of the curcuminoids (this gap increased from curcumin to bisdemethoxycurcumin). The same influence was noticeable with the water content of the SFME extraction system: the higher the water content of the SFME was, the more the gap between the different SFME curves from curcumin to bisdemethoxycurcumin increased. For the ratio 1:16, the influence of water was noticeable only to a small extent, due to the loss of the SFME extraction system. As can be seen, the curcuminoid content increase was not rigorously linear as for the weight ratio 1:24.

As written before, a saturation of the three curcuminoids was reached for the SFME extraction system containing 40 wt% of water after three cycles with the weight ratio 1:16. The SFME extraction system containing 30 wt% of water with the same ratio should be closed to saturation as the slopes of the curves decreased after two extraction cycles for the three curcuminoids. It can be expected that it should be saturated after 5 extraction cycles. After 4 extraction cycles, the SFME extraction system containing 15 wt% of water contained the highest amount of extracted curcuminoids (128.29 mg curcuminoids in the SFME extraction system, see Table S 7 of the Appendix). Bisdemethoxycurcumin and demethoxycurcumin were more abundant in the SFME extraction systems containing high amounts of water as they are more “polar” than curcumin. On the contrary, the amount of curcumin remained almost the same for the SFME extraction systems containing 15 wt% of water or less, because curcumin prefers hydrophobic solvents. No saturation, on the other hand, occurred with the ratio 1:24, because higher amounts of SFME extraction solvent were used and therefore, the loss of SFME extraction system after each cycle was not enough to prematurely reach a saturation. The SFME

extraction systems containing 30 and 40 wt% of water exhibited almost the same curcuminoid content. This indicated that beyond 30 wt%, water had no more influence on the curcuminoid extraction.

If only the curcuminoid content in the different SFME extraction systems is compared, a higher content could be reached with the ratio 1:24. This result was not surprising, because previously it was demonstrated that a higher weight ratio *C. longa* to SFME extraction system slightly increased the curcuminoid extraction efficiencies (see Figure 13). If the curcuminoid concentration (see Figure 15, on the bottom) is now compared, it can be seen that a higher concentration could be reached with the smaller weight ratio 1:16, due to the loss of SFME extraction system after each extraction cycle. This loss increased with the water content of the SFME extraction system for both ratios and no real differences were noted between the ratios. So, it is important to consider that the curcuminoid concentration and the curcuminoid content in the SFME extraction system should not be confused. The most concentrated extracts were reached with the ratio 1:16 and the higher curcuminoid content was achieved with the ratio 1:24. If the two different weight ratios are compared with the six principles of the green extraction and the principles of the green chemistry, it can be seen that the ratio 1:16 should be the best appropriate ratio. Indeed, less SFME extraction system is used. But with the ratio 1:24, a higher content was reached (almost 20-25% more curcuminoid in the SFME extraction system) and the practical effort was the same for both ratios to obtain the phytochemicals.

One of the goals of this study was to have curcumin solubilised in an aqueous solution containing as much water as possible. As curcumin is a hydrophobic compound, it is completely insoluble in water. The SFME extraction system containing 40 wt% of water and EtOH as co-solvent showed a very good ability to extract the curcuminoids. Adding water to dilute the SFME extraction system will result in phase separation because the SFME extraction system H₂O/EtOH/TriA 40/24/36 in weight is very close to the miscibility gap of the ternary mixture H₂O/EtOH/TriA (see Figure 6). A ternary mixture H₂O/EtOH/TriA 50/32.5/17.5 (in weight), on the contrary, was dilutable with water to the infinite. Therefore, to extract the curcuminoids with this ternary mixture should be advantageable. Indeed, the extract solution was dilutable with water after the extraction process and if no precipitation occurred, the curcuminoids will be solubilised in an aqueous solution containing a very high content of water (more than 99 wt%). As mentioned in the introduction and in section 3.3.1.2, the essential oils are extracted along with the curcuminoids. If they are not removed beforehand, a precipitation will occur during the infinite dilution of the extract solution because the essential oils are not water soluble, like curcumin. Moreover, the essential oils are also able to solubilize curcumin. Therefore, different techniques to remove the essential oils and keep a high amount of curcuminoids in *C. longa* were investigated. After each technique to remove the oils, the ability of the extract solution to be infinitely

dilutable with water has also been studied. Three different techniques were used: steam distillation, vacuum distillation, and freeze-drying (lyophilisation). Two different SFME compositions were investigated: H₂O/EtOH/TriA 40/24/36 and H₂O/EtOH/TriA 50/32.5/17.5 in weight. The results are shown in Figure 17 and Figure 18. The detailed curcuminoid contents are shown in Table S 9 of the Appendix.

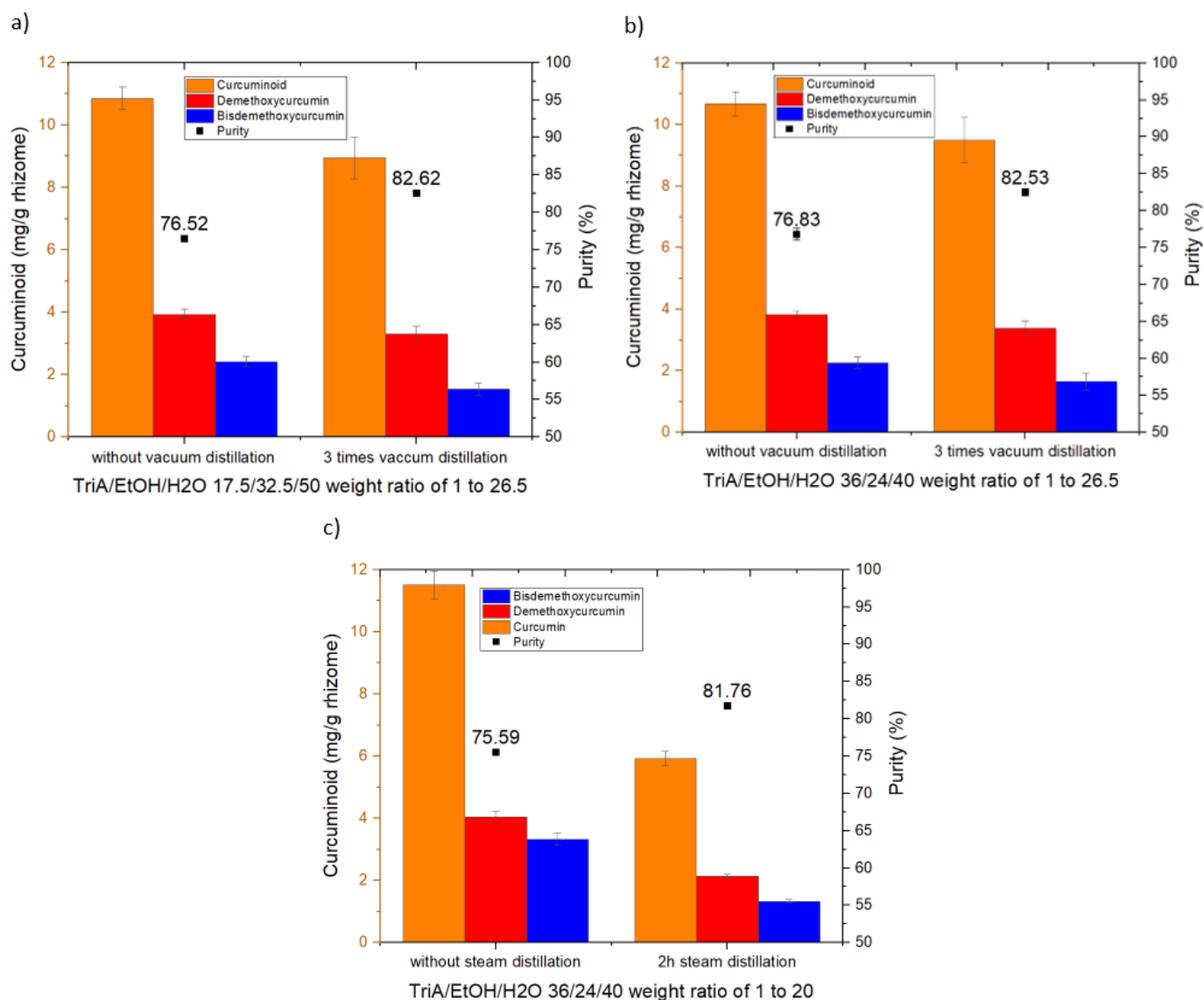


Figure 17: Comparison of the purification techniques: a) and b) vacuum distillation and c) steam distillation. Two different SFME compositions were used as extraction system: a) TriA/EtOH/H₂O 17.5/32.5/50 with a weight ratio *C. longa* to SFME extraction system of 1 to 26.5 and b) and c) TriA/EtOH/H₂O 36/24/40 with a weight ratio of *C. longa* to SFME extraction system of 1 to 26.5 and 1 to 20 for respectively the vacuum distillation and steam distillation purification processes. The reference with the same weight ratio and without any purification process was also done for comparison. The relative purity of the extract solutions has been also determined (Y-axis on the right) [85].

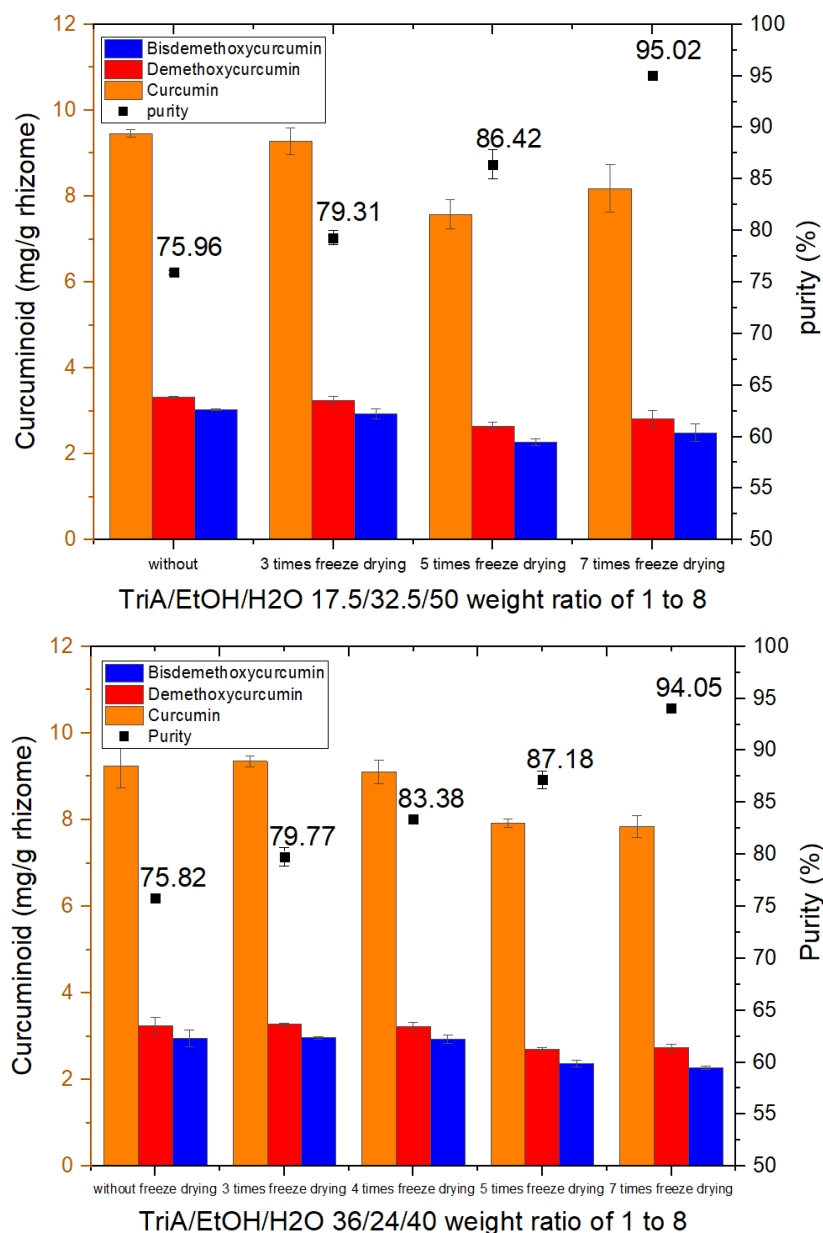


Figure 18: Extracted curcuminoids per g. *C. longa* with the two SFME extraction systems TriA/EtOH/H₂O 17.5/32.5/50 in weight (top) and TriA/EtOH/H₂O 36/24/40 in weight (bottom) with a weight ratio *C. longa* to SFME extraction system of 1 to 8 after several cycles of lyophilisation. The relative purity after each cycle of lyophilisation has been also determined (Y-axis on the right).

Steam distillation is the most popular and common method to extract the essential oil for the perfume industry. To avoid the permanent contact between the curcuminoids and the high temperature, a vacuum steam distillation was investigated also. Indeed, the curcuminoids are temperature sensitive and could be destroyed during the steam distillation. In Figure 17 the comparison between the two different purification processes is shown. As can be seen, both processes increased the relative purity of the extracts (almost 82% after the purification process, almost 76% without). The vacuum distillation gave a similar result as the steam distillation, but was not as effective. Only 2 h of steam distillation was required to achieve the same purity. The major difference between the two processes was the

curcuminoid content after purification and extraction. Both processes led to a decrease of the curcuminoid content. Only half of the curcuminoids have been extracted after the steam distillation in comparison with the non-processed *C. longa*. In contrast, only around 10% less curcuminoids have been extracted after the vacuum distillation in comparison with the non-processed *C. longa*. The vacuum distillation was a better alternative compared to the steam distillation, because no heat is required and therefore, the curcuminoids were not degraded thermally during the process. Moreover, the SFME extract containing 50 wt% of water was infinitely dilutable with water without precipitation upon the dilution. But a lot of SFME extraction mixture was used to extract the curcuminoids. Indeed, the used weight ratios *C. longa* to SFME extraction system were 1 to 20 and 1 to 26.5 for both purification processes. For this reason, lyophilisation was investigated as an alternative. This purification method did not require any heating and should permit the extraction of the essential oil without degrading the curcuminoids, like the vacuum distillation. The results are shown in Figure 18. As can be seen, a relative purity of around 94-95% could be reached through multiple cycles of lyophilisation. Moreover, the curcuminoid content decreased only slightly (comparable decrease as for the vacuum distillation). This decrease was due to the handling of the samples during the purification process. Indeed, small amounts of *C. longa* can be lost during one cycle of lyophilisation or it is possible that the *C. longa* powder was not completely water-free at the end of the lyophilisation process. The purity and curcuminoid extraction efficiencies were independent of the SFME extraction mixture compositions. For this purification process, a weight ratio of 1 to 8 (*C. longa* to SFME extraction system) was used. This weight ratio was in accordance with the six principles of green extraction [9], because less SFME extraction mixture was required in comparison to the steam and vacuum distillations. The only drawback was the time consumption. Indeed, one cycle of lyophilisation required between 2 to 3 days to be achieved in the lab. For this method, the applicational effort is minimal in comparison to the steam and vacuum distillation. For comparison, supercritical CO₂ could be used to achieve a same purity (or even more), but the applicational effort is much higher in this case.

The infinite water dilution of the extract solutions after the vacuum distillation and the lyophilisation was tested with the SFME extraction mixture H₂O/EtOH/TriA 50/32.5/17.5 in weight. In both cases, no precipitation occurred during the dilution. After some hours, a precipitation occurred, but it was resolvable, when the sample is gently shook. Therefore, the colour stability of the extract and the diluted extract solutions were investigated over the time after different cycles of lyophilisation (4, 5, and 6). Pictures have been taken after 3, 14, and 30 days. The samples were stored at day light and in darkness. The pictures are shown in Figure 19.

Sample		Type of lighting		Day 0	Day 3	Day 14	Day 30
4 times freeze drying	dilution	darkness	day light				
	extract	day light					
5 times freeze drying	dilution	darkness	day light				
	extract	day light					
6 times freeze drying	dilution	darkness	day light				
	extract	day light					

Figure 19: Pictures of the different extracts (at day light) and extract dilutions (at day light and in the darkness, 0.1 mL extract in 10 mL water) after extraction and different cycles of lyophilisation (4, 5, or 6 times of freeze drying) over time. The SFME H₂O/EtOH/TriA 50/32.5/17.5 in weight was used as extraction system using a weight ratio of 1 to 8 (C. longa to SFME extraction system). [85]

As said before, if the essential oils are not removed before the extraction, a phase separation will occur during the dilution of the extract after extraction with water. Here, all the extract solutions were clear and homogeneous after dilution. If the diluted extract was stored in the darkness, almost no change in the colouration was observed with the naked eye. On the contrary, if the diluted extract was stored at day light, a decolouration occurred over time. Indeed, the strong yellow colour had nearly disappeared after 30 days. On the other hand, the colour of the extract (not diluted) was stable over time, even though they were stored at day light. These results conformed with Figure 12. Indeed, here again, the light was the most degrading factor for the curcuminoids.

After three days, a precipitation occurred in the diluted samples, where the turmeric powder *C. longa* was freeze-dried four- and five-times (see Figure S 4 of the Appendix). This precipitate could be resolved by shaking. After 30 days, the corresponding extract solutions (after four- and five-times of freeze-drying) displayed a precipitation (see Figure S 5 of the Appendix). The samples, where the turmeric powder *C. longa* was six times freeze-dried, did not display any precipitation in the extract solution and almost no precipitation in the diluted extract (see Figure S 4 and Figure S 5 of the Appendix).

3.3.1.4 Overview

First, two edible, green, bio-based, and food-approved SFMEs consisting of H₂O/EtOH/TriA and H₂O/DiA/TriA were examined and developed to extract the major three curcuminoids from *C. longa*. The existence of SFMEs was proved by using DLS and conductivity measurements. Solubilizing measurements have demonstrated that there was a solubilizing synergy of curcumin in the binary mixture EtOH/TriA (up to a threefold increase compared to pure TriA). On the contrary, the binary mixture DiA/TriA did not show any solubilizing synergy. Upon addition of water, the solubility of curcumin in the two different SFME extraction systems decreased since curcumin is a hydrophobic compound. Surprisingly, the addition of water to the binary mixture EtOH/TriA resulted in an increase of the curcuminoid extraction efficiencies. More precisely, the bisdemethoxycurcumin extraction efficiency increased a lot compared to curcumin (from 2.19 mg bisdemethoxycurcumin per g *C. longa* in the binary mixture EtOH/TriA 40/60 in weight to 2.89 mg bisdemethoxycurcumin per g *C. longa* in the SFME extraction system consisting of 40 wt% of water (H₂O/EtOH/TriA 40/24/36 in weight)). It was also demonstrated using COSMO-RS calculations, that the polarity of the curcuminoids increased from curcumin to bisdemethoxycurcumin and therefore, the addition of water, a polar solvent, to the binary mixture of EtOH/TriA led to an improved curcuminoid extraction efficiency. The SFME extraction system containing EtOH as co-solvent was superior to the SFME extraction system containing DiA in solubilizing and extracting the curcuminoids from *C. longa*. Moreover, the mixture of EtOH/H₂O was

also used as reference extraction system of the industry and it was found, that the addition of a third (more hydrophobic) component, here TriA, led to an increase of the curcuminoid extraction efficiency. The big advantage of the SFME as extraction system was their edibility and their green and bio-based aspects.

To fully use the high solubilizing power of the SFME extraction system containing EtOH as co-solvent, it was re-used to perform several extraction cycles and, therefore, to concentrate the SFME extraction systems in curcuminoids. Moreover, the relative purity of the extracts was examined and improved through the use of three purification processes: steam and vacuum distillation and lyophilisation. Among them, it was found that the most adequate purification method was the lyophilisation of the ground rhizomes prior to their extraction because of the simplicity of the purification method, the high amount of extracted curcuminoid, and the high obtained purity. Removing the essential oils prior to the extraction of the curcuminoids enabled the extract solution to be infinitely dilutable with water (if the SFME extraction system did not cross the miscibility gap during the dilution). It led to stable aqueous solutions (diluted extract solution) of curcumin in darkness and to stable extract solutions at day light, if several cycles of lyophilisation (at least six) were achieved prior to extraction.

3.3.2 (Meglumine/PCA/H₂O)/EtOH/TriA

3.3.2.1 *Solubility and stability of curcumin in water with different additives*

Different additives (meglumine, ethanolamine, diethanolamine, triethanolamine, D-glucamine, D-(+)-glucosamine, PCA, NaSal and NaOH) were tested to further develop the high potential of the developed SFME extraction system consisting of H₂O/EtOH/TriA. First, a small kinetic experiment using meglumine as additive was done to determine the best agitation time (see Figure S 6 of the Appendix). Then, the interaction between meglumine and curcumin was investigated with NMR to understand the mechanism of solubilisation of curcumin in water using meglumine and, after that, the influence of the different additives on the curcumin solubility and stability in water was investigated. The different additives are shown in Figure 20.

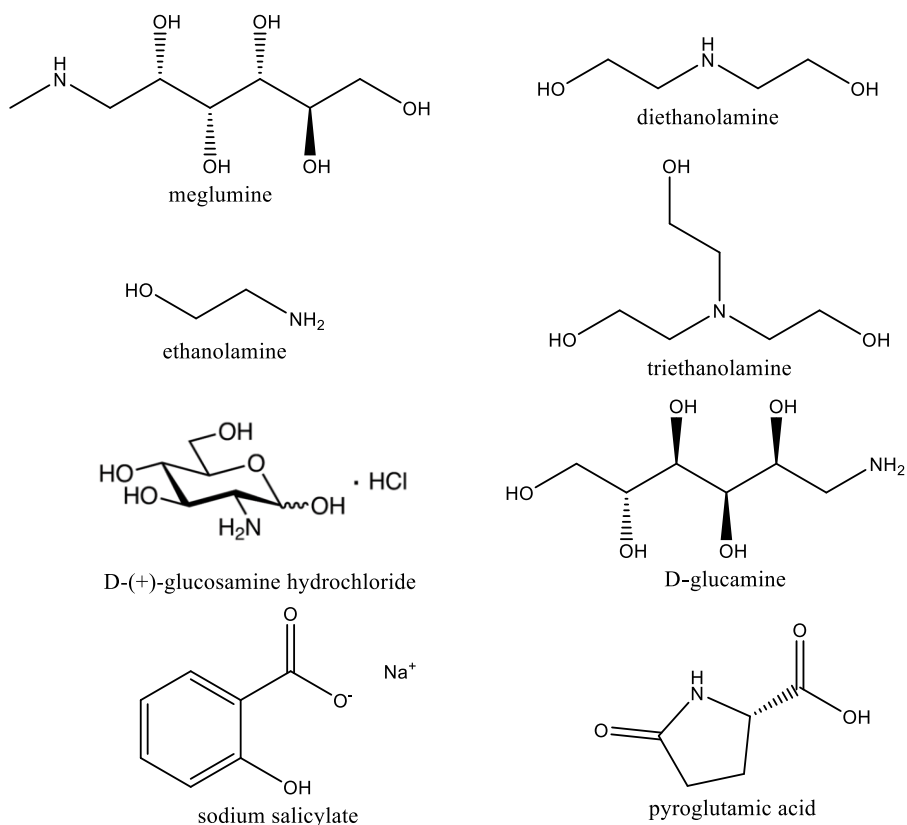


Figure 20: Structure of the different used additives

As can be seen in the Figure S 6 of the Appendix, after 10 minutes, the aqueous solution was already saturated with curcumin. This result indicated that meglumine and curcumin probably formed a salt in water and therefore, the solubilisation of curcumin happened instantly in the aqueous solution. This finding will be further investigated with NMR. The different $^1\text{H-NMR}$ spectra are shown in Figure 21.

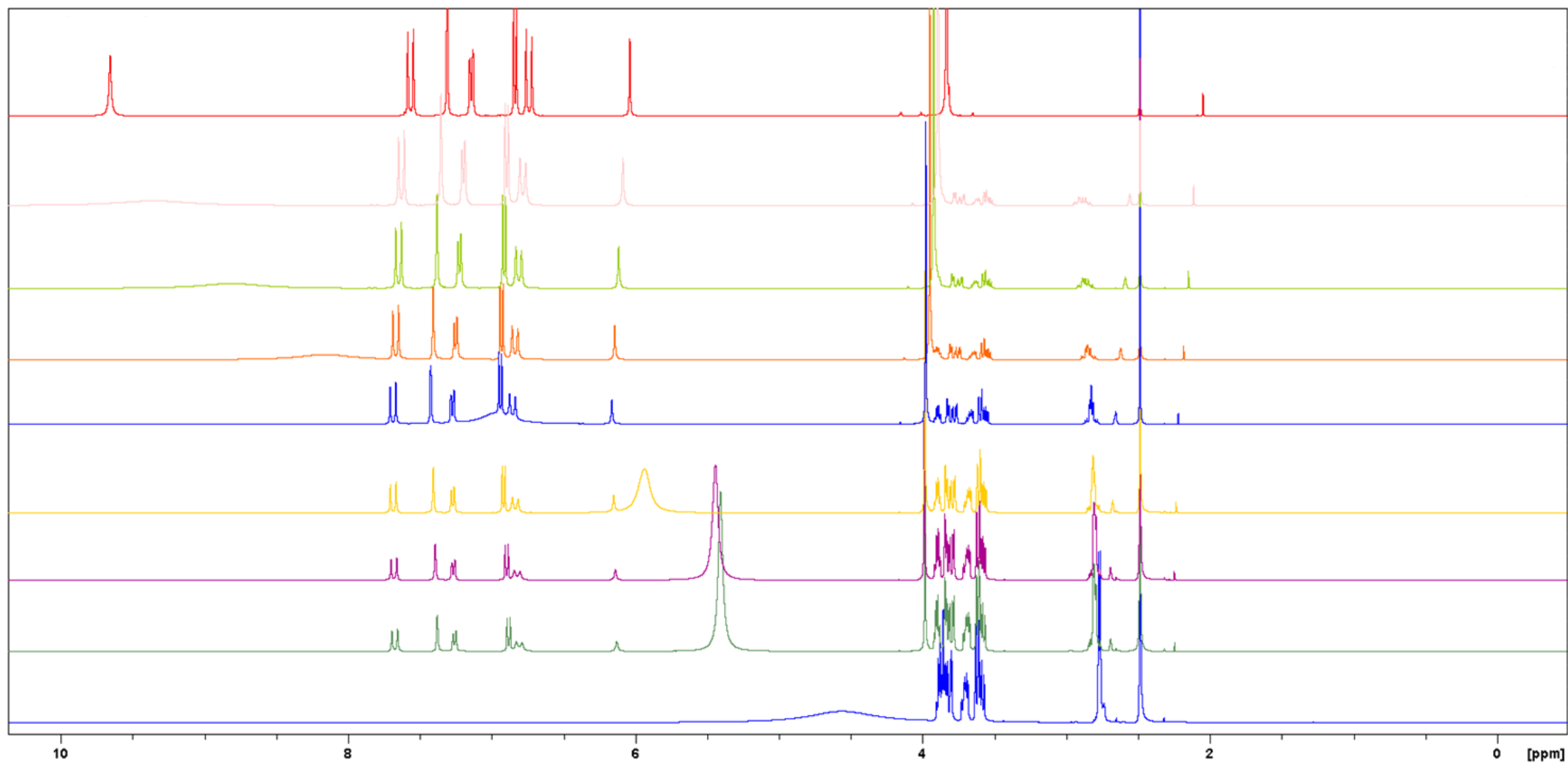


Figure 21: $^1\text{H-NMR}$ -spectra of the different mole ratios meglumine/curcumin: 0/1 (red), 1/4 (light pink), 1/3 (light green), 1/2 (orange), 1/1 (blue in the middle), 2/1 (yellow), 3/1 (violet), 4/1 (dark green), and 1/0 (blue at the bottom).

The detailed $^1\text{H-NMR}$ spectra of curcumin and meglumine alone are shown in Figure S 7 and Figure S 8 of the Appendix. The hydroxy groups of meglumine showed a broad peak at 4.4 ppm. It was not a sharp and defined peak because some residual water was present in DMSO-d_6 and therefore, they formed hydrogen bonds with water. With the addition of curcumin, this peak became sharpened and defined and was especially de-shielded (more than 1 ppm only with the addition of 1 mol curcumin to 4 mol meglumine). The more curcumin was present in the mixture curcumin/meglumine in mole, the more the hydroxy groups' peak of meglumine was shielded. The hydroxy groups' peak became broad again with a higher amount of curcumin (mole ratio meglumine/curcumin of 1/1 to 1/4), but was still de-shielded. Rotating frame Overhauser Enhancement Spectroscopy (ROESY) measurements (2D-NMR) have been done with the mole ratio meglumine/curcumin 2/1 to see if cross-peaks appeared or not. The 2D-spectra are shown in Figure S 9 and Figure S 10 of the Appendix. Cross-peaks appeared between the aromatic protons of curcumin and the protons of the sugar-chain and the methyl group of meglumine and between the methyl groups of curcumin and meglumine. These results supported the idea that meglumine and curcumin formed a salt in water. Aromatic rings (present in curcumin) could also act as hydrogen bond acceptors and therefore, may have a significant interaction with hydrogen bond donors like the N-H group (present in meglumine) [86] or to a small extent like the sugar-chain of meglumine. In fact, it is already known in the literature that carbohydrates have a specific interaction with aromatic compounds, including polyphenols [87,88]. Moreover, the fact that a salt is formed and that the N-H group and the OH groups of meglumine have a significant interaction with the aromatic rings of curcumin could explain the de-shielding of the hydroxy groups' peak of meglumine. The possible interaction between curcumin and meglumine is shown in Figure 22.

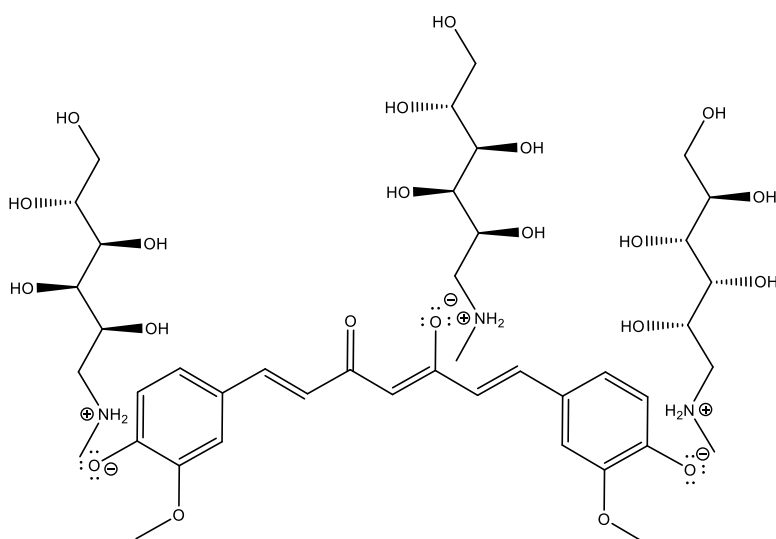


Figure 22: Possible interaction between curcumin and meglumine

concentrations of triethanolamine in water (10 wt%) and the lowest mass concentration of D-glucamine (1 wt%) and therefore was worse than the best co-solvents meglumine and ethanolamine. The high pH of water with NaOH allowed the solubilisation of curcumin in water, although curcumin is extremely hydrophobic. The pH of different water solutions with 15 wt% of co-solvent and NaOH at pH 11.5 was recorded before and after saturation with curcumin. The results are shown in Table 6. The pH was not the major reason for the solubilisation of curcumin in water with the different additives (if it were the case, the solubility should be pH-dependent, which was not the case, see Table 6). The solubilisation of curcumin was dependent on the additive, but no clear trend can be seen.

Table 6: pH before and after saturation with curcumin and maximum absorbance of different water solutions containing 15 wt% of additives (additive/water, 15/85 in weight) saturated with curcumin [89].

Additive (15 wt% in water)	pH before saturation	pH after saturation	Maximum absorbance 422 nm in acetone (undiluted)
Ethanolamine	12.15	11.07	5602
Diethanolamine	11.59	10.68	1118
Triethanolamine	10.90	10.30	126
Meglumine	11.60	10.84	1822
D-Glucamine	11.18	10.64	685
NaOH pH 11.5	11.47	10.40	67

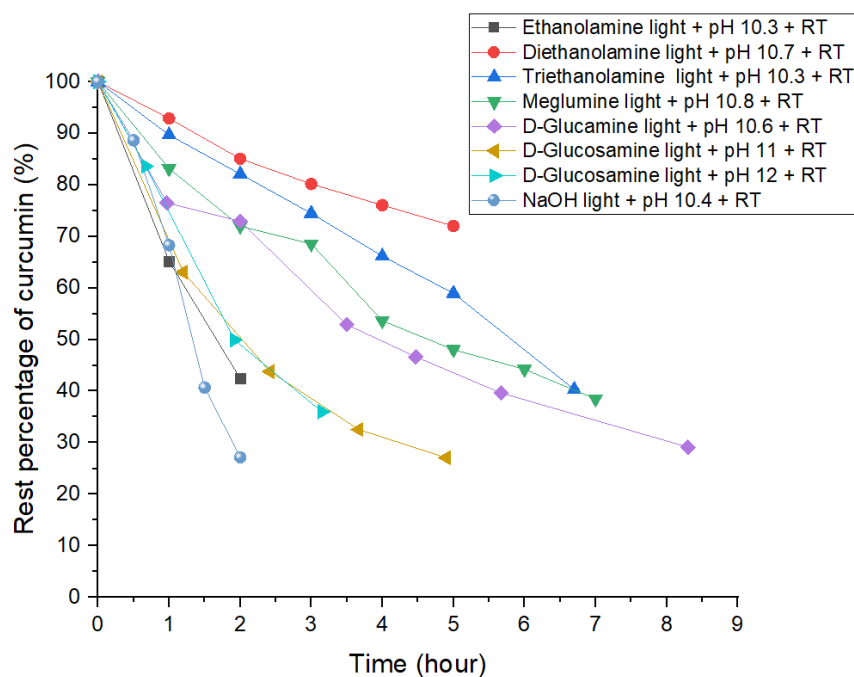


Figure 24: Stability of curcumin (saturated solutions) in water (85 wt%) with 15 wt% of additives under constant lighting: ethanolamine (dark square), diethanolamine (red circle), triethanolamine (blue up-facing triangle), meglumine (green down-facing triangle), D-glucamine (violet diamond), D-(+)-glucosamine at pH 11 (yellow left-facing triangle) and 12 (cyan right-facing triangle) and NaOH (sky blue sphere). For NaOH, the pH before saturation was set to 11.5. [89]

The stability against light was investigated for all additives at the highest concentration in water (15 wt%). For comparison, the stability with NaOH at pH 11.5 was also investigated. As can be seen in Figure 24, some additives, like diethanolamine, triethanolamine, and meglumine, stabilised curcumin in water more against light than NaOH, D-glucosamine, or ethanolamine. The best stabiliser was diethanolamine, followed by triethanolamine, meglumine, and D-glucamine respectively. NaOH, ethanolamine, and D-glucosamine were very bad stabilisers. Indeed, after 90 and 120 min lighting, almost 60% of curcumin was lost with NaOH and ethanolamine, respectively. After the same time of lighting, only 10-20% curcumin was lost with diethanolamine, triethanolamine, and meglumine. No correlation between solubilisation and stabilisation was found. But meglumine or diethanolamine seemed to be the best solubilizers and stabilators. Meglumine was chosen as additive to further investigate the solubilisation and stabilisation of curcumin in the green, biodegradable, and edible SFME as it solubilised more curcumin in water than diethanolamine. First, the stability against light was investigated under different condition: in darkness at room temperature, in darkness at 8 °C and under constant lighting. For comparison in the darkness, the same solution containing NaOH as additive was also investigated. The results are shown in Figure 25.

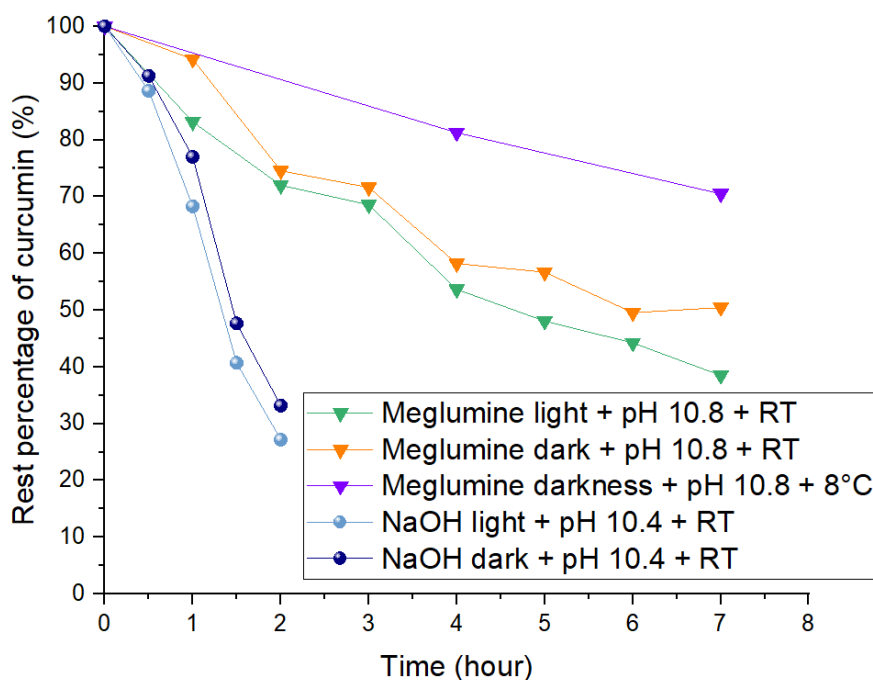


Figure 25: Stability of saturated curcumin solutions in water (85 wt%) with 15 wt% of meglumine (down-facing triangle) under constant lighting (green curve), in the darkness (orange curve) and in darkness at 8 °C (violet curve) and in water at a pH of 11.5 adjusted with NaOH (sphere) under constant lighting (sky blue) and in the darkness (dark blue). [89]

As can be seen in Figure 25, the pH was the major factor for the degradation of the sample and not the type of illumination. Indeed, the samples stored in the dark are slightly more stable than the ones under constant lighting. The stability in the fridge with meglumine as additive was the best one. After 7 hours, only 30% curcumin was lost. After the same time, half of curcumin was lost in the darkness and 62% under lighting. The temperature played a role in the degradation speed due to the high pH in water. The stability of curcumin in water could be extended to several hours in water but remained extremely low in comparison with the green, bio-based, and edible SFME. Therefore, the addition of meglumine to the best SFME extraction system consisting of H₂O/EtOH/TriA should enhance the solubility and maybe the extraction efficiencies of the curcuminoids in this system. The stability of curcumin in the SFME with meglumine should also be investigated to see if meglumine stabilizes or destabilizes curcumin.

3.3.2.2 Solubility, stability and extraction of curcumin with meglumine and PCA as additive in water in the SFME extraction system

As the pH played a major role in the degradation of curcumin, a pH regulator was added to regulate the pH of the SFME with meglumine. PCA was used as pH-regulator because PCA is allowed in the pharmaceutical industry and showed hydrotropic properties for curcumin. The addition of PCA to regulate the pH could also be beneficial for the solubility and the extraction efficiencies of the curcuminoids. First, the influence of meglumine at different weight per cent and PCA on the phase diagram was investigated. The given concentrations of meglumine are the concentrations in pure water before its use for the formation of the SFME with EtOH and TriA. The addition of PCA to regulate the pH was done also in water with the different weight concentrations of meglumine and not in the SFME. The results of the influence of meglumine and PCA on the phase diagram H₂O/EtOH/TriA are shown in Figure 26. Four different pH values were investigated: pH 7, pH 9, pH 11.3 and pH 11.5 (the pH values over 11 are the pH without PCA for the two meglumine concentrations, 5 wt% and 15 wt% respectively, in pure water). At pH7, meglumine is completely positively charged (the salt formation with curcumin should not be possible) and pH 9 was chosen because of the pK_a of meglumine (9.64, see Figure S 11 of the Appendix). The phase diagram without PCA was also investigated to see the influence of meglumine alone on the phase diagram. The water used to obtain the different phase diagrams was freshly prepared with meglumine and/or without PCA and the phase diagram was recorded on the same day. R represents the molar ratio between PCA and meglumine (the mole number of PCA divided by the mole number of meglumine). R_{pH7} and R_{pH9} represent the molar ratio at pH 7 and 9 respectively. In water at pH 7 and 9, R_{pH7} was equal to 0.88 ± 0.01, 0.91 ± 0.01 and 0.95 ± 0.01 for respectively 5 wt%, 15 wt% and 20 wt% of meglumine in water neutralised with PCA and R_{pH9} was equal to 0.82 ± 0.02 and 0.85 ± 0.02 for respectively 5 wt% and 15 wt% of meglumine in water neutralised with PCA.

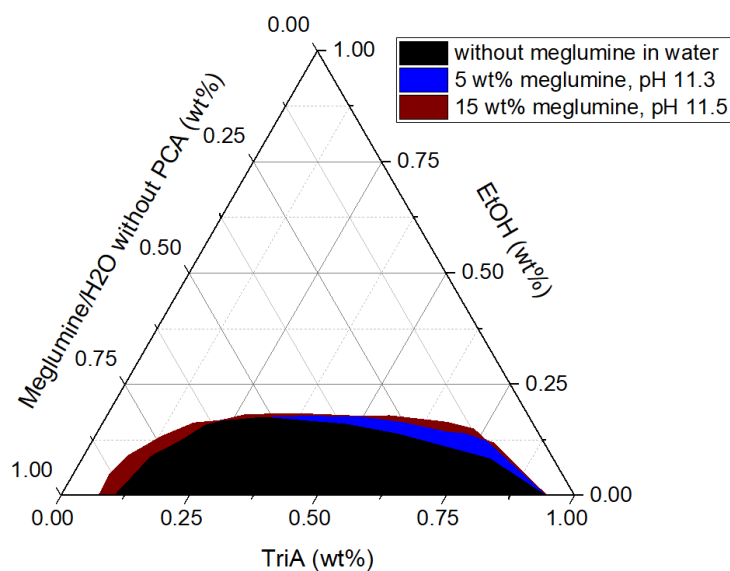
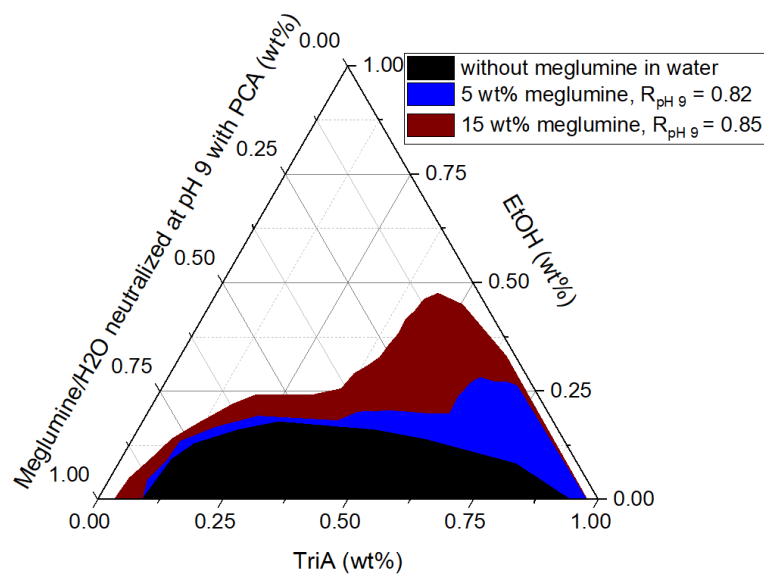
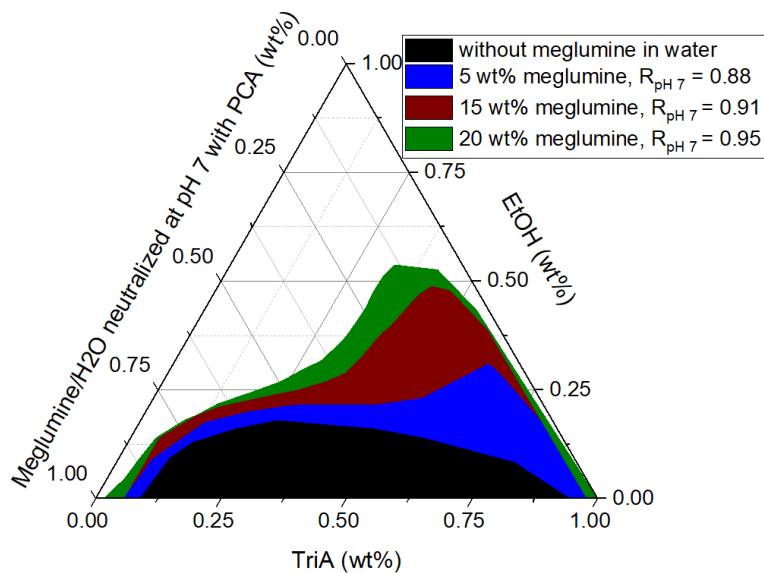


Figure 26: Ternary phase diagrams of the systems: H_2O with meglumine (5, 10, and 15 wt% in pure water) neutralised with PCA at pH 7/EtOH/TriA (top), H_2O with meglumine (5 and 15 wt% in pure water) neutralised with PCA at pH 9/EtOH/TriA (middle), and H_2O with meglumine (5 and 15 wt% in pure water) without PCA at pH 11.3 and 11.5 respectively/EtOH/TriA (bottom). The R values represent the molar ratio between PCA and meglumine at the different pH values (7 and 9) for the different weight concentrations of meglumine in pure water [71].

As can be seen in Figure 26, meglumine had almost no influence on the miscibility gap in the phase diagram compared to the phase diagram without additives. On the contrary, a salting-out effect of PCA was observed in the oil-rich phase of the phase diagram when the water pH was adjusted to pH 7 and 9 with PCA. To explain the salting-out effect, the charge of PCA and meglumine must be investigated at different pH values. As meglumine has a pK_a of 9.64, it is almost completely positively charged at pH 7 and a part of it is positively charged at pH 9. At pH 11.3 or 11.5 meglumine is not charged. PCA contains an amino group and a carboxylic function. Therefore, PCA can be charged at two different positions. At pH 7 and 9, the carboxylic function is negatively charged. The charge of the amino group, more precisely of the nitrogen, should be determined according to the pH values. Therefore, 2D-NMR measurements have been done for samples containing PCA in water at two different pH values: 1.3 and 10.2. The results are shown in Figure 27.

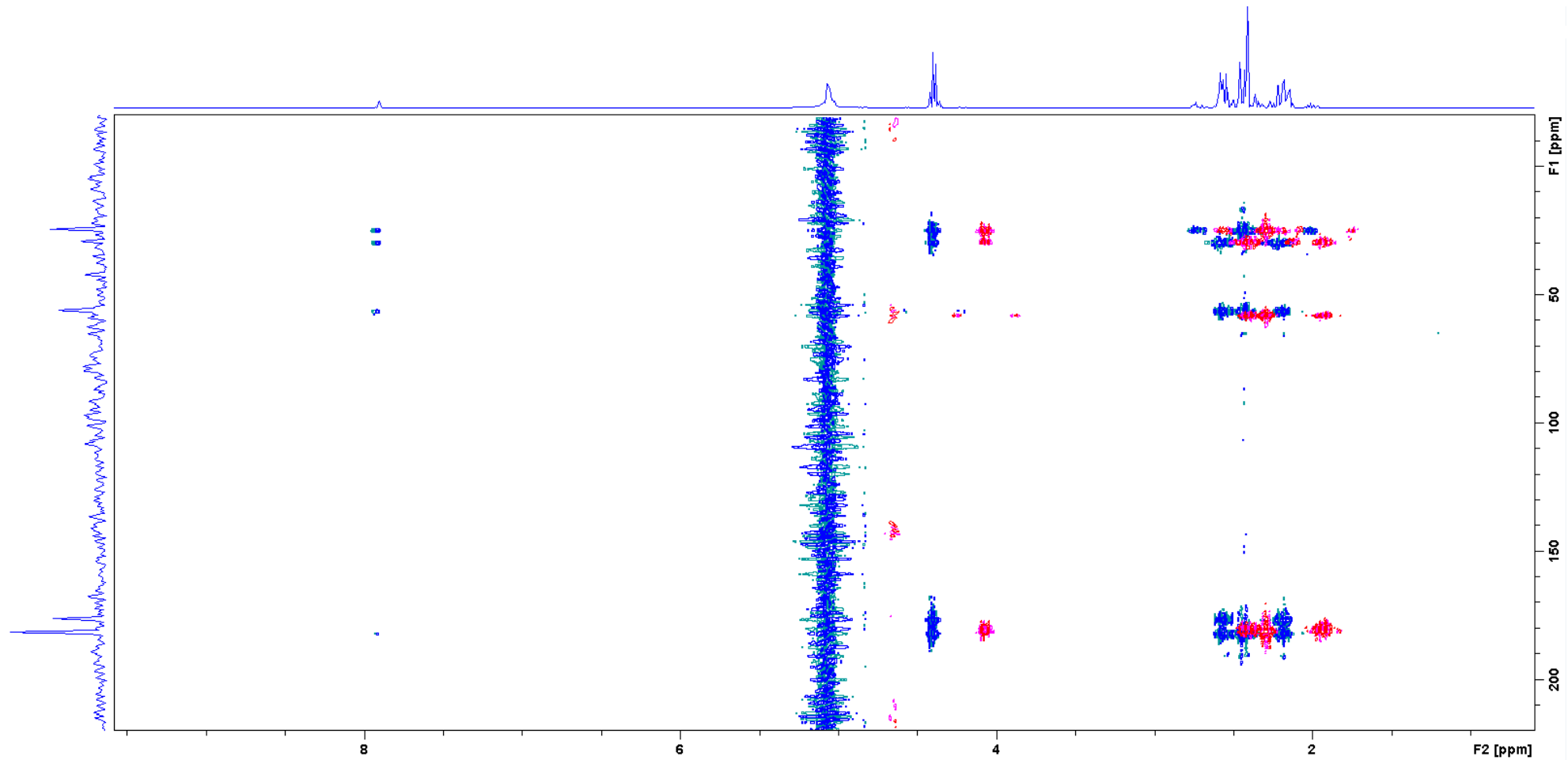


Figure 27: 2D-NMR spectra (HMBC) of PCA in water at pH 1.3 (blue cross peak) and at pH 10.2 (red cross peak).

The signal at around 7.9 ppm corresponds to the hydrogen atom linked to the nitrogen of PCA. The blue cross-peaks are the cross-peaks visible at pH 1.3 and the red ones were at pH 10.2. As can be seen, a correlation between the hydrogen atom linked to the nitrogen and the different carbon atoms around the nitrogen was visible at pH 1.3. This peak and the cross-peaks disappeared at pH 10.2 and therefore, the nitrogen did not share a bond with any hydrogen atom and was negatively charged. This means that PCA is partially negatively charged at pH 7 and 9 in the different phase diagrams. As a lot of charge is present in the ternary mixture of H₂O/EtOH/TriA at pH 7 and 9, it is responsible for the observed salting-out effect in the oil-rich-phase because more water is needed to solve the different ions (PCA and meglumine). The influence of PCA and meglumine on the structure of the SFME was also investigated via DLS. One sample composition was used: H₂O/EtOH/TriA 40/24/36 in weight. 5 different samples were recorded (with or without the addition of additives in the water phase before mixing the ternary mixture): 15 wt% of meglumine in water (pH 11.5), 5 wt% of meglumine in water (pH 11.3), 5 wt% of meglumine in water at pH 9 ($R_{pH9} = 0.82 \pm 0.02$), 5 wt% of meglumine in water at pH 7 ($R_{pH7} = 0.88 \pm 0.01$), and without additives in water. Two different conditions were analysed: one hour of stirring to simulate the conditions of the extraction and without stirring (simulate the conditions during storage). The results are shown in Figure 28 and Figure 29.

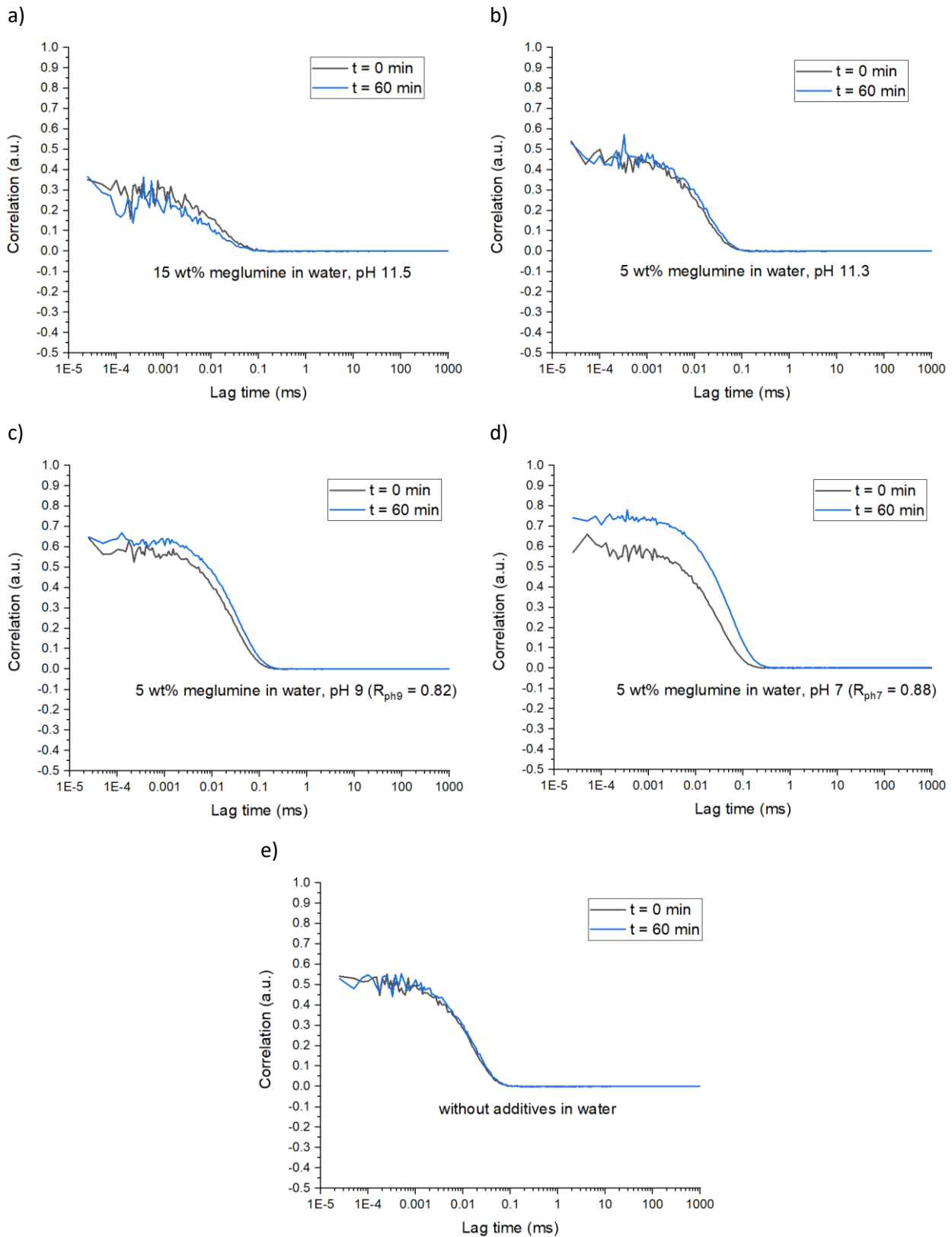


Figure 28: DLS measurements of the investigated ternary mixture $H_2O/EtOH/TriA$ 40/24/36 with a) 15 wt% meglumine in pure water at pH 11.5, b) 5 wt% meglumine in pure water at pH 11.3, c) 5 wt% meglumine in water at pH 9 ($R_{pH9} = 0.82$), d) 5 wt% meglumine in water at pH 7 ($R_{pH7} = 0.88$), and e) without additives in water. The measurements were done directly after mixing and after one hour of stirring time to simulate the extraction conditions.

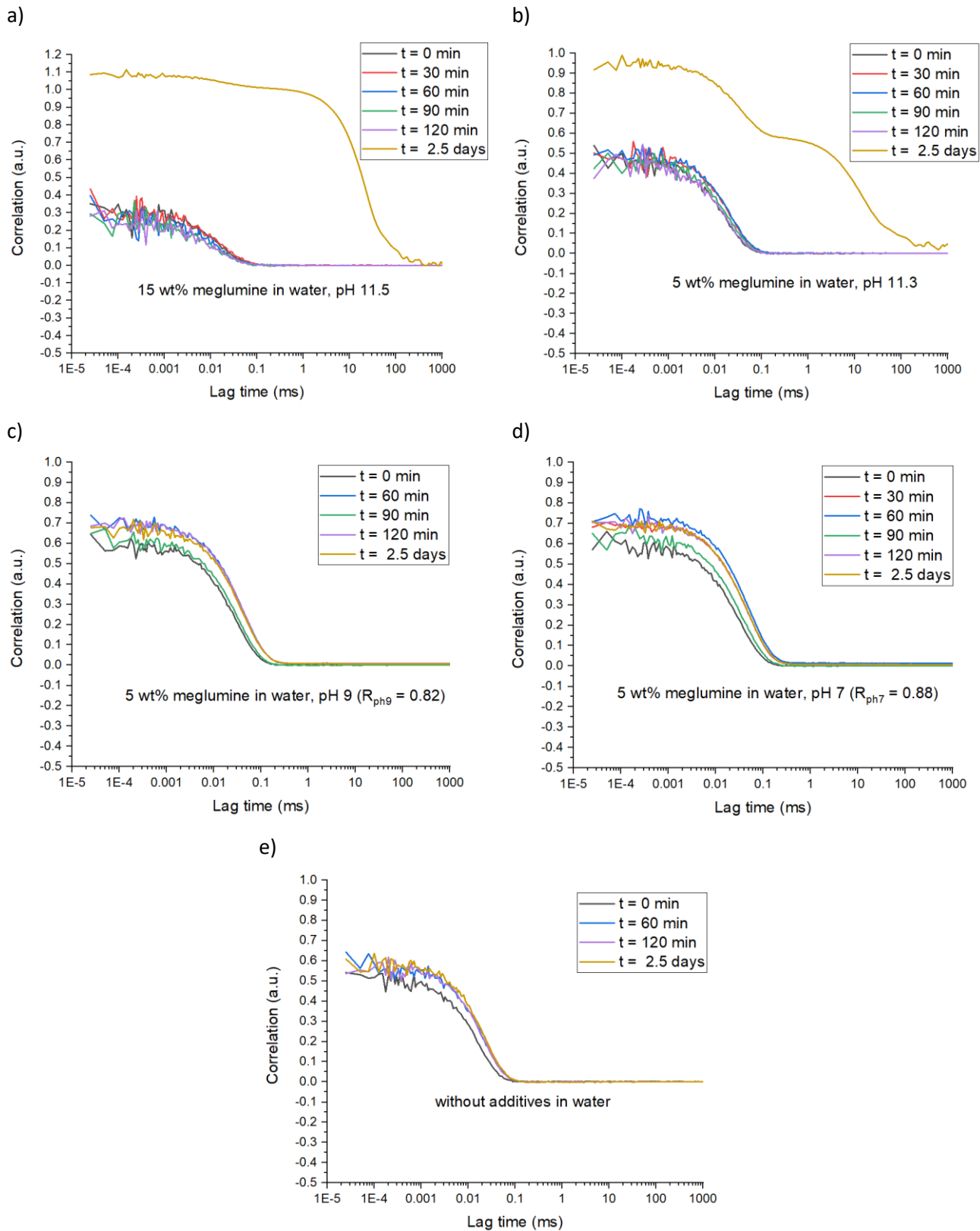
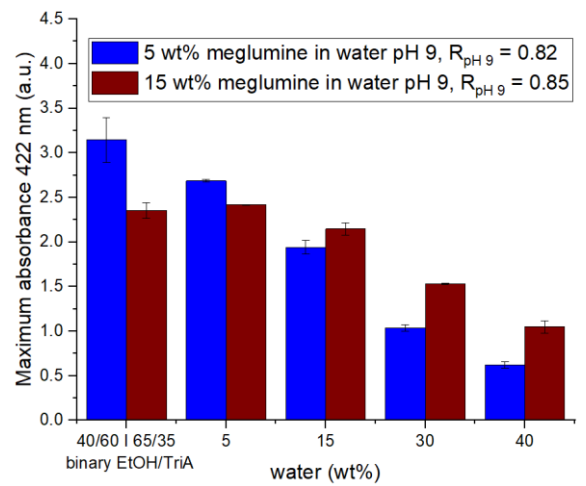
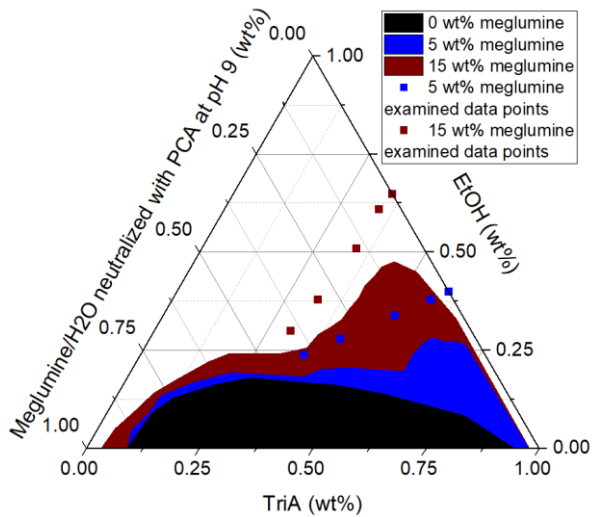
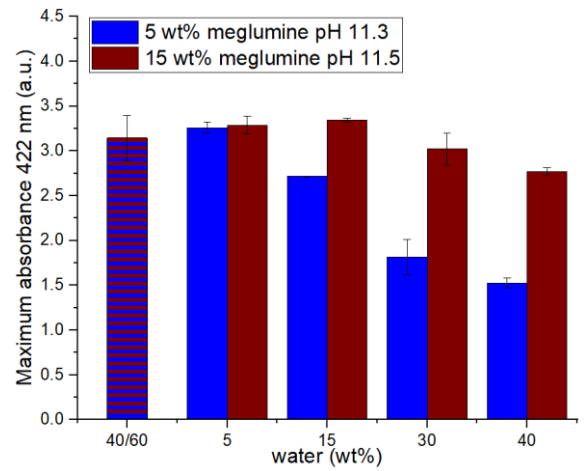
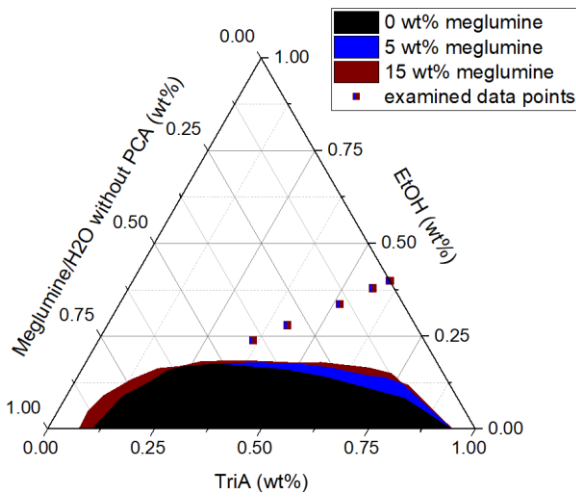
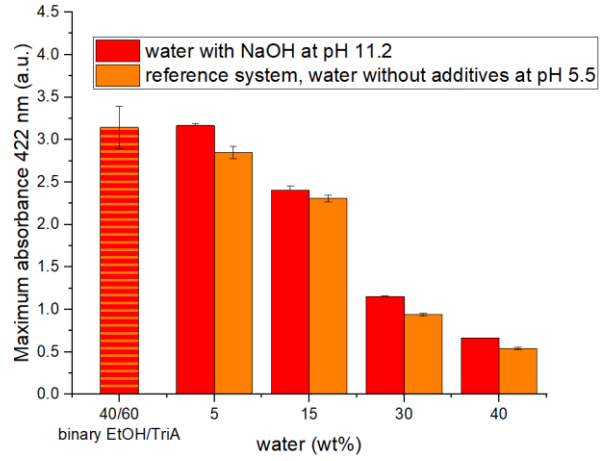
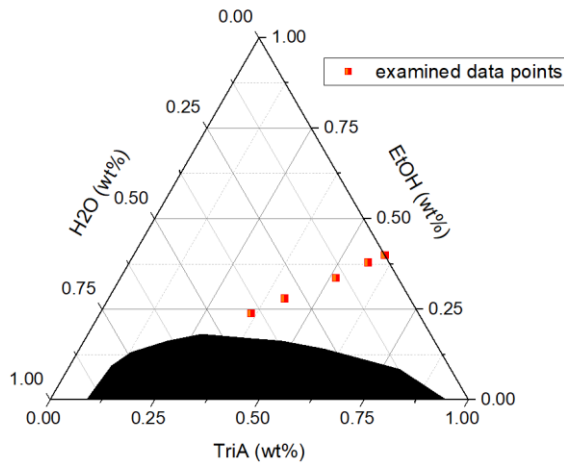


Figure 29: DLS measurements of the investigated ternary mixture $H_2O/EtOH/TriA$ 40/24/36 with a) 15 wt% meglumine in pure water at pH 11.5, b) 5 wt% meglumine in pure water at pH 11.3, c) 5 wt% meglumine in water at pH 9 ($R_{pH9} = 0.82$), d) 5 wt% meglumine in water at pH 7 ($R_{pH7} = 0.88$), and e) without additives in water. The measurements were done directly after mixing and after a certain time: after 30, 60, 90, 120 min and 2.5 days.

As can be seen in Figure 28, the addition of meglumine and PCA to the water phase at different pH had almost no influence on the SFME, if the samples were measured directly after mixing. In contrast, the addition of 15 wt% of meglumine to pure water decreased the correlation curve and therefore, the structuring was weaker than the reference system without any additives. Meglumine at high weight concentration destroys the structuring of the ternary system of H₂O/EtOH/TriA partially. After one hour of stirring, no change was observed for all the samples except for the two samples at pH 7 and 9. Indeed, a stronger and higher correlation curve was obtained after one hour of stirring, which indicates that the system showed stronger structuring than the reference system without additives. This was more significant for the system at pH 7 than at pH 9. Viscosity measurements have been made for several samples to investigate the potential increase of viscosity of the different systems leading, for example, to stirring problems and to worse extraction efficiencies of the curcuminoids. The results are shown in Table S 10 of the Appendix. For all the systems with additives investigated with DLS, the viscosity was higher than the reference system without additives. Moreover, the highest viscosities were found for the systems at pH 7 and 9 (3.38 and 3.32 mPa.s respectively). This increase of viscosity could be an explanation for the stronger structuring of the systems with meglumine and PCA at pH 7 and 9 in water after one hour of stirring. The same systems without stirring have also been investigated. The results were similar for all the measurements after two hours. The same systems have also been measured after 2.5 days (the samples were left in the measuring tubes so that the samples were not again filtered before measurement). For the samples with meglumine and PCA and without additives, no change occurred after 2.5 days. On the contrary, for the samples with only meglumine as additive in pure water, much bigger structuring occurred. A bimodal correlation curve was obtained with 5 wt% of meglumine in pure water after 2.5 days. After the same time, much bigger aggregates were built with 15 wt% of meglumine in pure water. The pH of the SFME was very high and TriA was not stable under basic conditions. TriA can be hydrolysed to glycerol and acetic acid under basic conditions [90]. Glycerol is completely soluble in water and short chain alcohols like EtOH, which is also the case for acetic acid. After 2.5 days, all the samples remain clear, although bigger aggregates were formed in the case of the samples with only meglumine as an additive in pure water.

Prior to the extraction, the maximum solubility of curcumin in the different ternary systems was investigated. Two different weight concentrations of meglumine (15 wt% and 5 wt% in pure water) and four different pH values (7, 9, 11.3, and 11.5) were investigated for the solubility and the extraction of the curcuminoids from *C. longa*. The results are shown in Figure 30.



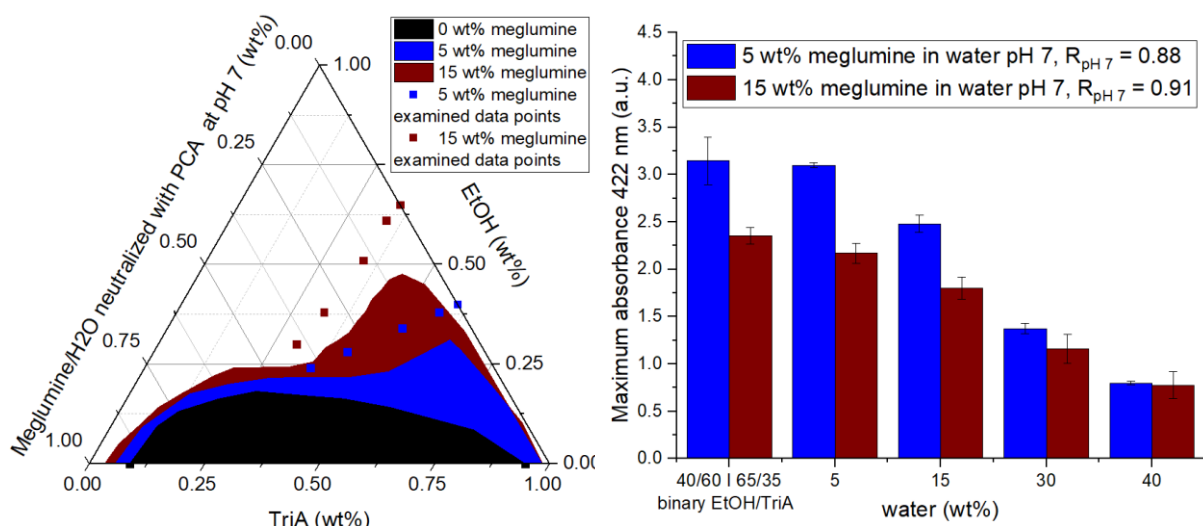


Figure 30: Ternary phase diagrams of the systems: $H_2O/EtOH/TriA$ the reference system (top), H_2O with meglumine (5 and 15 wt% in pure water) without PCA at pH 11.3 and 11.5 respectively/ $EtOH/TriA$ (second from the top), H_2O with meglumine (5 and 15 wt% in pure water) neutralised with PCA to pH 9 ($R_{pH9} = 0.82$ and 0.85 respectively for 5 and 15 wt% of meglumine in water)/ $EtOH/TriA$ (third from the top), and H_2O with meglumine (5 and 15 wt% in pure water) neutralised with PCA to pH 7 ($R_{pH7} = 0.88$ and 0.91 respectively for 5 and 15 wt% of meglumine in water)/ $EtOH/TriA$ (bottom). The ternary phase diagrams also contain the compositions of the mixtures used for curcumin solubilisation studies. The corresponding solubility data are given on the right side of each phase diagram corresponding to the different pH values. R values represent the molar ratio between PCA and meglumine at the different pH values for the two different weight concentrations of meglumine in pure water [71].

First, the influence of the pH on the maximum solubility of curcumin in the ternary phase diagram was investigated with NaOH. As meglumine in water had a high pH (11.3 or 11.5 for respectively 5 wt% and 15 wt% of meglumine in water) and the pH after the formation of the SFME did not change (i.e. the pH of the ternary mixture after mixing is equal to the pH of the water phase before mixing), the pH of the water phase was adjusted to 11.2 with NaOH in $OEtOH/TriA$ to compare with meglumine. As can be seen in Figure 30, the pH had no major impact on the maximum of solubility of curcumin in the SFME. It was only very slightly increasing. Thus, the pH did not impact the maximum solubility of curcumin. Regarding the solubility at pH 11.3 and 11.5 (i.e. without PCA but only with meglumine in water), the same trend was observed for both weight concentrations of meglumine in water as previously: upon addition of water, the maximum solubility of curcumin decreased. The decrease was more pronounced with 5 wt% of meglumine in pure water than with 15 wt% of meglumine. For both meglumine concentrations, the maximum of solubility of curcumin was more robust against small additions of water (i.e. meglumine/water) as previously without meglumine in water. The maximum of solubility of curcumin decreased only slightly with 15 wt% of meglumine in pure water. Regarding the maximum solubility of curcumin at pH 7 and 9, the same trend as before was also observed (the solubility of curcumin decreased upon the addition of water) for both weight concentrations of meglumine in water. It is important to notice that the dilution lines were different (due to the increase of the miscibility gap due to the addition of PCA) and therefore, a direct comparison is difficult. Only the same

weight concentration of meglumine in water at different pH are comparable. Moreover, the dilution lines at pH 7 and 9 with 15 wt% of meglumine in pure water were investigated close to the miscibility gap. Therefore, the ratio between EtOH and TriA remained not constant. The two investigated binary solutions EtOH/TriA (40/60 and 65/35 in weight) showed the same maximum of solubility as previously without any additive in water, as expected. First, the different pH with 5 wt% of meglumine in water will be compared. Upon addition of PCA to the SFME system to bring the pH from 11.3 to 9, the maximum solubility of curcumin decreased. Upon further addition of PCA to bring the pH from 11.3 to 7, the maximum solubility of curcumin also decreased, but not as strongly as at pH 9. It can be supposed that there was a synergism between PCA and meglumine for this SFME system (i.e. with 5 wt% of meglumine in pure water). On the contrary, the addition of PCA to the SFME system with 15 wt% of meglumine in water to bring the pH from 9 to 7 further decreased the maximum solubility of curcumin and in this case, no synergism can be observed or presumed.

The real advantage to use meglumine as an additive in pure water was the high increase of the maximum solubility of curcumin for the SFME containing 40 wt% of water (H₂O/EtOH/TriA 40/24/36) for all the systems without PCA. The comparison between the different SFME systems is shown in Figure 31.

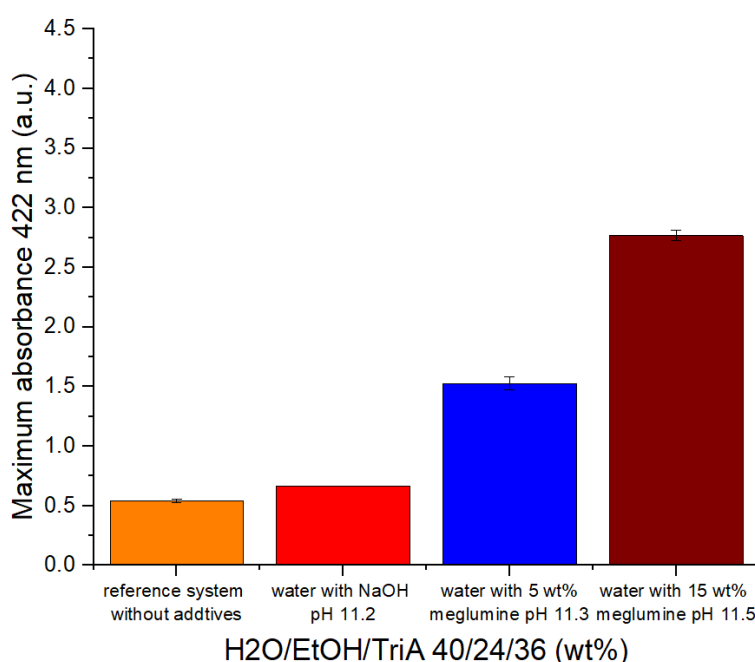


Figure 31: Maximum absorbance of curcumin (at $\lambda_{max} = 422$ nm) at saturation for the same SFME composition (H₂O/EtOH/TriA 40/24/36) with different additives in pure water: reference SFME without additives, water with NaOH at pH 11.2, water with 5 wt% of meglumine, and water with 15 wt% of meglumine (from the left to the right) [71].

As can be seen in Figure 31, the increase of the maximum solubility of curcumin was due to the addition of meglumine and not due to the pH. The maximum solubility of curcumin was higher for all the systems with additives than with the reference system without additives. Moreover, the maximum solubility of curcumin increased 5-fold with the addition of only 15 wt% of meglumine to pure water. Therefore, the different weight concentrations of meglumine should be tested for extraction. Prior to the extraction, the stability of curcumin in different SFME systems with additives at different pH values must be investigated. Indeed, curcumin is degrading under basic conditions (see section 3.3.2.2). Therefore, the change of colour of the saturated solutions for the investigation of the maximum of solubility of curcumin was observed for a certain time to obtain preliminary results. In some samples at pH 11.3 and 11.5 (i.e. with only meglumine in pure water) a precipitation occurred overnight or after 2 days. Moreover, a change of colour was observed: from red (high pH) to orange (decrease of the pH). The same change of colour occurs at pH 9, but the samples were less red at the beginning than at pH 11.3 and 11.5 and no precipitation was observed. No changes were noticed at pH 7 for both weight concentrations of meglumine in water. The UV samples were stored in the lab at day light.

First, the precipitation of curcumin along the dilution lines with 15 wt% and 5 wt% of meglumine in pure water without PCA at pH 11.3 and 11.5 respectively was investigated more precisely (for sample composition see Table 7). The samples were stored in darkness after saturation with curcumin and pictures of the sample were taken over the time. The pictures and the different investigated compositions of the ternary system are shown in Table 7.

Table 7: Sample composition (Sample 1 to 5; from the left to the right in the pictures) for the investigated precipitation of curcumin with 5 wt% and 15 wt% of meglumine in water and pictures of the samples after saturation with curcumin, after 1 and 2 days in the dark. [89]

Sample composition (wt%)	5 wt% of meglumine in pure water	15 wt% of meglumine in pure water
		Day 0
1: EtOH/TriA 40/60		
2: H ₂ O/EtOH/TriA 5/38/57	Day 1	
3: H ₂ O/EtOH/TriA 15/34/51		
4: H ₂ O/EtOH/TriA 30/28/42	Day 2	
5: H ₂ O/EtOH/TriA 40/24/36		

All samples were red after saturation with curcumin, except for the binary system, which was orange. The red colour was due to the high pH. The samples had a more pronounced red colour with an increasing water content of the SFME for both weight concentrations of meglumine. The red colour was more pronounced for the samples with 15 wt% of meglumine in water than with 5 wt% of meglumine. After one day of storage in the dark, all the red samples became brighter (due to the decrease of the pH over time) and for both weight concentrations of meglumine in water, a precipitation occurred in the samples 4 and 5 (with respectively 30 wt% and 40 wt% of water with meglumine in the SFME). The precipitation was stronger in the samples with 15 wt% of meglumine in water (judged with bare eyes) and stronger in sample 5 than sample 4 (see Figure S 12 of the Appendix). After two days, more curcumin has precipitated in samples 4 and 5 for both concentrations and all the samples are brighter again (except the binary system). No precipitation occurred in the others samples (sample 1 to 3). The more water was in the SFME and the more meglumine was dissolved in water, the more curcumin has precipitated in the samples. The pH and the different pK_a (meglumine and curcumin) seemed to play the major role for the precipitation of curcumin.

Therefore, the precipitation pH of curcumin and bisdemethoxycurcumin has been investigated first in water containing 5 wt% of meglumine, in order to know if the precipitation occurred at the pK_a of meglumine or of the polyphenol. Then, the pH of precipitation of curcumin in the SFME H₂O/EtOH/TriA 40/24/36 (in weight) at different meglumine concentrations in water (5 wt% and 15 wt%) was investigated. Further, the pH of the same SFME without curcumin has also been measured as comparison. The results are shown in Figure 32 and in Figure S 13 and Figure S 14 of the Appendix. In water with 5 wt% of meglumine, curcumin started to precipitate at a pH of 9.70 and bisdemethoxycurcumin began to precipitate at a pH of 10.48 (see the pictures of the centrifuge tubes in Figure S 13 and Figure S 14 of the Appendix). The precipitation of the polyphenols was not dependent on the pK_a of meglumine ($pK_a = 9.64$, see Figure S 11 of the Appendix) but on the pK_a of the polyphenols themselves. This means that if the curcuminoids could be extracted with a simple water/meglumine mixture, the separation of the three curcuminoids could be possible simply by lowering the pH step by step.

As previously mentioned, meglumine, more precisely the high pH, destroyed TriA and therefore, the SFME over the time, meaning that the pH of the SFME decreased over the time. In the SFME H₂O/EtOH/TriA 40/24/36 (in weight) with 15 wt% of meglumine in water, curcumin started to precipitate at a pH of 9.32 and with 5 wt% of meglumine at a pH of 8.94. The difference could be explained by the higher maximum solubility of curcumin in the SFME with 15 wt% of meglumine in pure water. Indeed, more curcumin was soluble and therefore, the precipitation should be started at a higher pH value. Over four hours, the pH of the SFME without curcumin decreased from 11.02 to 8.95 and from 10.01 to 9.32 over three hours with curcumin saturation. After one hour of stirring, no precipitation occurred, meaning that the extraction could be performed without any problems concerning the precipitation of curcumin from the extraction SFME system.

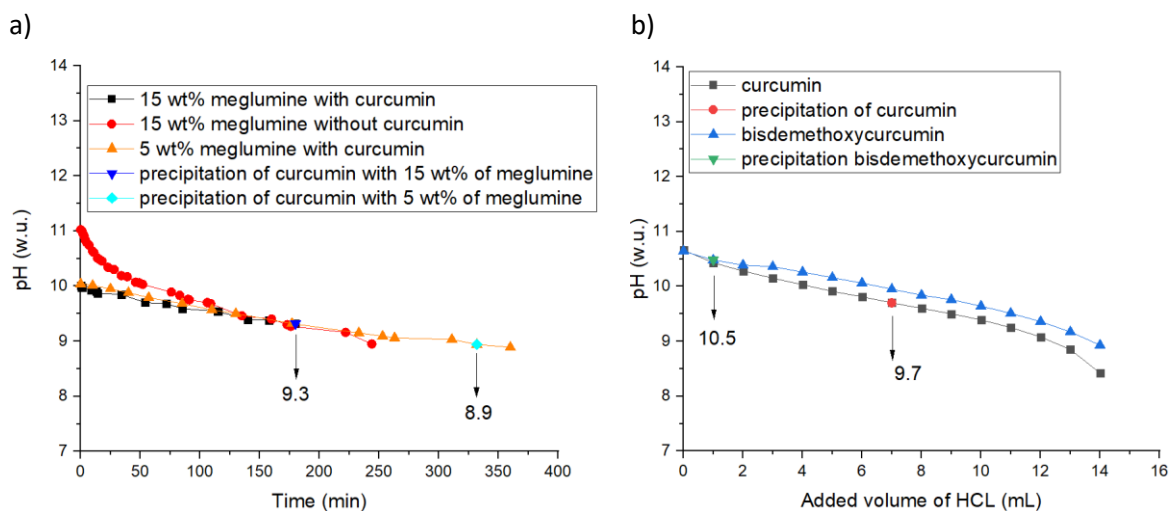


Figure 32: a) Evolution of the pH over the time in the SFME $H_2O/EtOH/TriA$ 40/24/36 with 15 wt% of meglumine in water without curcumin (black square), with curcumin at saturation (red circle) and with 5 wt% of meglumine in water with curcumin at saturation (up-facing orange triangle). The pH of precipitation of curcumin is indicated for both weight concentrations of meglumine in water. b) investigation of the pH of precipitation of curcumin (black square) and bisdemethoxycurcumin (up-facing blue triangle) in water containing 5 wt% of meglumine.

The only drawback of the use of meglumine with or without PCA in the SFME extraction system was the high pH. Therefore, the stability of curcumin in different SFME extraction systems with or without additives was investigated via UV/Vis measurements. As curcumin precipitated overnight in the SFME extraction system containing 30 and 40 wt% of water with additives, the highest water content used for the stability measurement of curcumin was 15 wt% (i.e. $H_2O/EtOH/TriA$ 15/34/51 or $H_2O/EtOH/TriA$ 15/51/34 in weight). Moreover, the pH of the samples stored in the dark and at day light was also measured over the UV-measurement time. NaOH as additive was also investigated as well as meglumine with and without PCA. The results at day light and in darkness are shown respectively in Figure 33 and Figure 34. Curcumin was not stable in the reference systems $H_2O/EtOH/TriA$ 15/34/51 and $H_2O/EtOH/TriA$ 15/51/34 in weight. Indeed, after 10 days almost no curcumin was detected via UV/Vis. Moreover, a change of the spectra was observed. Thus, all the curcumin was degraded after 10 days. The reference system with NaOH as additive at pH 11.5 showed the same results as the reference system without additives. It can be deduced that the high pH has no influence on the curcumin stability or instability in the SFME. The change of spectra occurred later for the samples with additives (meglumine with or without PCA), because the maximum of solubility of curcumin was much higher in the SFME with water containing additives than in the reference SFME. From all the results, it can be deduced that first, the high pH had no influence on the curcumin stability and that light was responsible for the curcumin degradation in the SFME.

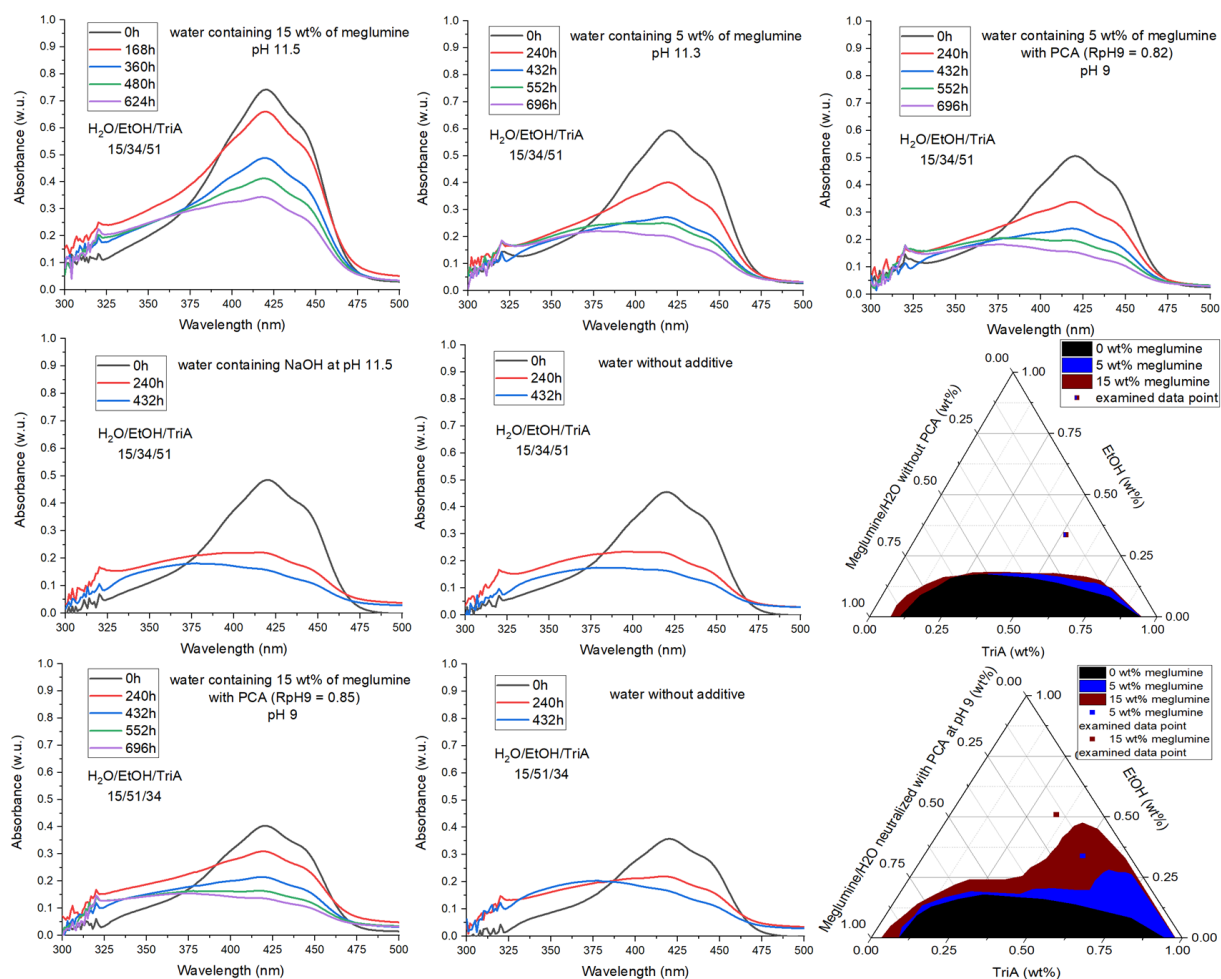


Figure 33: UV/Vis spectra of two different SFME systems H₂O/EtOH/TriA 15/34/51 and 15/51/34 in weight with different additives in water and without additives over time at curcumin saturation at day light. From the left to the right and from the top to the bottom: H₂O/EtOH/TriA 15/34/51 with water containing 15 wt% of meglumine (pH 11.5); with water containing 5 wt% of meglumine (pH 11.3); with water containing 5 wt% of meglumine with PCA at pH 9 ($R_{pH9} = 0.82$); with water containing NaOH (pH 11.5); without additives; ternary phase diagram without PCA with the composition of the investigated SFME; H₂O/EtOH/TriA 15/51/34 with water containing 15 wt% of meglumine with PCA at pH 9 ($R_{pH9} = 0.85$); without additives; ternary phase diagram with PCA at pH 9 with the compositions of the investigated SFME.

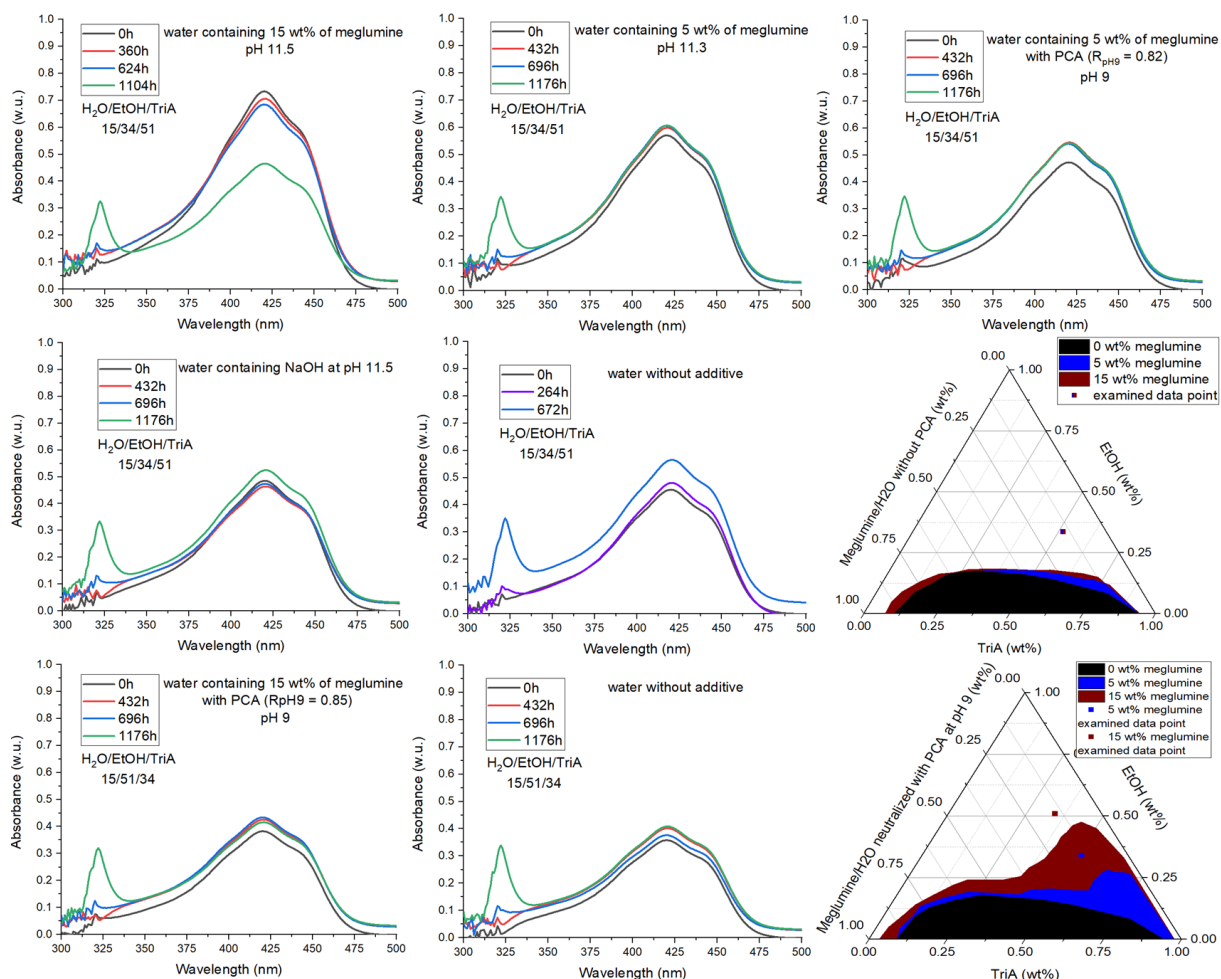


Figure 34: UV/Vis spectra of two different SFME systems $H_2O/EtOH/TriA$ 15/34/51 and 15/51/34 in weight with different additives in water and without additives over time at curcumin saturation in darkness. From the left to the right and from the top to the bottom: $H_2O/EtOH/TriA$ 15/34/51 with water containing 15 wt% of meglumine (pH 11.5); with water containing 5 wt% of meglumine (pH 11.3); with water containing 5 wt% of meglumine with PCA at pH 9 ($R_{pH9} = 0.82$); with water containing NaOH (pH 11.5); without additives; ternary phase diagram without PCA with the composition of the investigated SFME; $H_2O/EtOH/TriA$ 15/51/34 with water containing 15 wt% of meglumine with PCA at pH 9 ($R_{pH9} = 0.85$); without additives; ternary phase diagram with PCA at pH 9 with the compositions of the investigated SFME.

The fact that the pH had no influence on the curcumin stability was also supported and demonstrated by the measurements in darkness. Indeed, in the dark curcumin was stable over one month at least. Some samples showed a maximum absorbance higher than the initial one. As all the samples were diluted 5000-fold, this higher absorbance can be attributed to dilution mistakes. Only the sample with 15 wt% of meglumine in water at pH 11.5 showed a decrease of the maximum absorbance, but this decrease was due to the precipitation of curcumin in the sample. The precipitation can be explained by the degradation of TriA over the time (due to the high pH) and the decrease of the pH. The pH has also been measured and the results are shown in Table 8. As can be seen, the pH decreased very fast after two to three days only. Indeed, all the samples had a pH under 7.5. The pH decreased faster under light as in darkness. It can be deduced that the degradation of TriA occurred faster than the degradation of curcumin in darkness. After one month, a new peak appeared in the UV spectra of all

the samples. This unknown substance could be a degradation product of curcumin or TriA, but no accurate statement can be made.

Table 8: pH of the two SFME systems H₂O/EtOH/TriA 15/34/51 and 15/51/34 in weight with different additives in water and without additives over time at curcumin saturation at day light (L) and in darkness (D). n.m. means not measured [89].

pH at day			0		1	2	3	11
SFME system	H ₂ O/EtOH/TriA 15/34/51	without additives	L	6.2	6.7	5.3	4.7	3.4
			D	6.2	n.m.	6.8	n.m.	6.6
		5 wt% meglumine in water at pH 9	L	9	7.0	6.8	6.7	5.9
			D	9	n.m.	n.m.	7.0	6.3
		5 wt% meglumine in water at pH 11.3	L	11.3	8.0	7.6	7.4	6.0
			D	11.3	n.m.	7.0	n.m.	6.9
		NaOH pH 11.5	L	11.5	7.4	7.0	n.m.	4.1
			D	11.5	n.m.	7.7	n.m.	7.2
	15 wt% meglumine in water at pH 11.5	L	11.5	8.2	7.6	7.4	6.5	
		D	11.5	n.m.	n.m.	n.m.	7.0	
	H ₂ O/EtOH/TriA 15/51/34	without additives	L	6.0	6.7	5.9	5.2	3.8
			D	6.0	n.m.	6.8	n.m.	6.8
		15 wt% meglumine in water at pH 9	L	9	7.5	7.1	6.9	5.5
			D	9	8.2	n.m.	7.5	6.7

As the pH had no major influence on the curcumin degradation in the SFME, extraction could be performed. Moreover, after one hour, the pH of precipitation of curcumin was not reached in the SFME H₂O/EtOH/TriA 40/24/36 (in weight) with 15 wt% of meglumine in water, meaning that the extraction can be performed without curcumin precipitation from the SFME extraction system. As meglumine with and without PCA solubilised in water increased the maximum curcumin solubility in the SFME, it could be hoped that the extraction of the curcuminoids from *C. longa* could be enhanced even more

than in the reference system without additives in water. Indeed, previously the best extraction system was the ternary mixture with 40 wt% of water. Upon addition of water, the extraction efficiencies of demethoxycurcumin and bisdemethoxycurcumin were increased. Therefore, extraction experiments were conducted with different weight concentrations of meglumine with and without PCA at different pH values in water to be compared to the SFME extraction system without additives. The same extraction procedure was used with the same weight ratio *C. longa* to extraction SFME of 1 to 4 in weight. The results are shown in Figure 35. The detailed curcuminoid extraction efficiencies for all the SFME systems at different pH values and meglumine weight concentration in water are shown in Table S 11 of the Appendix.

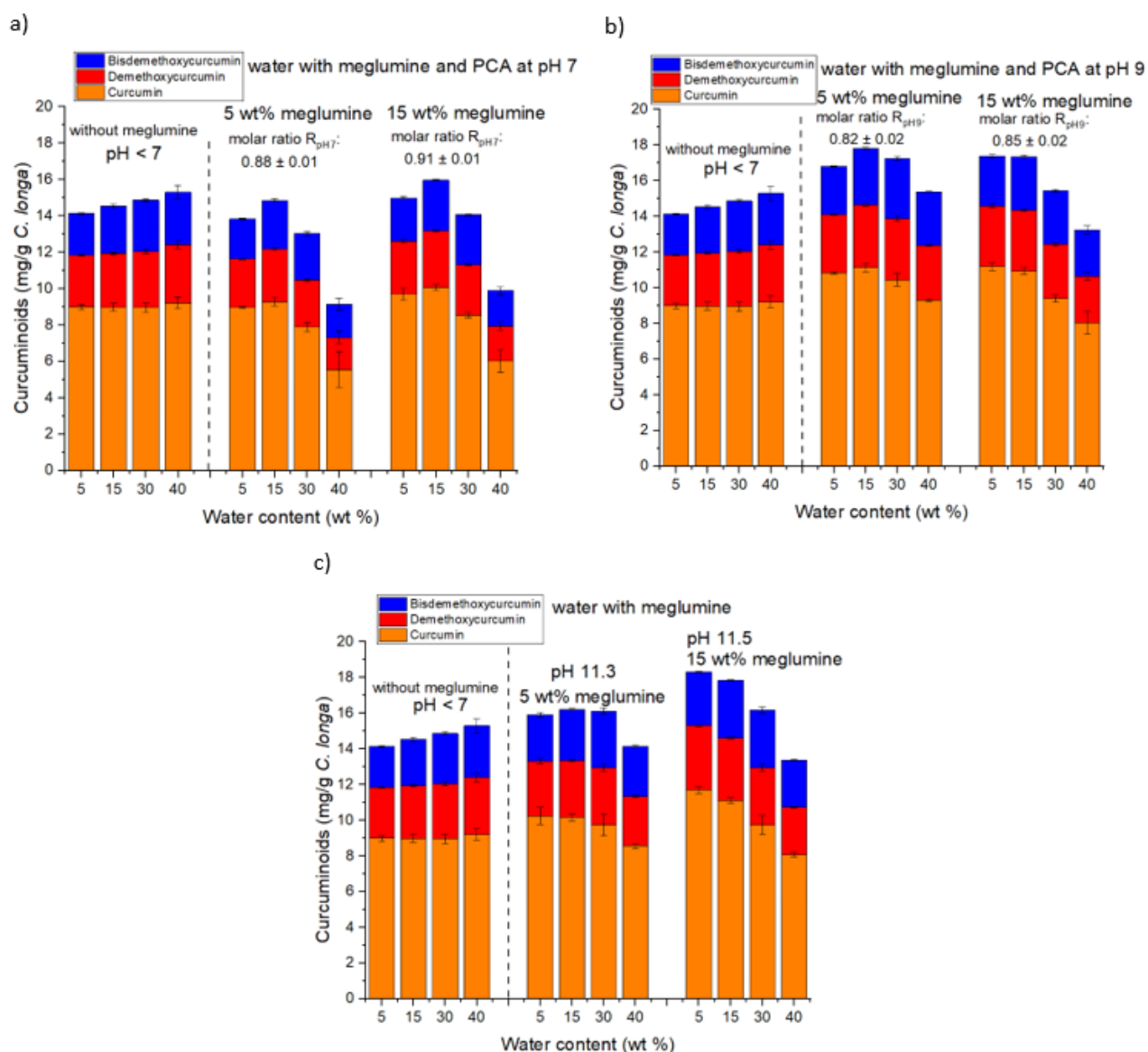


Figure 35: Overview of the total curcuminoid content (curcumin, demethoxycurcumin, and bisdemethoxycurcumin) for the SFME extraction systems with varying water content with 5 and 15 wt% of meglumine in pure water at a) pH 7, b) pH 9, and c) pH 11.3 and 11.5. R_{pH} values represent the molar ratio between PCA and meglumine at the different pH values [71].

First, the curcuminoid extraction efficiencies with the two weight concentrations of meglumine in water will be compared at constant pH and to the reference system without additives (see Figure 35). With a water pH of 7 (cf. Figure 35 a), all total curcuminoid extraction efficiencies were lower or equal for all SFME extraction systems with additives compared to the reference system without additives. Only the SFME system containing 15 wt% of water with 15 wt% of meglumine surprisingly exhibited a higher total extraction efficiency (the gain remaining very low). If the best SFME extraction system without additives (i.e. with 40 wt% of water) is compared to the same SFME extraction system with additives for both weight concentrations of meglumine, the curcuminoid extraction efficiencies of the SFME extraction system with additives were much lower. Many reasons could explain the bad extraction efficiencies: first, the viscosity was higher if the SFME extraction system contained additives (see Table S 10 of the Appendix), leading to agitation problems, second at pH 7 both additives were charged in the SFME extraction system (see Figure 27), meaning that a lot of water was needed to hydrate both additives so that less water could participate to the curcuminoid extraction, and last as meglumine was positively charged at pH 7, no salt formation with curcumin should occurred.

With a water pH of 9 (cf. Figure 35 b), all total curcuminoid extraction efficiencies of were better or equal for all SFME extraction systems with additives compared to the reference system without additives, in contrast with a water pH of 7. Only the SFME extraction system with 40 wt% of water exhibits a lower extraction efficiency, certainly due to a higher viscosity (see Table S 10 of the Appendix). In total, between 2 and 3 mg more curcuminoids per g *C. longa* could be extracted at low water contents (5 and 15 wt% of water) for both meglumine weight concentrations in pure water. Even the SFME extraction system with 30 wt% of water containing 5 wt% of meglumine showed a higher total curcuminoid extraction efficiency (17.24 mg curcuminoids per g *C. longa*, see Table S 11 of the Appendix) than the best SFME extraction system without additives (15.28 mg curcuminoids per g *C. longa*, see Table S 11 of the Appendix, H₂O/EtOH/TriA 40/24/36 in weight). The SFME extraction systems exhibited a similar trend for both meglumine weight concentrations: higher total curcuminoid extraction efficiencies at low water contents and a decrease upon increase of the water content of the SFME extraction systems. At a higher water content, the total curcuminoid extraction efficiencies were better with 5 wt% of meglumine in pure water than with 15 wt% of meglumine (the same total curcuminoid content was reached with the SFME extraction system with 40 wt% of water containing 5 wt% of meglumine than with 30 wt% of water containing 15 wt% of meglumine). The addition of meglumine and PCA led to higher curcuminoid extraction efficiencies than with the best SFME extraction system without additives (synergistic effect). Comparing the curcuminoids alone now: for curcumin, all extraction efficiencies were better than the reference system without additives, except

the SFME extraction system with 40 wt% of water containing 15 wt% of meglumine. The same trend as previously with the investigation of the maximum of solubility of curcumin was observed: upon addition of water (i.e. water/meglumine/PCA), the curcumin extraction efficiencies decreased. As curcumin is the most abundant curcuminoid, it was not surprising [91,92]. The same trend as for curcumin was observed for demethoxycurcumin. Only three SFME extraction systems (SFME with 40 wt% of water containing 5 and 15 wt% of meglumine and 30 wt% of water containing 15 wt% of meglumine) showed a lower demethoxycurcumin extraction efficiency than the best reference system without additives (respectively 3.04, 2.60, 3.04, and 3.18 mg demethoxycurcumin per g *C. longa*, see Table S 11 of the Appendix). The same trend as previously seen without additives could also be observed for bisdemethoxycurcumin. Indeed, upon addition of water, the bisdemethoxycurcumin extraction efficiency increased (except for the SFME extraction system with 40 wt% of water with additives, because of viscosity reasons and therefore, agitation problems, see Table S 10 of the Appendix). For both weight concentrations of meglumine, the SFME extraction system with 15 wt% and 30 wt% of water with additives extracted more bisdemethoxycurcumin than the reference system without additives (3.18 and 3.38 mg bisdemethoxycurcumin per g *C. longa* for respectively 15 wt% and 30 wt% of water containing 5 wt% of meglumine and 3.01 and 3.01 mg bisdemethoxycurcumin per g *C. longa* for respectively 15 wt% and 30 wt% of water containing 15 wt% of meglumine). In contrast to curcumin, bisdemethoxycurcumin and demethoxycurcumin are not that abundant in *C. longa* [91,92]. The extraction efficiencies of these two curcuminoids could be enhanced just with the addition of meglumine and PCA in the water phase of the SFME extraction system (~ 10% and ~ 17% for the best SFME extraction system for demethoxycurcumin and bisdemethoxycurcumin respectively).

With a water pH of 11.3 or 11.5, all SFME extraction systems with additives (i.e. only meglumine, without PCA) showed a higher total curcuminoid extraction efficiency, except again the SFME extraction system with 40 wt% of water for both meglumine weight concentrations in water (certainly due to viscosity reason, see Table S 10 of the Appendix). The total curcuminoid extraction efficiencies were better with 15 wt% of meglumine in pure water than with 5 wt% of meglumine. With 5 wt% of meglumine in water, the total curcuminoid extraction efficiencies were equal upon the addition of water. With 15 wt% of meglumine in water, they decreased upon addition of water. A maximum was reached with the SFME extraction system with 5 wt% of water containing 15 wt% of meglumine (18.3 mg curcuminoids per g *C. longa*, see Table S 11). This was a win of 3 mg of curcuminoids per g *C. longa* compared to the best SFME extraction system without additives (15.28 mg curcuminoids per g *C. longa*, see Table S 11 of the Appendix, H₂O/EtOH/TriA 40/24/36 in weight). Regarding the curcuminoids alone, the same trend as for pH 9 could be observed (the SFME extraction system with 40 wt% of water

will not be considered for the comparison of the curcuminoids alone): upon addition of water, the curcumin extraction efficiency decreased, the demethoxycurcumin extraction efficiency decreased also a little and the bisdemethoxycurcumin extraction efficiency increased. Remarkable, curcumin was extracted better with all investigated SFME extraction systems than with the reference system without additives (from 9.72 to 11.7 mg curcumin per g *C. longa* with the SFME extraction system additives compared to 9.21 mg curcumin per g *C. longa* with the reference system, see Table S 11 of the Appendix). The demethoxycurcumin and bisdemethoxycurcumin extraction efficiencies with the SFME extraction system with 15 wt% of meglumine in water were all better than the reference system. With 5 wt% of meglumine, a maximum was reached with the SFME extraction system with 30 wt% of water (3.20 and 3.17 mg demethoxycurcumin and bisdemethoxycurcumin respectively per g *C. longa*, see Table S 11 of the Appendix).

First, the total curcuminoid and the different curcuminoid extraction efficiencies were compared at constant pH for different weight concentrations of meglumine in pure water, now the pH effect at a constant weight concentration of meglumine in water will be compared. The results (same as in Figure 35, but reordered) are shown in Figure 36.

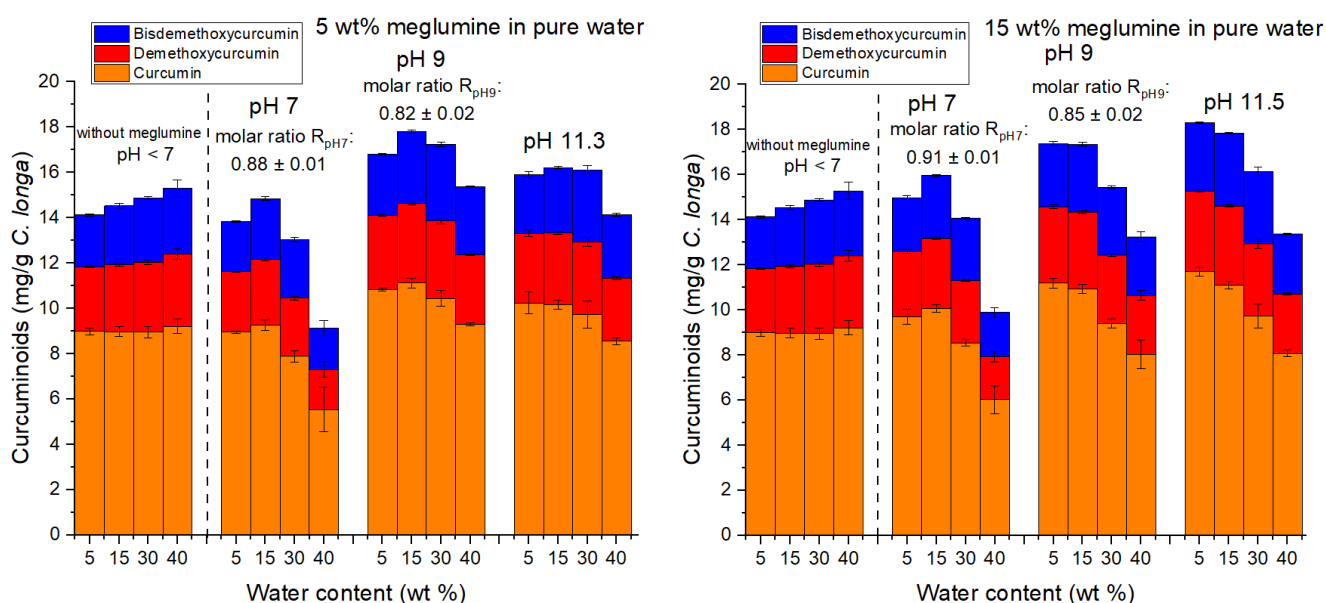


Figure 36: Overview of the total curcuminoid content (curcumin, demethoxycurcumin, and bisdemethoxycurcumin) for the SFME extraction systems with varying water content with 5 wt% (on the left) and 15 wt% (on the right) of meglumine in pure water at different pH. R_{pH} values represent the molar ratio between PCA and meglumine at the different pH values [71].

As can be seen, the best total curcuminoid extraction efficiencies were reached with a water pH of 9 with the SFME extraction system with 5 wt% of meglumine in water (the maximum is reached with the SFME extraction system containing 15 wt% of water) and with a water pH of 11.5 with the SFME extraction system with 15 wt% of meglumine in water (the maximum was reached with the SFME

extraction system containing 5 wt% of water). One explanation could be proposed to explain the difference. The charge of the two different additives (meglumine and PCA) should be considered at the two different pH values. At a water pH of 11.3 and 11.5, only meglumine was solubilised in water and was not charged (the salt formation with curcumin takes place), so that a higher weight concentration of meglumine led to higher total curcuminoid extraction efficiencies. At a water pH of 9, PCA and meglumine were charged. Indeed, as previously described in Figure 27, the nitrogen of PCA was negatively charged so that PCA could also participate in enhancing the total curcuminoid extraction efficiencies. Meglumine was also partially charged ($pK_a = 9.64$, see Figure S 11 of the Appendix) and considering all the charges in the SFME extraction system, a higher weight concentration of meglumine (and therefore also of PCA) led probably to a too higher overall charge in the SFME extraction system and therefore, to a lower total curcuminoid extraction efficiencies.

Previously, the stability of curcumin has been investigated to see if the high pH of the SFME extraction system could be a problem for the extraction of the curcuminoids. In order to see, if here the high pH played a major role on the extraction of the curcuminoids, the same SFME extraction systems have been tested with NaOH at pH 11.2 as additive to be compared with the best SFME extraction systems for both weight concentrations of meglumine in water. The results are shown in Figure 37. The detailed curcuminoid extraction efficiencies are shown in Table S 11 of the Appendix. The total curcuminoid extraction efficiencies could be enhanced with NaOH as additive (except for the SFME extraction system with 40 wt% of water) compared to the best reference system without additives, but lower than the best SFME extraction systems at pH 9 and 11.5. If the curcuminoids alone are compared, it can be seen, that NaOH had only an influence on the curcumin extraction efficiency. No influence on the demethoxycurcumin and bisdemethoxycurcumin extraction efficiencies was observed. The pH played then a minor role in the enhancement of the total curcuminoid extraction efficiencies. The pH after extraction was recorded for three SFME extraction systems with the same composition ($H_2O/EtOH/TriA$ 40/24/36 in weight) with the different additives: NaOH at pH 11.2, 5 wt% of meglumine in water (pH 11.3) and 15 wt% of meglumine in water (pH 11.5). After the extraction, the pH decreased to 6.6, 9.5 and 9.9 respectively. With the SFME extraction system with 40 wt% of water, the high pH destroyed the SFME over time which was then consumed by the plant material. It can be deduced, that NaOH was consumed more strongly by *C. longa* and TriA than meglumine.

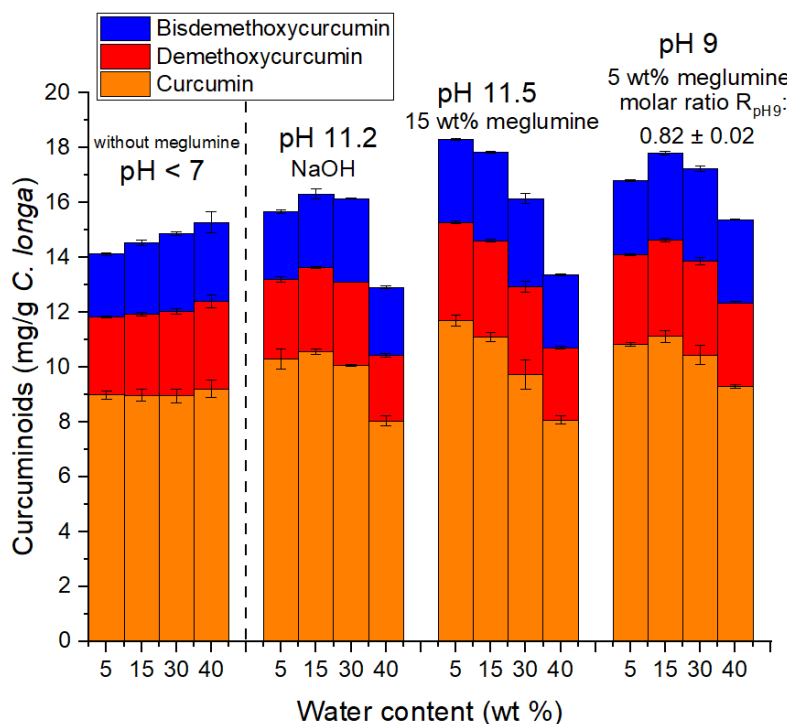


Figure 37: Comparison of the total curcuminoid extraction efficiencies between the best SFME extraction systems at pH 9 and 11.5, and the same SFME extraction system with NaOH at pH 11.2 as additive in water instead of meglumine and PCA. R_{pH9} represents the molar ratio between PCA and meglumine at pH 9 [71].

As the addition of meglumine to the water phase of the SFME extraction systems enhanced the total curcuminoid extraction efficiencies, a simple water extraction with only meglumine was investigated. Here, only water and meglumine were used, no organic solvents like EtOH or TriA were added. The same extraction procedure was performed with the same weight concentration of meglumine in water at the same pH (water/meglumine 85/15 in weight at pH 11.5 and water meglumine 95/5 in weight at pH 11.3). For comparison, NaOH as additive was also investigated at the same pH as before (11.2). The results are shown in Table 9. During the analytical process, the pH was decreased after the extraction to precipitate the curcuminoids and other phytochemicals from the extraction system. Acetonitrile was then used for analytical reasons because the curcuminoids and the essential oils were soluble in it. After the pH change, a part of the precipitated extract was neither soluble in water nor in acetonitrile. The results with NaOH are not presented in Table 9, because a too small amount of curcuminoids was extracted and therefore, the curcuminoid extraction efficiencies were not measurable.

Table 9: Curcuminoids extracted from *C. longa* with two aqueous extraction systems water/meglumine (95/5 and 85/15 in weight) [71].

Extraction systems (wt%)	Curcumin (mg/g <i>C. longa</i>)	Demethoxycurcumin (mg/g <i>C. longa</i>)	Bisdemethoxycurcumin (mg/g <i>C. longa</i>)
water/meglumine 95/5	4.03 ± 0.16	1.39 ± 0.08	1.51 ± 0.06
water/meglumine 85/15	7.70 ± 0.42	3.30 ± 0.62	3.46 ± 0.62

As can be seen, the more meglumine was solubilised in water, the higher the curcuminoid extraction efficiencies were. The high demethoxycurcumin and bisdemethoxycurcumin extraction efficiency was remarkable with only a mixture of meglumine (15 wt%) and water (85 wt%) as extraction system. Moreover, the bisdemethoxycurcumin extraction efficiency was the highest one of all investigated extraction systems. It was already demonstrated previously, that the addition of water to the binary mixture of EtOH and TriA enhanced the bisdemethoxycurcumin extraction efficiency, because bisdemethoxycurcumin had an affinity to polar solvents (supported also by COSMO-RS calculations [60]). Moreover, as bisdemethoxycurcumin possesses two methoxy groups less than curcumin, the salt formation should be in favour of bisdemethoxycurcumin instead of curcumin. All these assumptions could explain the high bisdemethoxycurcumin extraction efficiency, although bisdemethoxycurcumin is the least abundant of the curcuminoids [91,92]. For comparison, the relative purity of the extract was also measured via HPLC. A very good and high purity could be achieved (~87 to 88%) without any pre-treatment of *C. longa* before extraction, as previously done with freeze drying. If also pre-treatments were done before the extraction with a mixture of meglumine/water (85/15 in weight), an even higher purity should be reached.

3.3.3 Conclusion of the curcuminoids extraction from *C. longa* with the ternary systems H₂O/EtOH/TriA (with and without additives in the water phase) and H₂O/DiA/TriA

First, two different food-approved, bio-based, and edible ternary mixtures consisting of water, TriA as solvent, and EtOH or DiA as hydrotropes were investigated and examined concerning their ability to extract and stabilize curcuminoids from *C. longa*. Ternary phase diagrams were obtained and had an expected and similar miscibility gap like a ternary mixture consisting of water, oil, and hydrotrope. With the help of DLS measurements, it was demonstrated that both ternary mixtures build SFMEs.

The solubility of curcumin in the binary mixtures of EtOH/TriA and DiA/TriA and the SFMEs was then investigated using UV/Vis. A solubilising synergy of curcumin was found in the binary mixture of EtOH/TriA. On the contrary, no solubilising synergy was found with the binary mixture DiA/TriA. Upon

the addition of water to the best binary mixtures, a decrease of the maximum solubility of curcumin was found for both SFMEs. This was not surprising, as curcumin is a very hydrophobic compound. On the contrary, upon the addition of water, the curcuminoid extraction efficiencies were enhanced in the following way: curcumin < demethoxycurcumin < bisdemethoxycurcumin. The same order was found concerning the polarity of the curcuminoids (with the help of COSMO-RS calculations). As bisdemethoxycurcumin is the most polar curcuminoid, its extraction efficiency was enhanced the most upon the addition of water. The SFME extraction system containing EtOH as hydrotrope was superior to the SFME extraction system containing DiA. The different curcuminoids' extraction efficiencies were compared to the common water/EtOH 80/20 (in weight) extraction mixture: the addition of a third compound, here TriA, could improve the curcuminoid extraction efficiencies. The big advantage of the two SFME systems is the fact that they are edible and food-approved. Therefore, there is no need to remove the solvent after extraction. It was also demonstrated that keeping the solutions in the darkness enhanced the curcumin stability.

As the maximum curcumin solubility of the SFME H₂O/EtOH/TriA and the binary mixtures was quite high, the reuse of the SFME extraction system for further extraction was investigated. It was found that repeated extraction with fresh *C. longa* leads to a linear increase of the curcuminoid content in the SFME if no saturation occurred. A compromise had to be found between the water content of the SFME extraction system and the weight ratio of *C. longa* to SFME extraction system. Indeed, enough water was needed to swell the *C. longa* rhizomes, allowing a good solvent penetration and enhancing the curcuminoid extraction efficiencies. But too much water led to agitation problems and to saturation because too much SFME extraction system was lost after each cycle of extraction. A higher weight ratio of *C. longa* to SFME extraction system (1:24) would reduce the agitation problems and the risk to reach the saturation, but a smaller one (1:16) was greener and less SFME extraction system was needed or lost.

As further improvement, the relative purity of the SFME extract systems was increased with different pre-treatments of the *C. longa* (hydrodistillation, vacuum distillation, and lyophilisation). The lyophilisation has been found to be the best pre-treatment (high purity reached with a smaller loss of curcumin). Thanks to the pre-treatment, a high relative purity of ~ 94% could be reached. Due to the high purity, the extract was infinitely dilutable with water (unless the miscibility gap was crossed during the dilution with water). The curcumin was also very stable in the SFME extraction system if the samples were stored in the darkness. To even further improve the curcuminoid extraction efficiencies, different additives to the water phase of the SFME have been tested. Pre-tests were conducted in water. Regarding the solubility and the stability of curcumin, meglumine was chosen as the best

additive to be investigated for the SFME extraction system. Moreover, PCA was chosen as an additive for pH regulation and because it showed hydrotropic properties for curcumin and therefore, it could also enhance the curcuminoid extraction efficiencies. First, the stability of curcumin against the pH and light was investigated, because if meglumine was dissolved in water, the pH of the water phase was very high (up to 11.5). It was demonstrated that the high pH had no influence on the curcumin stability in the SFME extraction systems, opposed to light. Therefore, extraction experiments were conducted at different pH values and different meglumine weight concentrations in water. NaOH as additive has also been investigated, but the win in curcuminoids per g *C. longa* was smaller than with meglumine (with and without PCA). A win of 3 mg curcuminoids per g *C. longa* (corresponding to a win of 20 % curcuminoids) could be reached with the SFME extraction system with 5 wt% of water containing 15 wt% of meglumine at pH 11.5 (without PCA). With 5 wt% of meglumine, the best SFME extraction system was with 15 wt% of water at pH 9 (adjusted with PCA). Thus, the addition of meglumine and PCA to the water phase of the SFME extraction system could further improve the curcuminoid extraction efficiencies.

At last, a simple aqueous extraction (only meglumine and water as extraction mixture) was investigated. A very high bisdemethoxycurcumin and demethoxycurcumin extraction efficiency was achieved with only 15 wt% of meglumine in 85 wt% water as extraction system (the highest one for bisdemethoxycurcumin). Moreover, the relative purity of the extract reached ~ 87-88% without any pre-treatment of the *C. longa*.

As opposed to the SFME extraction systems without additive, meglumine and PCA are not agreed in food industry, but are allowed in pharmaceutical industry. The obtained extract solutions with meglumine and PCA could be used and investigated for different pharmaceutical assays.

3.3.4 H₂O/NaSal/EtOAc

3.3.4.1 Ternary phase diagram and solubility measurement

The ternary phase diagram H₂O/NaSal/EtOAc was first deeply investigated in cooperation with the Institut de Chimie Séparative de Marcoule (ICSM) [81]. The monophasic region was investigated using density measurements, DLS, small- and wide-angle X-ray scattering (SAXS) and small-angle neutron scattering (SANS). The critical point (CP) and the tie-lines in the miscibility gap liquid/liquid were also determined and compared to the ternary system H₂O/EtOH/1-octanol. The results will be briefly summarised to better to understand the meaning of the further investigation with curcumin. The ternary phase diagram H₂O/NaSal/EtOAc, as well the density excess map, are shown in Figure 38 (taken from El Maangar et al. [81]).

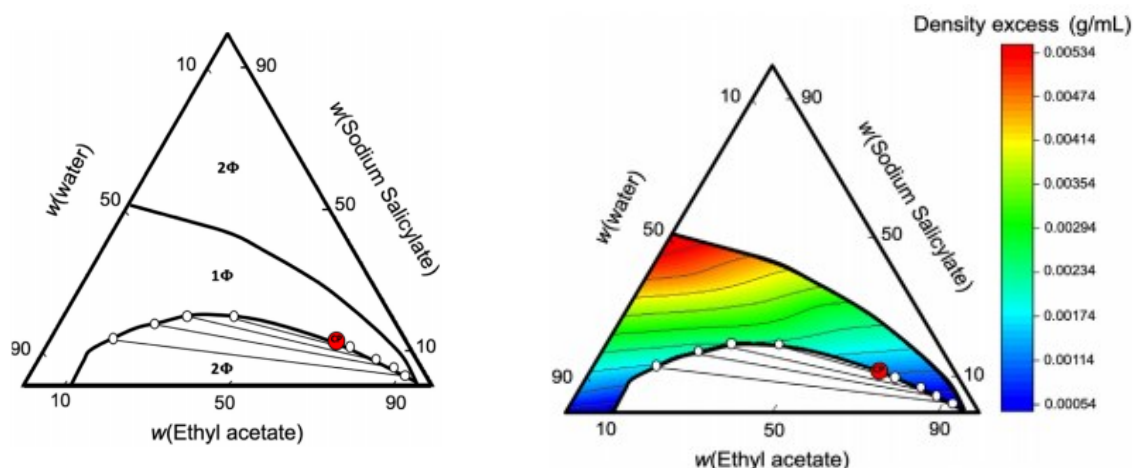


Figure 38: Ternary phase diagram H₂O/NaSal/EtOAc with the determined tie-lines and the critical point (CP) (on the left) and the obtained density excess map (on the right) taken from El Maangar et al. [81].

The ternary phase diagram showed two immiscible regions: one at low NaSal concentrations (common miscibility gap for a water/oil mixture with an hydrotrope, liquid-liquid equilibrium) and one at high NaSal concentration (common for charged molecules, solid-liquid equilibrium). A monophasic region was located in between. To quickly identify the region of interest in the monophasic area, a density excess map has been done. Two regions could be identified: the upper region in the monophasic area (EtOAc-poor region), where a density excess was measured and the region near the critical point. The first surprising result was the different location of the critical point and the area of density excess. Indeed, with a common hydrotrope like EtOH, the density excess was measurable around the critical point and it was not the case here. This means that the critical point in the phase diagram H₂O/NaSal/EtOAc was a common, classical critical point without pre-ouzo region. Indeed, if one drop of water was added to a composition near the phase-separation boundary, the phase separation occurred immediately in the case of H₂O/NaSal/EtOAc. On the contrary, no clear phase-separation occurs in the phase diagram H₂O/EtOH/1-octanol but an “Ouzo” solution was obtained (turbid and stable emulsion), if water was added to a composition near the critical point. The area of density excess was investigated with SAXS and SANS and revealed the presence of aggregates. The largest detectable and stable aggregates were near the crystallisation boundary and it involves 12 NaSal molecules. These 12 NaSal molecules were swollen with the same volume of EtOAc and no water was detected inside the aggregates.

The ternary mixture H₂O/NaSal/EtOAc showed different structuring in the monophasic region and could enhance the solubility and/or extraction efficiency of a hydrophobic compound. Moreover, the ternary mixture can be classified as a SFME and the SFME could also be helpful to stabilize a labile

hydrophobic compound from oxidation. Therefore, the SFME H₂O/NaSal/EtOAc has been investigated for the solubility, extraction, separation, and stabilisation of the curcuminoids from *C. longa*. First, the maximum solubility of curcumin in the monophasic region was investigated prior to extraction. Then the stability of curcumin was studied and finally, the separation of curcumin and the curcuminoids from the SFME extraction system was examined in the liquid-liquid biphasic region. The results concerning the maximum solubility of curcumin in the SFME are presented in Figure 39, as well as the different investigated compositions for extraction and the phase diagram in wt and mol %.

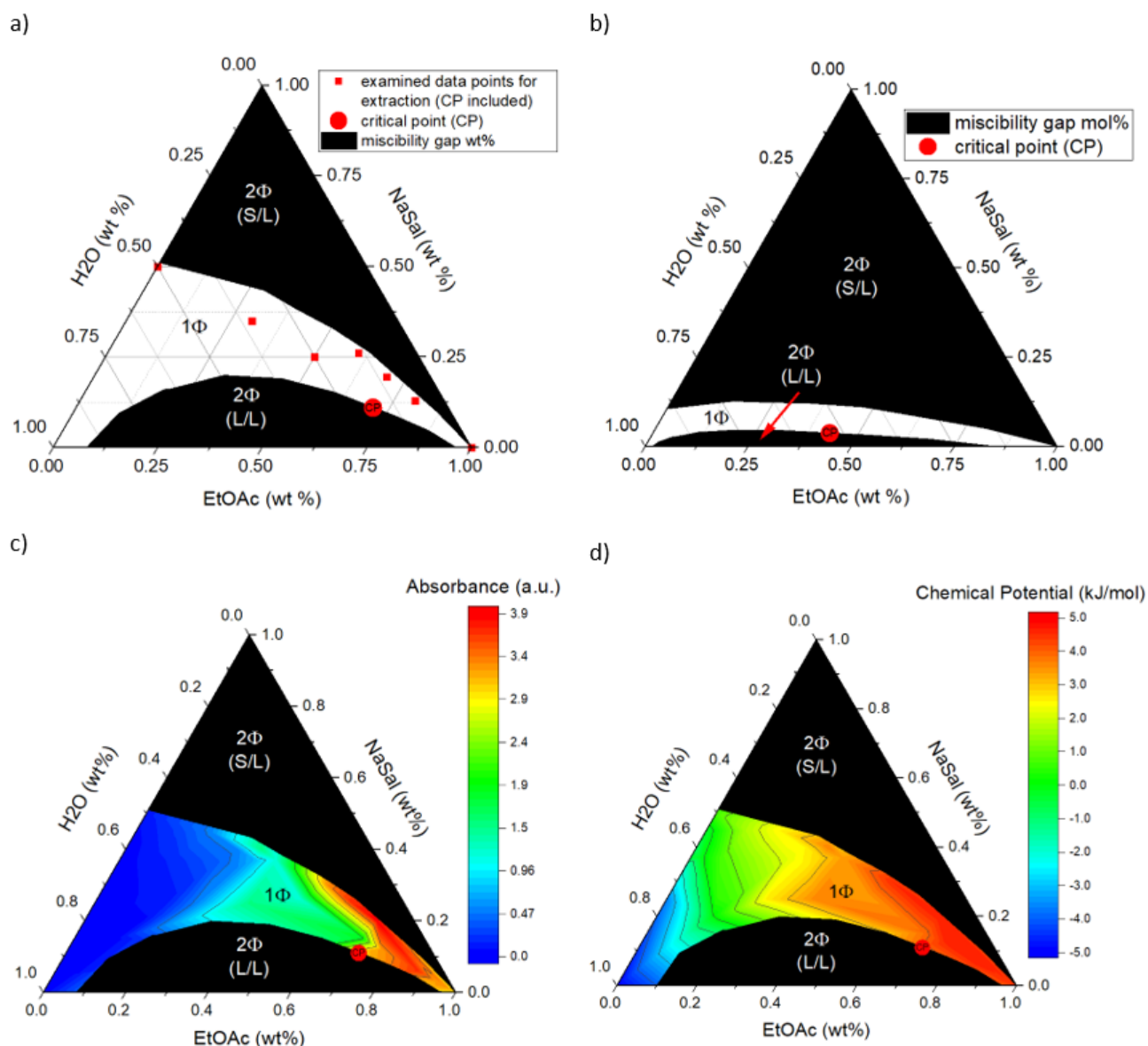


Figure 39: a) Ternary phase diagram H₂O/NaSal/EtOAc in weight percent with the investigated compositions for the extraction of the curcuminoids from *C. longa*. b) Ternary phase diagram in mol percent. c) Solubility map of curcumin in the ternary phase diagram H₂O/NaSal/EtOAc. High solubility is represented in red and low solubility in blue. d) corresponding map of the excess chemical potential, being plotted as the difference to a reference state ($RT \ln$ (concentration of curcumin in the SFME divided by a convenient reference state for curcumin (1 mg curcumin/mL SFME at the same temperature))). The excess chemical potential was calculated from the curcumin concentration in the SFME, which is calculated from the maximum absorbance and the calibration curve in acetone. The red dots represent the critical point (CP) [61].

The absorbance at λ_{\max} at 422 nm (maximum solubility of curcumin) was converted into the chemical potential (first into concentration and then into the chemical potential) to get a better idea of the cost of free energy of solubilisation of curcumin in the SFME system. As can be seen, the maximum solubility of curcumin was located in the EtOAc-rich region. In the left corner of the ternary phase diagram, i.e., in the water-rich region, the solubility of curcumin was unsurprisingly extremely low and the negative value of the chemical potential very large, as curcumin is a very hydrophobic compound and therefore, is not soluble in water. Starting from the same dilution line as investigated previously in the article of El Maangar et al. [81] (binary mixture of NaSal/H₂O 1/1 diluted with EtOAc), the maximum solubility of curcumin increased linearly (corresponding to an increase of chemical potential) with EtOAc content. This was not surprising, as curcumin is soluble in oil. In the aggregate region (upper left corner of the monophasic region), no enhancement of the solubility of curcumin could be detected. It may be difficult to solubilise a relatively large molecule such as curcumin in those aggregates. Between the critical point and the pure EtOAc, the maximum solubility of curcumin increased first then decreased again. Critical fluctuations can lead to an increase of solubility around the critical point [61].

Near the critical point, the pure EtOAc and the crystallisation border (meaning the liquid/solid border), the maximum solubility of curcumin increased again (by a factor of two at most). The gain in free energy of solubilisation (difference between a reference state, the critical point, and a final state, near the crystallisation border) was 0.6 to 0.8 kJ/mol. On the contrary, no gain was obtained near the upper crystallisation border, where the aggregates have been found in the paper of El Maangar et al. [81]. In this area, the water content of the SFME was probably too high, no free EtOAc was available and the aggregates were too small to solubilize curcumin. In the lowest region close to the solid/liquid phase border, the EtOAc content of the SFME is very high and probably some aggregates were formed (just before the crystallisation border) and the curcumin solubility was enhanced. Moreover, it is known in the literature that the intermolecular interactions between the ester group of EtOAc and the hydroxy group of NaSal may be responsible for the improvement of the maximum solubility of curcumin around the critical point [93].

If the two SFME systems (H₂O/NaSal/EtOAc and H₂O/EtOH/TriA) are compared, the maximum solubility of curcumin can be enhanced. Indeed, if the maximum solubility of curcumin is compared to the pure oils (EtOAc and TriA respectively), it was improved by a factor of two and three. Therefore, extraction will be performed, as previously done with the SFME extraction system H₂O/EtOH/TriA.

3.3.4.2 Extraction and stability of the curcuminoids

The extraction experiments were performed along the same dilution line as investigated previously in the study of El Maangar et al. [81] (binary mixture of NaSal/H₂O 1/1 diluted with EtOAc), at the critical

point and near the lower solid-liquid border (EtOAc-rich area of the monophasic region). First, the best weight ratio of *C. longa* to SFME extraction mixture (conducted with the composition at the critical point, H₂O/NaSal/EtOAc 17/12/71 in weight) was determined and then, extraction experiments were investigated. The results are shown in Figure 40. The detailed curcuminoid extraction efficiencies are shown in Table S 12 of the Appendix.

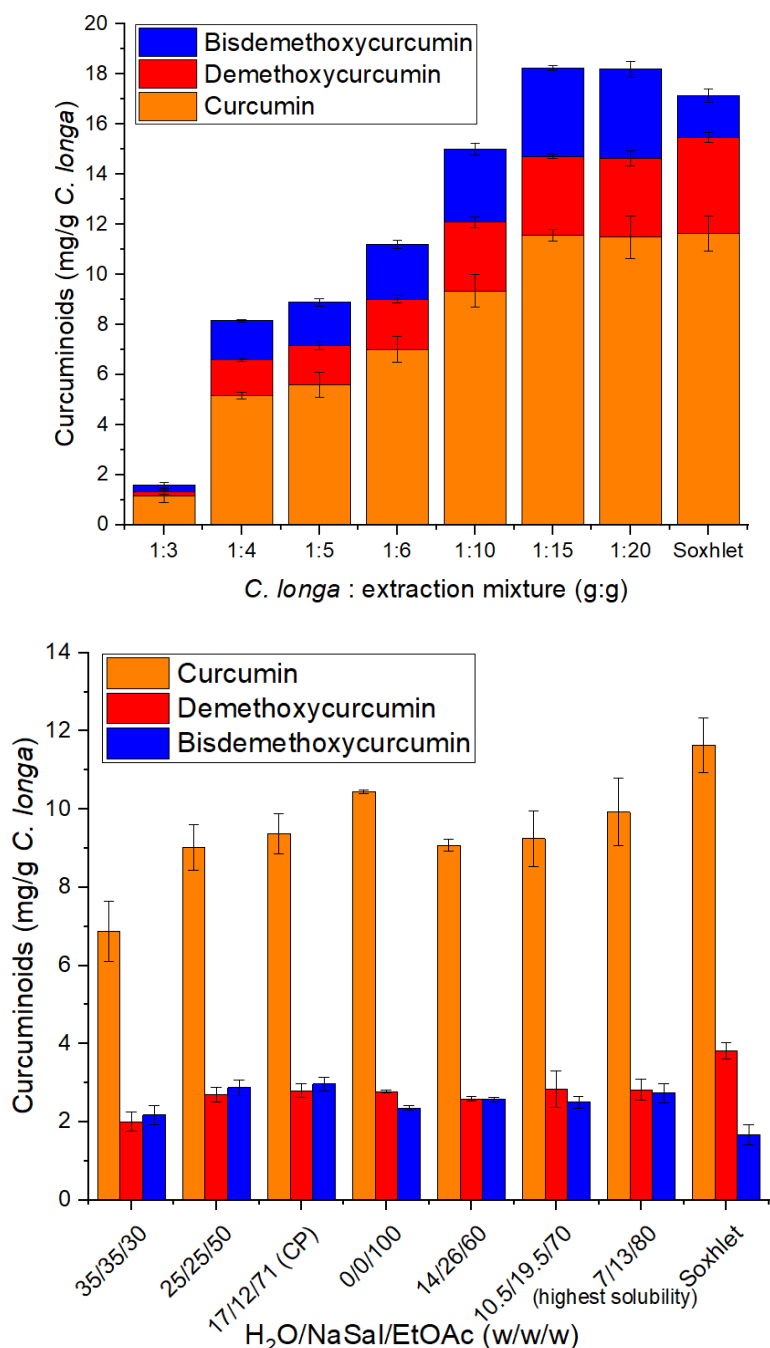


Figure 40: On the top: Curcuminoid yields in mg curcuminoids per g *C. longa* for varying *C. longa* to SFME extraction mixture weight ratios. The used extraction mixture was the SFME composition at the critical point H₂O/NaSal/EtOAc 17/12/71 in weight. The Soxhlet results are also given as a reference. On the bottom: Total curcuminoid extraction efficiencies at different SFME compositions given in weight percent. All extractions were conducted at a weight ratio of 1 to 10 *C. longa* to SFME extraction system and analysed via HPLC [61].

The SFME composition at the critical point was chosen for the investigation of the best weight ratio, because it was in the monophasic region of maximum of solubility of curcumin. The results obtained with Soxhlet were used as a reference. As mentioned before in section 3.3.1.2, the results are underestimated, because the curcuminoids are sensitive to elevated temperature and therefore, can be degraded during the extraction process. Indeed, the used solvent was acetone and the temperature used was above the boiling point of acetone ($> 56^{\circ}\text{C}$). Moreover, during the process, the curcuminoids were continuously exposed to high temperatures in the extraction flask for a long time. As can be seen in Figure 40, the total curcuminoid extraction efficiency increased with the weight ratio *C. longa* to SFME extraction system. At a low weight ratio (1:3), the total curcuminoid extraction efficiency remained very low due to agitation problems. Indeed, too much water was lost with this weight ratio, which was responsible for the swelling of the cells and the oil penetration of *C. longa*. The best weight ratio was 1:15 which reached a total curcuminoid extraction yield of 18.23 mg curcuminoids per g *C. longa* (see Table S 12 of the Appendix). It was higher than the reference Soxhlet extraction (17.13 mg curcuminoids per g *C. longa*, see Table S 12 of the Appendix). This is easily explained, because the extraction efficiency of bisdemethoxycurcumin is underestimated with Soxhlet (bisdemethoxycurcumin is the most sensitive curcuminoid to high temperature). Twice the amount of bisdemethoxycurcumin was extracted with the SFME at the critical point than with Soxhlet. Increasing the weight ratio from 1:15 to 1:20 led to an identical total curcuminoid extraction efficiency. Although the weight ratio 1:15 reached the best total curcuminoid extraction efficiency, the weight ratio 1:10 was chosen for the extraction experiments, because more SFME extraction system can be saved (almost 35%) and therefore, less waste will be produced, compared to the ratio 1:15. In general, the SFME extraction system $\text{H}_2\text{O}/\text{NaSal}/\text{EtOAc}$ seemed to be just as efficient as the Soxhlet extraction. In comparison, the SFME extraction system was less time and energy consuming and gentler than the Soxhlet extraction.

The free energy of extraction ($RT \ln$ (curcumin extracted with the SFME divided by the curcumin extracted with the Soxhlet)) has been calculated and compared to the excess chemical potential (solubility measurement, Figure 39 d)). The correlation is shown in Figure S 15 of the Appendix. The roughly linear correlation between the two proved that extraction and solubility are somewhat related.

The binary mixture $\text{NaSal}/\text{H}_2\text{O}$ (1/1 in weight) was tested for extraction, but no data could be collected, because too much solvent has been lost during the extraction process and therefore, no clear phase separation could be obtained after centrifugation. Two SFME compositions ($\text{H}_2\text{O}/\text{NaSal}/\text{EtOAc}$ 17/12/71 and 7/13/80) and the pure solvent EtOAc were of interest for extraction. Each of the three

extraction systems led to the highest total curcuminoid extraction yields (they differ only from one or two per cent from each other). The highest curcumin extraction yield was reached with the pure solvent EtOAc. It is not surprising, because curcumin is very soluble in oil, but surprising nevertheless, because the solubility map of curcumin showed, that the highest solubility of curcumin was located in the monophasic region and not in the pure solvent (although extraction and solubilisation are two different processes). Moreover, the curcumin extraction efficiency increased with the EtOAc content of the SFME (starting from the binary mixture NaSal/H₂O (1/1 in weight)). The highest demethoxycurcumin and bisdemethoxycurcumin extraction efficiency was reached respectively with the SFME composition at the composition of the highest curcumin solubility (H₂O/NaSal/EtOAc 7/13/80) and with the SFME composition at the critical point (H₂O/NaSal/EtOAc 17/12/71). Indeed, through the addition of water to the system, the extraction efficiencies of demethoxycurcumin and even more of bisdemethoxycurcumin were enhanced (almost 26% more bisdemethoxycurcumin has been extracted). Slightly less curcumin was extracted with the two SFME extraction systems, but the total curcuminoid extraction efficiency remained the same because of the improvement of the demethoxycurcumin and bisdemethoxycurcumin extraction efficiencies. Considering the fact, that curcumin is the most abundant curcuminoids in *C. longa* [91,92] and only 29% of the pure EtOAc was replaced by water and NaSal, the improvement of the bisdemethoxycurcumin extraction efficiency was remarkable (the less abundant curcuminoids). The reasons for this are the same as before: bisdemethoxycurcumin is the most “polar” curcuminoid and therefore, has a higher affinity to more polar solvents like water. In conclusion, it seemed that each SFME extraction system and pure EtOAc have one curcuminoid, which was preferably extracted: Curcumin with pure EtOAc, demethoxycurcumin with the SFME composition at the highest curcumin solubility and bisdemethoxycurcumin with the SFME composition at the critical point. Different SFME compositions could be chosen to obtain preferably one curcuminoid in the SFME extraction system. Globally, the highest total curcuminoid extraction efficiencies were obtained in the domain of highest curcumin solubility.

Once the curcuminoids could be well extracted with the SFME, the stability of curcumin should be investigated in it. Here again, the same dilution line as previously investigated by El Maangar et al. [81] has been looked into. Moreover, the dissolved oxygen has also been measured to give an idea of the potential reasons for the degradation or stabilisation of curcumin. The results are shown in Figure 41.

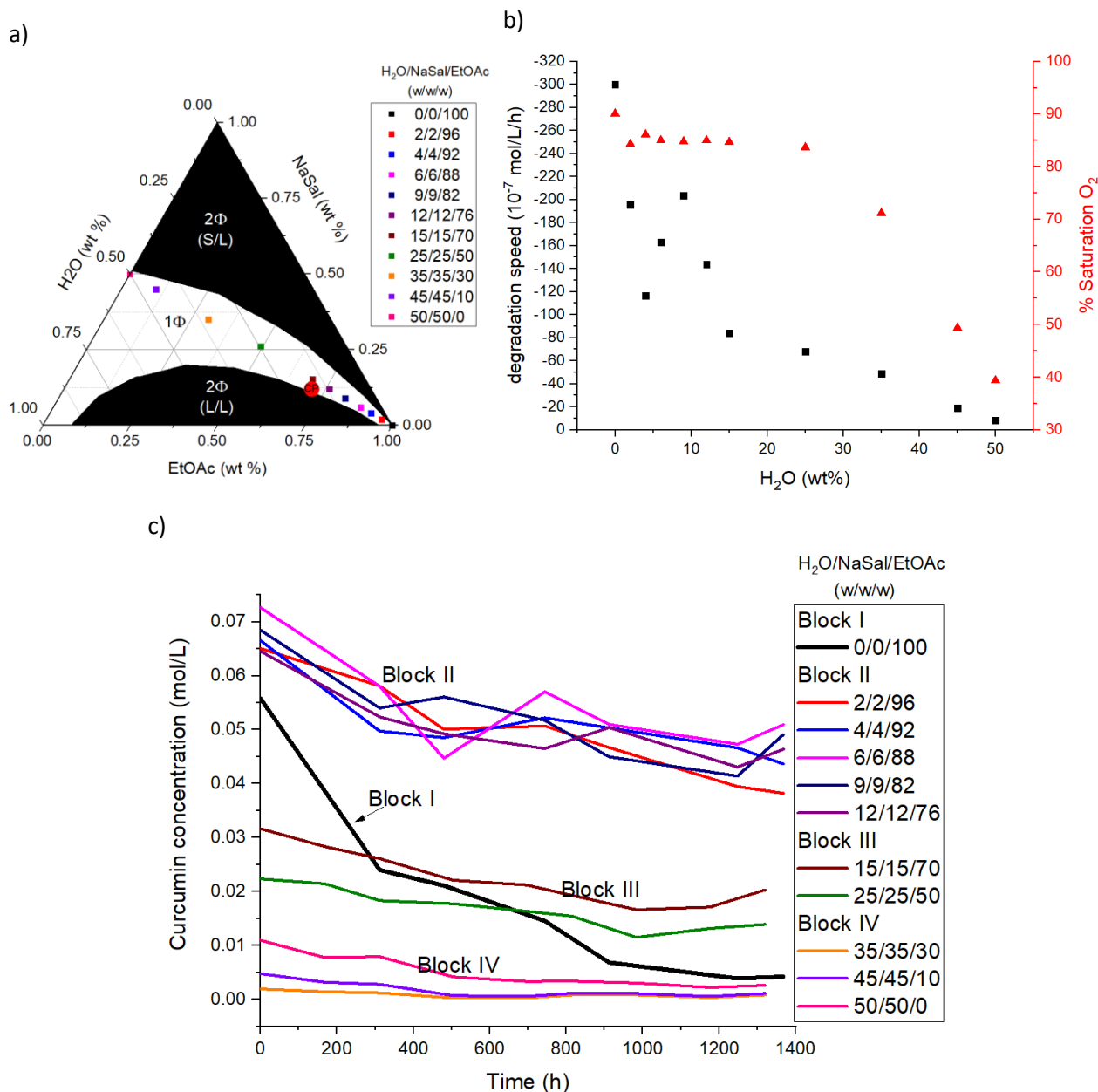


Figure 41: a) Ternary phase diagram with the examined data points for the stability of curcumin over time at day light. b) Calculated degradation speed of curcumin (mol/L/h, black square) and dissolved oxygen (red triangle) as a function of the water content of the SFME. c) Stability of curcumin over time in different SFME compositions and the pure solvent EtOAc [61].

As can be seen, the different investigated SFME samples can be classified into four blocks concerning the curcumin stability: block I (pure EtOAc), block II (SFME composition with low water content 2-12 wt%), block III (SFME composition with medium water content 15 and 25 wt%) and block IV (SFME composition with high water content 35, 45, and 50 wt%). The separation into four blocks for the curcumin stability resulted also follows the curcumin solubility. Indeed, the SFME systems with high water content had a very low curcumin concentration and the SFME systems with low water content (i.e. high EtOAc content) had a high curcumin concentration. The shape of the degradation curve of EtOAc (Block I) differed from the other degradation curves. It decreased exponentially and suggest a

degradation with a high reaction order. Curcumin was not protected and degraded very quickly in this case. On the contrary, all the SFME curves and the binary mixture NaSal/H₂O 1/1 showed a slow linear decrease and therefore, suggest a first order kinetic of degradation, although no interface was clearly present in solution. Normally, to have a first order kinetic reaction an interface is necessary. In the case of the different investigated SFME systems, a weak polar/nonpolar interface as described by Schöttl et al. [21] was present in solution due to the formation of the SFME and the critical fluctuations around the critical point. At this weak interface a first order degradation reaction could take place. Block II showed the SFME system with low water content and the highest curcumin solubility. It is not surprising, because the SFME compositions of block II were in the area of the monophasic region of high solubility. The addition of water and NaSal (1:1 in weight) to the pure solvent EtOAc seems to stabilize curcumin in the SFME system. Indeed, the shape of the degradation curves changed radically over time and the calculated degradation speed was clearly reduced (average of -165 mol/L/h for the SFME system and -300 mol/L/h for the pure solvent EtOAc). The oxygen content of the different investigated systems has been measured to maybe explain the stabilisation of curcumin. As can be seen in Figure 41 b), the oxygen content remained stable for block II and the pure solvent (around 90% O₂ saturation of the oxygen partial pressure in EtOAc and 85% in the SFME of block II). Oxygen is more soluble in oil than in water and in the case of the SFME of block II, the continuous outer-phase is EtOAc and therefore, the oxygen content remained stable. The formation of the SFME could be one reason for the stabilisation of curcumin, but the presence of NaSal could be another one. Indeed, NaSal is an antioxidant and UV-filter [94,95]. The aromatic moiety of NaSal can absorb light from the ultraviolet spectrum and can prevent the degradation of curcumin by photobleaching. The mechanism of degradation of curcumin is mostly an auto-degradation, meaning it needs light to generate a curcumin radical, which will react with the dissolved oxygen in solutions. If the light is previously filtered through the presence of NaSal, no activation of the radical takes place and, therefore no degradation occurs [63]. Derivates of NaSal, like ethylhexyl and octyl salicylate, are well known as UV-filters [95]. Another reason could be molecular interactions. Indeed, Sathisaran et al. [96] found that curcumin and NaSal form a eutectic through weak interactions between the acid group of NaSal and the keto-enol form of curcumin. These interactions are weak but may be strong enough to keep the two molecules very close together in solution and therefore, NaSal could stabilize curcumin and prevent its degradation. In block III and IV, the degradation of curcumin also showed a linear decrease. For block IV, the curcumin solubility and the oxygen content (from 40 % to 70 % O₂ saturation) were so low that the change in curcumin concentration over time was almost undetectable (result in a degradation speed near to 0). Curcumin was most stable in the SFME of block III. Here, the outer-phase was water and curcumin should be present mostly around or in the aggregates. NaSal was preferably in the water-rich phase. If

this was the case, NaSal protected curcumin from degradation by following the so-called polar paradox, which means that an antioxidant protects the most, when it is situated in another phase than the target compound [97].

In general, the curcumin stability was enhanced with an increasing amount of water and salicylate. In other words, the degradation speed was decreased with an increasing amount of water and if water was the outer phase, the degradation speed decreased linearly. Indeed, between 0 and 15 wt% of water in the SFME system, the outer phase was the oil, EtOAc and the degradation speed fluctuated (see Figure 41 b)) because of the fluctuation around the critical point and, because curcumin was mostly solubilised in the outer phase, and therefore was more subject to degradation.

To further look into the antioxidant properties of NaSal, four different samples (EtOAc, EtOAc/H₂O 96/4, EtOAc/H₂O/NaSal 96/2/2 and EtOAc/H₂O/NaSal 99.9/0.05/0.05 in weight per cent) were investigated at curcumin saturation with UV/Vis over time. The results are presented in Figure 42.

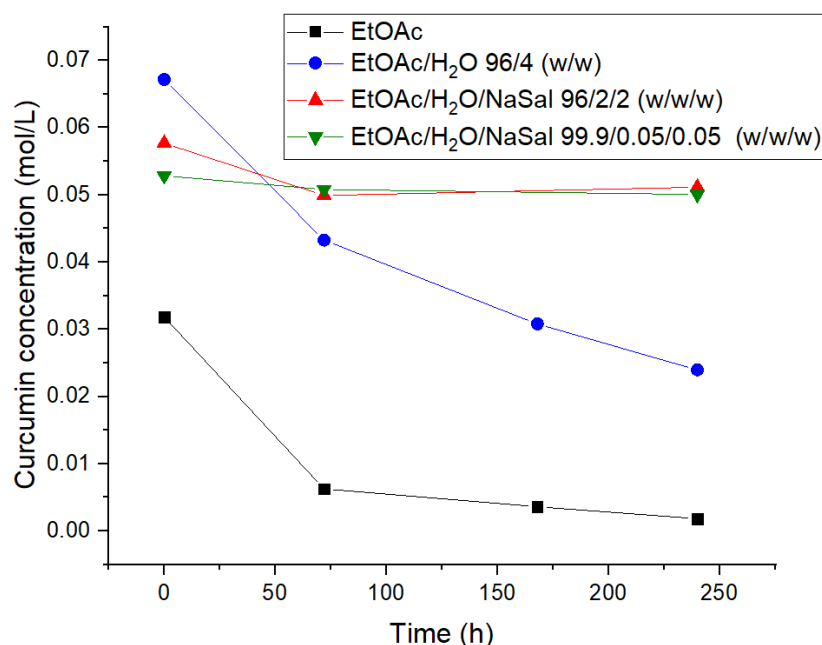


Figure 42: Overview of the curcumin concentration (calculated from the absorbance) in four different systems: EtOAc (black square), EtOAc/H₂O 96/4 in weight (blue point), EtOAc/H₂O/NaSal 96/2/2 in weight (red up-facing triangle) and EtOAc/H₂O/NaSal 99.9/0.05/0.05 in weight (green down-facing triangle) [61].

If no NaSal was present in solution, the shape of the degradation curves was exponential. The saturation of EtOAc with water led to an enhancement of the maximum of solubility of curcumin compared to pure EtOAc. However, this addition did not stabilize curcumin in solution but it took a longer time for curcumin to be degraded completely due to its higher solubility. If NaSal was present in solution, a drastic change of the shape of the degradation curves was noticed from exponential to linear. After 10 days, almost the same amount of curcumin was present in solution, only 50% in the

binary mixture EtOAc/H₂O and almost nothing was left in the pure solvent EtOAc. The measurements were not conducted over months but only over a period of 10 days to show the antioxidant property of NaSal. Obviously, a small concentration of NaSal was sufficient to first enhance the curcumin solubility and then to stabilize and prevent curcumin from degradation.

3.3.4.3 Precipitation and separation of the curcuminoids

The present SFME presents some disadvantages compared to the green, edible, and bio-based SFME consisting of H₂O/EtOH/TriA: the SFME is not edible (NaSal is not allowed in the food industry) and NaSal is not considered as bio-based, although it occurs naturally in some fruits and vegetables. But the SFME has one big advantage: curcumin and the curcuminoids could be separated from the SFME extraction medium after extraction. Indeed, NaSal could be washed with water and EtOAc is volatile. This was not the case for TriA for example. So once the curcuminoids are extracted, dissolved and stabilised in the monophasic region, they can be precipitated by adding water to the SFME extraction system. This phenomenon will be further investigated. First, the influence of curcumin on the tie-lines and the interfacial tension will be studied (using diffusion ordered spectroscopy (DOSY) and SAXS measurements), then the partition coefficient of the curcumin and the curcuminoids will be measured and analysed, and finally the precipitation of curcumin will be investigated. First, we consider the tie-lines. The results are shown in Figure 43. Two pictures of an SFME sample at the critical point composition saturated with curcumin, before (CP) and after addition of water (A8C3), are shown in Figure 44.

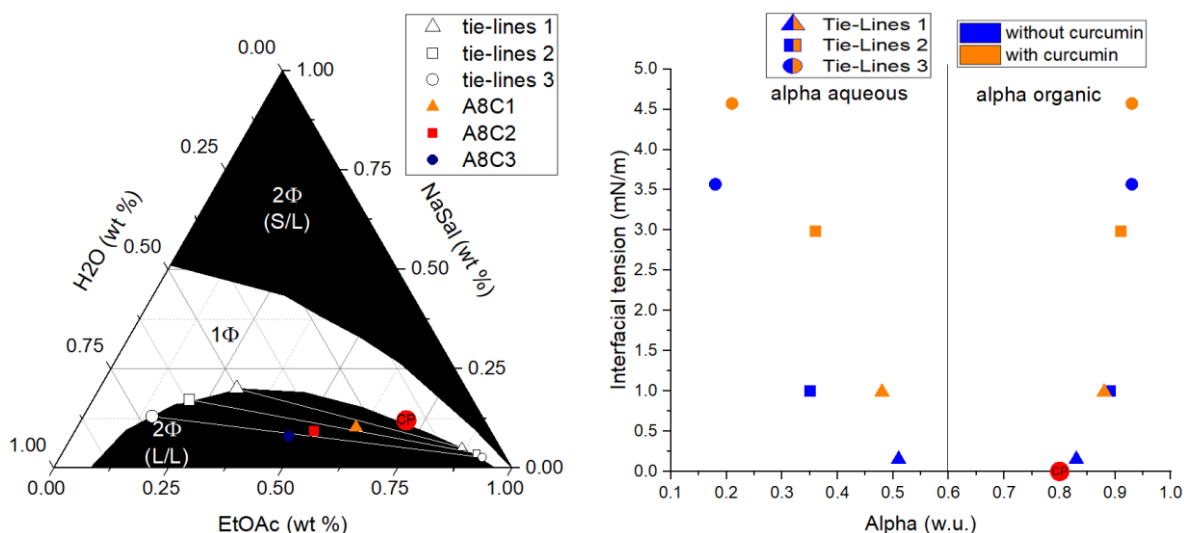


Figure 43: Phase diagram of water, NaSal, and EtOAc with the three different investigated tie-lines (on the left) linked to the interfacial tension with and without curcumin (on the right). The red point represents the critical point. The yellow triangle, red square and blue points in the phase diagram represent the three investigated tie-lines, where the partition coefficient and the DOSY measurements were done. Alpha corresponds to the oil/water ratio [61].



Figure 44: Colour photo of the SFME saturated with curcumin at the critical point composition, before (on the left) and after (on the right) addition of water. The pH varies between 6 and 7. The upper layer contains mostly EtOAc with a small amount of NaSal and H₂O. On the contrary, the lower phase contains mostly H₂O and NaSal with small amount of EtOAc [61].

The addition of 1 wt% of curcumin in the SFME composition at the critical point had no significant influence on the tie-lines. This result was further confirmed by the DOSY and SAXS measurements with and without curcumin. The results are presented in Table S 13 and Figure S 16 respectively. As can be seen, the diffusion coefficients of the single molecules of the SFME (H₂O, NaSal, and EtOAc) remained the same with and without curcumin in the SFME. Therefore, curcumin had no influence on the diffusion coefficients of the components of the SFME. Moreover, no structuring was found at the end of the tie-lines on the water-rich side. On the contrary, a significant structuring was found on the oil-rich side. Only one sample differs with and without curcumin: the water-rich phase of the sample of the first tie-line (meaning A8C1). On the water-rich side of the sample with the highest water content, structuring was found without curcumin, which was destroyed with the addition of curcumin. It seemed as if structuring similar to a bicontinuous microemulsion was present in the water-phase at the highest NaSal content of the SFME after phase separation by addition of water. All these experiments showed that curcumin had no significant influence on the tie-lines in the ternary phase diagram. As additional data, interfacial tension was measured between the oil- and water-rich phases with and without curcumin. As can be seen in Figure 43 on the right, the interfacial tension changed in presence of curcumin. Although curcumin is a hydrophobic compound, curcumin may accumulate at the liquid-liquid interface. The partition coefficient of curcumin $\log(k)$ (logarithm of the ratio between the curcumin concentration dissolved in the oil-rich phase and the curcumin concentration dissolved in the water-rich phase) has been investigated for the three tie-lines. First, the stability of the partition coefficient over time has been checked, then the partition coefficient of the three curcuminoids upon addition of water was investigated. The results are shown in Table 10.

Table 10: Partition coefficient of curcumin directly after solubilisation and after two days at the SFME composition of the critical point with addition of different amounts of water. Partition coefficient for the same SFME composition and the same addition of different amounts of water for curcumin, demethoxycurcumin, and bisdemethoxycurcumin after extraction [61].

Sample \ Log(k)	Day 0	Day 2	
A8C1	0.76 ± 0.01	0.66 ± 0.01	
A8C2	1.22 ± 0.04	1.17 ± 0.01	
A8C3	1.50 ± 0.03	1.59 ± 0.07	
Sample \ Log(k)	Curcumin	Demethoxycurcumin	Bisdemethoxycurcumin
A8C1	1.04	1.10	1.17
A8C2	1.62	1.70	1.64
A8C3	2.12	2.47	2.18

The partition of curcumin is stable over the time, as can be seen in Table 10. Moreover, upon addition of water, the partition coefficient of curcumin increased, meaning that curcumin went from the water-rich phase (depletion) to the oil-rich phase (enrichment). The same trend upon addition of water was observed for the three curcuminoids after extraction. It was expected, as curcumin is very hydrophobic ($\log(P) = 3.00$ [40]). The DOSY measurements and the curcumin solubility map also confirmed the depletion of curcumin in the water-rich phase, as the solubility of curcumin at the ends of the tie-lines on the water-rich side is very low and too low for the diffusion coefficient measurement (see Table S 13 of the Appendix).

Here the measurements were done with 1 wt% of curcumin and therefore, curcumin stayed in solution because the maximum of solubility of curcumin around the critical point was very high. The same experiments were done with an SFME at the critical point composition saturated with curcumin. Upon addition of water, the curcumin precipitated at the interface between the oil-rich and the water-rich phase. The precipitation was kinetic, it took time (at least one day) for curcumin to precipitate and therefore, no precipitate can be seen in the picture in Figure 44 on the right. Since curcumin may accumulate at the interface and upon the addition of water, the oil-rich phase was enriched and the water-rich phase was depleted, the excess of curcumin precipitated at the interface. The precipitate has been investigated with NMR. The presence of curcumin and NaSal was confirmed. By washing the precipitate three times with water, NaSal could be removed. After washing and drying, around 96 ± 23 mg of curcumin could be collected as precipitate. To see if the total amount of curcumin could be

recovered, the oil-rich phase was also collected. EtOAc was removed with a rotary evaporator and the remaining powder washed with water (three times) and dried. Around 411 ± 27 mg of curcumin could be recovered. On balance, almost all the curcumin could be recovered from the SFME extraction system.

As curcumin precipitated, the same procedure was used with an extract solution. Therefore, a SFME extraction system with the composition of the critical point was enriched in curcuminoids (same procedure as before studied in section 3.3.1.3) through 5 successive extraction cycles. After addition of water, the extraction solution was centrifuged to accelerate the precipitation. After separation, the precipitate, an oil with small orange particles, and the oil-rich phase (after evaporation of EtOAc, an orange-yellow oil) were both analysed using HPLC. It showed the presence of curcuminoids and also of the essential oils in both recovered oils. The oils are the essential oils of *C. longa* and the curcuminoids were dissolved in it. Indeed, no pre-treatment like a lyophilisation was performed before the enrichment of the SFME at the critical point composition and therefore, the essential oils were present in the extract solution and disturbed the precipitation process (obtention of a powder and not of an oil as precipitate if the *C. longa* was previously unflavoured).

3.3.5 Conclusion and outlook of the extraction of the curcuminoids from *C. longa* using a ternary mixture of H₂O/NaSal/EtOAc

The SFME H₂O/NaSal/EtOAc has been found to enhance the maximum solubility of curcumin in the EtOAc-rich area of the monophasic region. This was surprising, as curcumin usually is not soluble in water, as can be seen in the water-rich area of the monophasic region. However, an increase of 25% of the maximum solubility of curcumin could be reached using the SFME system compared to the pure solvent EtOAc. Thus, through the addition of an aqueous hydrotrope solution to EtOAc, the maximum solubility could be increased, reaching a maximum around the solid-liquid border in the EtOAc-rich region. Moreover, it was found that not only the maximum solubility of curcumin but also the extraction efficiencies of the curcuminoids from *C. longa* could be enhanced by an anionic hydrotrope. In the same area as the highest solubility of curcumin, extraction experiments were conducted with a weight ratio *C. longa* to SFME extraction system of 1 to 10. The results showed that the extraction efficiency of the curcuminoids was not a linear function of solubility and was dependent on the composition of the SFME extraction system. Indeed, EtOAc was most effective for solving curcumin, the SFME with a composition near the solid-liquid border for bisdemethoxycurcumin, and the SFME at the critical point composition for bisdemethoxycurcumin. The SFME was more polar than EtOAc alone and therefore, it extracted more bisdemethoxycurcumin and demethoxycurcumin, the more polar curcuminoids, due to their "affinity" to more polar solvents. The precipitation of curcumin from the

SFME extraction system has also been investigated. It was found that curcumin saturated in an SFME at the critical point composition was precipitated upon the addition of water. The precipitate could be isolated and purified by washing it with water. Moreover, the presence of curcumin did not change the tie-lines in the miscibility gap. This was also confirmed by DOSY and SAXS measurements.

Further advantages of using an anionic hydrotrope like NaSal are its antioxidant and anti-UV properties. Indeed, NaSal decelerated the degradation of curcumin in solution. It was confirmed by stability tests using UV/Vis measurements. NaSal stabilised curcumin in three different ways (antioxidative, UV-filtering, and lowering of the oxygen solubility) depending on its concentration in the SFME. At high concentrations, NaSal protected curcumin thanks to its anti-UV property, while also decreasing the oxygen solubility in the SFME. At low concentrations, NaSal could act as antioxidant to protect the curcumin. All these results make it an interesting hydrotrope for further investigation of extraction and stabilisation of other labile, hydrophobic compounds.

4 Phytochemical and pharmacological *in vitro* investigation of rhizomes and roots of *Iris germanica* L. growing in Bavaria

4.1 Introduction

4.1.1 *Iris germanica* L. in the history

The iris (*Iris spec.*) history is dating back to the Ancient Greek mythology. Iris means rainbow and is due to the Greek mythology a messenger of the gods. Indeed, the flower of the subgenus Iris (bearded iris rhizome, see section 4.1.3) can be found in every colour of the rainbow [98]. Since centuries, iris is a common garden flower. Its cultivation is dating back to approximately 1500 years before Christ to the pharaoh of Egypt Thutmose III. When Egypt conquered Syria, the pharaoh was captured by the beauty of irises. As avid gardener, he took the plants to his gardens. Since Thutmose III, iris was thought to have therapeutic properties and was used to treat several diseases: periodic fever, epilepsy, headaches, and bites from snakes. Later on, iris became very popular and thus was spread around Europe and Asia. During the middle age, iris was used as a medicinal plant and for perfumes. In Italy, more precisely in Florence, the rhizomes of some iris varieties (*Iris florentina* L., *Iris pallida* Lam. and *Iris germanica* L.) were traditionally used for the manufacture of perfumes. In India, they are still used for religious ceremonies and for medicinal purposes (especially *Iris germanica* L., see section 4.1.4). One of the most popular garden irises today is the German iris (bearded iris), known as *Iris germanica* L..

4.1.2 Genus *Iris*

The *Iris* genus is the largest of the tribe *Irideae* with approximately 300 species and also the largest genus of the family *Iridaceae* [99]. Carl Linnaeus (1707-1778), a Swedish botanist, was the first scientist to develop a classification for the plant kingdom (binomial nomenclature). He described and classified iris species in his book "*Species Plantarum*" (1753) [100]. The classification was then further developed and enriched over the years. The classification of the genus *Iris* is shown in Table 11.

Table 11: Systematic classification of the genus *Iris* in the plant kingdom

Taxon	Latin name	English name
Kingdom	<i>Plantae</i>	Plant
Clade	<i>Tracheophytes</i>	Vascular plant
Clade	<i>Angiosperms</i>	Flowering plant
Clade	<i>Monocots</i>	Monocotyledons
Order	<i>Asparagales</i>	Asparagoid lilies
Family	<i>Iridaceae</i>	Iridaceae
Subfamily	<i>Iridoideae</i>	Iridoideae
Tribe	<i>Irideae</i>	Irideae
Genus	<i>Iris</i>	Iris

Many scientists have tried to subdivide the genus *Iris*. It started with William Rickatson Dykes (1877-1925) in 1913, followed by George Hill Mathewson Lawrence (1910-1978), Georgi Ivanovich Rodionenko (1913-2014) and Brian Frederick Mathew (much more scientist have participated to the classification over the years) [101–105]. Briefly, Dykes divided the genus *Iris* in sections, on the contrary Lawrence and Rodionenko called these sections subgenera. Dykes was the first to term the subgenus *Iris* [101]. Rodionenko provided arguments to split the genus *Iris* in five genera and to classify all rhizomatous irises in the genus *Iris* [103], but this classification was not accepted by Mathew [104,105]. Nowadays, the modern classification of the genus splits into six subgenera (as determined by Mathew in 1981): *Iris* (bearded rhizomatous irises), *Limniris* (beardedless rhizomatous irises), *Xiphium* (smooth-bulbed bulbous irises), *Nepalensis* (bulbous irises), *Scorpiris* (smooth-bulbed bulbous irises) and *Hermodyloides* (reticulate-bulbed bulbous irises). Before, the three subgenera *Xiphium*, *Scorpiris* and *Hermodyloides* were considered as separated genera (*Xiphion*, *Juno* and *Iridodictyum* respectively) but now they are included in the genus *Iris* as subgenera. Today, the subdivision of the genus is still investigated and in constant modification with the development of new techniques (DNA analysis, Internal Transcribed Spacer ...) [98,106–109]. The two largest subgenera (*Iris* and *Limniris*) are further divided into sections: 6 sections for the subgenus *Iris* and 2 for the subgenus *Limniris*.

4.1.3 Subgenus *Iris*

The *Iris* subgenus is the largest subgenus of the *Iris* genus and has been divided into six sections: bearded or pogon irises, *Psamiris*, *Oncocyclus*, *Regelia*, *Hexapogon*, and *Pseudoregelia*. Previously, Rodionenko has reduced the number of sections in the subgenus *Iris* to two sections, *Hexapogon* and *Iris*, depending on the presence or absence of arils on the seeds [103]. On the contrary, John J Taylor

provided some arguments for not included all the arilate species in the section *Hexapogon* in 1976 [110]. *Iris germanica* L. is included in the section bearded irises, which is the largest section of the subgenus *Iris*. *Iris pallida* Lam. and *Iris florentina* L. are also included in the section bearded irises.

4.1.4 *Iris germanica* L.

Iris germanica L. is commonly known as the bearded iris or the German bearded iris in Europe and was first described by Carl Linnaeus in his book “*Species Plantarum*” (1753, volume 1 page 38) [111]. It is a natural hybrid of the subgenus *Iris*. Unfortunately, its parentage is unknown. A botanical view of *Iris germanica* L. is shown in Figure 45.



Figure 45: Botanical view of *Iris germanica* L. (from Koehler's Medicinal-Plants).

Iris germanica L. is an herbaceous perennial rhizomatous plant, growing up to 100-120 cm high and 30 cm wide and is present in Europe, Asia, Nord-Afrika and Nord-America. The straight stem is sparsely ramified and round. The leaves have a blade sword-shaped form. Indeed, *Iris germanica* L. is called “Deutsche-Schwertlilie” or “Ritter-Schwertlilie” (German or Knight sword-lilies) in Germany. The

sparthaceous bract is on the side-lines dry-skinned. The hermaphrodite flowers are triple blossoms and the tepal is most of the time dark purple or pale blue. The flowering period is from May until July, mid to late spring. The plant is an hemicryptophyte, meaning that the overwintering buds of the plant are located at the soil surface. The rhizomes are well-branched and contain the most interesting chemical compounds of the plants. The roots are up to 20-25 cm deep. In Middle-Europe, the plant is sterile. The reproduction occurs only through the division of the rhizomes. On the contrary, *Iris germanica* L. is fertile and bear fruits in the Mediterranean region. A picture of a Bavaria iris field during the bloom time is shown in Figure 46.



Figure 46: Iris field in Bavaria during the bloom time

4.1.5 Phytochemical composition and medicinal use of *Iris germanica* L.

The rhizomes of *Iris germanica* L. find mainly application in the perfume industry. The essential oil of *Iris germanica* L. is one of the most valuable natural products (approximately 15.000 €/Kg of essential oil) [112–114]. But the rhizomes are also used in the food industry for aromatisation of products like liqueur or cigarettes and in Asia, particularly in India, as medicinal plant (Ayurveda) [115]. Ayurveda or Ayurvedic medicine is a healing approach in India and counts to alternative medicine. The bearded iris is used for the preparation of various herbal medicines since centuries. The theory and practice of Ayurveda is pseudoscientific and is not recognised as medicine in Europe due to the absence of real scientific evidence. Almost 80% of the Indian and Nepalese population exert the ayurvedic medicine. The roots are used for example as blood or digestive tract purifier. The plant is also used to treat several skin problems, bronchitis, pneumonia, headache, toothache, muscles pain, to reduce joints inflammation and pain. The main producers of *Iris germanica* L. rhizomes are nowadays Morocco (~100-120 tons), China (~100 tons), France (~40 tons) and Italia (in the past more than 200 tons, but nowadays only ~30 tons, because of the unsustainable prices) [114].

The iris rhizomes contain different secondary metabolites like irones, fatty acids, polyphenols and terpenoids.

4.1.5.1 Irones and fatty acids

Today the irones (mainly α - and γ -irone) are the most valuable compounds of the rhizome of *Iris germanica* L. because of their pleasant odour (almost 63% cis- α -irone and 37% cis- γ -irone of the total irone content) [112,114,116]. They are not present in the fresh plant, but are formed upon degradation (oxidation) of some triterpenoids, the iridals, present in the fresh rhizome [113]. After the harvest, the rhizomes are stored in a stockroom or hangar at ambient air for at least 3-5 years to reach a high concentration of irones by oxidative degradation of the precursor molecules, the iridals. This process is known as aging process. Nowadays, many methods are developed to accelerate the aging process. High levels of irones can be obtained within weeks by storing the rhizomes under an elevated pressure and temperature in an oxygen containing atmosphere (a patented process of M. Flemming [117]). Irones are the main fragrant constituents of the iris butter, which contain about 15% of irones and 85% of fatty acids (mainly myristic acid). Iris butter is obtained by hydro distillation of the dried and ground rhizomes. 0.1 to 0.25% of essential oils can be recovered by hydro distillation. The composition of the different fatty acids present in *Iris germanica* L. rhizomes is shown in Table 12 [114]. The chemical structure of the cis- α -, cis- γ irones and of some iridals are shown in Figure 47.

Table 12: Composition of fatty acids contained in *Iris germanica* L. rhizomes [114].

Fatty acid	Relative proportion (%)
Caprylic acid	1.5
Capric acid	2.3
Lauric acid	3.2
Myristic acid	47.7
Palmitic acid	13.3
Linoleic acid	14.0
α -Linoleic acid	4.1
Oleic acid	4.7
Elaidic acid	3.4
Stearic acid	2.0
Arachidic acid	2.0
Behenic acid	1.6
Lignoceric acid	traces

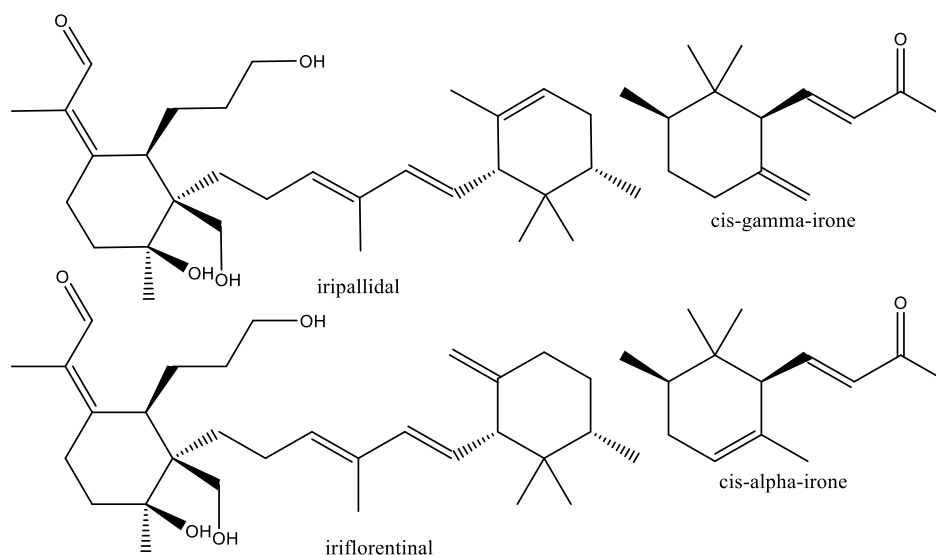


Figure 47: Structure of *cis-α-irone*, *cis-γ-irone*, and two iridals (*iripallidal* and *iriflorentinal*).

4.1.5.2 Flavonoids and isoflavonoids

One of the most important classes of secondary metabolites in the rhizomes of *Iris germanica* L. are polyphenols, especially the flavonoids and its subfamily the isoflavonoids [118,119]. The backbone structure of flavonoids (flavone) and isoflavonoids (isoflavone) is shown in Figure 48. Many flavonoids and isoflavonoids can be described as substituted flavones and isoflavones. Flavonoids and isoflavonoids are produced by plants from the amino acid phenylalanine through the action of several enzymes [120,121]. They are essential for plant growth and development as flavonoids tasks are critical for survival. Therefore, species from all orders of the higher plant kingdom produce them. Flavonoids such as anthocyanins are responsible for the flower colouration (plant pigments) [122]. Together with other flavonoids, they are responsible for the attraction of pollinator animal and seed dispersal [123,124]. They act as UV-protector, protect the plants from insects, mammalian herbivores or against pathogenic microbes as well as from temperature and oxidative stress [123–128]. The biosynthesis of flavonoids is a response of the plants to its environment and therefore, the accumulation of the different flavonoids in the plants differs according to the plant's environment [129–131].

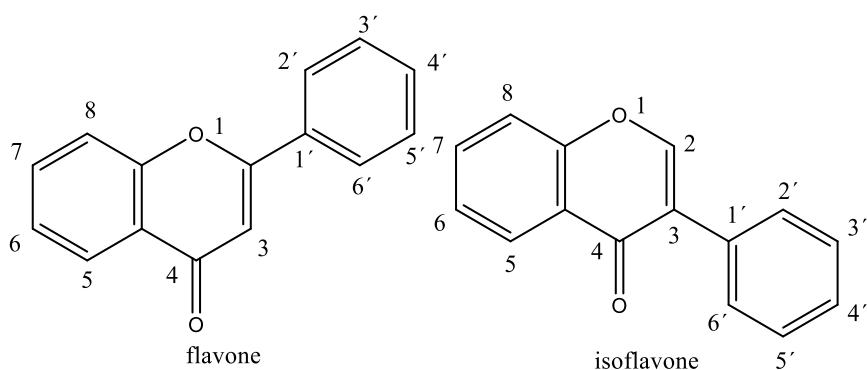


Figure 48: Structure of flavone and isoflavone, which is often the backbone structure of the flavonoids and isoflavonoids respectively.

The rhizomes of *Iris germanica* L. are known to produce the isoflavone irilone [132]. The chemical composition, and especially the phenolic compounds, of the rhizome has been studied over decades. Many different isoflavones are known, for irisfloreantin, irisflogenin, irigenin, irisolidone, and tectorigenin [118,133–136]. Isoflavonoids can be found as isoflavonoid-glycosides (isoflavonoids conjugated to or more sugar-units) or isoflavonoid-aglycones (isoflavonoid alone without any sugar) in the rhizome. Nowadays, isoflavonoids are widely investigated for their ability to protect the plants, but also to provide many health benefits [115,119,137,138]. According to the literature, isoflavonoids possess antioxidant, antimicrobial and anti-inflammatory properties [139–146]. They are mainly used in the pharmaceutical and food industry as food or dietary supplement [147], e.g. against the side effects of the menopause [148].

4.1.5.3 Xanthonoids and benzophenones

Xanthones (xanthonoids) and benzophenones are other classes of secondary metabolites accumulated in the rhizomes of *Iris germanica* L. and belong to the class of polyphenols, but are much less abundant than isoflavonoids. Xanthonoids are also biosynthesized from phenylalanine and benzophenones play a key role as intermediate in the xanthonoids' biosynthesis. The backbone structures of xanthonoids and benzophenones are shown in Figure 49. Like isoflavonoids, xanthonoids have been studied concerning their potential health benefits: they exert antimicrobial, antioxidant, anticarcinogenic or anti-inflammatory properties [149,150]. Benzophenones are used in the cosmetic and pharmaceutical industry, because of their UV-absorbing and fragrance properties [95,151,152], although some of them have been reported as potentially dangerous for human's health [152–155]. Benzophenones are also used as flavoured ingredients in other formulations such as plastics, coatings, adhesive, household cleaning or insecticide products [151,154].

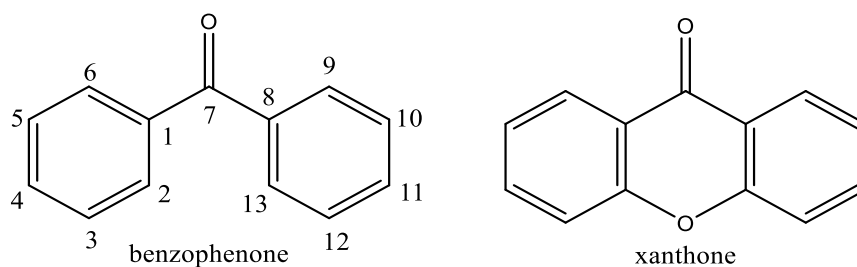


Figure 49: Structure of benzophenone and xanthone, which are the backbone structures of the benzophenones and xanthonoids respectively.

Some xanthonoids and benzophenones have been isolated from the leaves and rhizomes of *Iris germanica* L.: isomangiferin, mangiferin, 6-dehydrojacareubin, iriflophenone and 2,6,4'-trihydroxy-4-methoxybenzophenone [135,156–159].

4.1.6 HeLa, SK-Mel-28 and HMEC-1 cells

4.1.6.1 HeLa and SK-MEL-28

HeLa cells are cancerous cells and the first immortal cell line commonly used in scientific research. The cell line was developed in the John Hopkins Hospital in Baltimore by Dr. George Otto Gey. They are epithelium cells from a cervical cancer taken from **Henrietta Lacks** and were named after the first two letters of her name: HeLa. The HeLa cells grow easily and rapidly, making them of great interest for large scale testing in the research against cancer or virus for example. They are popular cellular models for scientists. SK-MEL-28 are like HeLa cancerous cells and one of a series of melanoma cell lines (type of skin cancer cells). They were established from patient tumour samples of the axillary lymph nodes.

4.1.6.2 HMEC-1

HMEC-1 cells are the first immortalised **H**uman **M**icrovascular **E**ndothelial **C**ells (HMEC) developed by Ades et al. in 1992 [160]. They were immortalised by transfection with a PBR-322-based plasmid containing a gene product of the simian virus 40 A. They retain many of the characteristics of endothelial cells and have a lifespan up to 95 passages without any sign of senescence. On the contrary, non-transfected cells have a lifespan of only 8-10 passages. The culture of HMEC-1 cells is possible without human serum.

4.1.7 MTT assay

The MTT (yellow tetrazole) assay is used to evaluate the cytotoxicity of extracts and isolates on different cell lines [161]. MTT is a yellow tetrazolium salt (3-(4,5-dimethylthiazol-2-yl)-2,5-diphenyltetrazolium bromide). It can be absorbed and reduced by living cells into formazan crystals (see Figure 50). MTT is water-soluble unlike formazan. After solubilisation of the formazan crystals

(blue purple solutions), the absorbance (at 560 nm) is measured to determine the metabolic activity of the cells which can be correlated to the number of viable cells (cytotoxicity). Thus, it is assumed that the concentration of formazan is proportional to the cell viability. The aim of the assay is on the one side to determine the half maximum inhibitory concentration (IC_{50}), meaning the concentration whereby 50 % of the cells are dead (or living), and on the other side to determine the extract and isolate concentrations which are not toxic for the cells in order to perform other assays. By testing the cytotoxicity first, false negative and positive results can be avoided.

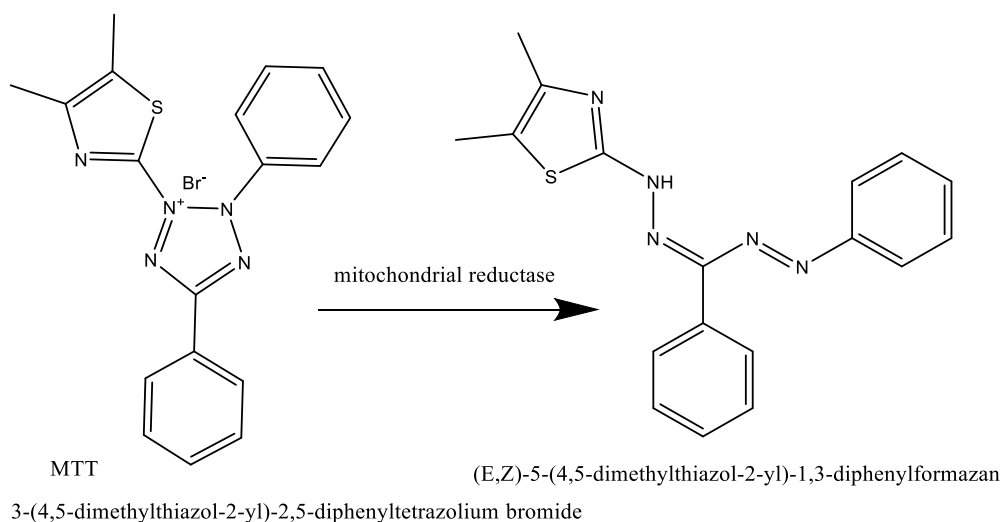


Figure 50: Reduction of MTT to formazan through the mitochondrial reductases.

4.1.8 Inflammatory processes and the role of the ICAM-1 molecule

Inflammation is a natural defence process which is activated by the body in the case of an infection, injury or disease. This process aims to struggle the presence of invading micro-organisms or noxious agents in the tissue. For that, a cascade of complex occurrences (known as signal cascade) is required, starting from the perception and notification of the present invading micro-organisms or noxious agent in the tissue (inflammatory cytokines) and ending with the migration of leukocytes from the blood vessels to the inflamed tissue to struggle them. The defence mechanism will be here explained only roughly. First, the role of different adhesion molecules, and especially the role of the intercellular adhesion molecule-1 (ICAM-1), will be described. After that the different transduction pathways, which lead to the production of ICAM-1, will be explained.

4.1.8.1 Adhesion molecules

Three different groups of adhesion molecules play a role in the extravasation of the leukocytes from the blood vessels to the inflamed tissue and the simplified mechanisms are shown in Figure 51 [162].

Selectin molecules represent the first group of adhesion molecules [163]. Three different selectin molecules are known: L-selectin (Leukocyte-selectin), P-selectin (Platelets-selectin) and E-selectin (Endothelium-selectin). L-selectin is located on the leukocytes. P-selectin and E-selectin are produced by endothelial cells. They are built and migrate to the surface of the cell membrane if an inflammation is detected and notified (through proinflammatory cytokines released from macrophages in the tissue) near the endothelial cells. Cytokines are cell signalling proteins. On the surface of the leukocytes, a selectin receptor (for all the selectins), P-selectin glycoprotein ligand-1 (PSGL-1), is located. By ligand-selectin binding, the leukocytes are decelerated and tethered up the endothelial membrane. Then, the leukocytes start to roll on the surface of the endothelial cells (“rolling”), because ligand-selectin binding is only a weak and not a strong interaction [163,164].

The second group of adhesion molecules are the integrins [165]. Integrins are glycoproteins acting as transmembrane receptors, that facilitate cell-cell and cell-extracellular matrix (consisting of all the macromolecules like glycoproteins, enzymes or proteins that help the cells to get structural and biochemical information on the cell surface) adhesion. Integrin consists of two different glycoprotein-chains, α - and β -subunits, that are not bound covalently. Many of them are known, but only four are of interest concerning the binding of leukocytes to endothelial cells: $\alpha_4\beta_1$, $\alpha_4\beta_7$, $\alpha_L\beta_2$ and $\alpha_M\beta_2$ integrin. If an inflammation is present in the tissue, the integrins are activated through chemokines (proteins of the cytokine family). Chemokines induce a change in conformation of the integrins and allow a strong binding of the leukocyte to the endothelial cell membrane and therefore, decelerate the “rolling”. Integrins also bind with other adhesion molecules present on the surface of the endothelial cells, such as ICAM-1 or VCAM-1 (vascular intercellular adhesion molecule-1) [165,166].

ICAM-1 and VCAM-1 belong to the third group of adhesion molecules, the immunoglobulin superfamily [166]. They are glycoprotein produced by the endothelial cells. They allow the leukocytes to move from the blood vessels to the inflamed tissue (see section 4.1.8.2). α_4 -Integrins bind exclusively with VCAM-1 adhesion molecule (decelerating of the “rolling”) and β_2 -integrins bind with ICAM-1 adhesion molecule (adhering and stopping of the “rolling”). The ICAM-1 molecule is responsible for the migration of the leukocytes to the inflamed tissue. Indeed, the adhesion molecule ICAM-1 plays also a role in the transmigration and is not only responsible for the adhesion and stopping of the “rolling” [163,167].

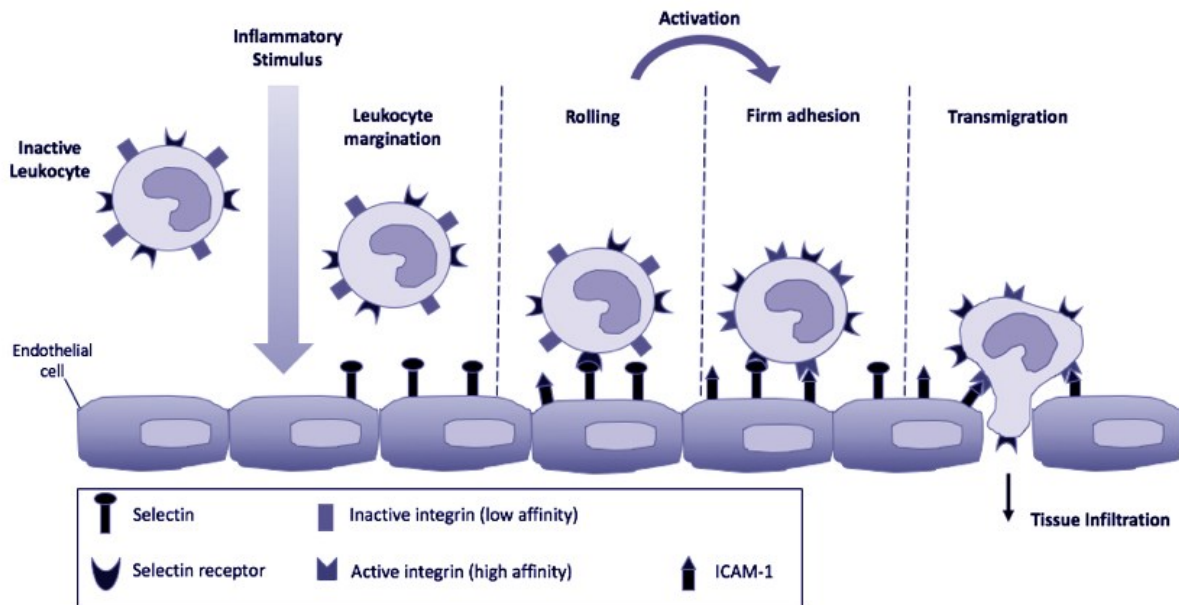


Figure 51: Simplified mechanism of the leukocyte migration from the blood vessels into the inflamed tissue, taken from Thorburn et al. [162].

4.1.8.2 Transduction pathway of the production of ICAM-1

The production and migration of ICAM-1 adhesion molecule to the surface of endothelial cells can be driven by different cytokines (for example TNF- α , IFN- γ , IL-1, LPS, ...) or physical and chemical stimuli like UV radiation, metal ions Co²⁺ or H₂O₂. A simplified signal transduction pathway activating the transcription of ICAM-1 induced by TNF α , IL-1 and IFN- γ is shown in Figure 52 [163,168–170]. Activation of two different signal cascades trigger the transcription of ICAM-1: one with NF- κ B (**N**uclear **F**actor **k**appa **B**) which is activated by the cytokine TNF- α (**T**umour **N**ecrosis **F**actor α) and the other one with STAT hetero- or homodimers (**S**ignal **T**ransducers and **A**ctivators of **T**ranscription) which are activated by the cytokine IFN- γ (**I**nterferon γ). LPS (**L**ipopolysaccharide) can activate both signal cascade (NF- κ B with IL-1 (interleukin) and STAT with IFN- γ). In both signal cascades, a phosphorylation takes place in order to release the transcription factors NF- κ B and STAT. IFN- γ activates the enzymes JAK-1 and JAK-2 (**J**anus **K**inase) by a phosphorylation cascade. JAK-1 and JAK-2 release the STAT hetero- and homodimers, which translocate into the cell nucleus. TNF- α activates the phosphorylation of the protein I- κ B (**I**nhibitor of κ B), which is a regulatory protein of NF- κ B. I- κ B is phosphorylated by IKK α and IKK β (**I**- κ B-**K**inase-**K**omplex). IKK α and IKK β are activated by the protein NIK (**NF**- κ B-**i**nducing **K**inase). The phosphorylation of I- κ B induces the dissociation of the complex I- κ B/NF- κ B and the release of the transcription factor NF- κ B, which translocate into the cell nucleus. Therein, the transcription factors bind to the corresponding promoter region and activate the transcription of the adhesion molecule ICAM-1. It is known that the transcription factor NF- κ B activates also the transcription of other pro-inflammatory genes like cytokines (TNF- α , IL-1 β , ...), chemokines and enzymes [169–173].

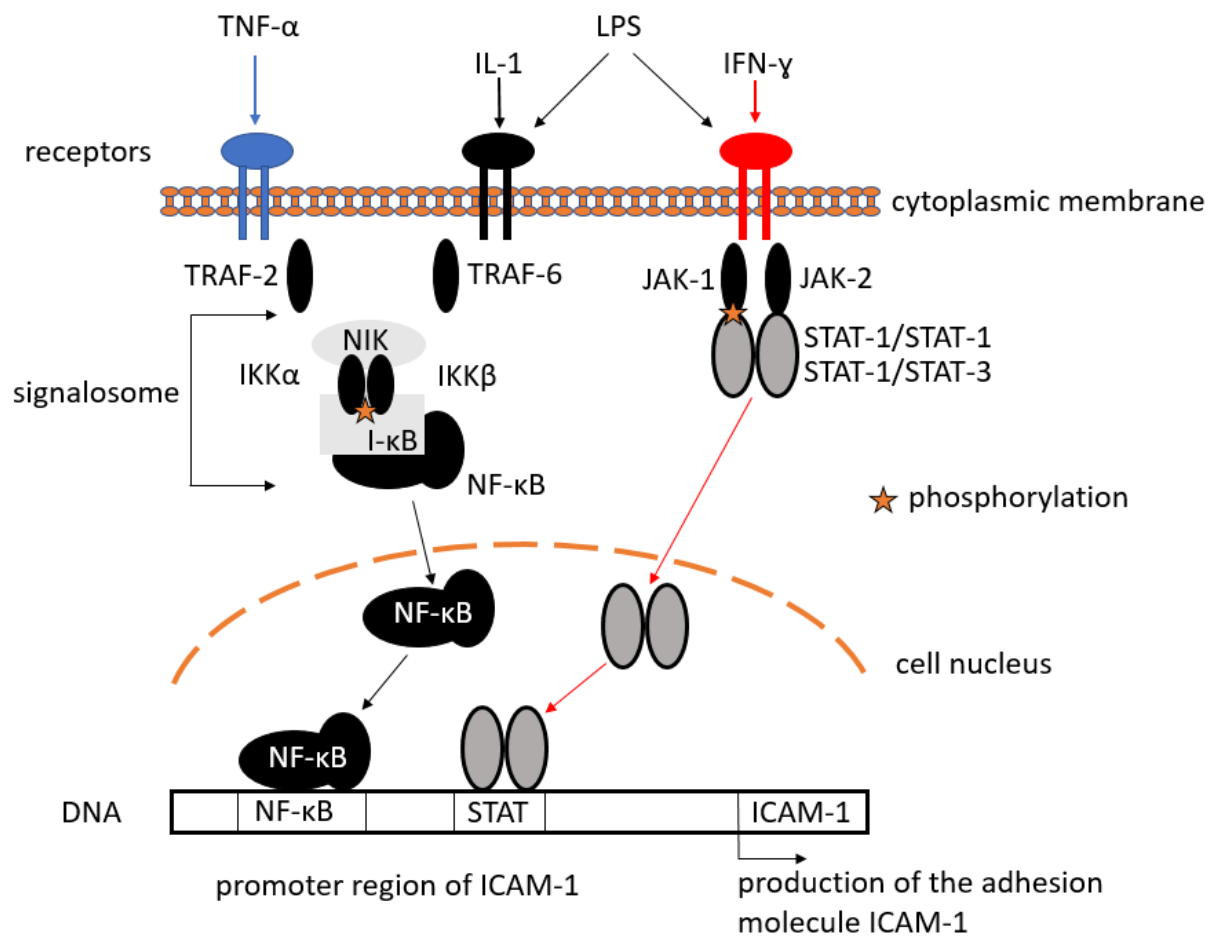


Figure 52: Very simplified pathway of the production of the adhesion molecule ICAM-1. Modified from the doctoral thesis of Marcel Flemming, Luo et al 2005 and Roebuck and Finnegan 1999 [168–170]. LPS (Lipopolysaccharide), TNF- α (Tumour Necrosis Factor α), IL-1 (Interleukin 1), IFN- γ (Interferon- γ), TRAF (Tumour Necrosis Receptor Associated Factor), JAK (Janus Kinase), NIK (NF- κ B Induced Kinase), IKK (I- κ B-Kinase-Komplex), I- κ B (Inhibitor of κ B), NF- κ B (Nuclear Factor Kappa B), STAT (Signal Transducers and Activators of Transcription), ICAM (Intercellular Adhesion Molecule).

The readout of the ICAM assay (see section 4.2.2.8.7 for the description of the assay) is the modified transcription of the adhesion molecule ICAM-1. Indeed, an unphysiologically increased transcription of ICAM-1 is a problem of chronic inflammations like rheumatism, asthma, or arteriosclerosis. Although no inflammation in the tissue is present, the transcription takes place and thereby the tissue can be damaged. In this case, inhibitors of ICAM-1 like parthenolide are of great interest. Parthenolide is a sesquiterpene lactone and reduces the transcription of ICAM-1. It inhibits the binding of NF- κ B to the corresponding promoter or the IKK α and IKK β [170,174,175]. Parthenolide is used as positive control in the ICAM-assay.

4.1.9 Antimicrobial assay: *Escherichia coli* and *Staphylococcus aureus*

Nowadays more and more microorganisms develop an antimicrobial resistance. Antimicrobial assays are very important to screen and test the ability of extracts or molecules to kill microorganisms like

bacteria [176,177]. In the literature, the most used and known methods are agar disk- diffusion and broth dilution methods [178,179].

The agar disk-diffusion method was developed in 1944 by Norman George Heatley [180]. This method is well-known and pretty common [178,179]. Basically, a disk containing the potential antimicrobial agent is placed on an agar surface in a petri dish. Previously, the agar surface was swabbed with the microorganism. The petri dish is then incubated under suitable conditions (commonly 37°C) and after a certain time, the ability to inhibit microbial growth of the antimicrobial agent (through diffusion in the agar) is observed and measured. Indeed, if the potential antimicrobial agent shows an antimicrobial effect, then an inhibition growth circle is obtained, where microorganisms could not germinate and grow. Afterwards, the diameter of the circle, which corresponds to the critical value, is measured and compared with other antimicrobial agents to estimate the antimicrobial property.

The broth dilution method is a liquid method used to determine a MIC (minimum inhibitory concentration). The MIC is the lowest concentration of an antimicrobial agent that is necessary to inhibit the growth of microorganism in a broth medium. Mostly the MICs are given in µg/mL. A defined volume of broth medium is mixed with a dilution of the microorganisms and a defined concentration of the antimicrobial agent. Then the solution is incubated under suitable conditions (mainly 37 °C) and the effect of the antimicrobial agent is observed with the naked eye. To avoid errors, colorimetric methods have been developed. Indeed, the usage of dyes like MTT is often used to measure the MIC with a photometric device like a UV-spectrometer [178,179,181,182]. The risk of errors compared to the observation and determination by the naked eyes is reduced.

In this thesis two different bacteria were used: *Escherichia coli* (*E. coli*) and *Staphylococcus aureus* (*S. aureus*). *E. coli* is an acid-forming and rod-shaped Gram-negative bacterium, whereas *S. aureus* is a spherical Gram-positive bacterium. The Gram's method (or Gram staining) is used to differentiate the bacteria into two large groups: Gram-negative and Gram-positive bacteria [183]. They are differentiated by the composition of their cell wall. The cell wall of a bacteria is composed of a plasma membrane, a periplasm and a murein layer [184]. The major difference between a Gram-positive and a Gram-negative bacterium is the thickness of the murein layer. Gram-positive bacteria possess a thicker murein layer than Gram-negative bacteria. Moreover, Gram-negative bacteria have an outer membrane whereas Gram-positive bacteria do not have one. In general, Gram-negative bacteria and rod-shaped bacteria are respectively more harmful than Gram-positive bacteria and spherical bacteria. Plant extracts are generally more active against Gram-positive than Gram-negative bacteria.

4.1.10 Goal of the investigation, cell biological tests and antimicrobial assays

As previously explained, the main application of the rhizomes of *Iris germanica* L. is found in the perfume industry. Therefore, the rhizomes are aged, distilled to obtain the so-called iris butter and then disposed of. Due to the low yield, iris butter is applied and sold only in small quantities in some perfumes. The main idea of the phytochemical investigation of iris rhizomes is to screen the waste of iris butter (meaning the remaining rhizomes and water in the distillation balloon) for valuable compounds. Moreover, the roots of *Iris germanica* L., which are co-harvested with the rhizomes, make up a huge amount of undesired waste and thus are removed during the harvest (as far as possible). As iris roots might contain valuable compounds too, they were also screened on their phytochemical profile and compared with the rhizomes. Therefore, different rhizome and root extracts of *Iris germanica* L. were compared via TLC. Then, the activity of these extracts on different cell lines, HeLa and SK-MEL, was studied to have a first idea of the cytotoxicity and will be compared and analysed with the TLC results. After that, the phytochemical composition of two iris extracts, 18I4A (EtOAc extract of the rhizomes of *Iris germanica* L.; the rhizomes were first extracted with DCM then with a binary mixture of water and EtOH (H₂O/EtOH 30/70 wt%) and after rotary evaporation of EtOH, the water remaining phase was shaken out with EtOAc; see Figure 54 in section 4.2.2.4) and 19IA (EtOAc extract of the roots of *Iris germanica* L.; the roots were first extracted with n-hexane and then with EtOAc; see Figure 53 in section 4.2.2.4), was investigated using different chromatographic methods (open silica gel column, analytical and semi preparative HPLC). Isoflavonoids and benzophenones were isolated from the rhizomes and the roots. Finally, some isolated compounds and two iris extracts 18I4A and 19IA were tested for anti-inflammatory and anti-microbial properties.

4.2 Material and methods

4.2.1 Material and chemicals

All used chemicals and materials are summarised in Table 13 and Table 14.

Table 13: Listing of all used chemicals.

Chemicals			
Name	Purity	Description/Grade	Company (city, country)
<i>Iris germanica</i> L. rhizomes, leaves and roots	n.a.	Plant growing in Bavaria	SKH GmbH (Ortenburg, Germany)
Ethanol (EtOH)	≥ 99.8%	p.a., Rotipuran®	Merck (Darmstadt, Germany) or Carl ROTH (Karlsruhe, Germany)
Acetonitrile	n.a.	HPLC grade, LiChrosolv®	Merck (Darmstadt, Germany)
Acetic acid	≥ 99.8%	p.a.	Merck (Darmstadt, Germany)
Ethyl acetate (EtOAc)	≥ 99.8%	analytical reagent grade	Thermo Fisher Scientific (Steingrund, Germany)
Dichloromethane (DCM)	≥ 99.8%	analytical reagent grade	Thermo Fisher Scientific (Steingrund, Germany)
Butan-1-ol	≥ 99.5%	p.a., ACS reagent	Sigma Aldrich (Darmstadt, Germany)
Toluene	≥ 99.8%	analytical reagent grade	Thermo Fisher Scientific (Steingrund, Germany)
Methanol (MeOH)	n.a.	HPLC grade, LiChrosolv®	Merck (Darmstadt, Germany)

N-Hexane	99%	analytical grade	Sigma Aldrich (Darmstadt, Germany)
Sulfuric acid 95-97%	95-97%	p.a.	Merck (Darmstadt, Germany)
Anisaldehyde (AA)	≥ 97.5%	FCC, Kosher	Merck (Darmstadt, Germany)
Anisaldehyde reagent (AA reagent)	n.a.	AA: 0.5 mL acetic acid: 10 mL MeOH: 85 mL sulfuric acid: 5 mL	n.a.
Celite®560	n.a.	filter agent, treated with sodium carbonate, flux calcined	Sigma Aldrich (Darmstadt, Germany)
Trifluoroacetic acid (TFA)	≥ 99.0%	for HPLC	Sigma Aldrich (Darmstadt, Germany)
2-Aminoethyl diphenylborinate	98%	for the natural product reagent	Alfa Aesar (Kandel, Germany)
Natural product reagent (N)	n.a.	10 g of 2-aminoethyl diphenylborinate in 1 L MeOH	n.a.
Vanillin	≥ 97.0%	FCC, FG	Sigma Aldrich (Darmstadt, Germany)
Vanillin reagent (V)	n.a.	Solution 1: 4 g vanillin in 400 mL MeOH	n.a.
		Solution 2: 80 mL sulfuric acid in 320 mL MeOH	
Acetone-d ₆	99.80% D	NMR solvent	Eurisotop (Saarbrücken, Germany)
Water	millipore	from a Milli-Q purification system	Merck Millipore (Billerica, MA USA)
Cyclohexane	≥ 99.8%	analytical reagent grade	Thermo Fisher Scientific (Steingrund, Germany)

Dimethyl sulfoxide (DMSO)	≥ 99.5%	for molecular biology	Carl ROTH (Karlsruhe, Germany)
3-(4,5-Dimethylthiazol-2-yl)- 2,5- diphenyltetrazoliumbromide	98%	(MTT) used solution: 4 mg/mL in PBS sterile filtered, conservation: -20 °C	Sigma Aldrich (Darmstadt, Germany)
Phosphate buffer saline (PBS)	n.a.	modified, without calcium chloride and magnesium chloride, sterile filtered	Sigma Aldrich (Darmstadt, Germany)
Trypsin/EDTA	n.a.	used solution: 10 % (v/v) Trypsin/EDTA (0.5%/0.2% in 10x PBS) in PBS	Biochrom AG (Berlin, Germany)
Minimum Essential Medium Eagle (MEM)	n.a.	Modified, with Earls's salt and reduced NaHCO ₃ (0.85 g/L), without L-glutamine, sterile-filtered, based medium for HeLa cells	Biochrom AG (Berlin, Germany)
L-Glutamine	n.a.	200 mM	Biochrom AG (Berlin, Germany)
Fetal Bovine Serum (FBS)	50 mL aliquoted	conservation: -20°C, defrosting with a water bath at 37 °C	Biochrom AG (Berlin, Germany)
Non-Essential Amino acid (NEA)	n.a.	100x-concentrate	Biochrom AG (Berlin, Germany)
HeLa medium	n.a.	MEM: 500 mL L-glutamine: 5 mL FBS: 50 mL NEA: 5 mL	n.a.
Dulbecco's Modified Eagle Medium (DMEM)	n.a.	+ 4.5 g/L D-Glucose and 2 mM glutamine	Gibco® (Paisley, United Kingdom)
HAM'S F-12 Medium	n.a.	With 1.176 g/L NaHCO ₃ , with stable glutamine	Sigma Aldrich (Darmstadt, Germany)
SK-MEL-28 medium	n.a.	DMEM: 500 mL HAM'S F-12: 500 mL FBS: 50 mL	n.a.

Endothelial Cell Growth Supplement (ECGS)	n.a.	2% FBS, EndoCGS (Endothelial Cell Growth Supplement), Heparin, bFGF (basic Fibroblast Growth Factor), EGF (Epidermal Growth Factor), Hydrocortisone, Glutamine	PeloBiotech GmbH (Planegg, Germany)
Endothelial Cell Basal Medium (ECBM)	n.a.	based medium for HMEC-1 cells w/o Glutamine	PeloBiotech GmbH (Planegg, Germany)
Antibiotic	n.a.	50 µg gentamicin /mL water	PeloBiotech GmbH (Planegg, Germany)
HMEC-1 medium (ECGM)	n.a.	ECBM: 500mL ECGS: 27 mL FBS: 50 mL Antibiotic: 1.5 mL	n.a.
Trypan blue solution: 3,3'-Dimethyl-4,4'-bis(5-amino-4-hydroxy-2,7-disulfonaphtyl-3-azo)-[1,1'-biphenyl]	dye content ~ 37%	used solution: 0.4% (m/V) trypan blue in PBS, sterile-filtered, conservation: 4°C	Sigma Aldrich (Darmstadt, Germany)
Sodium dodecyl sulfate (SDS)	92.5-100.5%	used solution: 10% (m/v) in water, sterile-filtered	Sigma Aldrich (Darmstadt, Germany)
Formaldehyde solution	phosphate buffered	10 wt% solution in water	AppliChem GmbH (Darmstadt, Germany)
TNF-α	≥ 97%, recombinant, human, <i>E. coli</i>	used solution: 17 µg/mL of a 0.1% Bovine Serum Albumin in PBS	Sigma Aldrich (Darmstadt, Germany)
IFN-γ	≥ 97%, recombinant, human, <i>E. coli</i>	used solution: 4 µg/mL PBS	PeproTech (Hannover, Germany)
Parthenolide	≥ 97%	used solution: 100 mM in DMSO	Callbiochem (Bad Soden, Germany)

Collagen G	4 mg/mL HCL from FBS	used solution: 0.25% collagen G in PBS (v/v)	Biochrom AG (Berlin, Germany)
FITC-marked antibody	n.a.	FITC-marked mouse antibody IgG1 for ICAM-1	Biozol (Eching, Germany)
Lysogeny broth (LB) // LB-medium	n.a.	LB-miller: NaCl 10g/L, Tryptone 10 g/L and yeast extract 5 g/L // 25 g of LB in 1 L H ₂ O	Merck (Darmstadt, Germany)
<i>S. Aureus</i>	n.a.	20231, type strain, ATCC 12600	DSMZ GmbH (Braunschweig, Germany)
<i>E. coli</i>	n.a.	K12	DSMZ GmbH (Braunschweig, Germany)
Iron	≥ 90% α-iron	Mixture of isomers (mainly the α-isomer)	Sigma Aldrich (Darmstadt, Germany)

Table 14: Listing of all used materials.

Materials		
Name	Description	Company
Cellulose filter	grade 1289, diameter 240 mm, 84 g/m ²	Sartorius (Göttingen, Germany)
Syringe filter 0.2	0.2 µm PTFE or CA Membrane, diameter 13 or 25 mm	VWR international (Ismaning, Germany)
Silica gel plate	TLC silica gel 60 F ₂₅₄ 20x20 cm	Merck (Darmstadt, Germany)
Silica gel plate RP-18	TLC silica gel 60 RP-18 F ₂₅₄ 20x20 cm	Merck (Darmstadt, Germany)
GC-HPLC vials	brown glass 1.5 mL ND9 with screw caps	Carl ROTH (Karlsruhe, Germany)
TLC-Chamber	twin through chamber for 100 x 100 mm plates	Camag (Muttens, Switzerland)
TLC apparat	Linomat 5 for the application Reprostar 3 for the documentation	Camag (Muttens, Switzerland)

	WinCats 1.4.2 as software	
Micropipette for TLC-application	Hirschmann® ringcaps®, 5 µL	Hirschmann (Eberstadt, Germany)
NMR tubes	NMR tubes borosilicate length 8 inch	Deutero (Kastellaun, Germany)
NMR spectrometer	Advance 400 MHz	Bruker Corporation (Billerica, MA USA)
NMR software	Topspin®3.2	Bruker Corporation (Billerica, MA USA)
Sea sand	extra pure	Merck (Darmstadt, Germany)
Silica gel column 1	length: 55 cm, diameter: 2.2 cm	Glass blowing workshop (University of Regensburg, Germany)
Silica gel column 2	length: 70 cm, diameter: 3.6 cm	
RP-18 column analytical HPLC	C-18 phase, 5 µm, 100 Å, 250 x 4.6 mm, Eurosphere	Knauer GmbH (Berlin, Germany)
Biphenyl column + precolumn analytical HPLC	Biphenyl phase, 5 µm, 100 Å, 250 x 4.6 mm Kinetex®/Phenomenex®	Phenomenex (Aschaffenburg, Germany)
RP-18 column preparative HPLC	Nucleodur C18 Isis, 5 µm, 100 Å, 250 x 21 mm	Machereynagel (Düren, Germany)
Biphenyl column + precolumn preparative HPLC	Biphenyl phase, 5 µm, 100 Å, 250 x 21.2 mm, Kinetex®	Phenomenex (Aschaffenburg, Germany)
Mass-spectrometer	Agilent MS Q-TOF 6540 UHD ion source: AJS ESI G6540A	Agilent (Santa Clara, USA)
Cell culture bottle	150 cm ²	TPP (Trasadingen, Germany)
Cell culture bottle	75 cm ²	Greiner Bio-One (Frickenhausen, Germany)
Falcon tubes for cell culture	15 and 50 mL, sterile	Greiner Bio-One (Frickenhausen, Germany)

C-chips	Grid pattern of Bürker-Türk, DHC-B02	NanoEntek Inc. (Pleasanton, USA)
Pipettes for cell culture	230 mm, sterile (done with an autoclave)	VWR (Darmstadt, Germany)
Pipettes, serological	5 and 10 mL, sterile	Greiner Bio-One (Frickenhausen, Germany)
Pipette tips	10, 200 and 1000 µL	Greiner Bio-One (Frickenhausen, Germany) and Sarstedt AG & Co. (Nümbrecht, Germany)
Cell culture bench	HeraSafe KS	Thermo Scientific (Langenselbold, Germany)
Cell culture incubator	AutoFlow IR Direct Heat NU-5500 E, temperature 37°C, 5% CO ₂	Integra Biosciences GmbH (Fernwald, Germany)
24-wells plate	sterile, for cell culture	Greiner Bio-One (Frickenhausen, Germany)
96-wells plate	sterile, for cell culture	TPP (Trasadingen, Germany)
Autoclave	Melag Autoclav 23 (small one, in the lab)	Melag Medizintechnik (Berlin, Germany)
	Systec VE-120	Systec GmbH (Linden, Germany)
Fluorescence-activated Cell Sorting (FACS)	Becton Dickinson FacsCalibur®, software: CellQuestPro	Becton Dickinson (Franklin, USA)
FACS-tubes	polystyrene pound bottom tube 5 mL	Becton Dickinson (Franklin, USA)
Vortex	Vortex mixer VV3	VWR (Darmstadt, Germany)
Plate reader	Spectra FluorPlus, software: Xfluor4 V 4.40	Tecan (Crailsheim, Germany)

Centrifuge cell culture	Heraeus Megafuge 1.0 R Sepatech	Thermo Scientific (Langensfeld, Germany)
Rotary evaporator	Glassware set G3, vacuum pump Rotavac Vario Pumping with digital vacuum control, Heidolph	Heidolph Instruments GmbH & Co. KG (Schwabach, Germany)
Eppendorf cup	1.5, 2 and 5 mL	Eppendorf (Hamburg, Germany)
Pipettes	0.1-2.5 μ L, 2.5-10 μ L, 10-100 μ L, 100-1000 μ L	Eppendorf (Hamburg, Germany)
Pipette controller	Accu-jet [®] pro	Brand GmbH & Co.KG (Wertheim, Germany)
Water bath	WB 22	Memmert GmbH & Co. KG (Schwabach, Germany)
Drying chamber	H3000	Binder GmbH (Tuttlingen, Germany)
	D-6450	Heraeus (Hanau, Germany)
Freeze dryer	Freeze Dryer Modulyo [®]	Edwards (Feldkirchen, Germany)
Separating funnel	3 liters	Carl ROTH (Karlsruhe, Germany)
Grinder	Cutting Mill Pulverisette 15	Fritsch (Idar-Oberstein, Germany)

4.2.2 Methods

4.2.2.1 Harvest and processing

The rhizomes, roots and leaves of *Iris germanica* L. were harvested in summer 2018 in Lower Bavaria. In summer 2019, only the roots were harvested. In summer 2020, only the rhizomes were harvested. For the denomination of the different extracts (see section 4.2.2.4), the two first number (18, 19 and 20) correspond to the year of the harvest. After being harvested, the different plant parts were washed, sun dried and finally ground (2 mm pieces). In 2018, one part of the rhizome harvest was aged before being ground (see section 4.2.2.2, aged rhizome). The other part of the rhizomes was directly used for the extraction process (unaltered rhizome). One part of the aged rhizomes was distilled after being ground (production of iris butter, see section 4.2.2.3), while the other part of the aged rhizomes was used for the extraction process (see section 4.2.2.4). Unaltered rhizomes were not distilled. In 2019, one part of the root harvest was aged (see section 4.2.2.2) before being ground. One part of the aged roots was used for the extraction process and the other part was distilled. The unaltered part of the root harvest was directly ground. One part of the unaltered roots was directly used for the extraction process and the other part was distilled. After the harvest in summer 2020 and after the distillation of some aged rhizomes in winter 2020, the residue in the distillation balloon was used as raw material for the extraction process.

4.2.2.2 Aging process

Roots (2019) and rhizomes (2018) were aged according to the aging process development by Marcel Flemming [117]. The rhizomes or roots were placed in a reactor under ambient air, at 10 bar and 45°C for 6 weeks.

4.2.2.3 Distillation

700 g of aged rhizomes were hydro distilled with 3.5 L of deionised water during approximately 8 hours using a Clevenger distillation. The rhizomes were previously macerated during 16-18 hours in water. Unaltered rhizomes were not distilled. 200 g of unaltered roots were hydro distilled using the same method, with and without maceration. 200 g of aged roots were hydro distilled without maceration using the same method.

4.2.2.4 Extraction process

The different extracts of the different parts of the plants were obtained using the extract pathway in Figure 53 and Figure 54. A summary of all achieved extracts with the description of the extraction process is shown in Table 15. The extraction procedure was repeated three times with all extraction solvents (one extract is the result of three successive extractions) except for the distillations, which was done only one. The plant material to extraction solvent in weight ratio was of 1 to 7 with the

rhizomes and leaves and 1 to 9 with roots. 1.2 kg of fresh (=unaltered) rhizomes (harvest 2018), 1 kg of aged rhizomes (harvest 2018), 0.8 kg of fresh roots (harvest 2018), 0.5 kg of leaves (harvest 2018), 0.18 kg of fresh (=unaltered) roots (harvest 2019), 0.15 kg of aged roots (harvest 2019) and three litres of the residue of the hydro distillation of aged rhizomes (harvest 2020) were used for the extraction processes (see Figure 53 and Figure 54).

Table 15: Summary of all achieved extracts, as described in Figure 53 and Figure 54.

Extract name	Plant material*	solvent	Description of the extraction process
18I1	fresh rhizomes	DCM	Plant material was extracted with DCM.
18I2	aged rhizomes	DCM	
18I3	fresh roots	DCM	
18I7	fresh leaves	DCM	
18I4A	fresh rhizomes	EtOAc	Plant material was first extracted with DCM then with a binary mixture of water and EtOH (H ₂ O/EtOH 30/70 wt%) and after rotary evaporation of EtOH, the water remaining phase was extracted with EtOAc.
18I5A	aged rhizomes	EtOAc	
18I6A	fresh roots	EtOAc	
18I4B	fresh rhizomes	BuOH	Plant materials were first extracted with DCM then with a binary mixture of water and EtOH (H ₂ O/EtOH 30/70 wt%) and after rotary evaporation of EtOH, the water remaining phase was extracted successively with EtOAc and BuOH.
18I5B	aged rhizomes	BuOH	
18I6B	fresh roots	BuOH	
18I4W	fresh rhizomes	Water	Plant materials were first extracted with DCM then with a binary mixture of water and EtOH (H ₂ O/EtOH 30/70 wt%) and after rotary evaporation of EtOH, the water remaining phase was extracted successively with EtOAc and BuOH. Finally, the remaining water phase was lyophilised to obtain the extract.
18I5W	aged rhizomes	Water	
18I6W	fresh roots	Water	
18I9	aged rhizomes	x	Iris butter obtained from hydro distillation.
19I9	fresh roots	x	
19I9a	aged roots	x	
19IH	fresh roots	n-hexane	Plant materials were extracted with n-hexane.
19IHa	aged roots	n-hexane	
19IA	fresh roots	EtOAc	Plant materials were first extracted with n-hexane and then with EtOAc.
19IAa	aged roots	EtOAc	
20IH	aged rhizomes	n-hexane	Residue of the hydro distillation (water and remaining plant materials) was extracted successively with n-hexane, EtOAc and BuOH.
20IA	aged rhizomes	EtOAc	
20IB	aged rhizomes	BuOH	

*fresh always mean unaltered, but dried plant material

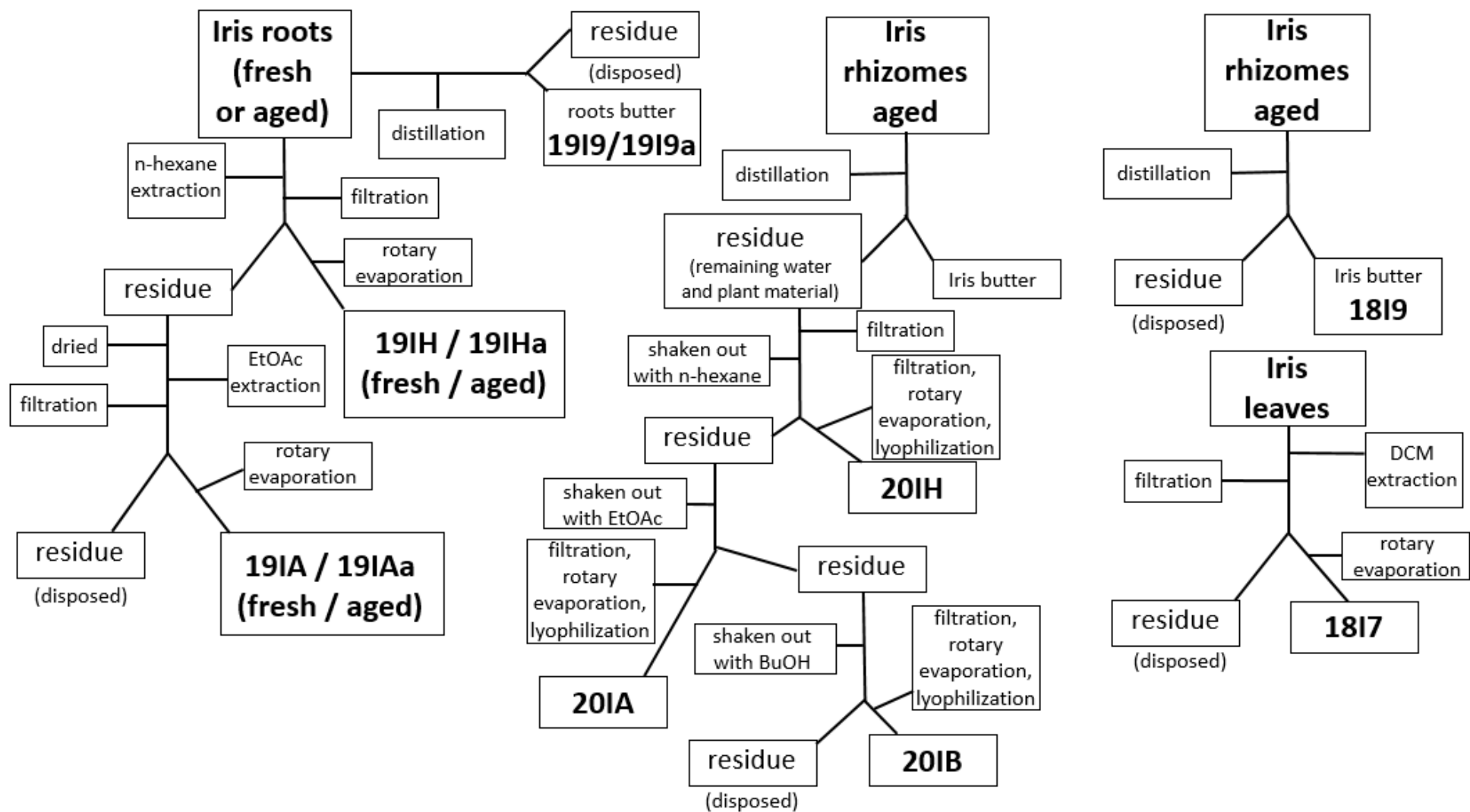


Figure 53: Extract pathway for the fresh (unaltered) and aged roots, the aged rhizomes, and the fresh (unaltered) leaves. For filtration, a Buchner filtration or a filtration using Celite®560 (if a Buchner filtration was not successful) were used. A drying chamber was used for drying, and a freeze dryer was used for lyophilisation. A separating funnel was used if a residue was shaken out with a solvent. The extract names as well as the used plant material part are underlined in bold.

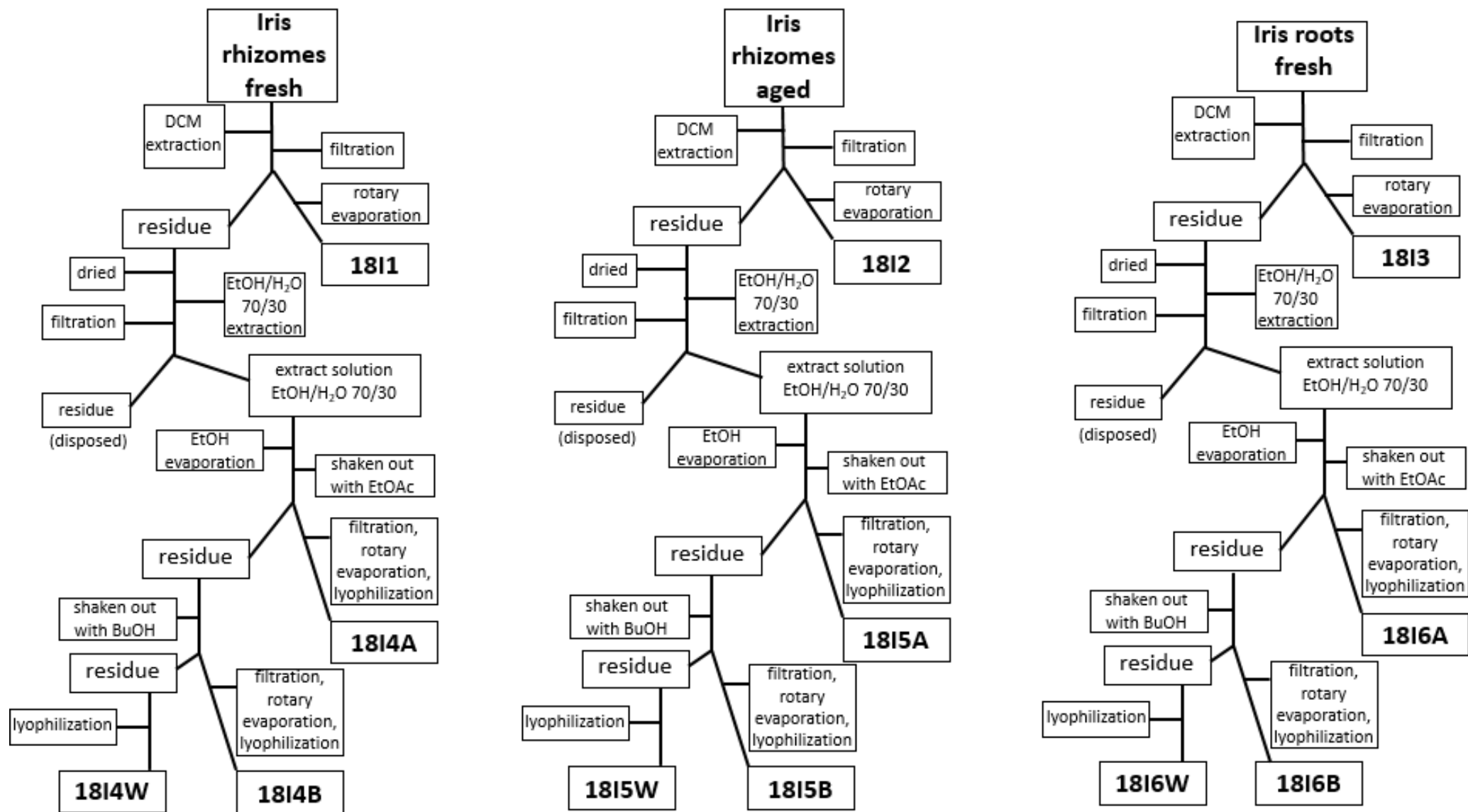


Figure 54: Extraction pathway for the fresh (unaltered) and aged rhizomes and the fresh (unaltered) roots. For filtration, a Buchner filtration or a filtration using Celite®560 (if a Buchner filtration was not successful) were used. A drying chamber was used for drying, and a freeze dryer was used for lyophilisation. A separating funnel was used if a residue was shaken out with a solvent. The extract names as well as the used plant material part are underlined in bold.

4.2.2.5 TLC comparison

TLC was used first to compare the different extracts with each other and second for monitoring the isolation methods. For the comparison, each extract (concentration 10 mg/mL) was applied to a TLC plate using a Linomat 5 (see section 4.2.1). The extract was applied with a 1 cm distance from the TLC plate bottom as 0.8 cm broad bands. The application volume was of 10 μ L and the spray speed of 150 nL/s with air as spray gas. For monitoring of the isolation process, the different fractions were applied using a TLC spotter micropipette. The TLC spots were made manually on the TLC plate, the applied volume varied between 2 and 3 μ L.

After application, TLC plates were developed in a TLC chamber containing the mobile phase (level < 1 cm height). First, the TLC-chamber was filled with the mobile phase, and a paper towel was taped on the wall of the chamber, soaked with the mobile phase and left for few minutes to ensure the saturation of the chamber with solvent vapor. Then the TLC plate was placed into the chamber. Once the mobile phase front reached the marked level, the TLC plate was removed from the chamber and dried at ambient air and temperature. After that, pictures at 254 nm and 366 nm were taken using the Linomat 5 apparatus.

Derivatisation of the TLC plates was carried out with different reagents (see section 4.2.1): anisaldehyde reagent (AA), natural product reagent (N) and vanillin reagent (V). After the derivatisation, pictures at 366 nm and day light were taken.

AA-reagent: the TLC plate was sprayed with the AA-reagent homogeneously and left on a heating plate at 105°C for 5-10 minutes.

N-reagent: the TLC plate was first heated on a heating plate at 100 °C, then sprayed homogeneously with N-reagent and finally dried at ambient temperature and air. After several minutes, different spots were detectable with naked eyes.

V-reagent: the TLC plate was first sprayed homogeneously with a vanillin solution (solution 1, see Table 13), then with a sulfuric acid solution (solution 2, see Table 13) and heated to 105 °C on a heating plate for 5-10 minutes.

All different mobile phases are summarised in the following Table 16.

Table 16: Composition (volume%) of the mobile phases for the comparison of the extracts with each other on TLC plates.

Eluent name	Composition (volume%)						
	hexane	DCM	EtOAc	MeOH	Toluol	EtOH	cyclohexane
TLC_1	75	20	5	10	/	/	/
TLC_2	/	/	13.3	3.3	80	3.3	/
TLC_3	/	/	40	5	/	45	10
TLC_4	/	/	35	15	50	/	/
TLC_5	70	20	20	10	/	/	/
TLC_6	65	20	15	10	/	/	/
TLC_7	/	/	40	/	60	/	/
TLC_8	30	30	30	10	/	/	/
Eluent name	Composition (volume%)						
	BuOH		Acetic acid		H ₂ O		only the upper phase is used as eluent
TLC_9	40		10		50		

4.2.2.6 Cell culture, cytotoxicity and MTT assay

4.2.2.6.1 Cytotoxicity of several extracts on HeLa and SK-MEL-28

All cell biological work steps were performed in a sterile bench under sterile conditions. All used chemicals or mediums (except trypsin/EDTA solution) were previously heated at 37°C for 30 minutes before usage. All the used devices, glass, and consumption items were purchased sterile or sterilised (with autoclave or dryer chamber). All the culture bottles or plates were cultivated in an incubator at 37 °C, 95% air humidity and 5% CO₂ content. The growing cells were monitored with a microscope to control split time or medium change.

4.2.2.6.2 Production of medium for cell culture

HeLa

L-Glutamine (5 mL), FBS (50 mL) and NEA (5 mL) were added to 500 mL MEM and well mixed. Then the medium was stored in the fridge.

SK-MEL-28

FBS (50 mL) was added to a mixture of 500 mL DMEM and 500 mL of HAM'S F-12 medium and was well mixed. The medium was preserved in the fridge for storage.

4.2.2.6.3 Defrosting of the cells

All the cells were stored in DMSO at -196 °C. As quickly as possible, the desired cell line was defrosted to 37 °C and transferred in a falcon-tube with approximately 8-10 mL of corresponding medium. Then the cell containing medium was centrifuged (HeLa: 700 rpm, 3 min; SK-MEL-28: 700 rpm, 5 min). The supernatant was removed. The remaining cell pellet was resuspended with 5 mL of medium and filled in a culture bottle containing 15 mL of medium. After one day in the incubator at 37 °C, the medium was changed (see section 4.2.2.6.4) to ensure a complete elimination of DMSO.

4.2.2.6.4 Medium change

The old medium was removed from the culture bottle. The cell layer was washed with 5 mL of PBS and 20 mL of fresh medium was added. The procedure was used for both cell lines HeLa and SK-MEL-28. After 2 or 3 days, the medium was changed again.

4.2.2.6.5 Splitting of the cells

HeLa

The old medium was removed, and the cell layer washed with 5 mL of PBS. After that 2 mL of a trypsin/EDTA solution was added and the cell culture bottle was incubated for 3-5 min at 37 °C (5% CO₂). Then the cell culture bottle was taped to detach the cell layer from the bottle base. 8 mL of medium was used to transfer the detached cells in a falcon tube. The cell containing medium was centrifuged (700 rpm, 3 min). The supernatant was removed, and the remaining cell pellet was resuspended in 5 mL medium. 20 mL medium were filled in a new culture bottle and 500 µL of the cell suspension was added. Generally, the cells were split every 5-7 days.

SK-MEL-28

The old medium was removed, and the cell layer washed with 5 mL of PBS. After that 3 mL of a trypsin/EDTA solution was added. The cell culture bottle was incubated for 3-5 min at 37 °C (5% CO₂). Then the cell culture bottle was taped to detach the cell layer from the bottle base. 7 mL of medium was used to transfer the detached cells in a falcon tube. The cell containing medium was centrifuged (700 rpm, 5 min). The supernatant was removed, and the remaining cell pellet was resuspended in 5 mL of medium. 19 mL of medium were filled in a new culture bottle and 1 mL of the cell suspension was added. Generally, the cells were split every 5-7 days.

4.2.2.6.6 Cell counting

The same procedure as described for the splitting (see section 4.2.2.6.5) was used, but the cells were resuspended and homogenised in 5-7 mL of medium. After that 10 µL of cell suspension was mixed with 10 µL of trypan blue solution (the dead cells were coloured in blue, the living cells not). Then 5-

10 μ L of the cell suspension was filled in a C-chip and the cells were counted in the four large squares. Finally, the cell number was determined (cell from the four large squares multiplied by 10^4) and the desired cell concentration was prepared (120 000 HeLa cells per mL medium and 60 000 SK-MEL-28 cells per mL medium for the MTT assay, see section 4.2.2.6.8).

4.2.2.6.7 Processing of the studied extract solutions

The different extracts were solubilised in DMSO or a mixture of EtOH/H₂O (70/30, v/v) at a defined concentration for the MTT assay (see section 4.2.2.6.8). The concentrations of the stock solutions are given in Table 17 for each extract and for the corresponding used solubilisation solvent. The final maximum concentration tested in the MTT assay is also given.

Table 17: Used concentration in the MTT assay with HeLa cells and SK-MEL-28 cells. See Figure 53, Figure 54 and Table 15 in section 4.2.2.4 for the different extract denomination.

HeLa			
Extract	Solvent (volume%)	Concentration stock solution (mg/mL)	Maximum concentration tested for the MTT assay (μ g/mL)
18I1/18I2/18I3/18I9	DMSO	9.75	65
18I4A/18I5A/18I6A	EtOH/H ₂ O 70/30	9.75	65
18I4B/18I5B/18I6B	EtOH/H ₂ O 70/30	97.5	650
SK-MEL-28			
18I1/18I2/18I3	DMSO	9.75	65
18I9	DMSO	9.75/52.2	65/348
18I4A	EtOH/H ₂ O 70/30	67	447
18I5A	EtOH/H ₂ O 70/30	65	431
18I6A	EtOH/H ₂ O 70/30	71	472
18I4B/18I5B/18I6B	EtOH/H ₂ O 70/30	97.5	650

4.2.2.6.8 MTT assay

96-wells plates were used to perform the MTT assay. First, all outers wells were filled with 150 μ L medium. Then 1 μ L of the stock solution was added to 149 μ L of medium in the first 6 wells (B2 to G2). All the other wells were filled with 75 μ L of medium (B3 to G11). After that, a 1 to 1 dilution was done: 75 μ L of the highest concentration solution were taken from the 6 wells B2 to G2 and mixed with the next 6 wells B3 to G3 (5-10 times aspirating and dispensing). Then 75 μ L were taken from the 6 wells B3 to G3 and mixed with next 6 wells B4 to G4 (5-10 times aspirating and dispensing). The process was

repeated until the 6 wells B10 to G10 and after that 75 μ L were removed from the last 6 wells (B10 to G10). Finally, the cell number was determined as explained previously in section 0 and 75 μ L of the cell suspension (120 000 HeLa cells per mL and 60 000 SK-MEL-28 cells per mL) was added to the wells in the middle (B2 to G11). The 6 wells B11 to G11 were used as reference (100% cells are alive, only cells and medium in the wells, no substances).

The 96-wells plate was incubated for 68 hours. After that, 15 μ L of the MTT solution (4 mg/mL) was added to the wells in the middle (B2 to G11) and the plate was incubated for 4 hours. Then, the medium was removed and 150 μ L of a SDS solution (10% in water) was added. The plate was kept in the darkness overnight and finally, it was measured at 560 nm with the plate reader (TECAN).

Every time, a 96-wells plate with only the solvent or solvent mixture (no extract solution) was prepared as solvent control. The maximum concentration of DMSO or EtOH/H₂O tested in the MTT assay was of 0.33%. The solvent control elucidated the solvent effect in the MTT assay (more precisely, that the solvent did not kill cells during the assay).

If the remaining activity of the highest tested concentration was over 50% (i.e., the average absorbance of the highest tested concentration was higher than 50% of the average absorbance of the reference), no IC₅₀ was determined. The determination of the IC₅₀ was calculated from the average of 3 to 6 experiments.

The IC₅₀ of the BuOH extracts 18I4B, 18I5B, and 18I6B (BuOH extracts of respectively the fresh (=unaltered) and aged rhizomes and the fresh roots of *Iris germanica* L.; see Figure 54 or Table 15 in section 4.2.2.4) on the SK-MEL 28 cells is not precise, because in some experiments no determination of the IC₅₀ was possible as the average absorbance of the highest tested concentration was higher than 50% of the average absorbance of the reference (see Figure S 26 of the Appendix). In this case, only the plates with determinable IC₅₀ were used to calculate the averaged IC₅₀ of the BuOH extract (18I4B (fresh rhizomes), 18I5B (aged rhizomes), or 18I6B (fresh roots)).

4.2.2.7 Isolation process

4.2.2.7.1 Chromatographic methods

Different chromatographic methods (open silica gel column, HPLC and semi preparative HPLC) were used for the investigation of the phytochemical profile of 18I4A (EtOAc extract of the fresh rhizomes of *Iris germanica* L.; see Figure 54 or Table 15 in section 4.2.2.4) and 19IA (EtOAc extract of the fresh roots of *Iris germanica* L.; see Figure 53 or Table 15 in section 4.2.2.4). An overview all used methods is shown in Table 18. The described methods for the semi preparative HPLC varied sometimes from the analytical methods (analytical HPLC methods had to be adjusted for the semi preparative HPLC).

Therefore, only the semi preparative HPLC methods and one analytical HPLC method are shown in Table 18 and in the two different isolation patterns in Figure 55 and Figure 56 respectively in sections 4.2.2.7.2 and 4.2.2.7.3.

Table 18: Overview of all used HPLC and open silica gel column (SGC) methods for the phytochemical investigation of 1814A and 191A. Solvent A and B are given in volume %. MeOH = methanol; TFA = trifluoroacetic acid; ACN = acetonitrile.

HPLC chromatographic methods				
Methods name	Solvent A (%)	Solvent B (%)	Time (min)	Type of column
HPLC_1	H ₂ O + 0.1% TFA 60 60	ACN 40 40	0 40	RP-18
HPLC_2	H ₂ O + 0.1% TFA 60 60	MeOH 40 40	0 80	RP-18
HPLC_3	H ₂ O + 0.1% TFA 40 40	MeOH 60 60	0 60	biphenyl
HPLC_4	H ₂ O + 0.1% TFA 55 55 40 40	MeOH 45 45 60 60	0 40 50 70	RP-18
HPLC_5	H ₂ O + 0.1% TFA 30 30	ACN 70 70	0 20	RP-18
analytical HPLC_6	H ₂ O + 0.1% TFA 80 80 20 80 80	ACN 20 20 80 20 20	0 2 22 42 45	RP-18
Silica gel column (SGC) methods				
Methods name	Eluent composition (volume%)			
SGC_1	Toluol/EtOAc/MeOH/EtOH 80/13.3/3.3/3.3			
SGC_2	Toluol/EtOAc 60/40			
SGC_3	Hexane/DCM/EtOAc/MeOH 65/20/15/10			
SGC_4	Hexane/DCM/EtOAc/MeOH 30/30/30/10			

4.2.2.7.2 Isolated compounds from 1814A (EtOAc extract of the fresh (=unaltered) rhizomes)

5 g of 1814A (EtOAc extract of the fresh rhizomes of *Iris germanica* L.; see Figure 54 or Table 15 in section 4.2.2.4) was dissolved in 8-10 mL of a mixture of a EtOAc/EtOH mixture (1/1 V/V) and separated over four silica gel columns (silica gel column 1, see section 4.2.1). TLC was used for monitoring the

fractionation of the extracts resulting in 25 fractions including 3 main fractions (Z1, Z2 and Z3). Fraction Z2 (500 mg) was then analysed with HPLC and semi preparative HPLC (RP-18 column) resulting in two main subfractions Z2P1 and Z2P2. Z2P1 (34 mg) was further analysed with HPLC and semi preparative HPLC (biphenyl column). Z1 (1.7 g) was further eluted over a silica gel column (silica gel column 1, see section 4.2.1). After monitoring with TLC, 5 main fractions were obtained: Z1F1, Z1F2, Z1F3, Z1F4 and Z1F5. Only Z1F4 (247 mg) was further analysed with HPLC and semi preparative HPLC (RP-18 column).

After isolation via semi preparative HPLC, LC-MS, ¹H- and 2D-NMR data were collected to elucidate the molecular structure.

A summary of the isolation process is given in Figure 55 with the different isolated compounds from 18I4A.

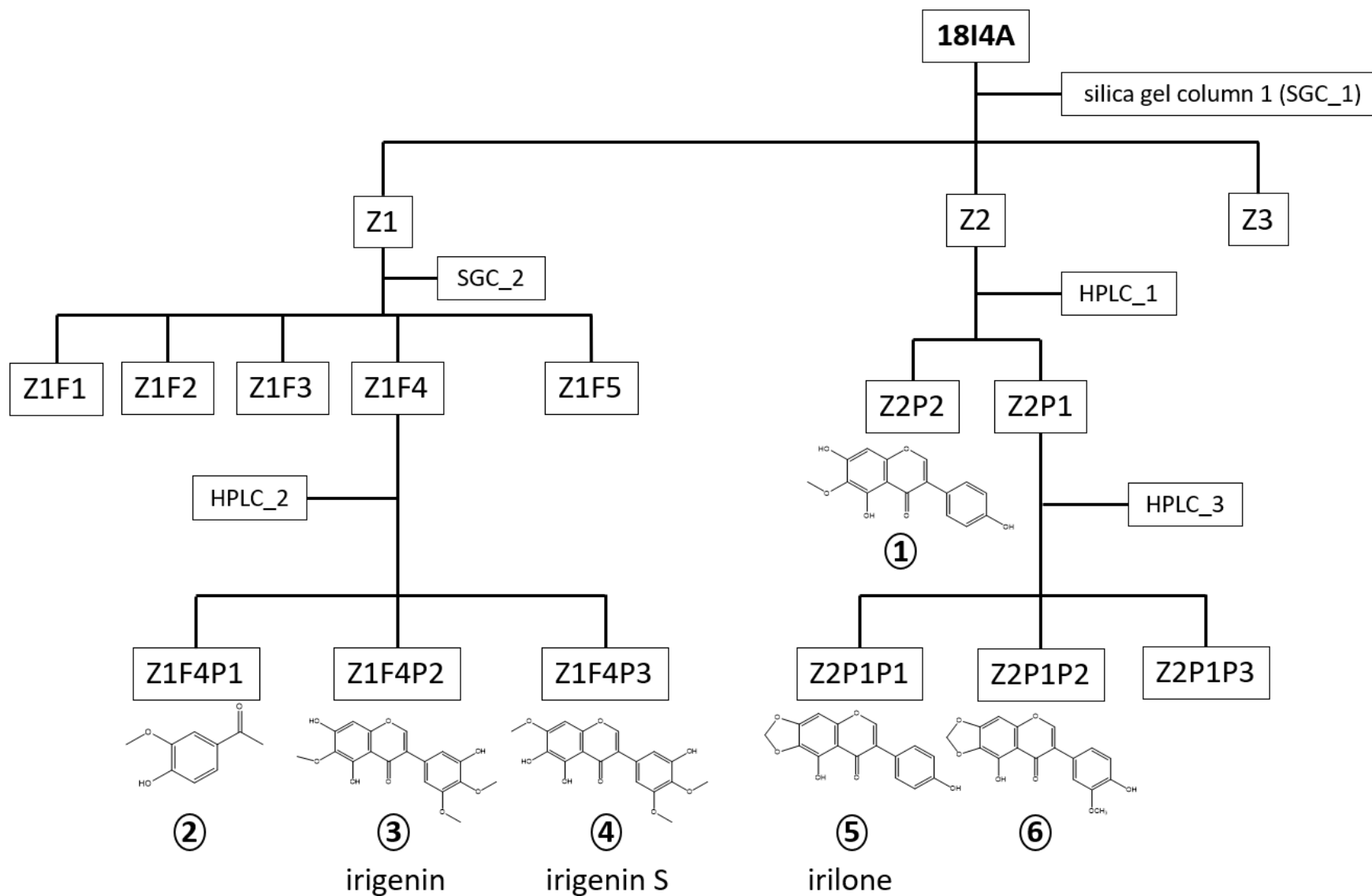


Figure 55: Isolation pattern of the different compounds from 18I4A (EtOAc extract of the rhizomes of *Iris germanica* L.; see Figure 54 or Table 15 in section 4.2.2.4). The different chromatographic methods (SGC: silica gel column, SGC_1, SGC_2, HPLC_1, HPLC_2, and HPLC_3) are shown in Table 18 in section 4.2.2.7.1.

4.2.2.7.3 Isolated compounds from 19IA (EtOAc extract of the fresh roots)

5 g 19IA (EtOAc extract of the fresh roots of *Iris germanica* L.; see Figure 53 or Table 15 in section 4.2.2.4) was dissolved in EtOAc and separated over an open silica gel column (silica gel column 2, see section 4.2.1). 7 main fractions (F1 to F7) were obtained after monitoring with TLC. The fraction F6 (570 mg) was then analysed with HPLC and semi preparative HPLC (RP-18 column). The fraction F4 (1.5 g) was separated again over an open silica gel column (silica gel column 1, see section 4.2.1). 5 main fractions were collected (F4F1 to F4F5). The fraction F4F1 was analysed with HPLC, the fraction F4F3 (502 mg) with HPLC and semi preparative HPLC.

After isolation via semi preparative HPLC, LC-MS, ¹H- and 2D-NMR data were collected to elucidate the molecular structure.

A summary of the isolation process is given in Figure 56 with the different isolated compounds from 19IA.

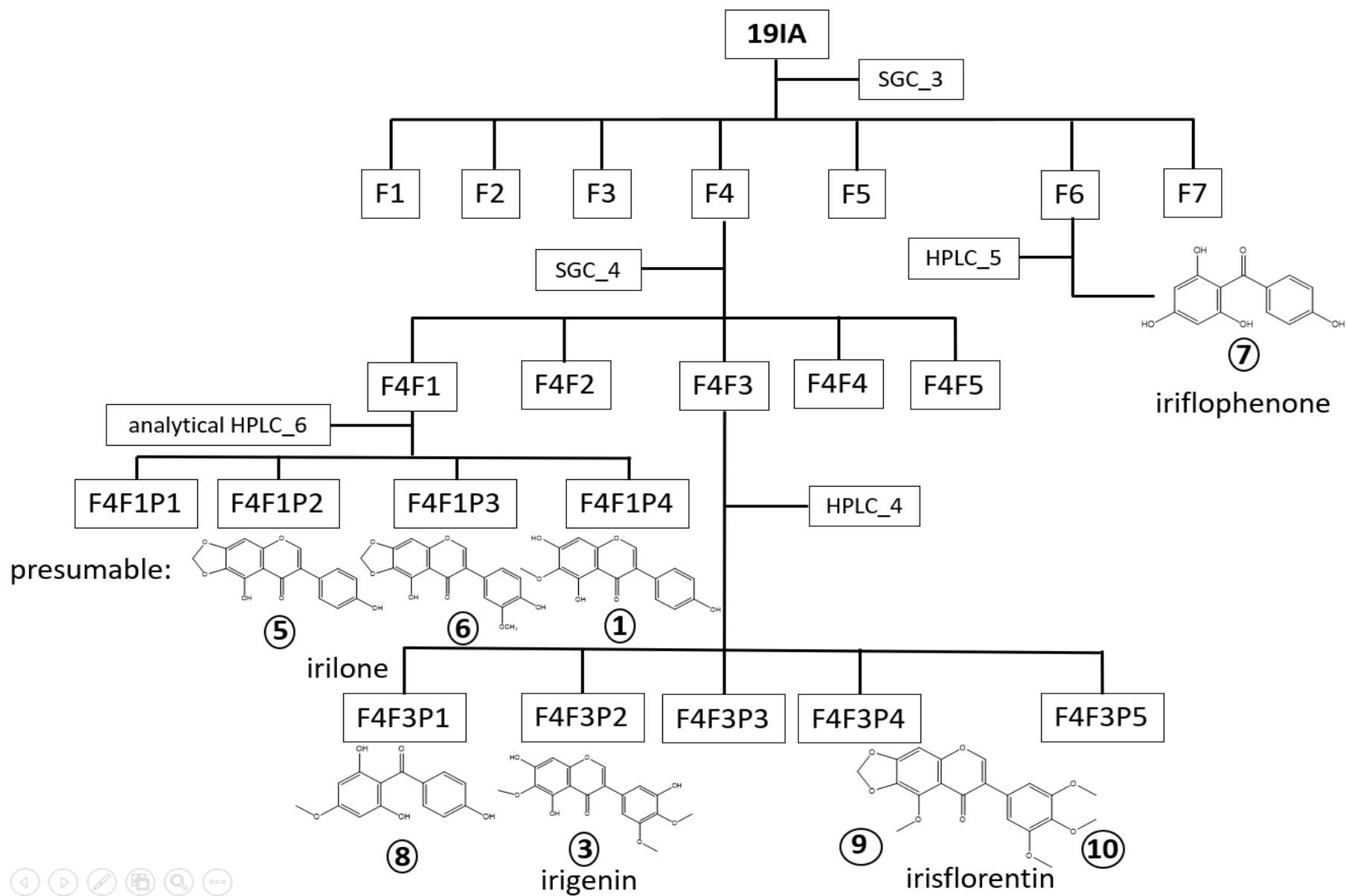


Figure 56: Isolation pattern of the different compounds from 19IA (EtOAc extract of the roots of *Iris germanica* L.; see Figure 53 or Table 15 in section 4.2.2.4). The different chromatographic methods (SGC: silica gel column, SGC_3, SGC_4, HPLC_4, HPLC_5, and analytical HPLC_6) are shown in Table 18 in section 4.2.2.7.1.

4.2.2.8 ICAM assay with HMEC-1 cells

All cell biological work steps were done in a sterile bench under sterile conditions. All the used chemicals or mediums (except trypsin/EDTA solution) were previously heated to 37°C for 30 minutes before usage. All the used devices, glass or consumption items were purchased sterile or sterilised (with an autoclave or dryer chamber). All the culture bottles or plates were cultivated in an incubator at 37 °C (95% air humidity and 5% CO₂). The growing cells were monitored with the microscope to control split or medium change time.

4.2.2.8.1 Collagen and production of medium

To facilitate the growth of HMEC-1 cells in culture bottles, collagen G can be used. Collagen G is a structural protein from the connective tissue. 25 µL of a collagen G solution was dissolved in 10 mL of PBS, transferred in a small culture bottle (50 µL in 20 mL were used for a big culture bottle) and incubated at 37 °C for 30 min. After that, the collagen solution was extracted and the culture bottle was coated.

For the ICAM assay, a 24-wells plate was also coated to facilitate the growth of HMEC-1 cells. Therefore, the same collagen G solution was used (25 or 50 µL in 10 or 20 mL of PBS respectively) and 300 µL was added per well. After 30 min incubation (incubator, 37 °C), the plate was left alone in the sterile bench for at least 15 min (may help to have more adhesion). Finally, the collagen G solution was removed resulting in a coated plate.

ECGS (growth supplement), FBS and an antibiotic (gentamicin) were added to the ECBM and well mixed. The obtained ECGM (growth medium) was used for the culture of HMEC-1 cells. In this case, antibiotic was used to protect the HMEC-1 cells from bacteria, because they are more sensitive and much more expensive than HeLa or SK-MEL-28 cells.

4.2.2.8.2 Defrosting

HMEC-1 cells were stored in DMSO at -196°C like the other cells. The same method as described in section 4.2.2.6.3 was used with small modifications. As quick as possible, the HMEC-1 cells were defrosted with 10 mL of ECGM, transferred in a 15 mL falcon tube and centrifuged (1000 rpm, 3 min). Then the supernatant (ECGM with DMSO) was removed, 5 mL of fresh ECGM was added to the remaining HMEC-1 cell pellet and the cell suspension was homogenised. The cell suspension was finally transferred in a culture bottle (previously coated with collagen G, see section 4.2.2.8.1) containing 10 mL of fresh ECGM. The bottle was cultivated in an incubator at 37 °C for one day and the medium was changed (see section 4.2.2.6.4, same procedure with ECGM) to ensure the complete elimination of DMSO.

4.2.2.8.3 Splitting

The same method was used as described for the SK-MEL-28 cells in section 4.2.2.6.5, with only small modifications. The old medium was removed, and the cell layer washed with 5 mL of PBS (10 mL for a big culture bottle). After that 3 mL (5 mL for a big culture bottle) of a trypsin/EDTA solution was added and the cell culture bottle for 3-5 min incubated at 37 °C (5% CO₂). Then the cell culture bottle was taped to detach the cell layer from the bottle base. 10 mL of ECGM was used to transfer the detached cells in a falcon tube. The cell containing medium was centrifuged (1000 rpm, 3 min). The supernatant was extracted, and the remaining cell pellet was resuspended in 5 mL of ECGM. 20 mL of fresh ECGM was filled in a new culture bottle (previously coated with collagen G) and 1 mL of the cell suspension was added.

4.2.2.8.4 Cell counting

The same procedure as described in 4.2.2.8.3 was used until the resuspension of the cells. The cell pellet was resuspended in 10 mL of fresh ECGM. Then 50 µL of the cell suspension was mixed with 50 µL of fresh ECGM, 50 µL of the first dilution was mixed again with 50 µL of fresh ECGM (1 to 4 dilution). Between 5 and 10 µL of the final dilution cell suspension was filled in a C-chip and the HMEC-1 cells were then counted in the four large squares. The cell number was determined and the desired cell concentration, 900 000 HMEC-1 cells per mL medium for the MTT assay, was prepared.

4.2.2.8.5 Processing of the studied extracts and isolates

All the extract solutions, 18I4A (EtOAc extract of the fresh rhizomes of *Iris germanica* L.; see Figure 54 or Table 15 in section 4.2.2.4) and 19I4A (EtOAc extract of the fresh roots of *Iris germanica* L.; see Figure 53 or Table 15 in section 4.2.2.4), were dissolved in DMSO at a concentration of 100 000 µg/mL, the isolates at a concentration of 70 000 µM (stocks). For the MTT and ICAM assays, the dilutions with ECGM were previously done in Eppendorf cups and then in a reservoir. The tested concentrations were 25, 50, and 70 µM for the isolates and 12.5, 25, 50 and 100 µg/mL for the extracts in MTT and ICAM-1 assay. In the case of irilone, 12.5, 25 and 50 µM have been tested. Pure DMSO was also diluted the same way but only the highest concentration was used as solvent control.

4.2.2.8.6 MTT assay

First, the cells were counted as described in section 4.2.2.6.6 and a cell suspension was adjusted to 900 000 cells per mL ECGM. A 96-wells plate (without coating) was filled with 100 µL of the cell suspension in all inner wells (B2 to G11). The outer wells were filled with 100 µL PBS. Then, the 96-wells plate was incubated for 24 hours. The old medium was removed and replaced by 100 µL of the DMSO solution (6 wells), extract or isolate dilution (6 wells per concentration). Pure ECGM was added in 6 wells and used as zero value. Then, the plate was incubated again for 24 hours. The warmed MTT

solution was diluted 1:10 with ECGM. The sample (DMSO, extract and isolate) dilutions and the pure ECGM medium were extracted and 100 μ L of the MTT solution were added in all inner wells. The plate was incubated at 37 °C for 3 hours. After that, the MTT solution was removed and replaced by 100 μ L of a SDS solution (10% in water). The plate was kept in the darkness overnight. Finally, the absorbance was measured at 560 nm with the plate reader. A solvent control and a zero value were measured for each plate, even if more than one plate was prepared. The results were indicative for the ICAM assay.

4.2.2.8.7 ICAM assay

For the ICAM assay only concentrations which are not toxic for the HMEC-1 cells (meaning at least 90% cell viability) were used. The sample dilutions were the same as for the MTT assay (pure ECGM and dilution of the extracts, isolates and pure DMSO as solvent control).

The same procedure as described in section 4.2.2.6.5 (splitting of the HMEC-1 cells) was used until the resuspension of the cells. The cell pellet was resuspended in 9 mL of fresh ECGM. 3 mL (6 mL if two plates were prepared) of the cell suspension was mixed with 10 mL (20 mL for two plates) of fresh ECGM. A 24-wells plate was used (previously coated with collagen G) for the ICAM assay. 500 μ L of the cell suspension was added in each well. The 24-wells plate was incubated for 48 hours.

After 48 hours, the prepared aliquoted stock solution (10 μ L, 100 mM) of parthenolide (positive control) was mixed with 990 μ L of fresh ECGM, followed by a 1 to 1 dilution (100 μ L parthenolide solution in 100 μ L fresh ECGM). The old medium was removed and replaced by 500 μ L of the sample dilution (2 wells per concentration, DMSO dilution also). 4 wells were filled with pure medium (500 μ L) and 5 μ L of the final parthenolide solution was added to 2 of the 4 wells (resulting in a final concentration of 5 μ M). In the 2 other wells, only the TNF- α solution was added (100 % value). Then, the 24-wells plate was incubated for 30 min. In the meantime, the TNF- α solution was prepared. 160 μ L of fresh ECGM was added to a prepared aliquoted TNF- α solution (10 μ L at a concentration of 17 μ g/mL). After 30 min incubation, 5 μ L of this solution was added to all wells (final concentration of 10 ng/mL per well) except the two wells with DMSO (solvent control). Then, the plate was incubated for 24 hours.

After 24 hours, FACS-tubes were prepared and 100 μ L of formalin was added to each tube (to fix the cells). The sample dilutions, the solvent control, the positive control (parthenolide), and the 100% value solution were extracted. The HMEC-1 cell layers were washed with 10 mL of PBS. Then, PBS was removed and 200 μ L of a trypsin/EDTA solution was added in each well. The 24-wells plate was incubated for 3 min. Then, the cells were transferred into the FACS tubes by aspirating and dispensing many times with a 1000 μ L pipette. The FACS tubes were vortexed and left alone for 15 min. After that,

1000 μ L PBS was added to each tube, vortexed, centrifuged (1200 rpm, 5 min) and the supernatant was tipped away. 5 μ L of antibody was added to each tube, vortexed and left alone for 20 min. Then, 1000 μ L PBS was added to each tube, vortexed, centrifuged (1200 rpm, 5 min) and the supernatant was tipped away. Finally, 400 μ L of PBS were added to each tube and the tubes were then ready to be measured with the FACS instrument.

IFN- γ was used as a second stimulator. Exact assay set-up was used, but 5 μ L of IFN- γ solution in PBS (4 μ g/mL) was added to each well (except the wells with the DMSO dilution) instead of 5 μ L TNF- α solution. The final concentration of IFN- γ was 40 ng/mL per well.

The FACS instrument was used to determine the ICAM-1 expression. First the cells were separated according to size (Forward-Scattered Light, FSC) and granularity (Side-Scattered Light, SSC). The ICAM-1 proteins produced by the cells through the stimuli TNF- α or IFN- γ were located on the surface of the cells and bound to the antibody. The ICAM-1 proteins were thereby fluorescence-labelled and the ICAM-1 expression is proportional to the fluorescence-intensity. As 100% value the fluorescence-intensity of the cells stimulated with TNF- α or IFN- γ was used (without test compound, average of two wells). All the other results were based and compared to this value. The corresponding device setup is summarised in Table 19.

Table 19: Parameters and settings of the FACS device for the determination of the ICAM-1 expression

Parameters	Settings
FSC	0.1 V
SSC	320 V
Flow	60 μ L/min
stimulation wavelength	495 nm
emission wavelength	519 nm
tension FL1 (green fluorescence)	500 V

4.2.2.9 Antimicrobial assays

4.2.2.9.1 Defrosting and cultivation of *S. aureus* and *E. coli*

The bacteria were stored at -80 $^{\circ}$ C in a mixture of glycerol 40%/LB-medium (40/60 in volume). The bacteria suspension was defrosted and 10 μ L were added in 25 mL fresh LB-medium in an Erlenmeyer flask. Then the flask was shaken for 24 hours at 37 $^{\circ}$ C. After that, the bacteria suspension was streaked on an agar plate and stored in the fridge. Doing so, a single colony can be obtained and used to set new bacteria suspensions. If a new bacteria suspension was required, 1 or 2 colonies were taken from

the agar plate with an inoculation loop (previously sterilised with a Bunsen burner) and added to 20-25 mL of fresh LB-medium in an Erlenmeyer flask, which was shaken for 24 hours at 37 °C.

4.2.2.9.2 Determination of the colony-forming unit

A dilution of the prepared bacteria suspension was done with LB-medium (1 to 1 or 100 million). Then, 50 µL of the diluted bacteria suspension was used to coat an agar plate. After that, the agar plate was cultivated in the incubator at 37 °C for 24 hours. The single colonies were then counted, and the colony-forming unit (CFU) was calculated. CFU allows a rough estimation of the number of viable bacteria in a sample.

4.2.2.9.3 Broth dilution method

All extracts were dissolved in DMSO at a concentration of 1000 µg/mL. All the isolates were dissolved in DMSO at a concentration of 1000 µM. Chloramphenicol was used as positive control (3 mg/mL in EtOH). Two different concentrations of MTT were used: 0.25 wt% for *S. aureus* and 0.5 wt% for *E. coli*. The final tested concentrations for the extracts were 250, 125, 62.5, 31.25, and 15.625 µg/mL. The final tested concentrations for the isolates were 250, 125, and 62.5 µM.

The same preparation method has been used as described for the MTT assay with HeLa and SK-MEL-cells (see section 4.2.2.6.8). A 96-wells plate was prepared with the diluted samples (5 different concentrations for the extracts and 3 for the isolates). All outer wells were filled with 200 µL of water. 2 extracts and 2 isolates were tested per plate. Therefore, 100 µL of the extract or isolate solution was added to 3 wells (12 wells were filled, B2, C2, D2 with the first extract, E2, F2, G2 with the second extract, B7, C7, D7 with the first isolate, E7, F7, G7 with the second isolate). 50 µL of DMSO was added to all the other residual wells. After a 1 to 1 dilution as described for the MTT assay in section 4.2.2.6.8, 50 µL LB-medium were added to all the wells, except the 6 last wells (B11 to G11). In these 150 µL were added (zero value). A dilution (1 to 50 for *S. aureus* and 1 to 5 for *E. coli*) of the bacteria suspension was prepared and 100 µL of the bacteria dilution was added to all the wells except the last 6 wells (B11 to G11). Then, chloramphenicol (30 µL) was added to 3 wells (B10 to D10). The 3 wells E10, F10, and G10 contain only bacteria with LB-medium and DMSO (100% value). Then, the 96-wells plate was shaken for 30 min and incubated at 37 °C for 20 hours. After 20 hours, the MTT solution (20 µL for *S. aureus* and 100 µL for *E. coli*) was added to all the wells and incubated at 37 °C for 4 hours. After that, the plate was measured at 560 nm with the plate reader and a picture of the plate was taken.

4.2.2.9.4 Agar diffusion

The inhibition zone assay (or disk diffusion test) was used as agar diffusion test. The irones were dissolved in DMSO at a concentration of 250 and 125 µg/mL. DMSO alone was used as solvent control.

First, an agar plate was swabbed uniformly with the bacteria solution (with a cotton swab). Then a filter paper disk was immersed in the sample dilution and deposited on the surface of the agar plate. After 24 hours incubation, the diameter of the inhibition zone was measured.

4.2.2.10 Statistical analysis

The results of the ICAM-1 assay were tested for statistical significance (significance level p of 95, 99.5 and 99.9%) using the statistical program SPSS (SPSS, Statistics 19, IBM).

4.3 Results and discussion

4.3.1 Yield and TLC comparison of the different extracts

The yields of all extracts (Figure 53, Figure 54, and Table 15 in section 4.2.2.4 for the extract denomination and the extraction process) are given in Table 20.

Table 20: Overview on the extraction yields. See Figure 53, Figure 54 and Table 15 in section 4.2.2.4 for the different extract denomination.

Extract name	Mass (g)	Yield (%)
18I1	24.6	2.1
18I2	23.8	2.4
18I3	13.7	1.7
18I4A	14.6	1.2
18I5A	14.6	1.5
18I6A	5.6	0.7
18I4B	7.3	0.6
18I5B	9.7	1.0
18I6B	11.0	1.4
18I4W	169.7	14.1
18I5W	138.8	13.9
18I6W	n.a.	n.a.
18I7	15.4	3.1
18I9	1.07	0.152
19IH	1.0	0.6
19IA	6.1	3.8
19IHa	0.54	0.36
19IAa	10.0	6.8
19I9 (with/without maceration)	0.107/0.17	0.05/0.09
19I9a	0.081	0.04
20IH	0.025	n.a.
20IA	2.0	n.a.
20IB	2.7	n.a.

The highest yields were obtained for 18I4W and 18I5W (water remaining extracts of respectively fresh and aged rhizomes of *Iris germanica* L.) followed by 19IA (EtOAc extract of the fresh roots of *Iris germanica* L.) and 18I1, 18I2 and 18I3 (DCM extracts of the fresh and aged rhizomes and fresh roots of *Iris germanica* L.). 18I4A, 18I5A, 18I6A (EtOAc extracts of the fresh and aged rhizomes and the fresh roots of *Iris germanica* L.), 18I4B, 18I5B, and 18I6B (BuOH extracts of the fresh and aged rhizomes and the fresh roots of *Iris germanica* L.) achieved low extraction yields as well as 19IH and 19IHa (hexane extracts of the fresh and aged roots of *Iris germanica* L.). The lowest yields were obtained for 18I9, 19I9 and 19I9a (iris butter from aged rhizomes and iris butter from fresh and aged roots of *Iris germanica* L. from hydro distillation). The yield obtained with the aged rhizomes (18I9) was 0.152% comparable to the hydro distillation yields (0.1-0.25% in average). For the fresh and aged roots, the achieved yields were even lower: 0.04, 0.05 and 0.09% respectively for aged roots without maceration, fresh roots without maceration and fresh roots with maceration before hydro distillation. Maceration of the roots in water for several hours before starting the hydro distillation seemed to reach higher yields. The maceration method was already used for the rhizomes. The aging process of the rhizomes did not influence the extraction yields. On the contrary, the aging process of the roots changed the yield: about twice the extraction yield was obtained for 19IAa (EtOAc extract of aged roots of *Iris germanica* L.) as for 19IA (EtOAc extract of the fresh roots of *Iris germanica* L.). It was not the case for 19IH and 19IHa (n-hexane extracts of respectively the fresh and aged roots of *Iris germanica* L.). Meaning, that the aging process had no influence on the volatile part of the root's composition. The extraction after the hydro distillation led to a low amount of extract (20IH, 20IA and 20IB; respectively n-hexane, EtOAc and BuOH extracts of the hydro distillation residue of the aged rhizomes of *Iris germanica* L.). In this case, no yield could be calculated. About three litres of the hydro distillation residue have been used for the extraction. The residue was composed mostly of water with rhizome residue, therefore it was not homogenous and filtration was difficult. Thus, only the mass of the obtained extract and not of the starting material was indicated in the Table 20.

Comparison of the hydro distillation extracts 1919 and 1919a:

The two different iris root's butter 1919 and 1919a (respectively iris root's butter obtained from fresh and aged roots from hydro distillation; Figure 53 or Table 15 in section 4.2.2.4) were compared using gas chromatography coupled to mass spectrometry (GC-MS). A direct and quantitative comparison was complicated, but the results of the GC-MS could give some information on the composition of both root's butters. The chromatograms of the GC-MS are shown in Figure S 17 of the Appendix (same concentration for the two butters) and a zoom of these chromatograms (between 5 and 14 minutes) is shown in Figure 57. The two butters were alike concerning the major constituent (end of the chromatograms). The four main components (peaks at 11.35, 12.24, 13.07 and 13.83 min) were alkanes (hexa-, hepta-, tetracosane, ...) for the two butters (as determined with the MS-spectrograms and the help of databanks). This result was not surprising because some of these compounds were already detected as components in some iris oils [116]. The other components (peak at 7.22, 9.62 and 10.67 min) were fatty acid (n-decanoic acid, tetradecanoic acid and n-hexadecanoic acid) and again it was not surprising because it is a butter and some fatty acids should be present and detected with the GC-MS [114]. The aging process did not change the major constituent of the root's butter but had an influence on the fatty acid part. The intensity of the peaks at 7.22, 9.62 or 10.67 min increased if the roots were aged before the hydro distillation. The major difference between the iris rhizome's and root's butters was the absence of irones in the fresh and aged root's butter. Concerning the odour, the fresh root's butter smelled earthy and rooty. The odour of the aged root's butter was more complex and smelled woody.

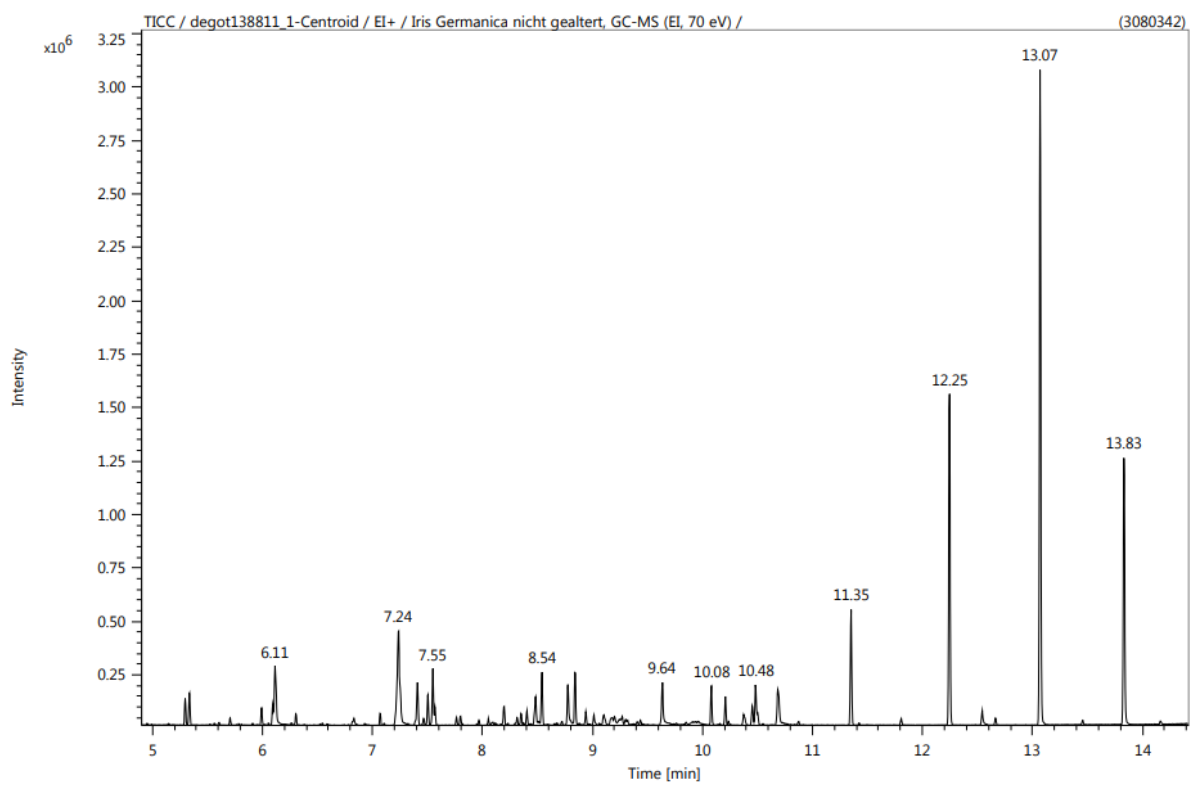
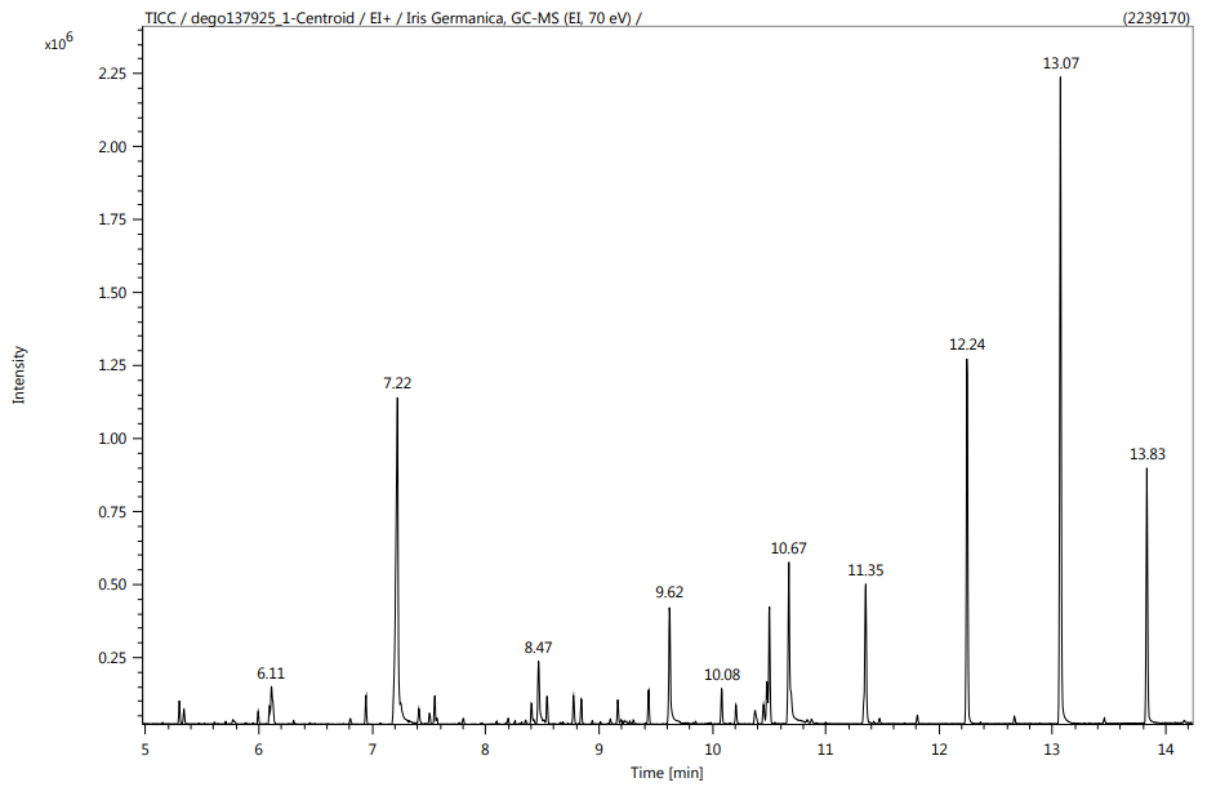


Figure 57: GC-chromatograms (5 and 14 minutes) of the iris aged root's (top) and the iris fresh root's (bottom) butter of Iris germanica L. (Figure 53 or Table 15 in section 4.2.2.4).

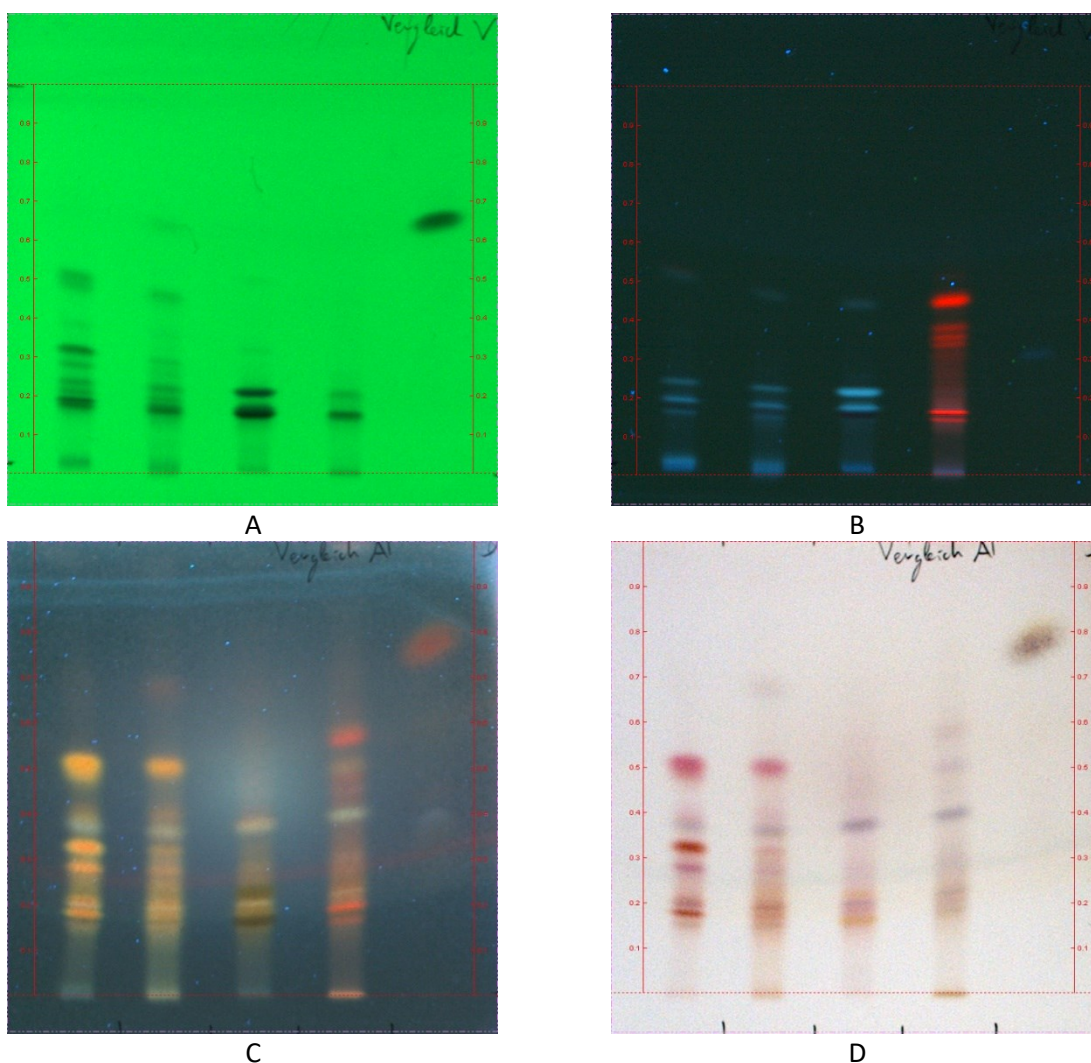
Comparison of the different solvent extracts:

The different solvent extracts were compared with each other.

DCM extracts 1811, 1812, 1813, 1817, and the iris rhizome's butter 1819:

First the DCM extracts 1811 (fresh rhizomes), 1812 (aged rhizomes), 1813 (fresh roots), 1817 (fresh leaves), and 1819 (iris butter from aged rhizomes from hydro distillation; see Figure 53, Figure 54 and Table 15 in section 4.2.2.4) were compared using TLC (same concentrations and volumes). The TLC plates were derivatised with three different reagents: AA, N and V to have a first idea about the phytochemical composition of the aged and fresh rhizomes and the fresh roots.

The comparison between the DCM extracts 1811 (fresh rhizomes), 1812 (aged rhizomes), 1813 (fresh roots), 1817 (fresh leaves), and 1819 (iris butter from aged rhizomes from hydro distillation) is shown in Figure 58. 1819 is used for comparison to determine the R_f values of the irones on the TLC. The TLC results on the extracts are shown in Figure S 18, Figure S 19 and Figure S 20 of the Appendix.



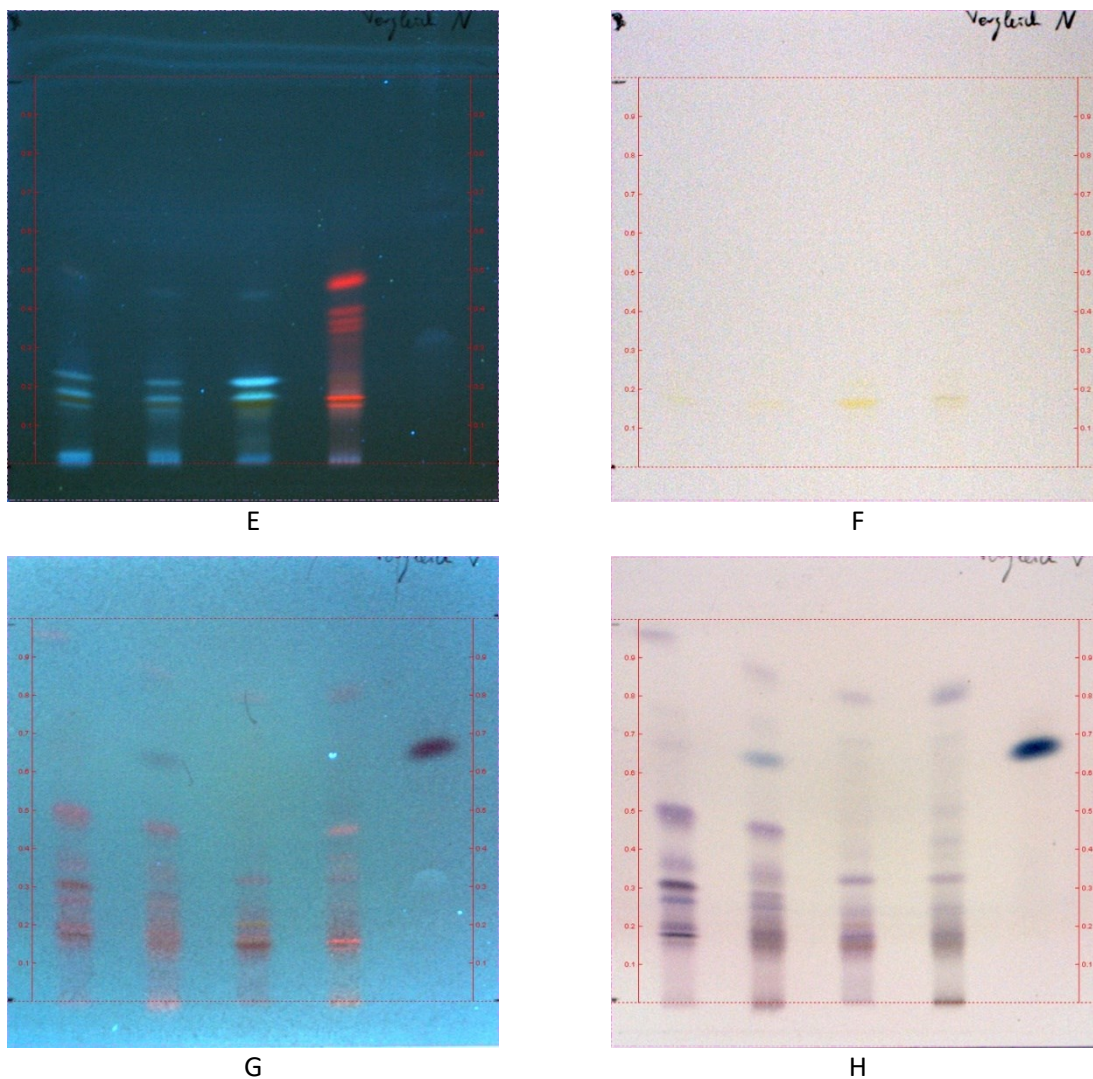


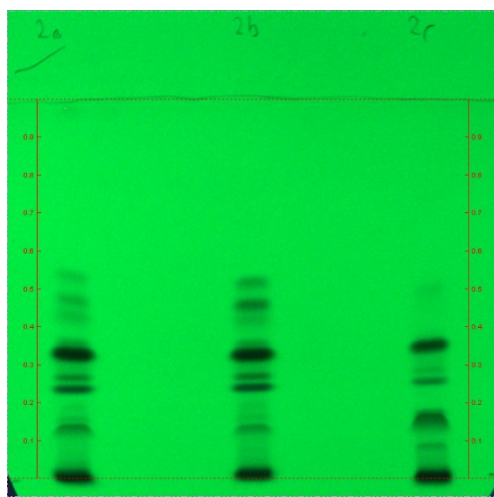
Figure 58: TLC comparison between the DCM extracts 1811 (fresh rhizomes), 1812 (aged rhizomes), 1813 (fresh roots), 1817 (fresh leaves), and 1819 (iris rhizome's butter from aged rhizome won by hydro distillation; see Figure 53, Figure 54 and Table 15 in section 4.2.2.4). The five spots on every plate correspond from the left to the right to 1811, 1812, 1813, 1817, and 1819. A/B: TLC plates without derivatisation under UV-light at 254 nm (left) and 366 nm (right). TLC plates derivatised with AA (C/D), N (E/F), and V (G/H) under UV-light at 366 nm (left) and under white light (right). Eluent for every plate: TLC_1 (see Table 16 in section 4.2.2.5).

First, the results obtained by GC-MS were reproduced with the TLC analysis. As expected, the irones ($R_f \approx 0.65$) were only present in 1812 (DCM extract of aged rhizomes) and not in 1811 (DCM extract of fresh rhizomes; see Figure 52 or Table 15 in section 4.2.2.4). 1811 and 1812 seemed very similar, as no major difference was seen on the TLC plates (except the irones). 1813 (DCM extract of fresh roots; see Figure 52 or Table 15 in section 4.2.2.4) contained less different compounds than the rhizome's extracts 1811 and 1812. Obviously, the compounds of 1813 were present in 1811 and 1812, but some were qualitatively more abundant in 1813 than in 1811 and 1812 like the two spots with R_f -values of 0.2 and 0.15 in Figure 58. After derivatisation with N, it seemed that these two spots were polyphenols and the lowest spots with $R_f \approx 0.15$ flavones or isoflavones, due to their green fluorescence under UV-light at 366 nm (Figure 58, TLC plate E derivatised with N on the left). 1817 (DCM extract of the fresh

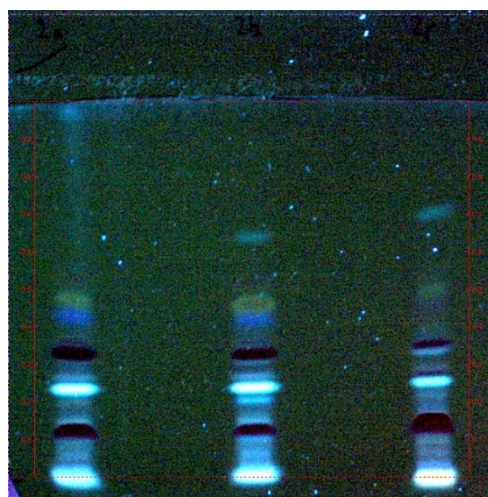
leaves; see Figure 54 or Table 15 in section 4.2.2.4) contained mostly chlorophyll and seemed to be similar to 1813. The chlorophyll should be removed in further separation steps, but due to lack of time, 1817 was not investigated.

EtOAc extracts 1814A, 1815A, 1816A, and the iris rhizome's butter 1819:

The EtOAc extracts 1814A (fresh rhizomes), 1815A (aged rhizomes) and 1816A (fresh roots) were compared (the plant materials were first extracted with DCM then with a binary mixture of water and EtOH (H₂O/EtOH 30/70 wt%) and after rotary evaporation of EtOH, the water remaining phase was extracted with EtOAc; Figure 54 or Table 15 in section 4.2.2.4). 1819 (iris butter from aged rhizomes from hydro distillation; Figure 53 or Table 15 in section 4.2.2.4) the presence or absence of irones was controlled also. No irones should be detected in the different extracts even for 1815A. The irones are polar compounds and should not be soluble in a mixture of EtOH/H₂O (70/30 V/V). Moreover, they were already detected in 1812 (DCM extract of aged rhizomes; Figure 54 or Table 15 in section 4.2.2.4) and therefore, should not be present in further subsequent extractions. The TLC comparison of EtOAc extracts 1814A (fresh rhizomes), 1815A (aged rhizomes), and 1816A (fresh roots) are shown in Figure 59. The TLC comparison of EtOAc extracts 1814A, 1815A, and 1816A with 1819 (iris rhizome's butter from aged rhizomes from hydro distillation) are shown in Figure 60. As previously, the TLC plates were derivatised with AA, N and V. The TLC plate of the comparison with 1819 was derivatised only with AA.



A



B

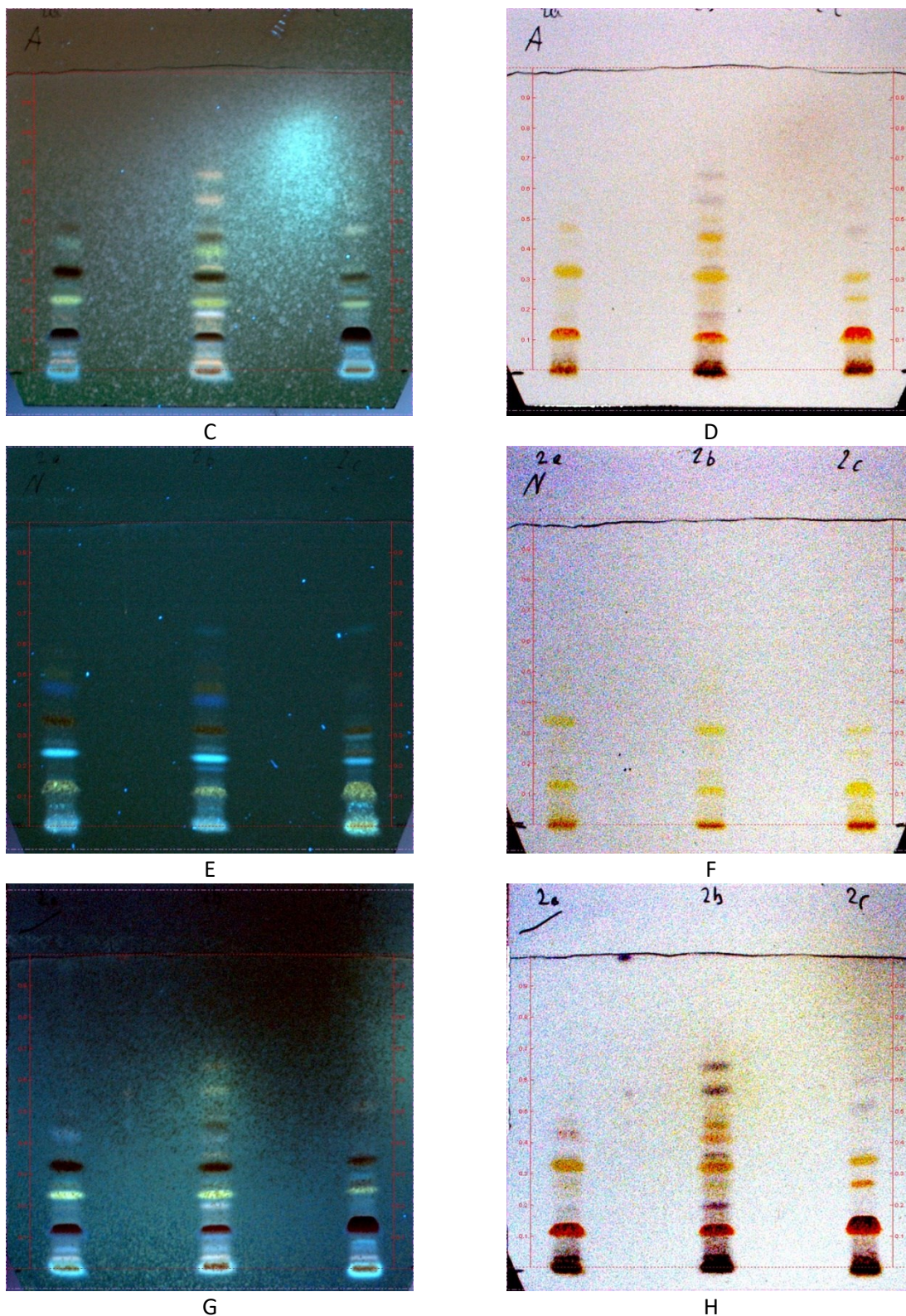


Figure 59: TLC comparison between the EtOAc extracts 1814A (fresh rhizomes), 1815A (aged rhizomes), and 1816A (fresh roots; Figure 54 or Table 15 in section 4.2.2.4). The three spots on every plate correspond from the left to the right to 1814A, 1815A, and 1816A. A/B: TLC plates without derivatisation under UV-light at 254 nm (left) and 366 nm (right). TLC plates derivatised with AA (C/D), N (E/F) and V (G/H) under UV-light at 366 nm (left) and under white light (right). Eluent for every plate: TLC₂ (see Table 16 in section 4.2.2.5).

As can be seen in Figure 59, the three EtOAc extracts 18I4A (fresh rhizomes), 18I5A (aged rhizomes), and 18I6A (fresh roots; Figure 52 or Table 15 in section 4.2.2.4) were very similar. After derivatisation with AA or V, some differences were detected between the fresh and aged rhizomes (respectively 18I4A and 18I5A). Several spots were revealed after derivatisation of 18I5A. The aging process had a strong influence on the phytochemical profile of 18I4A and 18I5A. Likely, the EtOAc fresh root's extract 18I6A contained compounds also present in the EtOAc extract 18I5A (aged rhizomes) but not in 18I4A (fresh rhizomes; R_f -values around 0.5, TLC plate D derivatised with AA under white light in Figure 59). The derivatisation with N confirmed the presence of flavonoids or isoflavonoids in the three EtOAc extracts (R_f -values of 0.15, 0.25 and 0.3). Qualitatively, the compound corresponding to the spot with the R_f -value of 0.15 seemed to be more abundant in the EtOAc extract 18I6A (fresh roots) than in the EtOAc extracts 18I4A and 18I5A (same concentrations and volumes). The three EtOAc extracts 18I4A, 18I5A, and 18I6A were of interest because they likely contain more polyphenols than the DCM extracts, because of the green, fluorescent spot at 366 nm and the yellow, yellow-orange spots under visible light after derivatisation with N (TLC E/F in Figure 59).

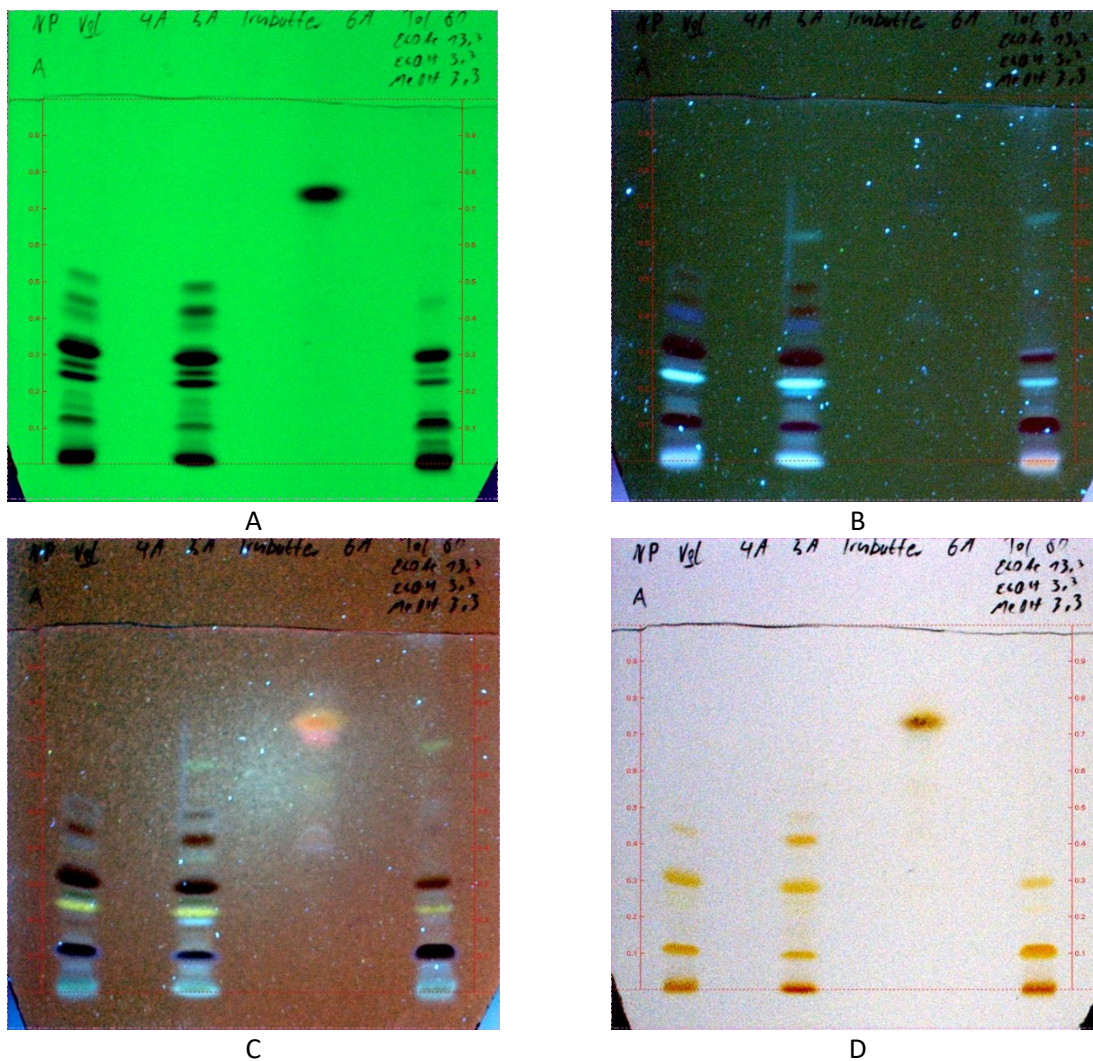


Figure 60: TLC comparison between the EtOAc extracts 1814A (fresh rhizomes), 1815A (aged rhizomes), and 1816A (fresh roots) and 1819 (iris rhizome's butter from aged rhizome won by hydro distillation; Figure 53, Figure 54 and Table 15 in section 4.2.2.4). The four spots on every plate correspond from the left to the right respectively to 1814A, 1815A, 1819, and 1816A. A/B: TLC plates without derivatisation under UV-light at 254 nm (left) and 366 nm (right). C/D: TLC plates derivatised with AA under UV-light at 366 nm (left) and under white light (right). Eluent for every plate: TLC_2 (see Table 16 in section 4.2.2.5).

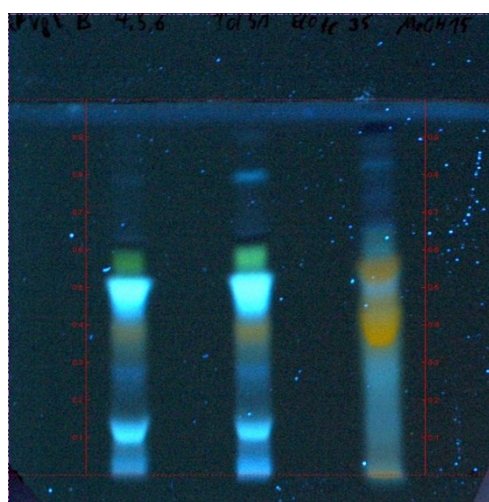
As can be seen in Figure 60, irones (spot with a R_f -value of 0.75 for 1819 (iris butter from aged rhizomes from hydro distillation) were not present in the EtOAc extracts 1814A (fresh rhizomes), 1815A (aged rhizomes), and 1816A (fresh roots).

BuOH extracts 18I4B, 18I5B, 18I6B, and the iris rhizome's butter 18I9:

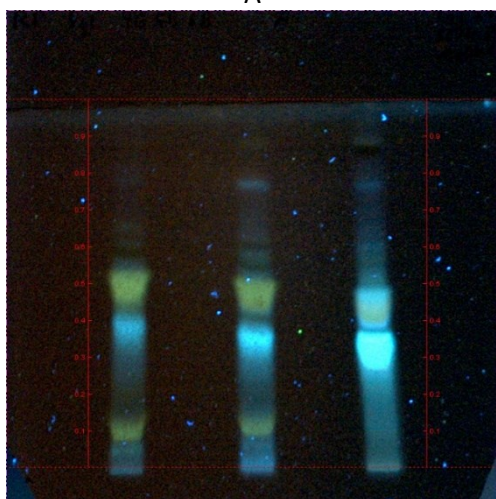
The BuOH-extracts 18I4B (fresh rhizomes), 18I5B (aged rhizomes), and 18I6B (fresh roots) (the plant materials were first extracted with DCM then with a binary mixture of water and EtOH (H₂O/EtOH 30/70 wt%) and after rotary evaporation of EtOH, the water remaining phase was extracted successively with EtOAc and BuOH; Figure 54 or Table 15 in section 4.2.2.4) were also compared with TLC (see Figure S 21 of the Appendix), but only the separation of polar compounds from non-polar compounds was possible. The use of RP-18 TLC plate gave the best separation. The results are shown in Figure 61.



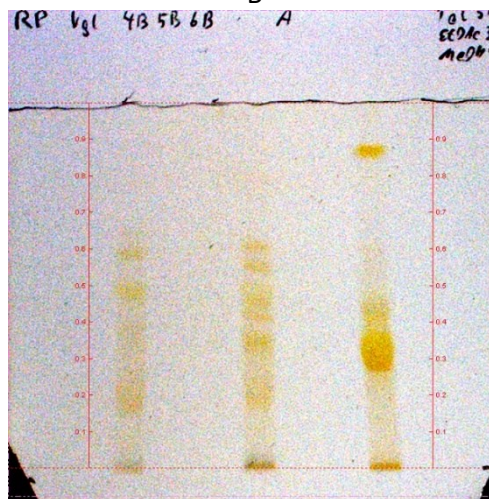
A



B



C



D

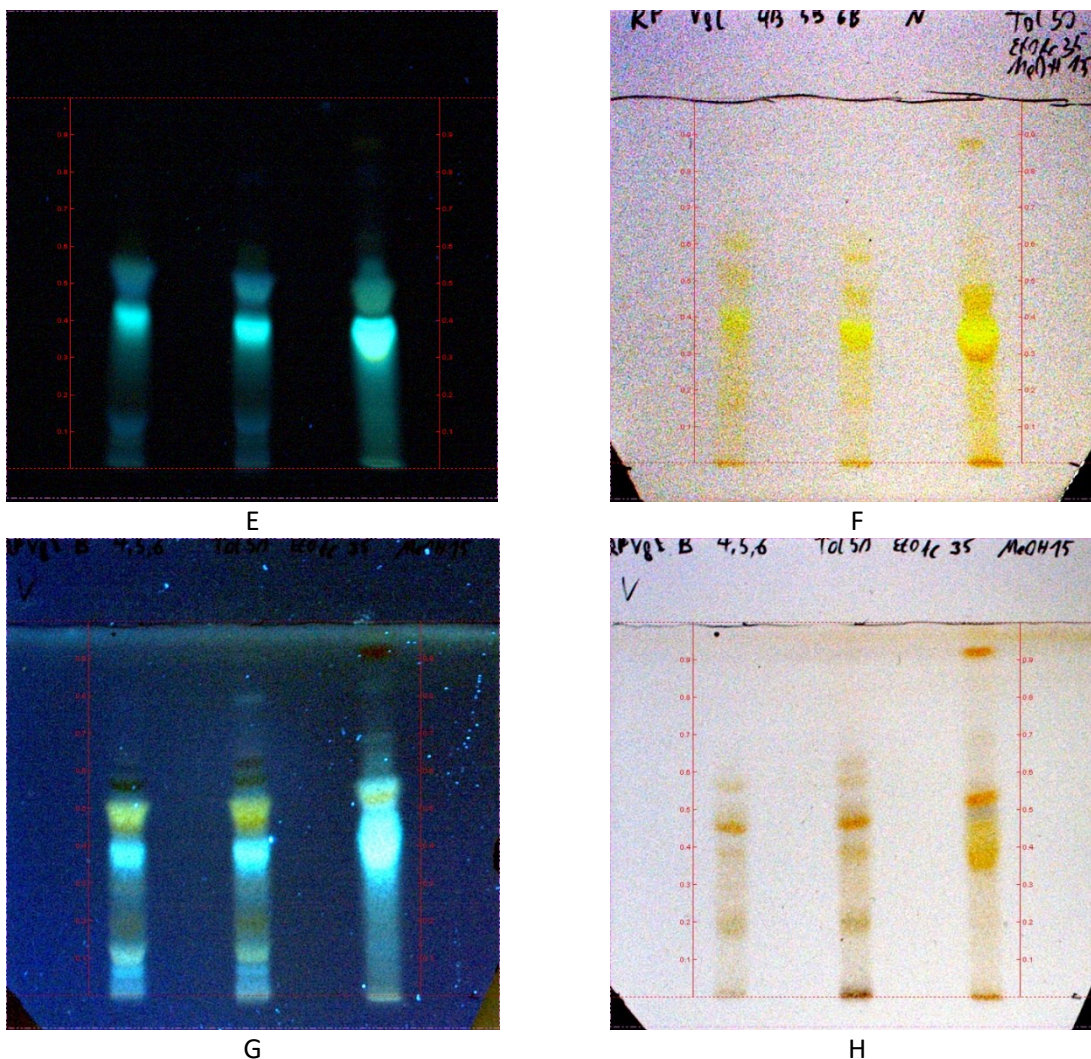


Figure 61: TLC (RP-18) comparison of the BuOH extracts 18I4B (fresh rhizomes), 18I5B (aged rhizomes), and 18I6B (fresh roots; Figure 54 or Table 15 in section 4.2.2.4). The three spots on every plate correspond from the left to the right to 18I4B, 18I5B, and 18I6B. A/B: TLC plates without derivatisation under UV-light at 254 nm (left) and 366 nm (right). TLC plates derivatised with AA (C/D), N (E/F) and V (G/H) under UV-light at 366 nm (left) and under white light (right). Eluent for every plate: TLC_4 (see Table 16 in section 4.2.2.5).

As can be seen in Figure 61, the BuOH rhizome extracts 18I4B (fresh rhizomes) and 18I5B (aged rhizomes) were very similar and differ from the BuOH root extract 18I6B (fresh roots). The derivatisation with AA and N gave indications that the three BuOH extracts 18I4B (fresh rhizomes), 18I5B (aged rhizomes), and 18I6B (fresh roots) should contain many polyphenols, saponins and/or bittering agents and especially flavonoids and isoflavonoids (E/F derivatised derivatised with N in Figure 61; R_f -values \approx 0.6 and 0.9). The presence of irones (see Figure S 22 of the Appendix) has also been checked by TLC comparison between 18I9 (iris butter from aged rhizomes from hydro distillation; Figure 53 or Table 15 in section 4.2.2.4) and the three BuOH-extracts 18I4B (fresh rhizomes), 18I5B (aged rhizomes), and 18I6B (fresh roots). As expected, no irones were present in these extracts.

Comparison between 19IH, 19IA, 19IHa, 19IAa (fresh and aged roots' extracts) and the DCM extracts 18I1, 18I2, and 18I3:

As the extract 18I3 (DCM extract of fresh roots; Figure 52 or Table 15 in section 4.2.2.4) had a very good and complex odour, it could be interesting for perfumers. It was decided to investigate the roots further with other extraction media (because DCM is not suitable for applications in the perfume industry). The roots, used for the extraction, were also aged like the rhizomes. Two extractions were performed with the fresh and aged roots with hexane and EtOAc successively. First, the different fresh root extracts 19IH (n-hexane extract of the fresh roots of *Iris germanica* L.) and 19IA (EtOAc extract of the fresh roots of *Iris germanica* L.; see Figure 53 or Table 15 in section 4.2.2.4) were compared (see Figure 62 and Figure S 23 of the Appendix). Then, the fresh and aged roots' extracts 19IH, 19IHa (n-hexane extract of the aged roots of *Iris germanica* L.), 19IA, and 19IAa (EtOAc extract of the aged roots of *Iris germanica* L.; see Figure 53 or Table 15 in section 4.2.2.4) were compared (see Figure 63). The DCM-extracts 18I1 (fresh rhizomes), 18I2 (aged rhizomes), and 18I3 (fresh roots; Figure 52 or Table 15 in section 4.2.2.4) were compared to the extract 19IA.

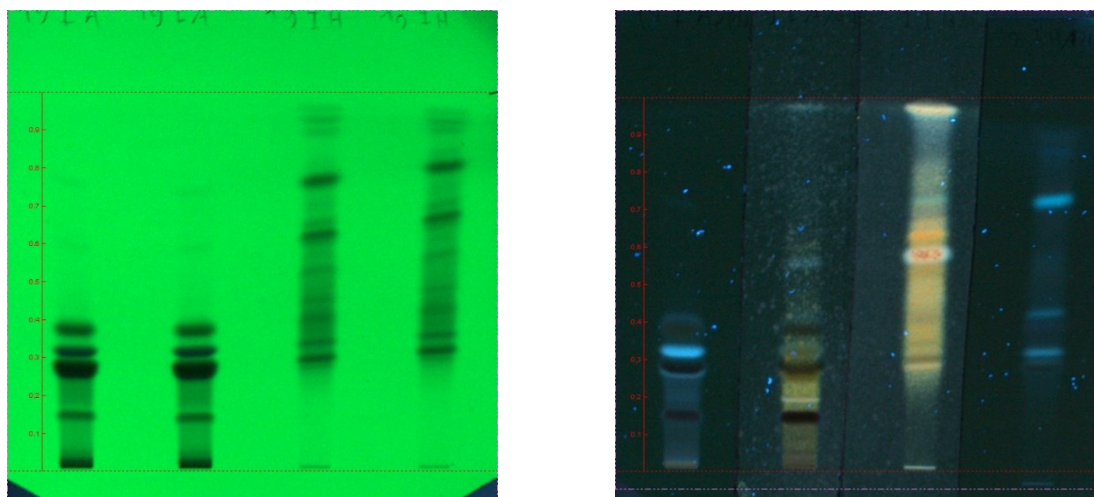


Figure 62: TLC comparison of root extracts 19IA (EtOAc extract of the fresh roots of *Iris germanica* L.) and 19IH (n-hexane extract of the fresh roots of *Iris germanica* L.; Figure 53 or Table 15 in section 4.2.2.4) under UV-light at 254 nm (left) and at 366 nm (right). The four spots on every plate correspond from the left to the right respectively to 19IA, 19IA, 19IH and 19IH. The plate on the left is not derivatised. The plate on the right is partially derivatised with AA (for the two spots in the middle, 19IA and 19IH). Eluent: TLC_6 (see Table 16 in section 4.2.2.5).

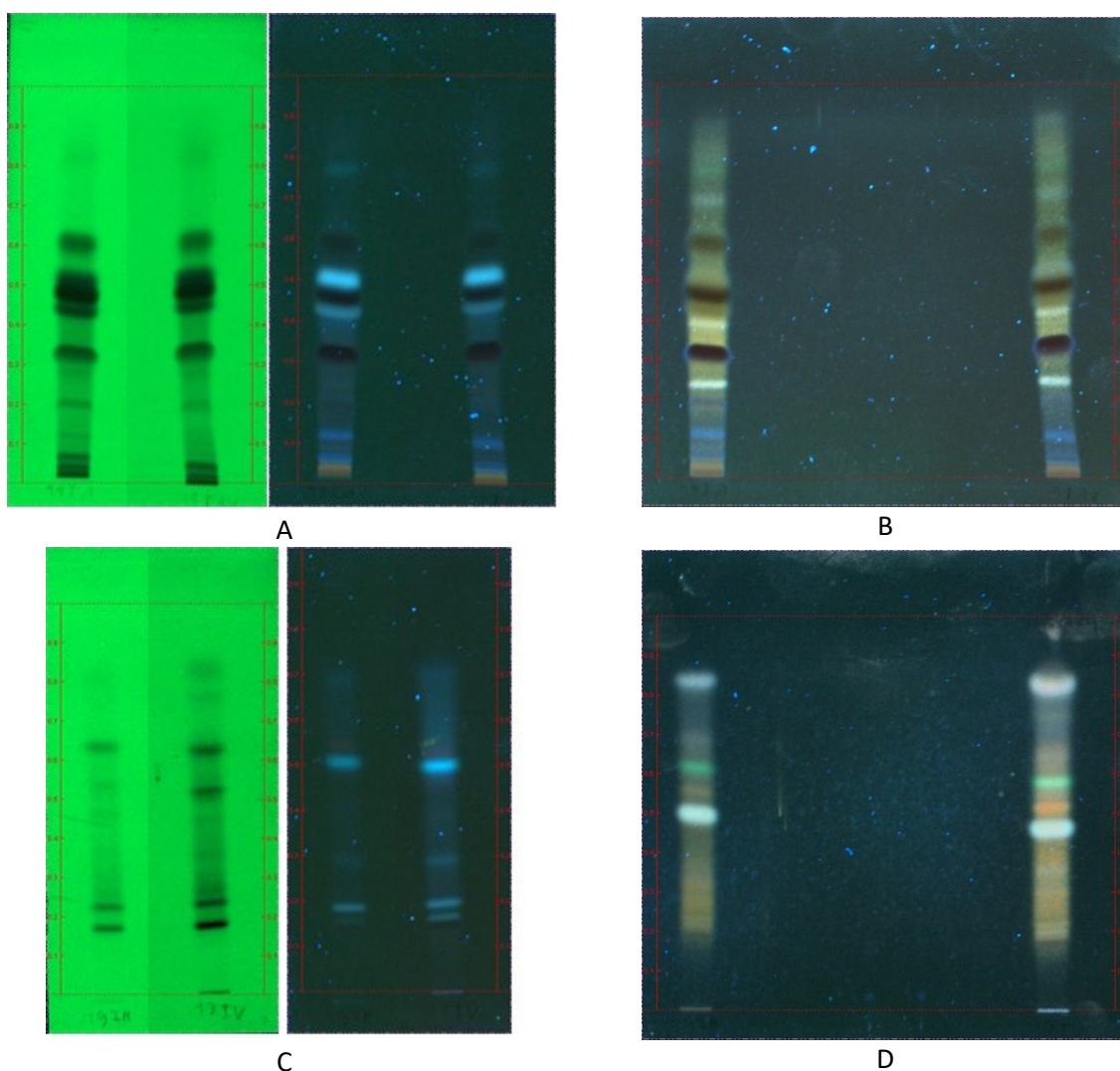
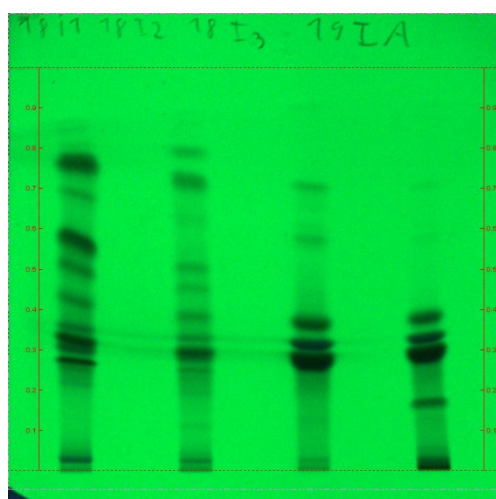


Figure 63: TLC comparison of fresh and aged root extracts 19IA (EtOAc extract of the fresh roots of *Iris germanica* L.), 19IAa (EtOAc aged roots' extract), 19IH (n-hexane extract of the fresh roots of *Iris germanica* L.) and 19IHa (n-hexane extract of the aged roots of *Iris germanica* L.; see Figure 53 or Table 15 in section 4.2.2.4) under UV-light at 254 nm (left) and at 366 nm (middle and right). The TLC plates on the left and the middle are not derivatised. The TLC plate on the left is derivatised with AA. A/B: the two spots on every TLC plate correspond from the right to the left to 19IA and 19IAa. C/D: the two spots on every TLC plate correspond from the right to the left to 19IH and 19IHa. Eluent: TLC_5 (see Table 16 in section 4.2.2.5).

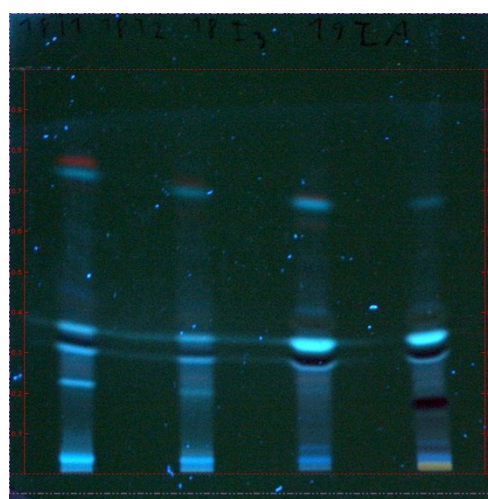
As can be noticed, 19IH (n-hexane extract of the fresh roots of *Iris germanica* L.) and 19IA (EtOAc extract of the fresh roots of *Iris germanica* L.) were different. Moreover, the aging process did not influence the phytochemical profile of the roots (TLC plates A/B in Figure 63) unlike for the rhizomes (TLC plates C/D in Figure 59 for the comparison of the EtOAc extracts 18I4A (fresh rhizomes) and 18I5A(aged rhizomes)). Indeed, no new spots on the TLC plate were detected between the fresh and aged root extracts, even with the derivatisation. This result supported the fact that neither irones nor precursors of irones were present in the roots of *Iris germanica* L., they were only present in the rhizomes. The odour of the extracts 19IH, 19IHa (n-hexane extract of the aged roots of *Iris germanica* L.), 19IA, and 19IAa (EtOAc extract of the aged roots of *Iris germanica* L.; see Figure 53 or Table 15 in section 4.2.2.4) did change and evolve if the roots were previously aged or not, but no difference could

be detected concerning the change of the phytochemical profile of the roots with TLC. The same result was obtained concerning the GC-MS analysis of the iris roots butter as no significant difference could be detected for the major constituents.

The DCM-extracts 1811 (fresh rhizomes), 1812 (aged rhizomes), and 1813 (fresh roots; Figure 52 or Table 15 in section 4.2.2.4) were compared to the extracts 19IH and 19IA. The results are shown in Figure 64 and Figure S 24 of the Appendix. As reflected, 19IA was very similar to 1813 and had like 1813 similarities with 1811 and 1812 especially for the spots with low R_f -values ($R_f < 0.4-0.5$ in Figure 64). An additional spot ($R_f = 0.18$) was detected in 19IA, obviously belonging to an isoflavone as the spot appears green under UV-light at 366 nm after derivatisation with N (see Figure S 23 of the Appendix). On the contrary, 19IH was similar to 1813 with regard to the spots with high R_f -values ($R_f > 0.5$, Figure S 24 of the Appendix). Meaning that the non-polar part of 1813 was similar to 19IH and the polar part to 19IA. 19IA was further investigated to isolate some compounds using different chromatographic methods (open silica gel column and semi preparative HPLC).



A



B

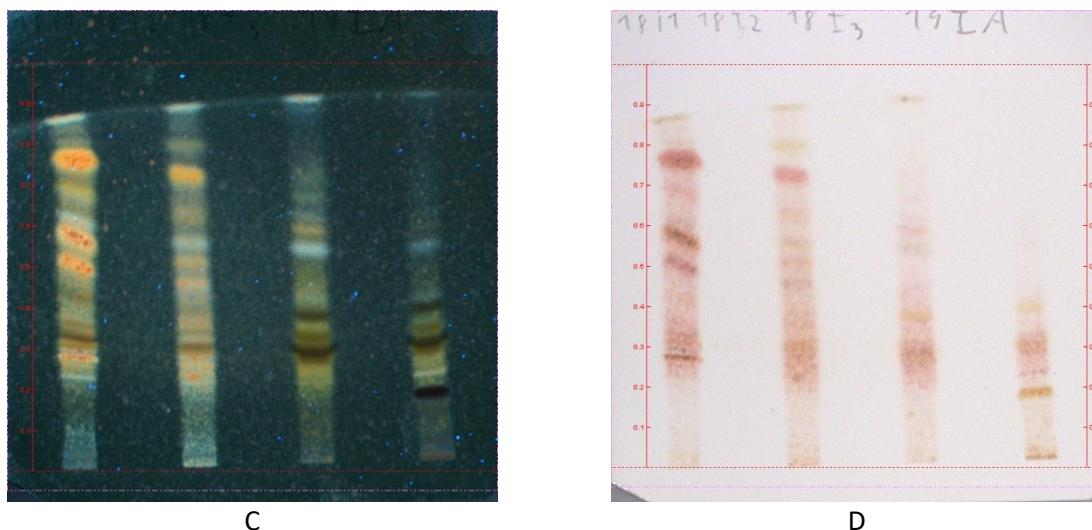


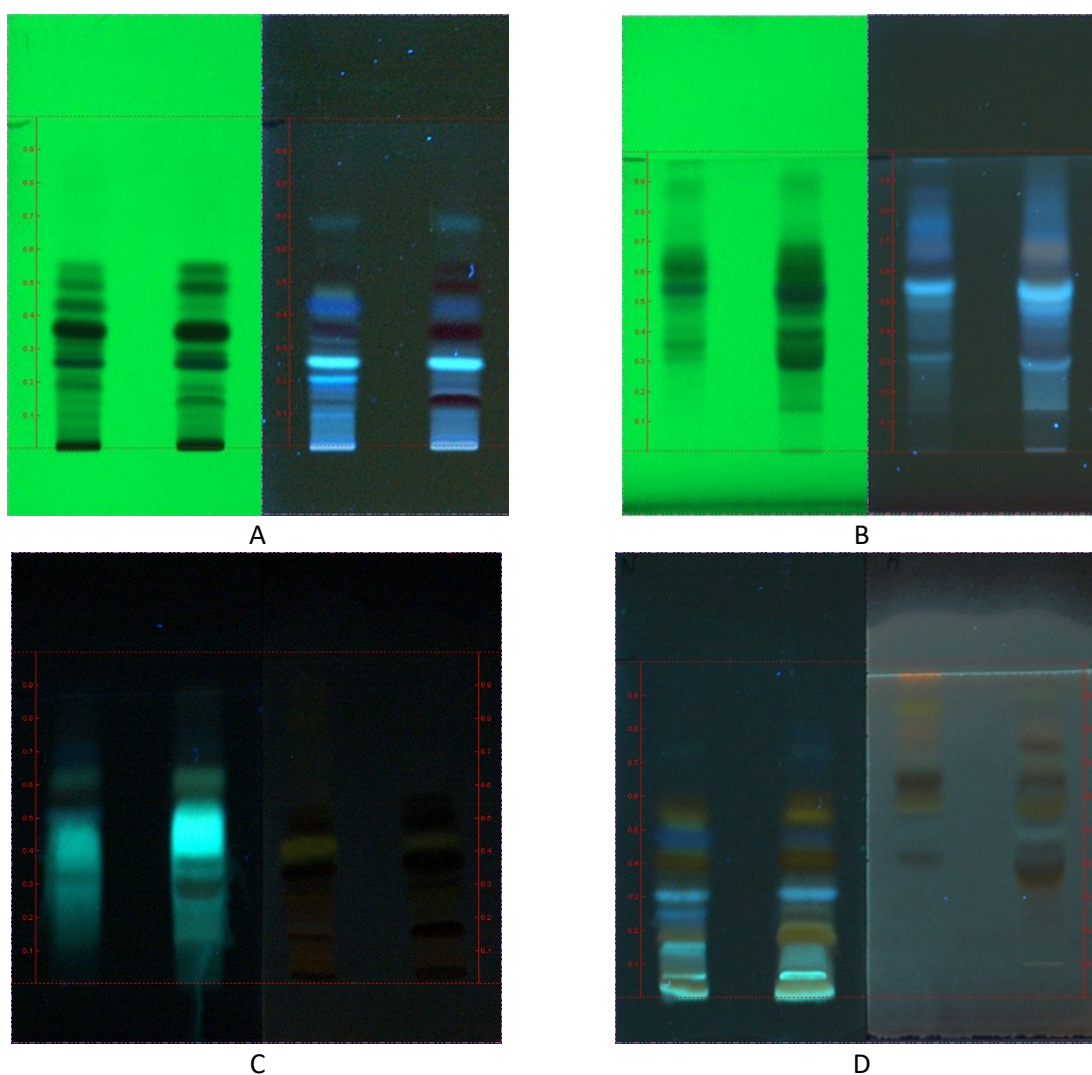
Figure 64: TLC comparison between the DCM extracts 1811 (fresh rhizomes), 1812 (aged rhizomes), and 1813 (fresh roots), and 191A (EtOAc extract of the fresh roots of *Iris germanica* L.; see Figure 53, Figure 54, and Table 15 in section 4.2.2.4). The four spots on every plate correspond from the left to the right to 1811, 1812, 1813 and 191A. A/B: TLC plates without derivatisation under UV-light at 254 nm (left) and 366 nm (right). C/D: TLC plates derivatised with AA under UV-light at 366 nm (left) and under white light (right). Eluent for every plate: TLC_5 (see Table 16 in section 4.2.2.5).

Comparison between the solvents extracts 201A (EtOAc extract) and 201B (BuOH extract) from the residue of the hydro distillation and the EtOAc (1815A) and BuOH (1815B) extracts of aged rhizomes:

Finally, 201A (EtOAc extract of the residue of the hydro distillation, aged rhizomes of *Iris germanica* L.) and 201B (BuOH extract of the residue of the hydro distillation, aged rhizomes of *Iris germanica* L.; see Figure 53 or Table 15 in section 4.2.2.4) were compared with two extracts performed in 2018, 1815A (EtOAc extract of the aged rhizomes of *Iris germanica* L.) and 1815B (BuOH extract of the aged rhizomes of *Iris germanica* L.; see Figure 54 or Table 15 in section 4.2.2.4). The goal of the comparison was to see if the residues can be used as extraction material. Indeed, the residues are normally categorized as waste, because the most valuable compound of the rhizomes of *Iris germanica* L. is the iris butter and there is no other use or application for the rhizomes. Simultaneously, 191A (EtOAc extract of the fresh roots of *Iris germanica* L.; see Figure 53 or Table 15 in section 4.2.2.4) was also investigated because roots of *Iris germanica* L. are also classified as waste after harvesting. The results of the comparison between 201A, 201B, 1815A, and 1815B are shown in Figure 65. 1815A and 1815B showed aged rhizomes previously used for hydro distillation. 201H (n-hexane extract of the residue of the hydro distillation of aged rhizomes of *Iris germanica* L.; see Figure 53 or Table 15 in section 4.2.2.4) was not included due to its low amount (~25 mg), but its composition was analysed with GC-MS because the odour was very interesting (it smelled very honey-like). The GC-MS chromatogram of 201H is shown in Figure S 25 of the Appendix. The major component (peak at 8.01 min) responsible for the honey-like

odour was apocynin (also known as acetovanillone). The other major peaks were fatty acids (from n-decanoic acid to n-hexanoic acid).

As depicted in Figure 65, 201A and 201B were very similar to 1815A and 1815B, respectively. All the EtOAc and especially BuOH extracts contained a lot of flavonoids and isoflavonoids. Moreover, only a few differences can be observed between the EtOAc (201A) and BuOH (201B) extracts of the residue of the hydro distillation of aged rhizomes and the EtOAc (1815A) and BuOH (1815B) extracts of the aged rhizome done in 2018 (see Figure 65). Meaning, that the extraction could be performed after the hydro distillation to recover other valuable compounds in the rhizomes. Qualitatively, it can be noticed that some secondary metabolites are more abundant in the solvent extract, if this was done with aged rhizomes as extracting material and not with the residue of the hydro distillation of the aged rhizomes (the same concentration is applied on the TLC plates in Figure 65).



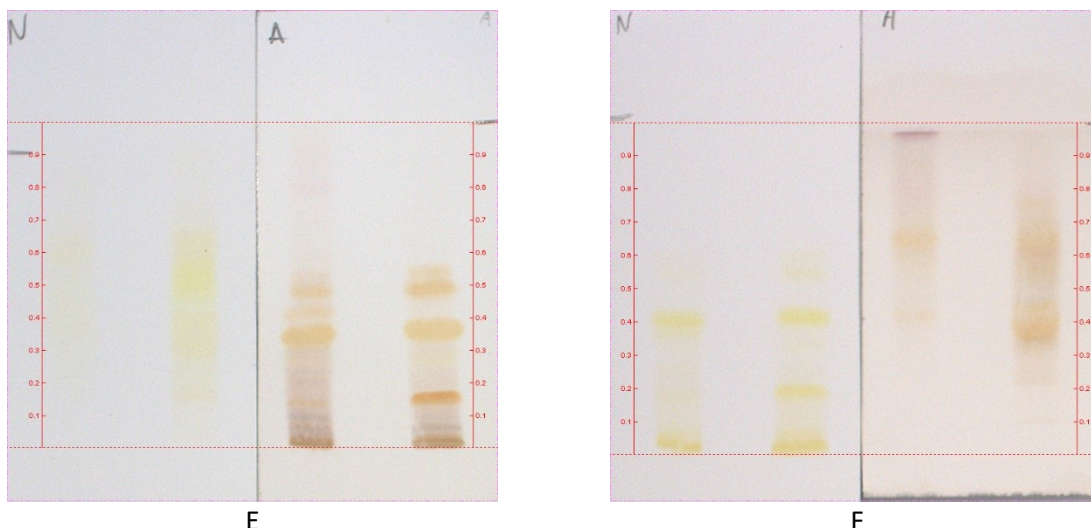


Figure 65: TLC comparison of 20IA (EtOAc extract of the residue of the hydro distillation of aged rhizomes of *Iris germanica* L.) and 20IB (BuOH extract of the residue of the hydro distillation of aged rhizomes of *Iris germanica* L.) with 1815A (EtOAc extract of the aged rhizomes of *Iris germanica* L.) and 1815B (BuOH extract of the aged rhizomes of *Iris germanica* L.; see Figure 53, Figure 54, and Table 15 in section 4.2.2.4) respectively. For every plate on the left, the four spots correspond from the left to the right to 20IA, 1815A, 20IA and 1815A. For every plate on the right, the four spots correspond from the left to the right to 20IB, 1815B, 20IB and 1815B. A/B: TLC plates without derivatisation under UV-light at 254 nm (left) and at 366 nm (right). C/D: TLC plates derivatised with N (left) and AA (right) under UV-light at 366 nm. E/F: TLC plates derivatised with N (left) and AA (right) under white light. Eluent for 20IA and 1815A: TLC_2 (see Table 16 in section 4.2.2.5). Eluent for 20IB and 1815B: TLC_9 (see Table 16 in section 4.2.2.5).

4.3.2 Cytotoxicity on HeLa and SK-MEL-28 cells

The DCM extracts (1811 (fresh rhizomes), 1812 (aged rhizomes), 1813 (fresh roots)), EtOAc extracts (1814A (fresh rhizomes), 1815A (aged rhizomes), 186A (fresh roots)), and BuOH extracts (184B (fresh rhizomes), 185B (aged rhizomes), 186B (fresh roots)); see Figure 54 or Table 15 in section 4.2.2.4) done in 2018 were tested in the cell culture on HeLa and SK-MEL-28 cells. The cytotoxicity was determined using MTT and a spectrophotometric method (see section 4.2.2.6.8). The aim of the cell culture test was to estimate the activity of the different extracts on cancer cells and then to relate the results of the cell culture with the results of the TLC analyses. The results of the cytotoxicity experiments are presented in Figure 66.

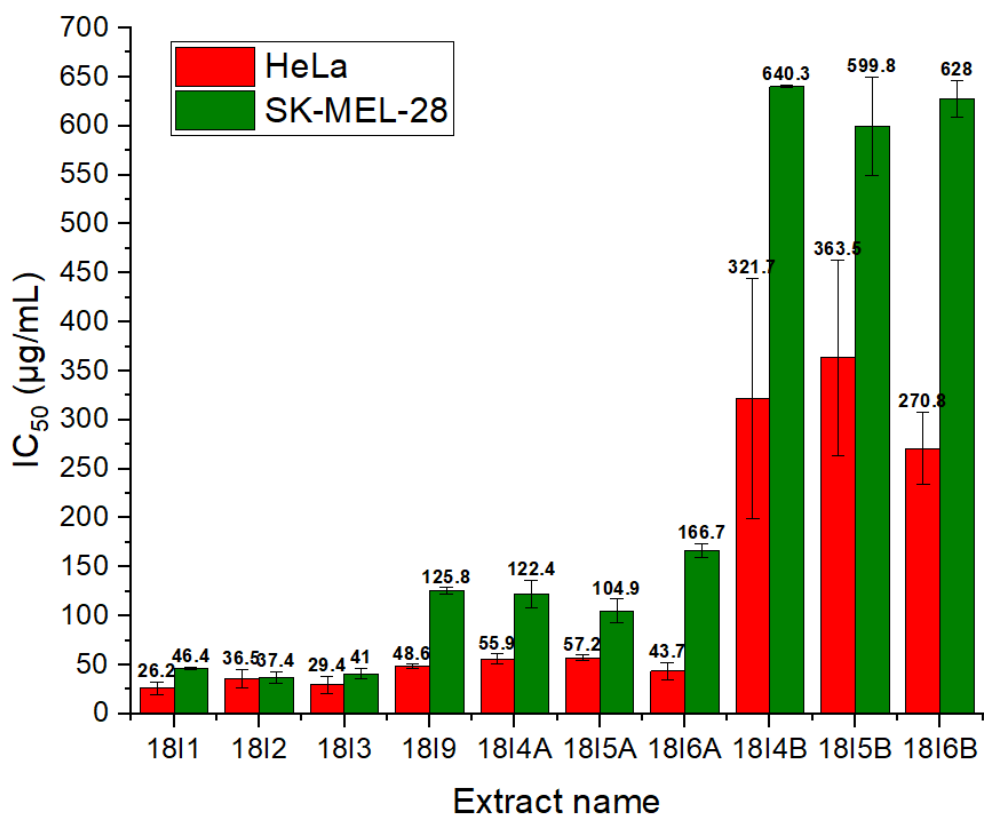


Figure 66: IC₅₀ in µg/mL of DCM extracts (1811 (fresh rhizomes), 1812 (aged rhizomes), 1813 (fresh roots)), EtOAc extracts (1814A (fresh rhizomes), 1815A (aged rhizomes), 186A (fresh roots)), and BuOH extracts (184B (fresh rhizomes), 185B (aged rhizomes), 186B (fresh roots)); see Figure 54 or Table 15 in section 4.2.2.4) done in 2018 on HeLa (red) and SK-MEL-28 (green). The given IC₅₀ with the calculated standard deviation is the average of 3-6 determined IC₅₀.

The IC₅₀ of the different solvent extracts decreased (= higher activity) with increasing lipophilicity of the extracts (for both tested cell line). It was not surprising, because lipophilic compounds easily penetrate through the cell membrane. The determination of the IC₅₀ for the BuOH extracts 1814B (fresh rhizomes), 1815B (aged rhizomes), and 1816 (fresh roots) was very complicated because of solubility problems and the very high tested concentrations. Therefore, the standard deviations are extremely large (see Figure 66 and Figure S 26 of the Appendix). Moreover, it was not possible to determine the IC₅₀ for the three Bu-OH extracts 1814B (fresh rhizomes), 1815B (aged rhizomes), and 1816 (fresh roots; see Figure 54 or Table 15 in section 4.2.2.4) with the SK-MEL-28 cells in every experiment because the highest concentration had a remaining activity over 50 % (see Figure S 26 of the Appendix), meaning that more than 50% of the cells were alive. Thus, the given IC₅₀ with the standard deviation in Figure 66 is not the average of all tested plates but only the average of the plates where the determination of the IC₅₀ was possible. Therefore, the given IC₅₀ is underestimated.

In general, the extracts were more active on HeLa than SK-MEL-28. Only the DCM-extracts had a similar IC₅₀ on both cell lines.

If the IC_{50} were compared with the TLC comparison, some interesting results can be observed. Indeed, the IC_{50} of 18I4A (fresh rhizomes) and 18I5A (aged rhizomes; see Figure 54 or Table 15 in section 4.2.2.4) were very similar for both cell lines cell lines and concerning the phytochemical profile. In contrast, TLC comparison between 18I4A (fresh rhizomes), 18I5A (aged rhizomes) and 18I6A (fresh roots), revealed more spots for 18I5A (aged rhizomes) as for 18I4A (fresh rhizomes) coming certainly from the aging process (see Figure 67).

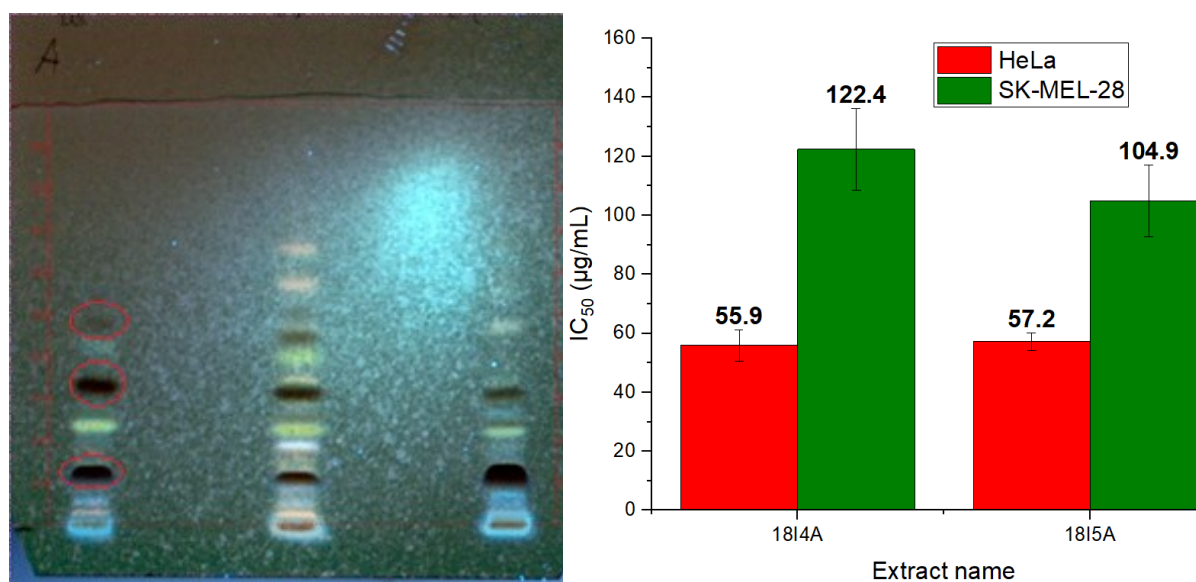


Figure 67: On the left: TLC comparison between the EtOAc extracts 18I4A (fresh rhizomes), 18I5A (aged rhizomes) and 18I6A (fresh roots; see Figure 54 or Table 15 in section 4.2.2.4). The spots from the right to the left correspond to 18I4A, 18I5A, and 18I6A derivatised with AA. The red circles represent the future investigated common spots between 18I4A and 18I5A. Eluent: TLC_2 (see Table 16 in section 4.2.2.5). On the right: IC_{50} of the EtOAc extracts 18I4A and 18I5A in $\mu\text{g/mL}$ with the calculated standard deviation on HeLa (red) and SK-MEL-28 (green) cells.

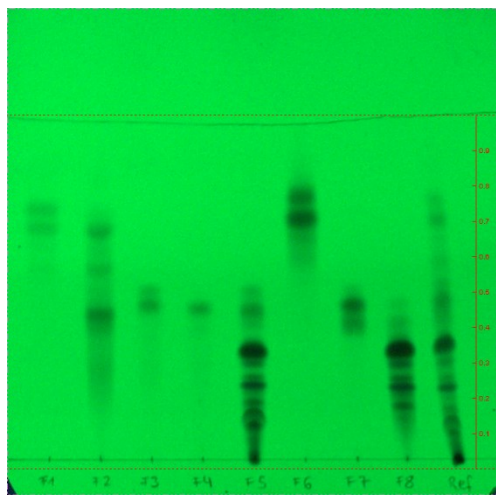
The three spots marked with a red circle in the Figure 67 correspond to spots present in 18I4A and 18I5A (the green spot ($R_f \approx 0.25$) could be also attributed to the common spots). They were probably responsible for the cytotoxic activity on HeLa and SK-MEL-28 cells. The aim was to isolate these three compounds using chromatographic methods and to investigate their structure. Simultaneously, the extract 19IA (EtOAc extract of the fresh roots of *Iris germanica* L.; see Figure 53 or Table 15 in section 4.2.2.4) was also investigated because of the presence of isoflavonoids (see section 4.3.4).

4.3.3 Isoflavonoids and a phenone in the EtOAc extract 18I4A from the fresh rhizomes of *Iris germanica* L.

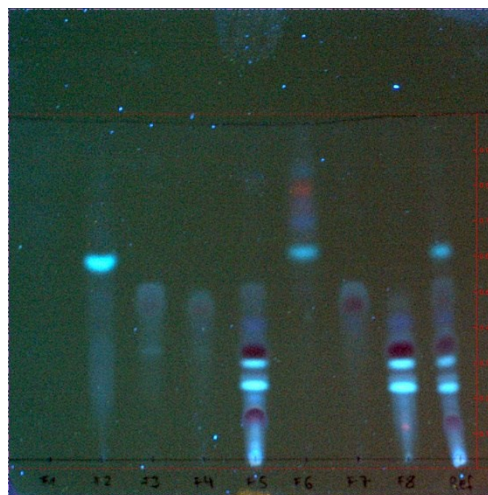
4.3.3.1 Isolation of the compounds 1, 5 and 6 (three isoflavonoids)

The separation of 18I4A (EtOAc extract of the fresh rhizomes of *Iris germanica* L.; see Figure 54 or Table 15 in section 4.2.2.4) with four silica gel columns (elution solvent: SGC_1, see Table 18 in section 4.2.2.7.1) resulted in 25 fractions. The TLC monitoring is shown in Figure 68 (eluent: TLC_2, see Table

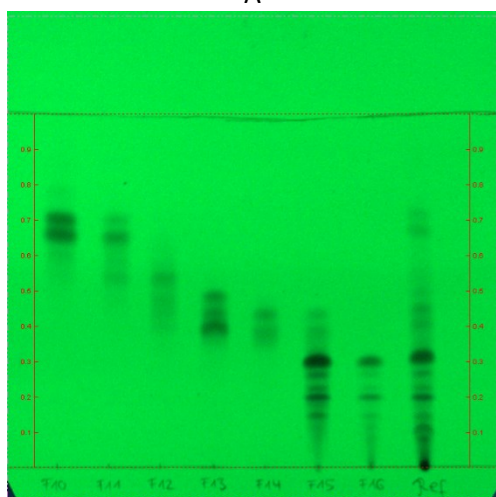
16 in section 4.2.2.5). As a result, three main fractions from the 25 fractions were combined: Z1, Z2 and Z3. The obtained amounts of the 25 fractions and the combination is shown in Table S 14 of the Appendix. A new mobile phase was developed for the separation of fraction Z1. The overview TLC plate with Z1, Z2, and Z3 is shown in Figure 69 (mobile phase: TLC_7, see Table 16 in section 4.2.2.5).



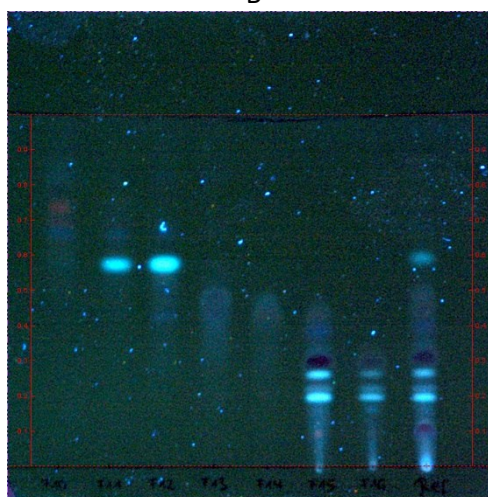
A



B



C



D

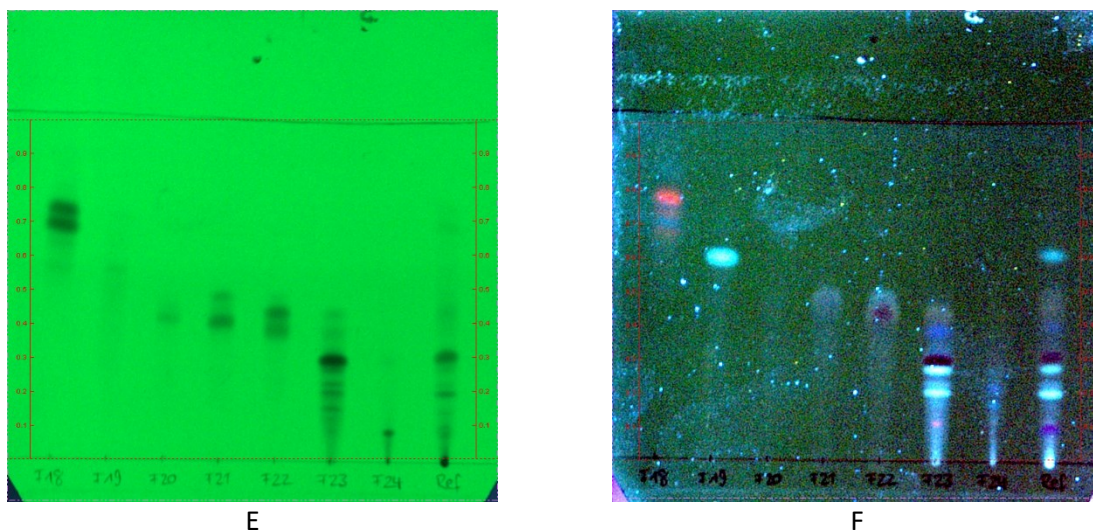


Figure 68: TLC monitoring of the 25 fractions obtained from the four open silica gel columns (mobile phase: SGC_1, see Table 18 in section 4.2.2.7.1) under UV-light at 254 nm (left) and at 366 nm (right). A/B: fractions F1 to F8 (see Table S 14 of the Appendix) with 18I4A (EtOAc extract of the fresh rhizomes of *Iris germanica* L.; see Figure 54 or Table 15 in section 4.2.2.4) as reference on the right. C/D: fractions F10 to F16 (see Table S 14 of the Appendix) with 18I4A (as reference on the right. E/F: fractions F18 to F24 (see Table S 14 of the Appendix) with 18I4A as reference on the right. The fractions F9, F17 and F25 were not spotted. Eluent: TLC_2 (see Table 16 in section 4.2.2.5). The spots were applied manually.

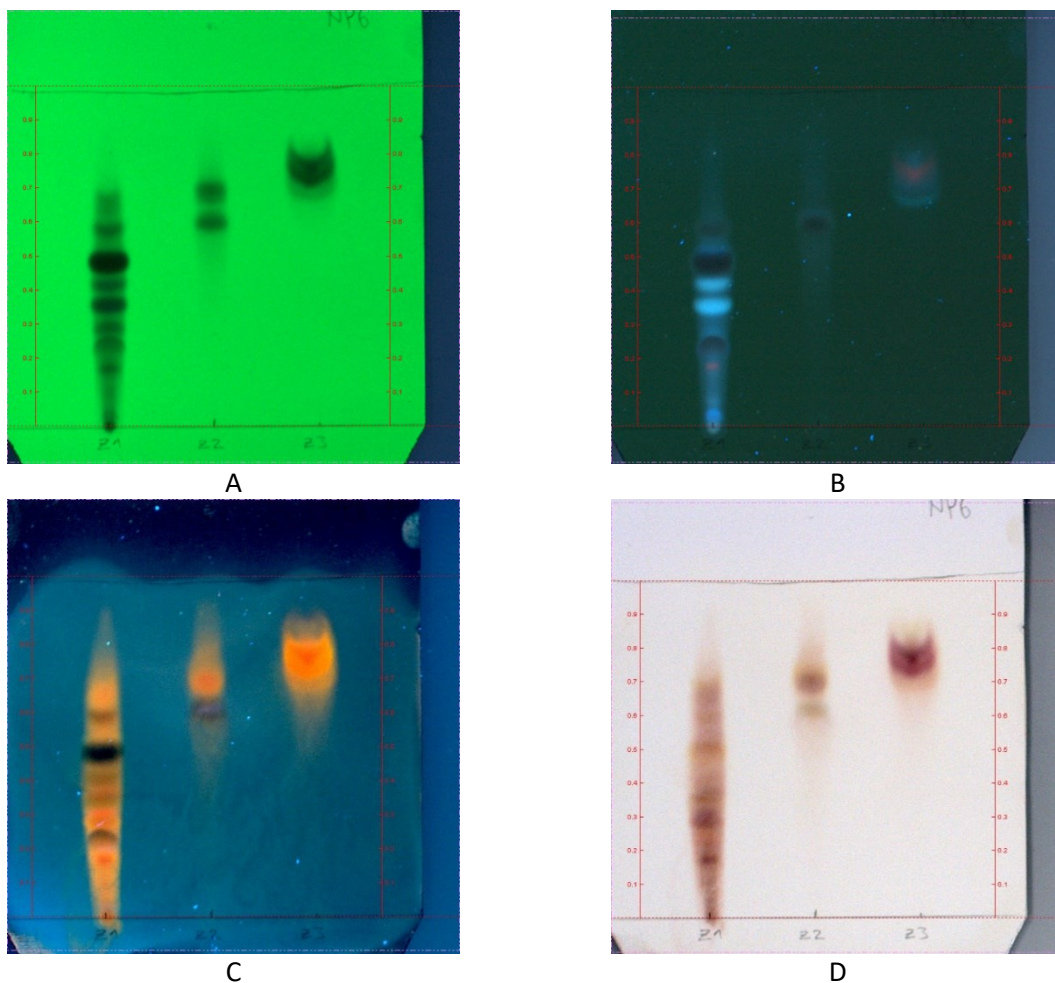


Figure 69: Overview TLC plate of the elution of 1814A (EtOAc extract of the fresh rhizomes of *Iris germanica* L.; see Figure 54 or Table 15 in section 4.2.2.4). The three spots on every plate are from the left to the right Z1, Z2 and Z3. A/B: TLC plates without derivatisation under UV-light at 254 nm (left) and 366 nm (right). C/D: TLC plates derivatised with AA under UV-light at 366 nm (left) and visible light (right). Eluent for every plate: TLC₇ (see Table 16 in section 4.2.2.5).

The isolation process was started one year after the preparation of 1814A. Thus, the EtOAc extract 1814A could contain irones as part of the phytochemical profile of Z3. A TLC comparison of Z3 and 1819 (iris butter from the aged rhizome of *Iris germanica* L. from hydro distillation; see Figure 54 or Table 15 in section 4.2.2.4) revealed, that Z3 did not contain irones (Figure S 27 of the Appendix). From all the fractions obtained, the fraction F4_1814A (spot with a R_f -value of 0.45 in A/B in Figure 68 of the fourth applied spot (corresponding to the fraction F4, see Table S 14 of the Appendix)) solely contained the desired first compound of 1814A (first spot with a R_f -value between 0.45 and 0.50 circle in red in Figure 67). Therefore, F4_1814A was not combined with other fractions. The fraction Z2 contained also the first wanted compound of 1814A (spot of Z2 (spotted in the middle of the TLC plate) with the lowest R_f -value on the TLC plates in Figure 69) together with another compounds (spot of Z2 (spotted in the middle of the TLC plate) with the highest R_f -value on the TLC plates in Figure 69). The compounds of F4_1814A were also present in the fraction Z2 (see Figure S 28 of the Appendix). The fractions, F4_1814A

and Z2 were further analysed with HPLC. The analytical HPLC-chromatograms of Z2 (RP-18 column) and of F4_1814A (alike Z2P1, fraction of Z2 isolated with the semi preparative HPLC (RP-18 column). Z2P1 contained the first three peaks detected in the analytical HPLC-chromatogram of Z2 (biphenyl column) as shown in Figure 70 and Figure 71, respectively.

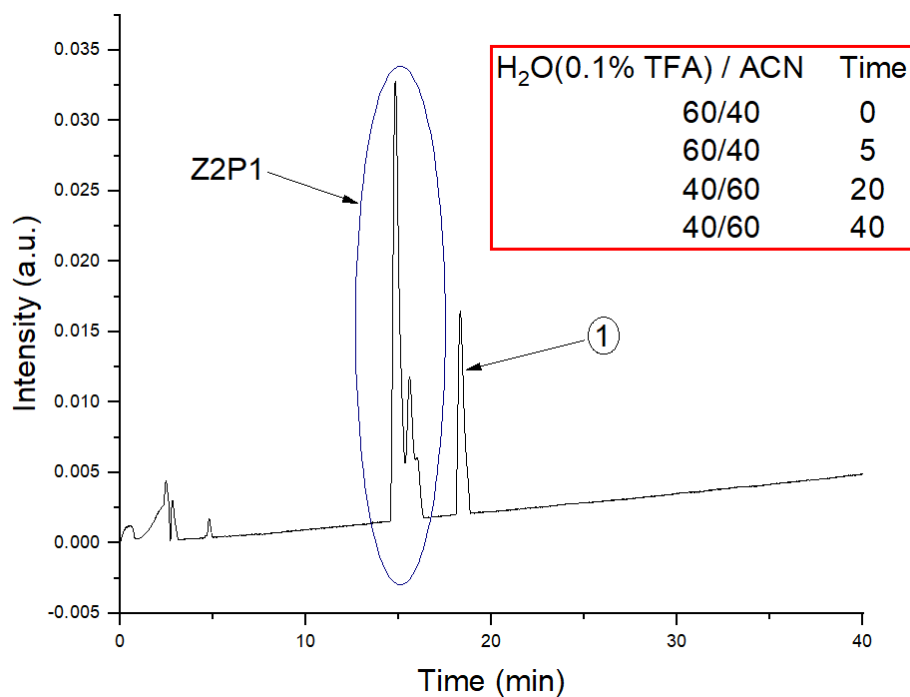


Figure 70: Analytical HPLC-chromatogram of Z2 (RP-18 column) from 1814A (EtOAc extract of the fresh rhizomes of *Iris germanica* L.; see Figure 54 or Table 15 in section 4.2.2.4). The substance 1 (see Figure 55) and subfraction Z2P1 (first three peaks of the analytical HPLC-chromatogram of Z2) were isolated using semi preparative HPLC with gradient method HPLC_1 (see Table 18 in section 4.2.2.7.1).

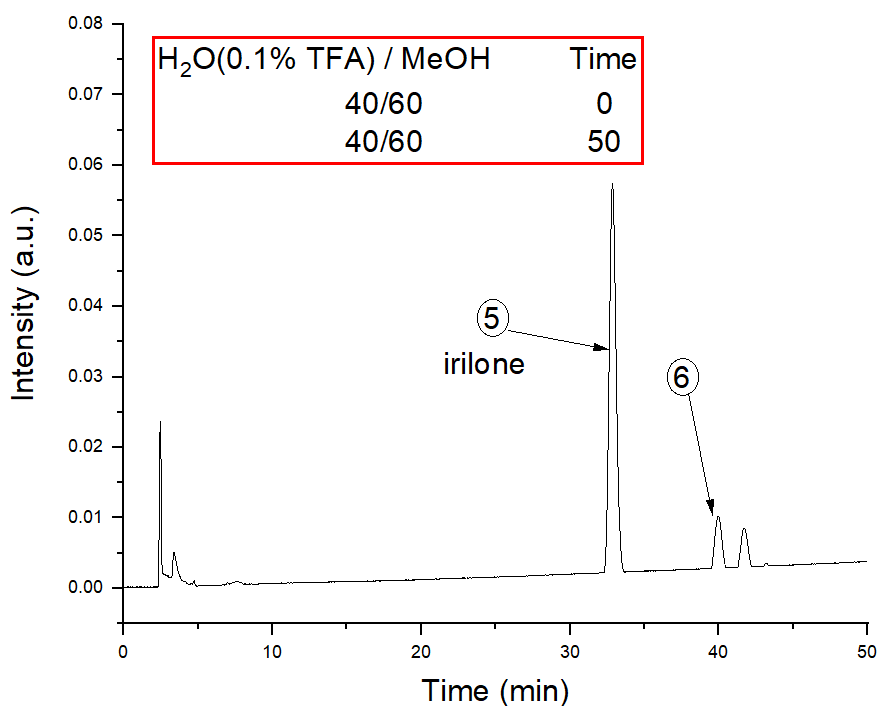


Figure 71: Analytical HPLC-chromatogram of F4_18I4A (alike Z2P1, fraction of Z2 isolated by semi preparative HPLC (RP-18)). Z2P1 contained the first three peaks of the analytical HPLC-run of Z2 (see Figure 70) using a biphenyl column. F4_18I4A is the spot with a R_f -value of 0.45 on the TLC plates A/B in Figure 68 of the fourth applied spot. Compounds **5** (irilone) and **6** (see Figure 55) were isolated using the semi preparative HPLC with the gradient method HPLC_3 (see Table 18 in section 4.2.2.7.1).

The fraction Z2P1 was isolated with the semi preparative HPLC (RP-18) and contained the first three peaks detected in the analytical HPLC-chromatogram of Z2 (see Figure 70). It was also analysed with semi preparative HPLC (applying the method HPLC_1, see Table 18 in section 4.2.2.7.1). The peaks of F4_18I4A (spot with a R_f -value of 0.45 on the TLC plates A/B in Figure 68 of the fourth applied spot, corresponding to the fraction F4, see Table S 14 of the Appendix) and Z2P1 showed the same NMR-spectra and the same LC-MS data. 2.1 mg of the compound **1**, 8 mg of the compound **5** (irilone) and 1.3 mg of the compound **6** were isolated from the fractions Z2 and F4_18I4A.

4.3.3.2 Isolation of the compounds **2** (phenone), **3** and **4** (two isoflavonoids)

The fraction Z1 (1.7 g) was further separated by open silica gel column (mobile phase: SGC_2, see Table 18 in 4.2.2.7.1). Separation resulted in 5 main fractions: Z1F1, Z1F2, Z1F3, Z1F4 and Z1F5. The overview plate is shown in Figure 72 below. The obtained amount of each fraction is summarised in Table 21.

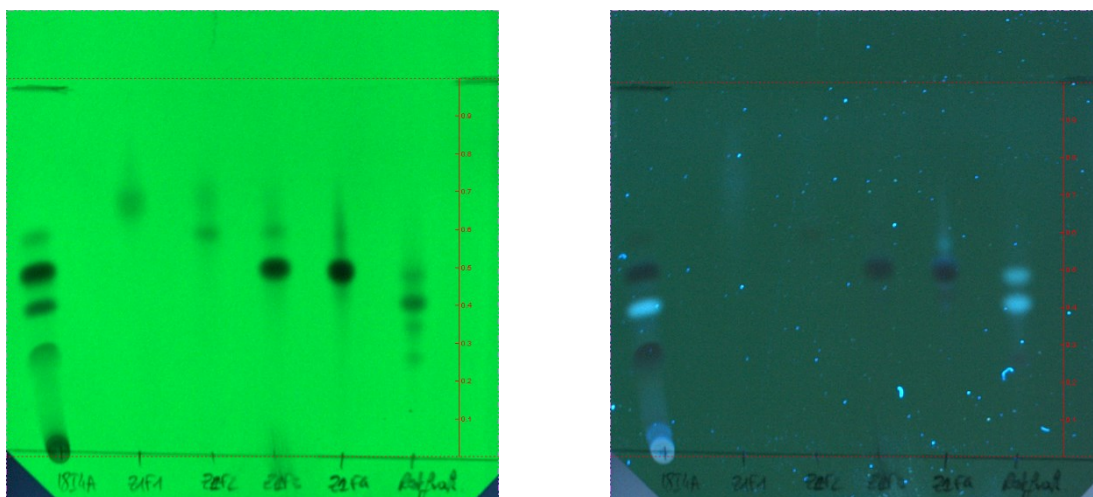


Figure 72: Overview TLC on separation of fraction Z1 (elution solvent: SGC_2, see Table 18 in 4.2.2.7.1) under UV-light at 254 nm (left) and 366 nm (right). The spots are from the left to the right: 1814A (EtOAc extract of the fresh rhizomes of *Iris germanica* L.; see Figure 54 or Table 15 in section 4.2.2.4), Z1F1, Z1F2, Z1F3, Z1F4 and Z1F5. Eluent: TLC_7 (see Table 16 in 4.2.2.5).

Table 21: Overview of the obtained amount of each fraction from the elution of Z1 (elution solvent: SGC_2, see Table 18 in 4.2.2.7.1).

Fraction name	Mass (mg)	Fraction name	Mass (mg)
Z1F1	70.3	Z1F4	247
Z1F2	n.a. (too low amount)	Z1F5	591
Z1F3	217.2	Total Z1F1 to Z1F5	1124.5

The fractions Z1F3 and Z1F4 contained the spot with a R_f -value of 0.50 (1814A, in Figure 72). Fractions Z1F1 and Z1F2 were similar to Z3 and Z2 (main fractions from separation of 1814A (EtOAc extract of the fresh rhizomes of *Iris germanica* L.; see Figure 54 or Table 15 in section 4.2.2.4) using the elution solvent SCG_1, see Table 18 in 4.2.2.7.1). Only the fraction Z1F4 was further analysed with HPLC. The HPLC-chromatogram of Z1F4 is shown in Figure 73. The three main compounds and a mixture of **3** and **4** were isolated from the fraction Z1F4: 6 mg of **2** (4-hydroxy-3-methoxyacetophenone), 15.8 mg of **3** (irigenin), 10 mg of **4** (irigenin S) and 40 mg of a mixture of **3** and **4**.

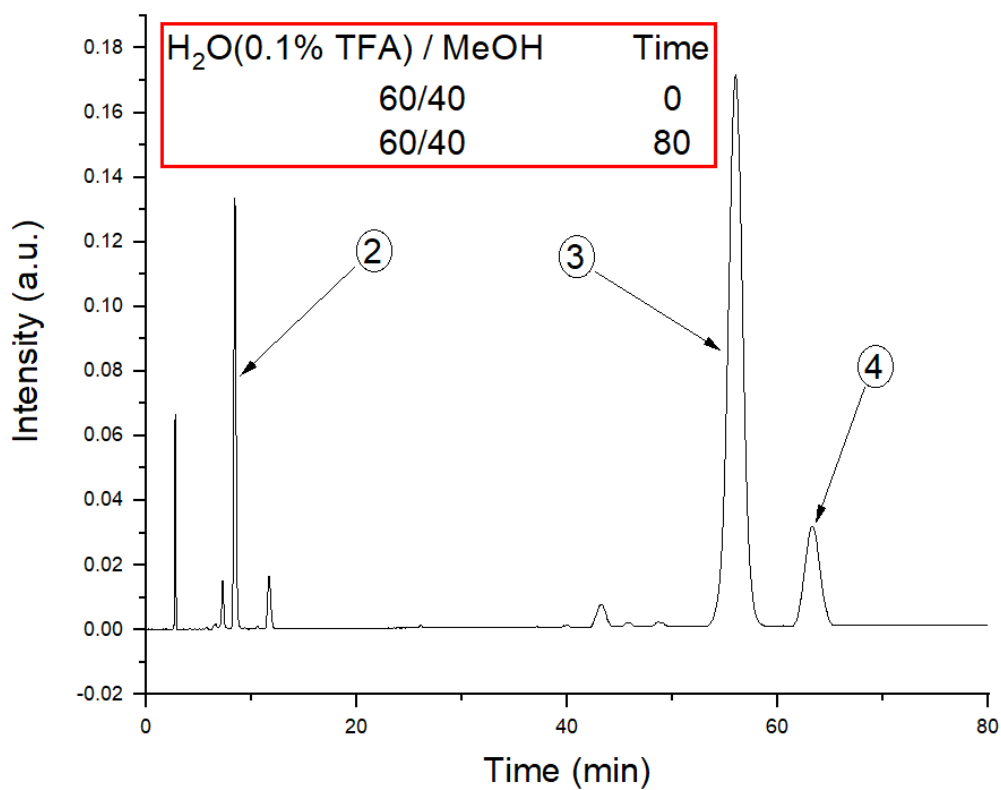


Figure 73: Analytical HPLC-chromatogram of Z1F4, one of the main fractions obtained from Z1 separation (RP-18). Z1 is the residual fraction of the separated 18I4A (EtOAc extract of the fresh rhizomes of *Iris germanica* L.; see Figure 54 or Table 15 in section 4.2.2.4) using the mobile phase SCG_1, see Table 18 in 4.2.2.7.1). The substances **2**, **3** (irigenin) and **4** (irigenin S, see Figure 55 for the structures) were isolated using semi preparative HPLC with the gradient method HPLC_2 (see Table 18 in 4.2.2.7.1).

4.3.3.3 Structure elucidation

The molecular structure of the isolated compounds was revealed with NMR-spectra in acetone- d_6 (1D and 2D) and with LC-MS data. The structures of the 6 compounds are shown in Figure 74. The LC-MS and NMR-data are shown in Table 22 and Table 23.

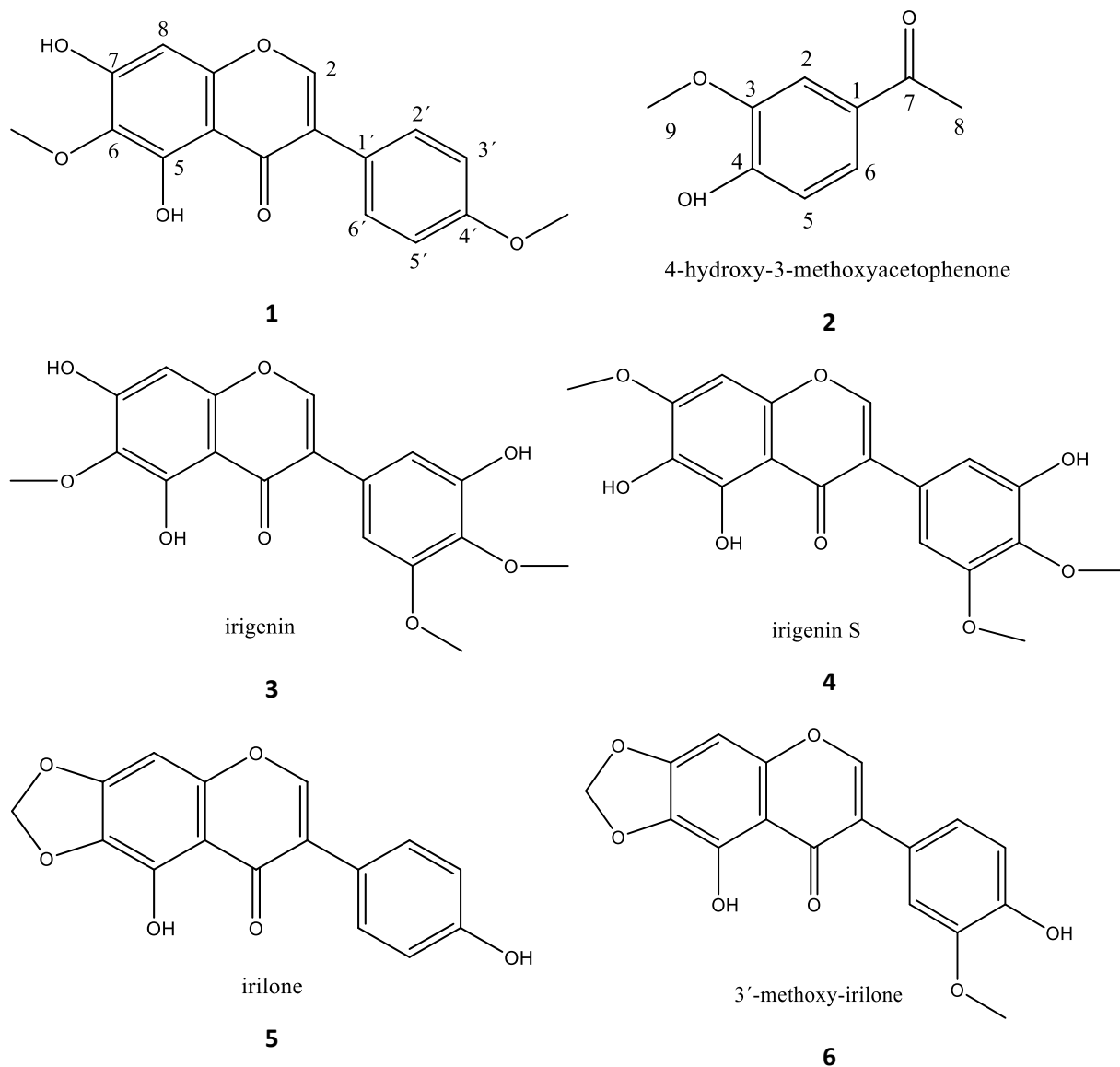


Figure 74: Structure of the isolated compounds **1-6** from 18I4A (EtOAc extract of the fresh rhizomes of *Iris germanica* L.; see Figure 54 or Table 15 in section 4.2.2.4).

Table 22: LC-MS and NMR-data of compound **1** (5,7-dihydroxy-6-methoxy-3-(4-methoxyphenyl)-4H-chromen-4-one) and **2** (4-hydroxy-3-methoxyacetophenone). See Figure 74 for the structures.

Compound 1 , LC-MS: (M-H) ⁺ : 315.0868 C ₁₇ H ₁₄ O ₆				Compound 2 , LC-MS: (M-H) ⁺ : 167.0704 C ₉ H ₁₀ O ₃			
H	δ _H (ppm)	Number of H, multiplicity, J (Hz)	group	H	δ _H (ppm)	Number of H, multiplicity, J (Hz)	group
2	8.21	1H, s	/	2	7.54	1H, d, 1.95	/
5	13.19	1H, s	hydroxy + H intramolecular	3	3.91	3H, s	methoxy
6	3.87	3H, s	methoxy	4	/	/	hydroxy
7	/	/	hydroxy	5	6.92	1H, d, 8.26	/
8	6.52	1H, s	/	6	7.57	1H, dd, 1.95; 8.26	/
2'/6'	7.54	2H, d, 8.73	/				
3'/5'	6.99	2H, d, 8.73	/	8	2.5	3H, s	methyl
4'	3.83	3H, s	methoxy				

Compound **1** is an isoflavone (5,7-dihydroxy-6-methoxy-3-(4-methoxyphenyl)-4H-chromen-4-one) as the compounds **3** (irigenin), **4** (irigenin S), **5** (irilone) and **6** (3'-methoxy-irilone). The position of the different substituents was determined by 2D-NMR (CORrelation SpectroscopY COSY and Nuclear Overhauser Enhancement SpectroscopY, NOESY). The NOESY-spectrum of compound **1** is shown in Figure 75.

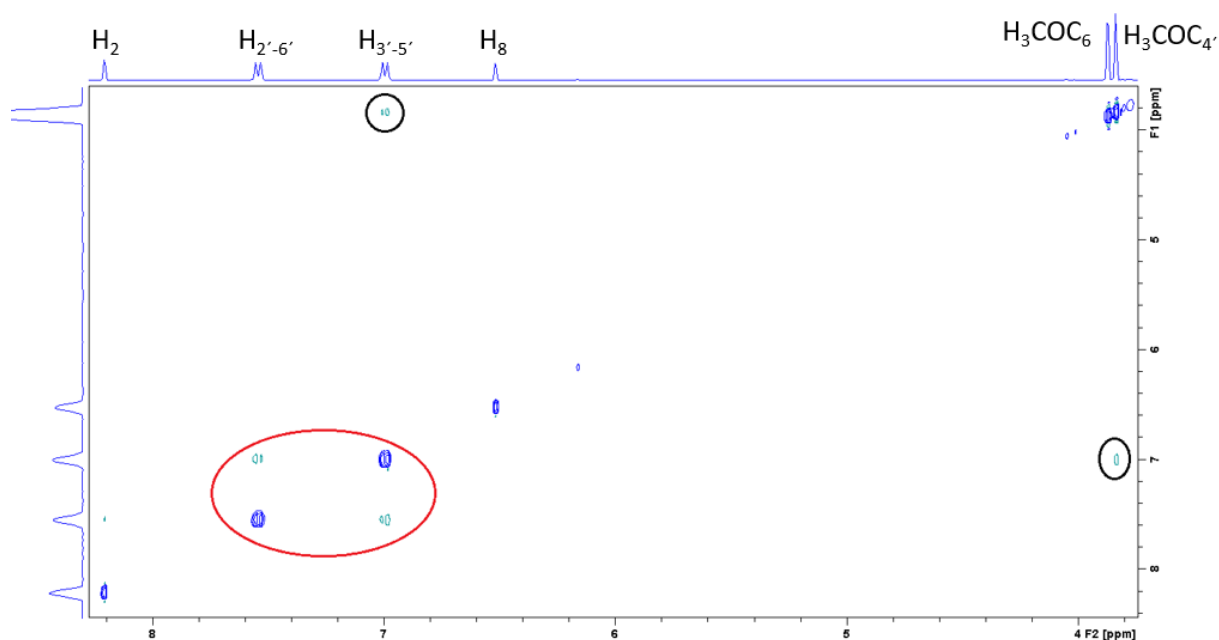


Figure 75: NOESY-spectrum of compound **1** (5,7-dihydroxy-6-methoxy-3-(4-methoxyphenyl)-4H-chromen-4-one, see Figure 74 for the structure) enhanced between 3.8 and 8.2 ppm. The red circle shows the cross peaks between the protons H-2'/6' and H-3'/5'. The black circle shows the cross peaks between the methoxy group H₃CO-C₄ and the protons H-3'/5'. H₃CO-C₆ represents the methoxy group at carbon C₆ (see Figure 74 for numbering of the carbons).

The presence of cross peaks between the protons H-3'/5' and the methoxy group H₃CO-C₄ as well as for protons H-2'/6' and H-3'/5' indicated that these pairs are neighbored. Moreover, a coupling constant ($^3J = 8.73$ Hz) can be obtained from the ¹H-spectrum (see x-axis in Figure 75). The absence of a cross peak between the methoxy group at C-6 and the proton H-8 gave the indication that they were not neighbours. Unfortunately, the region around 13 ppm (intramolecular H bond between OH group and ketone) was not included in the ¹H-spectrum to ensure the position of the methoxy group.

Compound **2** (4-hydroxy-3-methoxyacetophenone) is a phenone derivate. The position of the methoxy group for the compound **2** was also investigated and determined with 2D-NMR. The enhanced NOESY-spectrum is shown in Figure 76. The presence of cross peaks was noticed between H-6 and H-2, H-2 and the methoxy group at C-3 and between H-2/6 and H-8. Moreover, the signals for H-5 and H-2 are doublets with different coupling constants: $^3J = 8.26$ Hz for H-5 and $^4J = 1.95$ Hz for H-2. The same two coupling constants were found in the signal of H-6 (doublet of doublet), meaning that H-6 is neighbour of H₅ (3 bonds between the two protons, $^3J = 8.26$ Hz) and coupled long range to H-2 (4 bonds between the two protons, $^4J = 1.95$ Hz). The fact, that no cross peak was noticed between the methoxy group and H-5, indicated that the hydroxy group is neighbored to H-5 and the methoxy group is the direct neighbour of H-2 as a cross peak was detected between them.

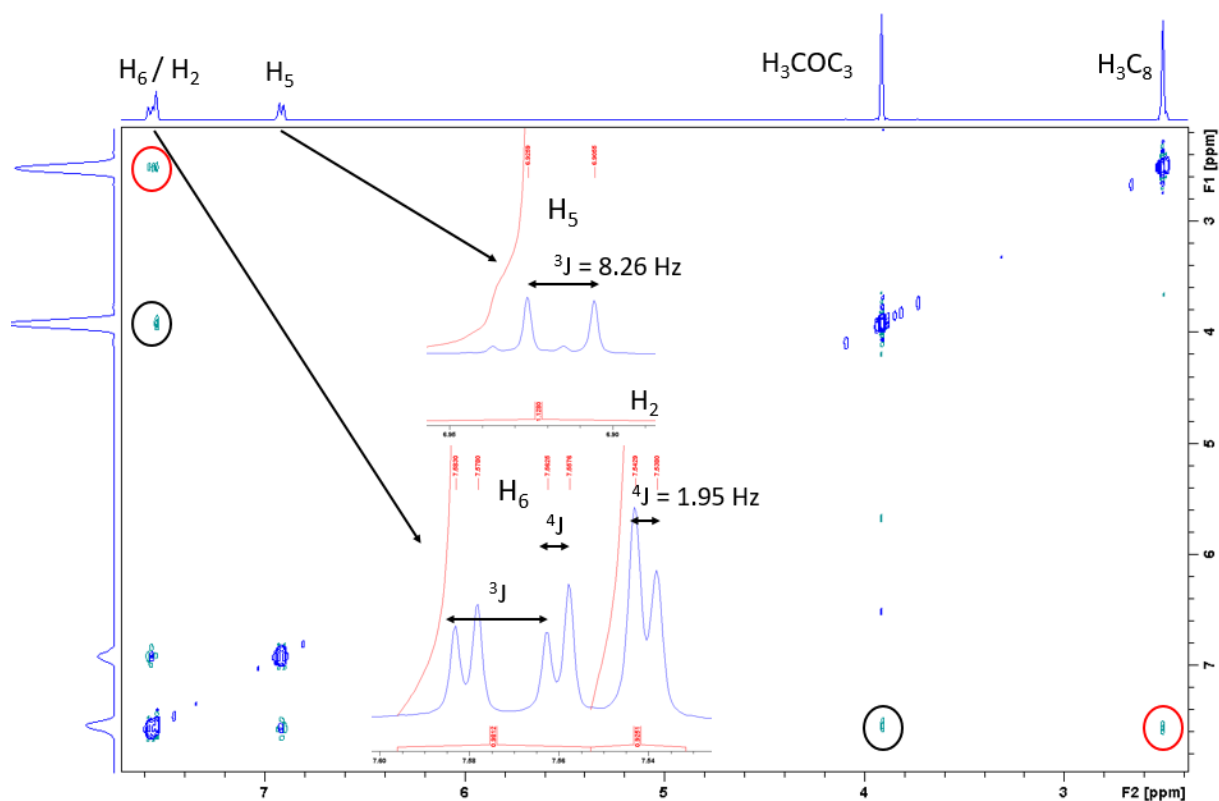
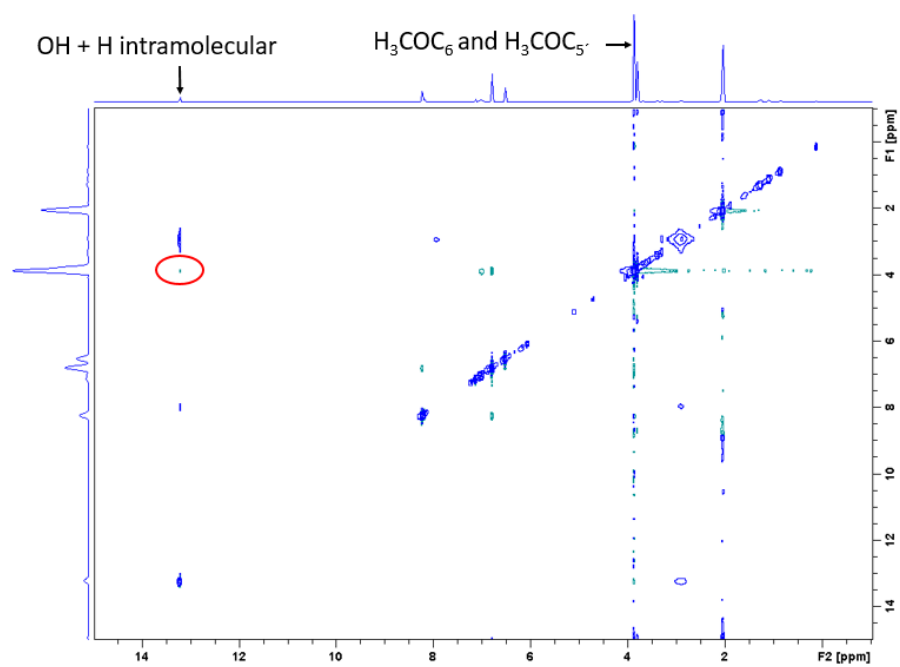


Figure 76: NOESY-spectrum of compound **2** (4-hydroxy-3-methoxyacetophenone, see Figure 74 for the structure) enhanced between 2.4 and 7.6 ppm. Zoom of the ^1H -spectrum with signals for H-2, H-5 and H-6 is shown including the different coupling constants ^3J and ^4J . The red and black circles indicate the cross peaks between H-6/H-2 and the $\text{H}_3\text{C}-\text{C}_8$ and H-2 and the methoxy group at C-3 respectively. $\text{H}_3\text{CO}-\text{C}_3$ represents the methoxy group at C-3 (see Figure 74 for numbering of the carbons).

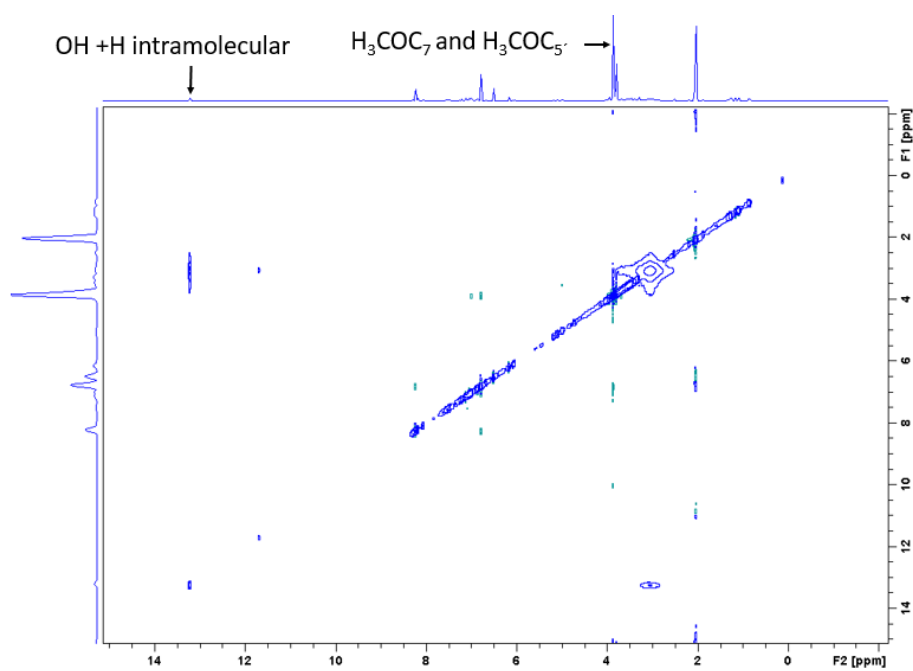
Structure elucidation of compounds **3** (irigenin), **4** (irigenin S), **5** (irilone) and **6** (3'-methoxy-irilone) was done the same way. First the structure elucidation of the compounds **3** (irigenin) and **4** (irigenin S) will be discussed. As can be seen in Figure 74, they differed only from the position of one methoxy group and one hydroxy group (on positions 6 and 7) and had the same ^1H -spectrum. To determine the position of the methoxy group a NOESY-spectrum was measured to potentially detect a cross peak between the methoxy group and the hydroxy group at C-5 (having an intramolecular H bond with the ketone at C-3). The NOESY-spectra of **3** and **4** are shown in Figure 77. The respective cross peak was detected for the ^1H -signal at 3.86 ppm (integration for 2 x 3 protons) of compound **3**, but not seen for the compound **4**. The position of the other substituents (two methoxy resonating at 3.86 and 3.79 ppm and one hydroxy group) was also determined with a NOESY-experiment for both compounds. The NOESY spectrum of **4**, enhanced between 3.2 and 8.4 ppm, is shown in Figure 78.

Table 23: LC-MS and NMR-data for the compound **3** (irigenin), **4** (irigenin S), **5** (irilone) and **6** (3'-methoxy-irilone). See Figure 74 for the structures.

Compound 3 , LC-MS: (M-H) ⁺ : 361.0919 C ₁₈ H ₁₆ O ₈				Compound 4 , LC-MS: (M-H) ⁺ : 361.0919 C ₁₈ H ₁₆ O ₈			
H	δ _H (ppm)	Number of H, multiplicity, J (Hz)	group	H	δ _H (ppm)	Number of H, multiplicity, J (Hz)	group
2	8.23	1H, s	/	2	8.23	1H, s	/
5	13.21	1H, s	hydroxy + H intramolecular	5	13.21	1H, s	hydroxy + H intramolecular
6/5'	3.86	6H, s	2x methoxy	6	/	/	hydroxy
7	/	/	hydroxy	7/5'	3.86	6H, s	2x methoxy
8	6.52	1H, s	/	8	6.52	1H, s	/
2'/6'	6.79	2H, s	/	2'/6'	6.79	2H, s	/
3'	/	/	hydroxy	3'	/	/	hydroxy
4'	3.79	3H, s	methoxy	4'	3.79	3H, s	methoxy
Compound 5 , LC-MS: (M-H) ⁺ : 299.0553 C ₁₆ H ₁₀ O ₆				Compound 6 , LC-MS: (M-H) ⁺ : 329.0654 C ₁₇ H ₁₂ O ₇			
H	δ _H (ppm)	Number of H, multiplicity, J (Hz)	group	H	δ _H (ppm)	Number of H, multiplicity, J (Hz)	group
2	8.24	1H, s	/	2	8.28	1H, s	/
5	13	1H, s	hydroxy + H intramolecular	5	13.03	1H, s	hydroxy + H intramolecular
6/7	6.14	2H, s	acetal	6/7	6.16	2H, s	acetal
8	6.66	1H, s	/	8	6.67	1H, s	/
2'/6'	7.45	2H, d, 8.59	/	2'	7.07	1H, dd, 1.65; 8.24	/
				3'	6.88	1H, d, 8.24	/
3'/5'	6.9	2H, d, 8.59	/	4'	/	/	hydroxy
				5'	6.16	3H, s	methoxy
4'	/	/	hydroxy	6'	7.25	1H, d, 1.65	/



A



B

Figure 77: NOESY-spectra of compounds **3** (A, irigenin) and **4** (B, irigenin S), see Figure 74 for the structures. The red circle indicates the cross peak between the methoxy group at C-6 and the proton from the hydroxy group at C-5 (the hydroxy has an intramolecular H bond with the ketone at C-3). H_3COC_7 , H_3COC_6 , and $H_3COC_{5'}$ represent the methoxy group at C-7, C-6, and C-5', respectively (see Figure 74 for numbering of the carbons).

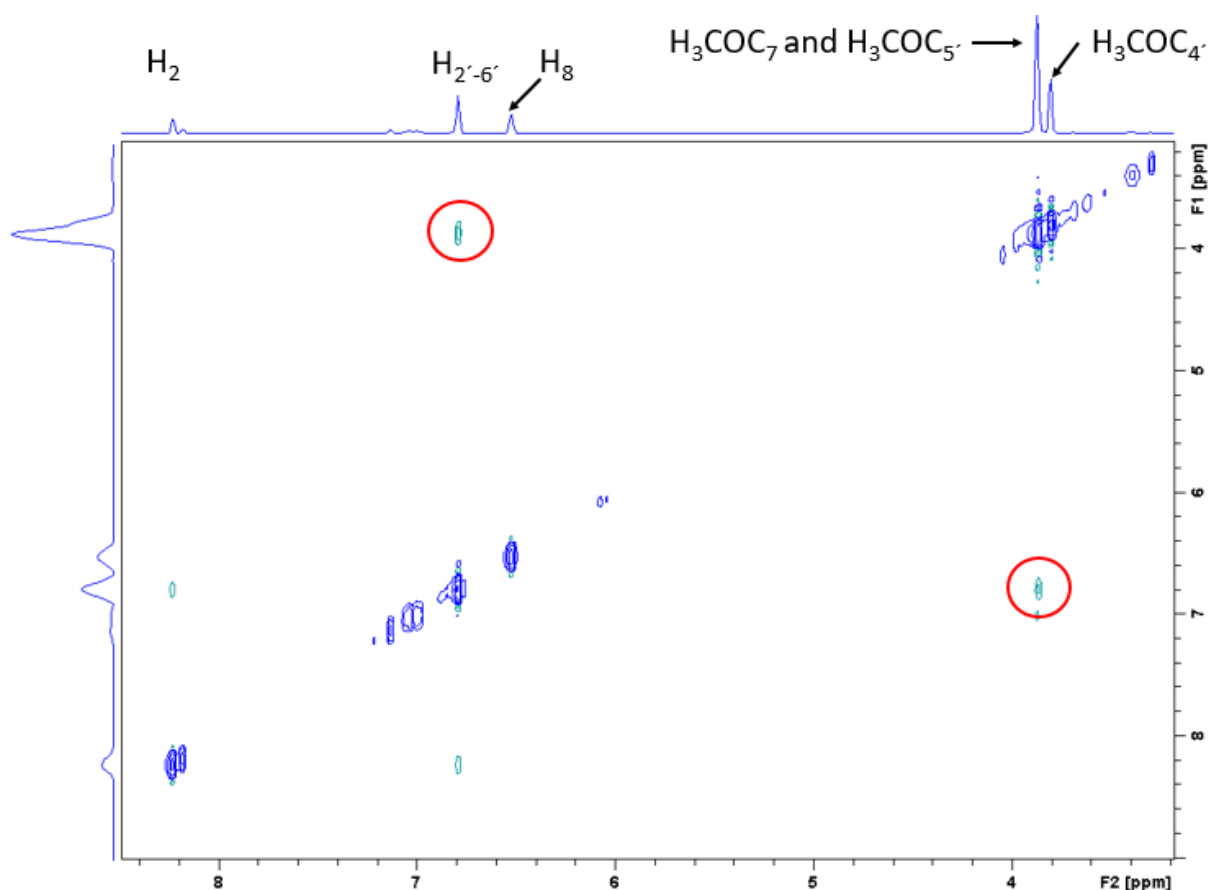


Figure 78: NOESY-spectrum of compound **4** (irigenin *S*, see Figure 74 for the structure) enhanced between 3.2 and 8.4 ppm. The red circles show the cross peaks between the protons H-2',6' and the methoxy group at C-5'. H₃COC₇, H₃COC_{4'}, and H₃COC_{5'} represent the methoxy groups at carbons C-7, C-4', and C-5', respectively (see Figure 74 for numbering of the carbons).

NOESY-spectra of compounds **3** and **4** seems to be identical between 3.2 and 8.4 ppm. A cross peak between H-2',6' and the methoxy group resonating at 3.86 ppm allowed to place one methoxy group at C-5' in **3** and **4**. Whereas in **3** the ¹H-signals for the methoxy groups at C-6 and C-5' overlapped at 3.86 ppm, in **4** methoxy groups at C-7 and C-5' overlapped at the same shift value (3.86 ppm). The ¹H-signal at 3.79 ppm (3 H) showed no cross peaks to other protons in **3** and **4**, and thus it corresponds to the methoxy group at C-4'. Cross peaks between the hydrogens H-2 and H-2'/6' are also detectable.

The structure elucidation of compound **5** (irilone) was simpler than for irigenin and irigenin *S* due to its close structural similarity with **1** showing nearly identical ¹H-signal pattern and shift values. The ¹H-signal at 6.14 ppm is characteristic for the presence of an acetal and substituted the signal of the methoxy group, pointing to its presence at C-6/C-7. Cross peaks were detected only between the protons H-2'/6' and H-3'/5'. The NOESY-spectrum is shown in Figure 79.

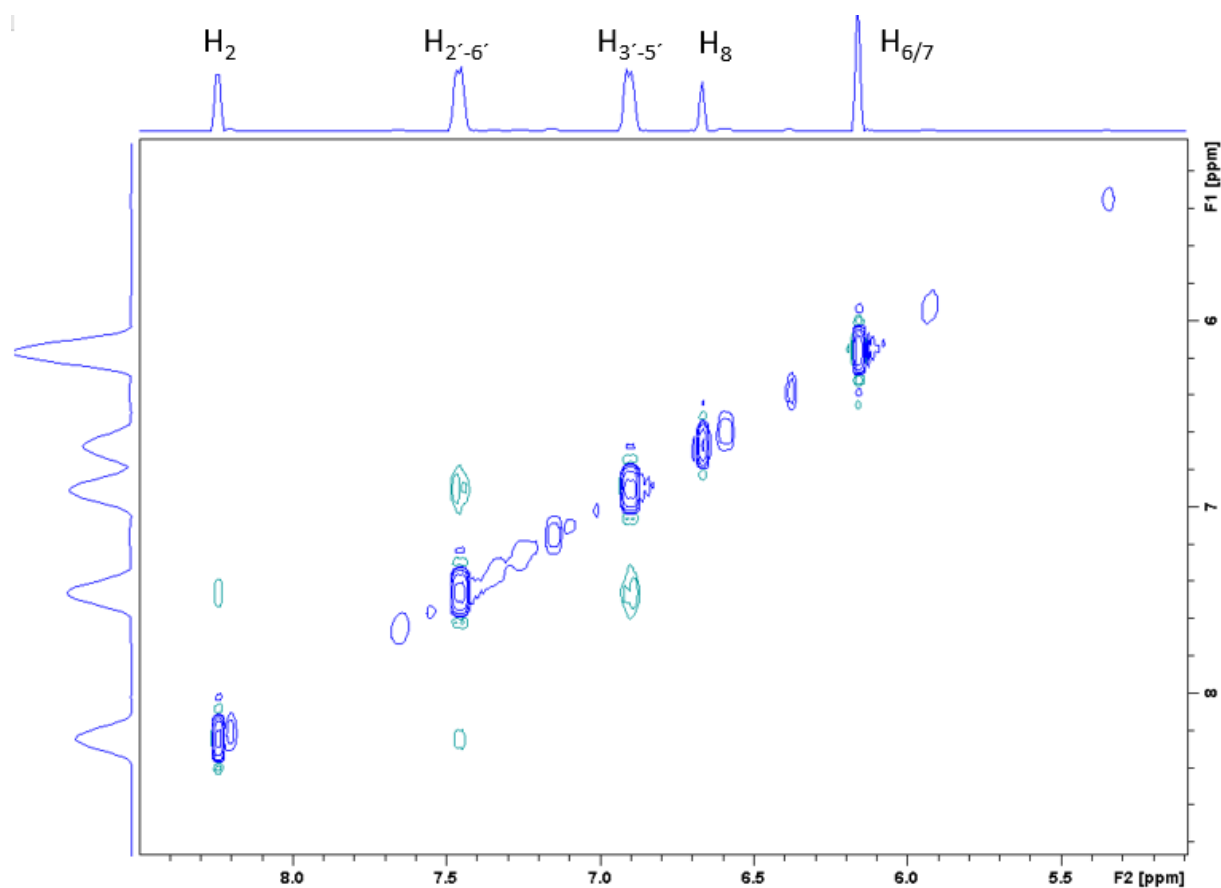


Figure 79: NOESY-spectrum of compound **5** enhanced between 5.1 and 8.5 ppm.

The same characteristic ^1H -signal was found in the ^1H -spectrum of compound **6** (9-hydroxy-7-(4-hydroxy-3-methoxyphenyl)-8H-[1,3]dioxolo[4,5-g]chromen-8-one, 3'-methoxy-irilone) together with the presence of one additional methoxy group was detected. The zoomed NOESY-spectrum is shown in Figure 80. The same type of coupling was observed as for compound **2** showing two coupling constants: $^3J = 8.24$ Hz for H-3' and $^4J = 1.65$ Hz for H-6'. The signals at 6.88 (H-3') and 7.25 ppm (H-6') are doublets and the signal at 7.07 ppm (H-2') is a doublet of doublet. The presence of a cross peak between the signal at 7.25 ppm (H-6', showing the smaller coupling constant $^4J = 1.65$ Hz) and the methoxy group indicated that the methoxy group is placed at C-5'.

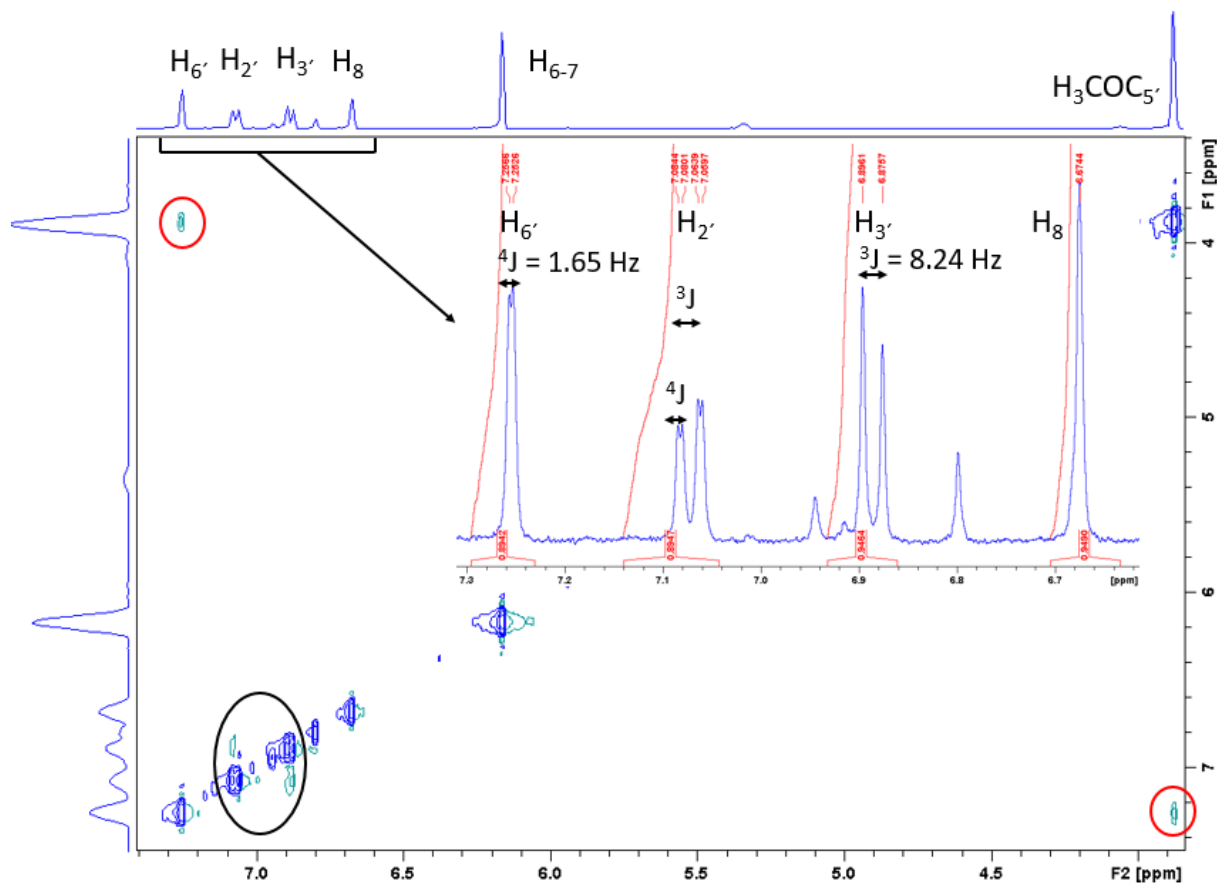


Figure 80: NOESY-spectrum of compound 6 (3'-methoxy-irilone, see Figure 74 for the structure) enhanced between 4.0 and 7.4 ppm. Zoom of the ¹H-spectrum of the signals for H-8, H-2', H-3' and H-6' is shown with the different coupling constants ³J and ⁴J. The red and black circles indicate the cross peaks between H-6' and the methoxy group at C-5' and between H-2' and H-3' respectively. H₃COC_{5'} represents the methoxy group at C-5' (see Figure 74 for numbering of the carbons).

4.3.4 Isoflavonoids and benzophenones in the EtOAc extract 19IA from the fresh roots of *Iris germanica* L.

4.3.4.1 Isolation of compound 7 (benzophenone)

5 g of 19IA (EtOAc extract of the fresh roots of *Iris germanica* L.; see Figure 53 or Table 15 in section 4.2.2.4) was separated over an open silica gel column (elution solvent: SGC_3, see Table 18 in section 4.2.2.7.1) and thereby 7 fractions were obtained. The elution was monitored by TLC. The overview TLC plate of the fractions is shown in Figure 81 and their obtained amount in Table 24.

Table 24: Overview on the obtained amounts of each fractions from separation of 19IA (EtOAc extract of the fresh roots of *Iris germanica* L.; see Figure 53 or Table 15 in section 4.2.2.4). Mobile phase: SGC_3, see Table 18 in section 4.2.2.7.1.

Fraction name	Mass (mg)	Fraction name	Mass (mg)
F1	500	F5	250
F2	200	F6	570
F3	90	F7	500
F4	1960	Total F1 to F7	4070

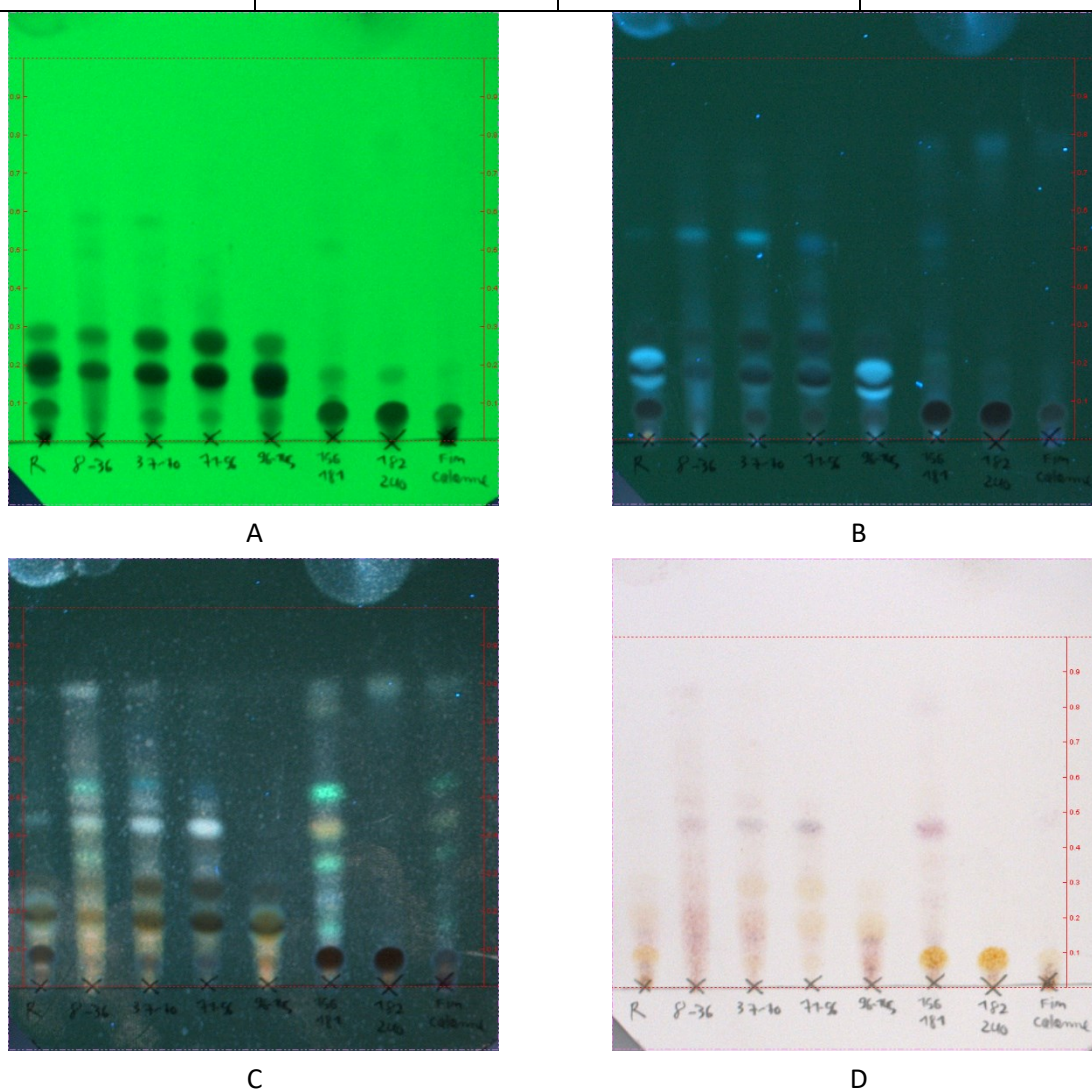


Figure 81: Overview TLC plate of the separation of 19IA (EtOAc extract of the fresh roots of *Iris germanica* L.; see Figure 53 or Table 15 in section 4.2.2.4). The spots on every plate are from the left to the right 19IA, F1, F2, F3, F4, F5, F6 and F7. The spots are made manually. A/B: TLC plates without derivatisation under UV-light at 254 nm (left) and 366 nm (right). C/D: TLC plates derivatised with AA under UV-light at 366 nm (left) and visible light (right). Mobile phase: TLC_6 (see Table 16 in section 4.2.2.5).

Fractions F4 and F6 were nearly poor (meaning that not too many spots are seen on the TLC plates in Figure 81) and were therefore further analysed. As only two spots (the major with the lower R_f -value and the minor with the higher R_f -value) were detected in the fraction F6, it was directly analysed with

HPLC. Only one peak was detected in the chromatogram and 53.1 mg of compound **7** (iriflophenone) were isolated from 19IA (EtOAc extract of the fresh roots of *Iris germanica* L.; the fresh roots were first extracted with n-hexane and then with EtOAc; Figure 53 in section 4.2.2.4) using the semi-preparative HPLC and the gradient method HPLC_5 (see Table 18 in section 4.2.2.7.1). As the fraction F4 contained at least three to four spots (see TLC plate C derivatised with AA under 366 nm in Figure 81), the fraction was further separated.

4.3.4.2 Isolation of compounds **3** (irigenin), **8** (benzophenone), **9** and **10** (two isoflavonoids) from fraction F4

F4 was separated over an open silica gel column (mobile phase: SGC_4, see Table 18 in section 4.2.2.7.1) and 5 fractions (F4F1, F4F2, F4F3, F4F4 and F4F5) were obtained. The obtained amount of each fraction is shown in Table 25 and the overview TLC plate of F4 is shown in Figure 82.

Table 25: Overview of the obtained amount of each fraction from the separation of F4 (fourth fraction obtained from the elution of 19IA (EtOAc extract of the fresh roots of *Iris germanica* L.; see Figure 53 or Table 15 in section 4.2.2.4) using the mobile phase SGC_3, see Table 18 in section 4.2.2.7.1). Mobile phase for separation of F4: SGC_4, see Table 18 in section 4.2.2.7.1.

Fraction name	Mass (mg)	Fraction name	Mass (mg)
F4F1	111	F4F4	81.7
F4F2	688.5	F4F5	21.1
F4F3	502	Total F4F1 to F4F5	1404.3

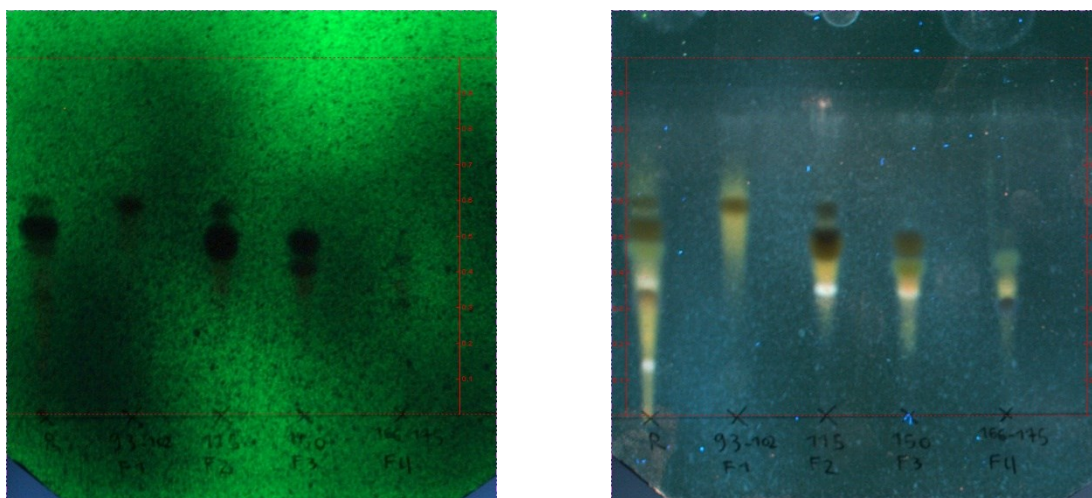


Figure 82: Overview TLC plate of separated fraction F4 (fourth fraction obtained from the elution of 19IA (EtOAc extract of the fresh roots of *Iris germanica* L.; see Figure 53 or Table 15 in section 4.2.2.4) derivatised with AA under UV-light at 254 nm (left) and 366 nm (right). The spots on every plate are from the left to the right F4, F4F1, F4F2, F4F3 and F4F4. The spots are spotted manually. Mobile phase: TLC_8 (see Table 16 in section 4.2.2.5).

The fraction F4F1 showed only one spot and was therefore analysed with HPLC. The HPLC-chromatogram is shown in Figure S 29 of the Appendix together with the HPLC-chromatogram of

Z2_18I4A (second main fraction isolated using silica gel columns from 18I4A (EtOAc extract of the fresh rhizomes of *Iris germanica* L.; see Figure 54 or Table 15 in section 4.2.2.4)) for comparison. As can be seen, the same peaks (and the same UV-spectra) as for compounds **5** (irilone), **6** (3'-methoxy-irilone) and **1** (see Figure 74 in section 4.3.3.1 for the structures) were detected. Therefore, it was very likely that the roots of *Iris germanica* L. also contained compounds **5**, **6** and **1**.

The fraction F4F3 was also further analysed with HPLC as it contains a low number of spots on the TLC (see Figure 83). The two main peaks (compounds **3** and **9**) and two other compounds were isolated using semi preparative HPLC. The peak eluting just before compound **8** coincided with EtOAc traces. 1.1 mg of compound **8** (4-methoxy-iriflophenone), 13.1 mg of compound **3** (irigenin), 15.2 mg of compound **9** (irisflorentin) and 7.5 mg of compound **10** were obtained.

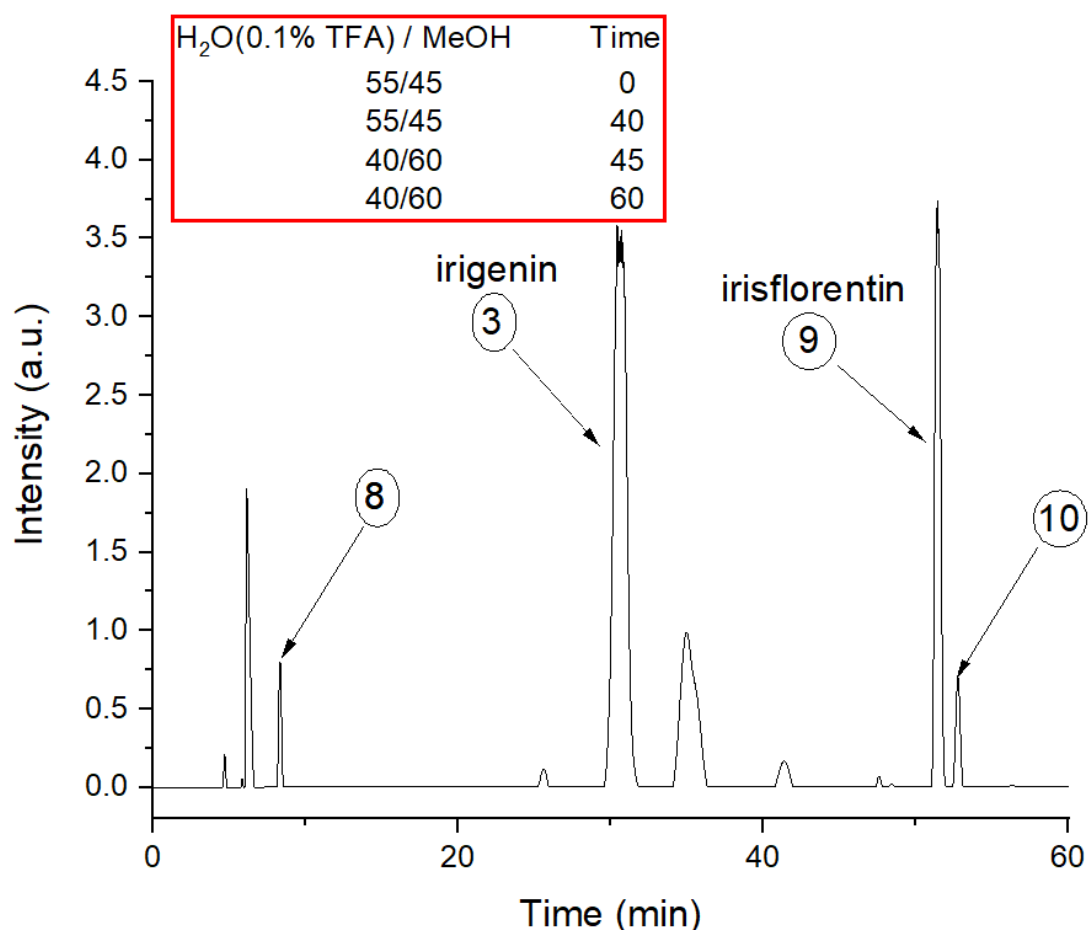


Figure 83: Analytical HPLC-chromatogram of F4F3 (third fraction of the elution of F4 (fourth fraction obtained from the elution of 19IA (EtOAc extract of the fresh roots of *Iris germanica* L.; see Figure 53 or Table 15 in section 4.2.2.4) using the mobile phase SGC_3, see Table 18 in section 4.2.2.7.1), see Table 25 in section 4.3.4.2) using a RP-18 column. The compounds **8** (4-O-methyl-iriflophenone), **3** (irigenin), **9** (irisflorentin) and **10** (see Figure 56 for the structures) have been isolated using the semi preparative HPLC with the gradient method HPLC_4 (see Table 18 in section 4.2.2.7.1).

4.3.4.3 Structure elucidation

The elucidation of the isolated compounds from 19IA (EtOAc extract of the fresh roots of *Iris germanica* L.; see Figure 53 or Table 15 in section 4.2.2.4) was done with the help of NMR- (in acetone- d_6 , 1D and 2D) and LC-MS data, as for the compounds of 18IA (EtOAc extract of the fresh rhizomes of *Iris germanica* L.; see Figure 54 or Table 15 in section 4.2.2.4). The structures of the 5 isolated compounds are shown in Figure 84. The LC-MS and NMR-data are shown in Table 26 and Table 27.

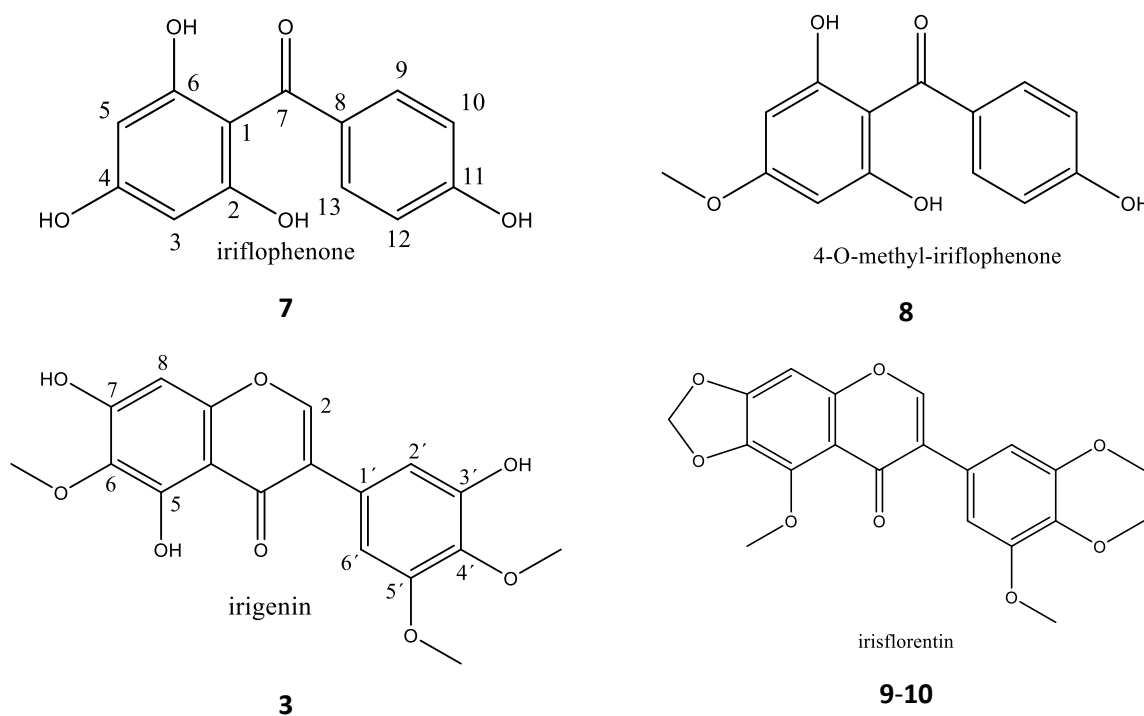


Figure 84: Structure of the isolated compounds (3 and 7-9) from 19IA (EtOAc extract of the fresh roots of *Iris germanica* L.; see Figure 53 or Table 15 in section 4.2.2.4).

Table 26: LC-MS and NMR-data for compounds 7 (iriflophenone) and 8 (4-O-methyl-iriflophenone). See Figure 84 for the structures.

Compound 7, LC-MS: (M-H) ⁺ : 247.0606 C ₁₃ H ₁₀ O ₅				Compound 8, LC-MS: (M-H) ⁺ : 261.0759 C ₁₄ H ₁₂ O ₅			
H	δ_H (ppm)	Number of H, multiplicity, J (Hz)	group	H	δ_H (ppm)	Number of H, multiplicity, J (Hz)	group
2/6	10.25	2H, s	hydroxy	2/6	/	/	hydroxy
3/5	6.05	2H, s	/	3/5	6.05	2H, s	/
4	9.18	1H, s	hydroxy	4	3.79	3H, s	methoxy
9/13	6.93	2H, d, 8.39	/	9/13	6.85	2H, d, 8.67	/
10/12	7.69	2H, d, 8.39	/	10/12	7.62	2H, d, 8.67	/
11	9.06	1H, s	hydroxy	11	/	/	hydroxy

Compounds **7** (iriflophenone) and its O-methylated derivative **8** ((2,6-dihydroxy-4-methoxyphenyl)(4-hydroxyphenyl)methanone, 4-O-methyl-iriflophenone) are benzophenones (see Figure 84). The NOESY-spectrum of compound **7**, zoomed between 5.8 and 10.6 ppm, is shown in Figure 85.

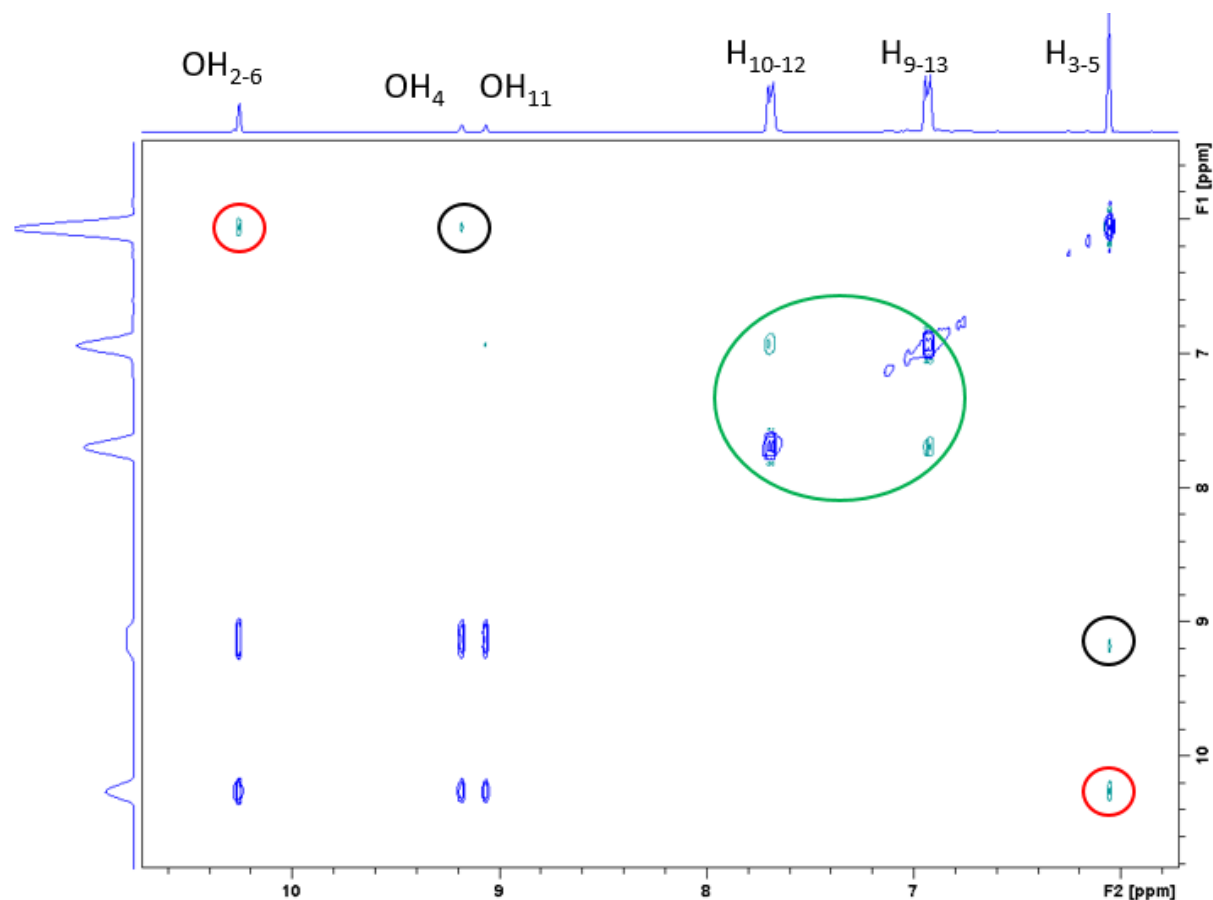


Figure 85: NOESY-spectrum of compound **7** (iriflophenone, see Figure 84 for the structure) enhanced between 5.8 and 10.6 ppm. The red, black and green circles show the cross peaks between hydroxy groups at C-2 and C-6 and protons H-3/5, the hydroxy group at C-4 and the protons H-3/5 as well as the protons H-10/12 and H-9/13, respectively (see Figure 84 for numbering of the carbons).

Elucidation of the substituent positions and the assignment of the signals were done with the help of a NOESY-spectrum. Indeed, the hydroxy signals were detectable because high amount of iriflophenone (compound **7**) were measured. The assignment of the signals at 9.06 and 9.18 ppm (integrated for one hydrogen each one, two hydroxy groups) was not possible only with the ¹H-spectrum. It could be assumed that the signal being the most de-shielded should be the signal for the hydroxy group on position 4, because of the presence of the two other neighbored hydroxy groups. On the contrary, the hydroxy group on position 11 has only neighbored protons and therefore, should be less de-shielded, what was confirmed with the NOESY-spectrum. As expected, cross peaks not only between the protons H-3/5 and the hydroxy group resonating at 9.18 ppm were detected but also between the

two hydroxy groups at C-2 and C-6 and OH₄ (9.18 ppm). Moreover, no cross peaks were detected for OH₁₁.

The NOESY-spectrum of compound **8** (4-O-methyl-iriflophenone) is shown in Figure 86. The hydroxy groups were not detectable because too low amount have been isolated.

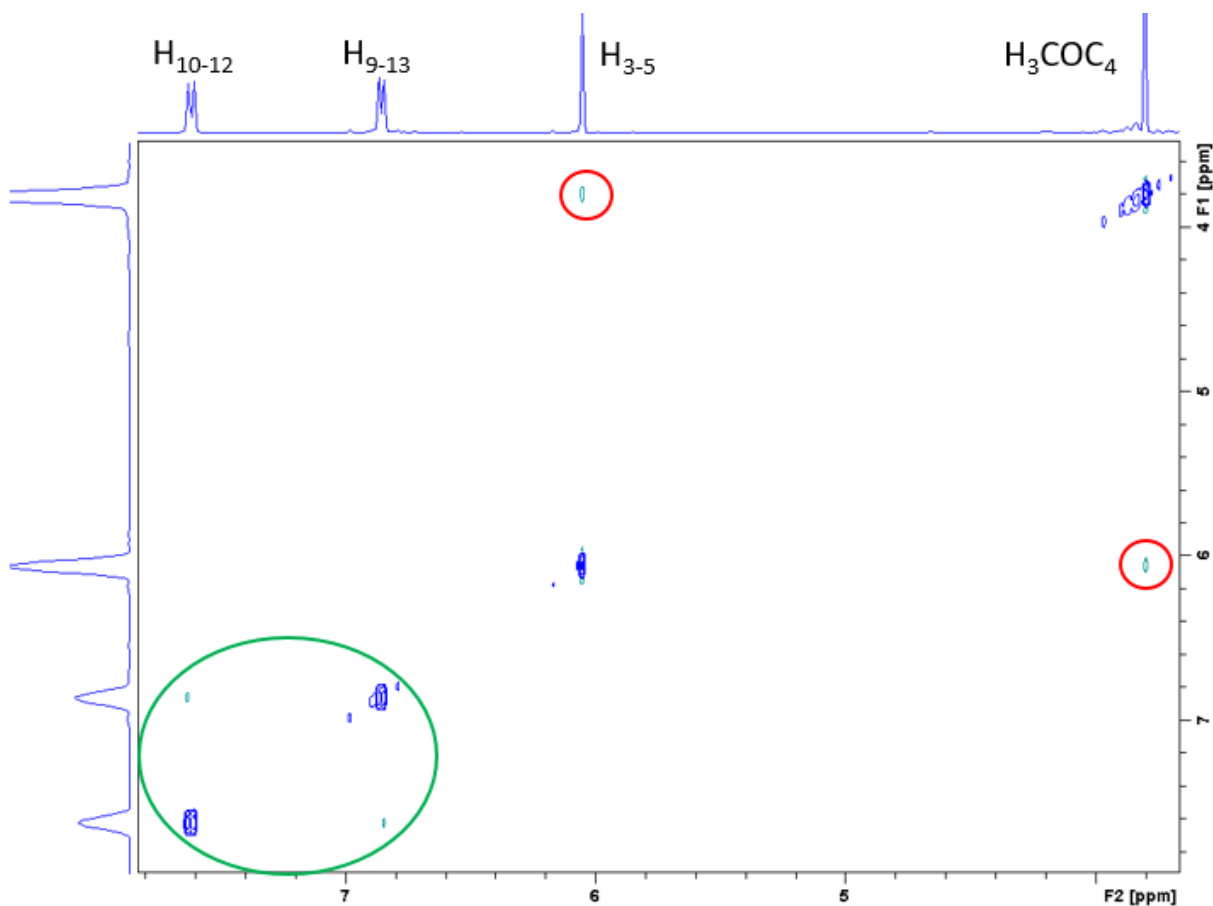


Figure 86: NOESY-spectrum of compound **8** (4-O-methyl-iriflophenone, see Figure 84 for the structure) enhanced between 3.8 and 7.8 ppm. The red and green circles show the cross peaks respectively between the methoxy group at C-4 and the protons H-3/5 and between the protons H-10/12 and H-9/13. H₃COC₄ represents the methoxy group at C-4 (see Figure 84 for numbering of the carbons).

As explained before and according to LC-MS and NMR data, compound **7** and **8** differed from each other only by an additional o-methylation in **8**. The only question was the position of the methoxy group. Only OH-4 and OH-11 were possible as the two hydroxy groups at C-2 and C-6 were not involved due to the presence of the signal at 6.05 ppm (singlet, 2H, H-3/5). Indeed, if one of the two hydroxy groups was a methoxy group, the two hydrogens would not be equivalent anymore, meaning that two different signals (doublet with a small coupling constant ⁴J) should be detected. The detection of cross peaks between protons H-3/5 and the methoxy group indicated that **8** is methylated at OH-4.

Compounds **3** (irigenin) and **9** (irisfloreantin) are isoflavones (see Figure 84). The NOESY-spectra of compound **3** are shown in Figure 87 and Figure 88. The NOESY-spectrum of compound **9** is shown in Figure 89.

Table 27: LC-MS and NMR-data for the compounds **3** (irigenin) and **9** (irisfloreantin). See Figure 84 for the structures.

Compound 3 , LC-MS: (M-H) ⁺ : 361.0924 C ₁₈ H ₁₆ O ₈				Compound 9 , LC-MS: (M-H) ⁺ : 387.1074 C ₂₀ H ₁₈ O ₈			
H	δ_H (ppm)	Number of H, multiplicity, J (Hz)	group	H	δ_H (ppm)	Number of H, multiplicity, J (Hz)	group
2	8.23	1H, s	/	2	8.11	1H, s	/
5	13.21	1H, s	hydroxy + H intramolecular	5	3.98	3H, s	methoxy
6/5'	3.86	6H, s	2x methoxy	6/7	6.17	2H, s	acetal
7/3'	/	/	hydroxy	8	6.79	1H, s	/
8	6.51	1H, s	/	2'/6'	6.89	2H, s	/
2'/6'	6.79	2H, s	/	3'/5'	3.86	6H, s	2x methoxy
5'	3.80	3H, s	methoxy	4'	3.75	3H, s	methoxy

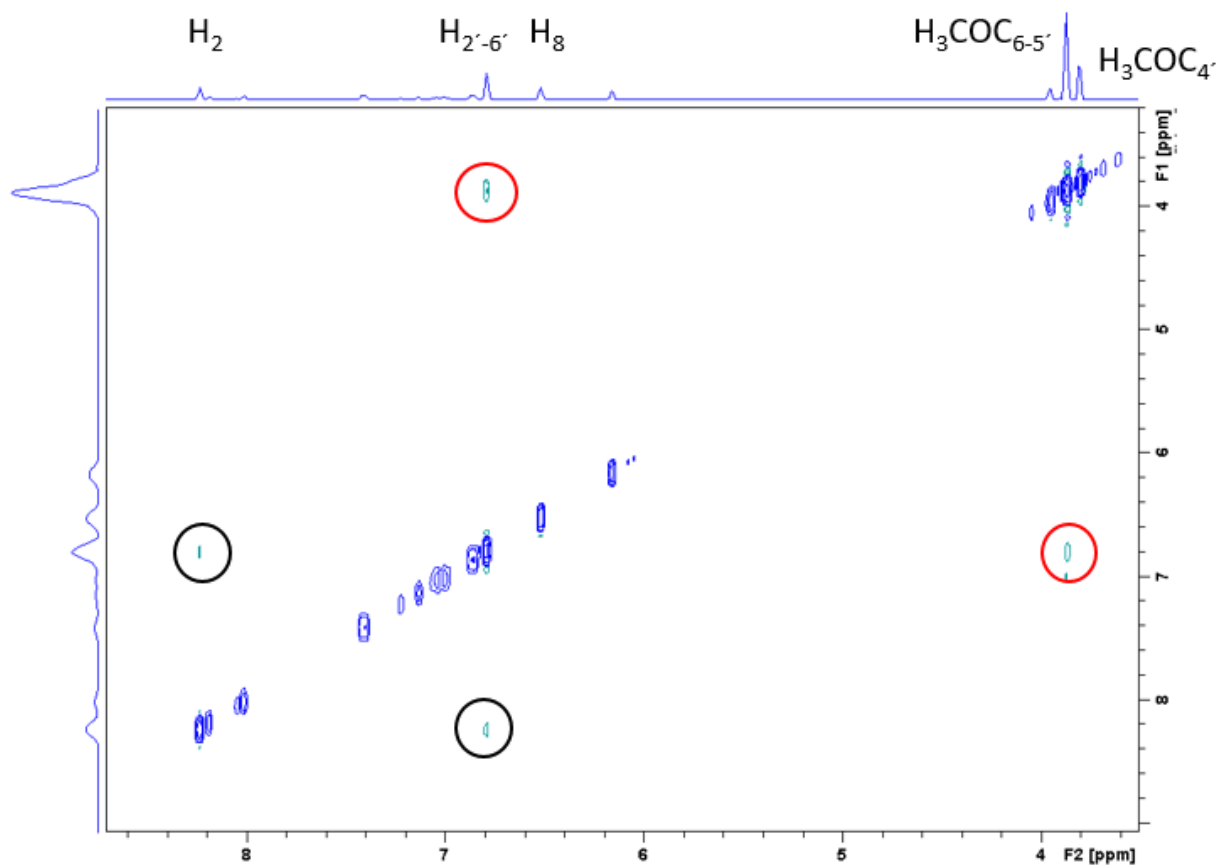


Figure 87: NOESY-spectrum of compound **3** (irigenin, see Figure 84 for the structure enhanced between 3.6 and 8.6 ppm). The red and dark circles show the cross peaks between the methoxy group H_3COC_5' and protons $H-2'/6'$, and between the protons $H-2'/6'$ and $H-2$. H_3COC_6 , H_3COC_4' , and H_3COC_5' represent the methoxy groups on the carbons $C-6$, $C-4'$, and $C-5'$, respectively (see Figure 84 for numbering of the carbons).

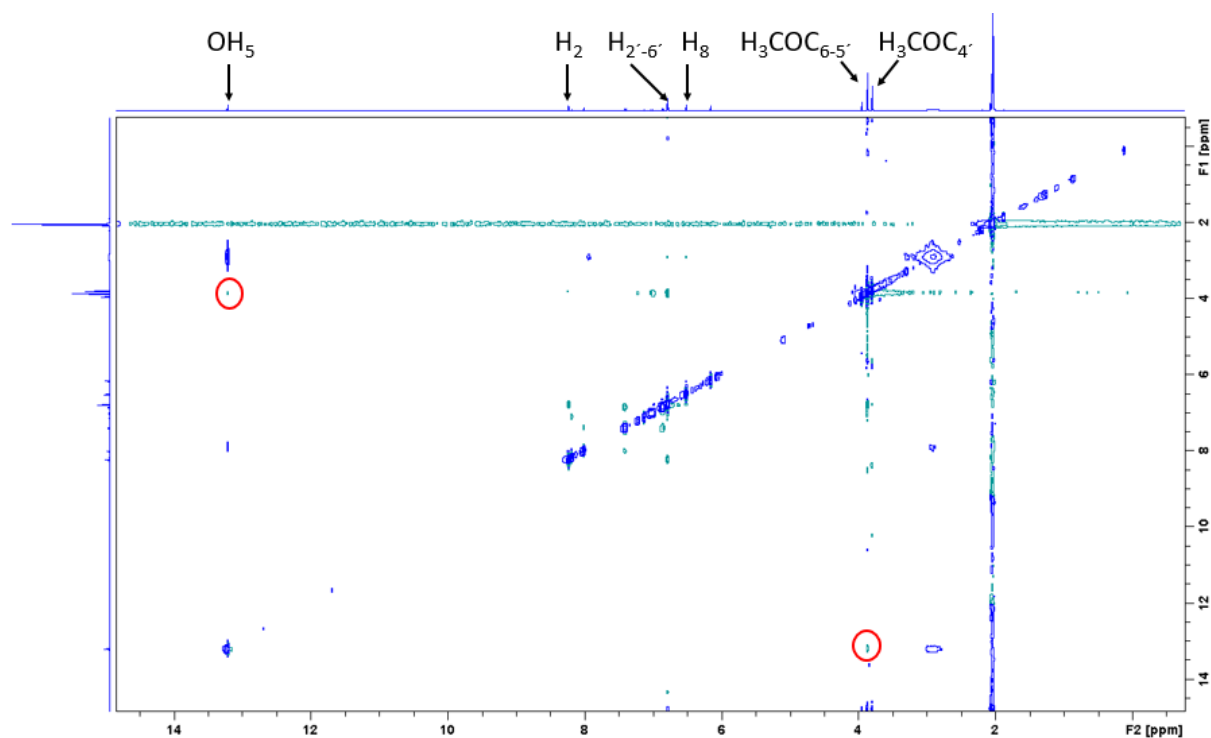


Figure 88: NOESY-spectrum of compound **3** (irigenin) isolated from the roots of *Iris germanica* L. (see Figure 84 for the structure). The red circles show the cross peaks between the hydroxy group OH_5 at C-5 and the methoxy group H_3COC_6 , H_3COC_5 , $\text{H}_3\text{COC}_{4'}$, and $\text{H}_3\text{COC}_{5'}$ represent the methoxy group on the carbon C-6, C-4' and C-5' (see Figure 84 for numbering of the carbons).

The two NOESY-spectra in Figure 87 and Figure 88 are identical to Figure 77 and Figure 78 in section 4.3.3.3, respectively and indicated that again compound **3** was isolated.

Compound **9** (irisflorentin) is an isoflavone. ^1H -signals were detected at 8.11 ppm (H-2), 6.89 ppm (H-2'/6'), 6.79 ppm (H-8), and 6.17 ppm (H-6/7). The NOESY showed the same cross peaks between H-2 and H-2'/6' (dark circles in Figure 89) as for irilone (**5**), irigenin S (**4**) or irigenin (**3**). The ^1H -signal at 6.17 ppm was attributed to an acetal function as for irilone (**5**). The four other substituents were methoxy group (^1H -signals resonating at 3.98, 3.86, and 3.75 ppm integrating for 3, 6, and 3 hydrogens respectively). No ^1H -signal was detected around 13 ppm, meaning that no hydroxy group was present to form a hydrogen bond with the keto group. Two methoxy groups are located near the hydrogens $\text{H}_{2'-6'}$ (cross peaks between the ^1H -signal at 3.86 ppm and the two hydrogens $\text{H}_{2'-6'}$, red circles in Figure 89). The last methoxy group is located on position 4' (see Figure 84 for numbering of the carbons).

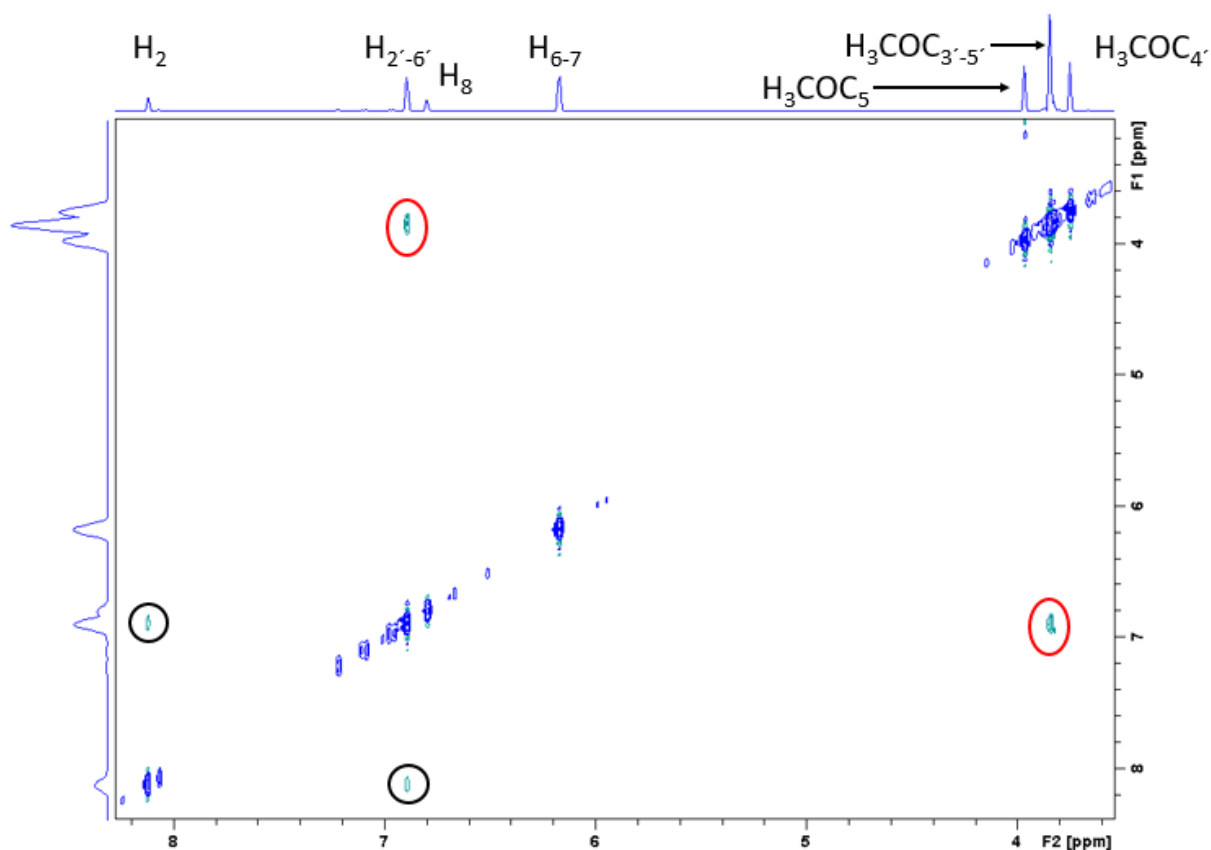


Figure 89: NOESY-spectrum of compound **9** (irisfloreantin, see Figure 84 for the structure) enhanced between 3.6 and 8.2 ppm. The red and dark circles show the cross peaks between the methoxy groups on C-3' and C-5' and the protons H-2'/6' as well as between the protons H-2'/6' and H-2. H₃COC_{3'}, H₃COC_{4'}, and H₃COC_{5'} represent the methoxy groups at C-3', C-4', and C-5', respectively (see Figure 84 for numbering of the carbons).

Compound **10** is an isoflavone and had exactly the same molecular weight, ¹H-, and NOESY-spectra as compound **9** (see Figure 90). Compound **10** was a yellow powder and compound **9** was a white powder. It can be assumed that they are structural isomers differing in their oxy-methylene substitution.

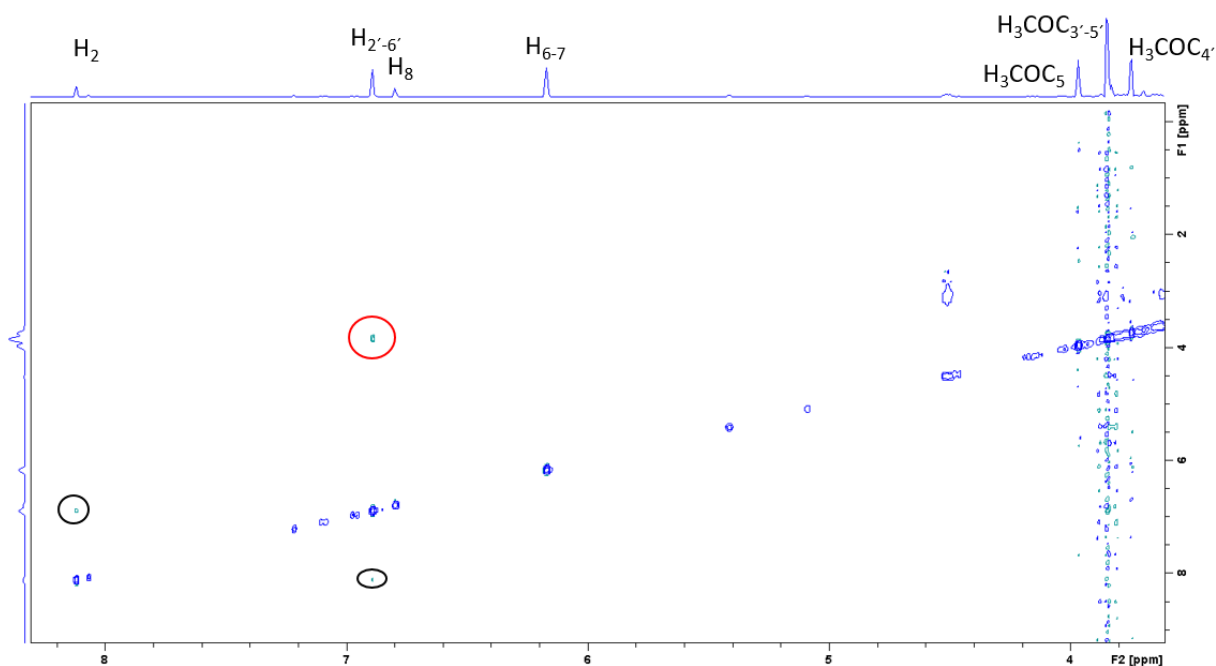
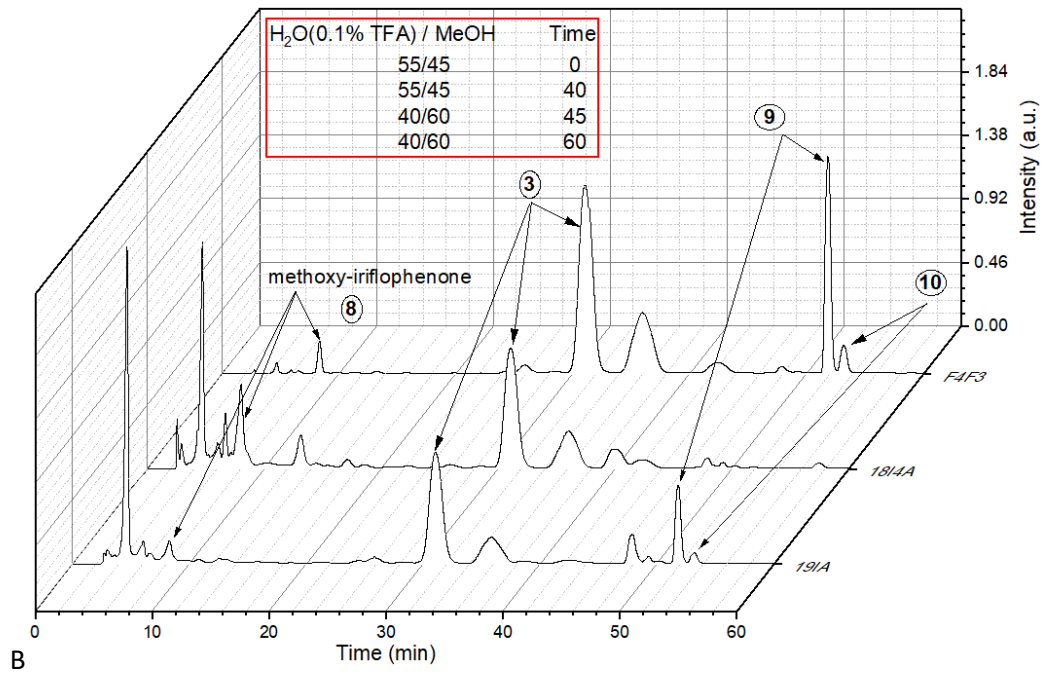
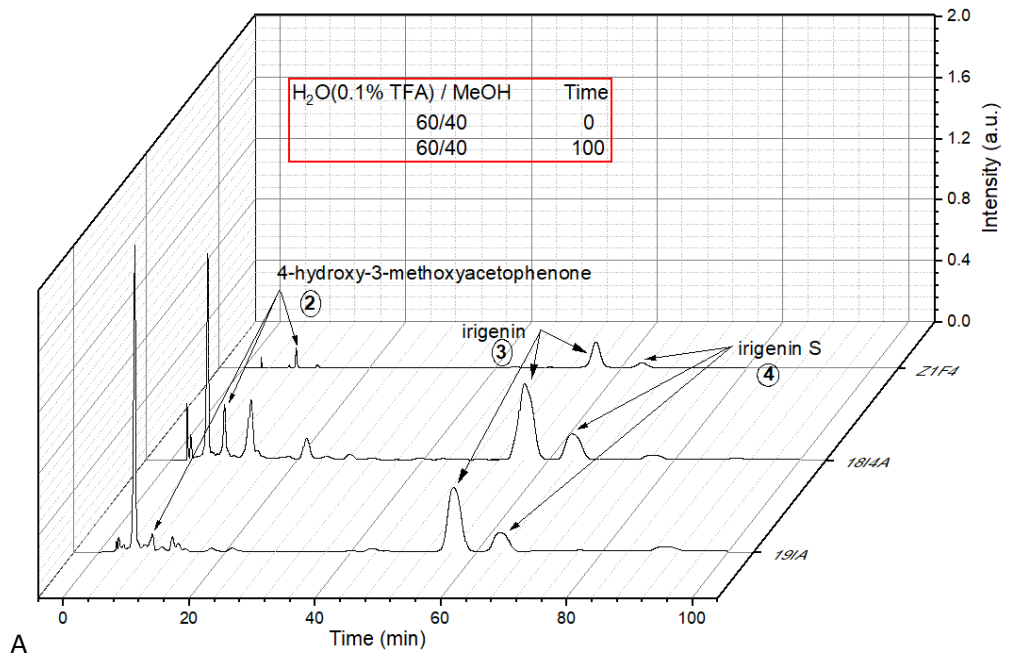


Figure 90: NOESY-spectrum of compound **10** (same as for compound **9** (iriflorentin), see Figure 84 for the structure) enhanced between 3.6 and 8.2 ppm. The red and dark circles show the cross peaks between the methoxy groups at C-3' and C-5' and the protons H-2'/6' and between the protons H-2'/6' and H-2. H₃COC_{3'}, H₃COC_{4'}, and H₃COC_{5'} represent the methoxy group at C-3', C-4', and C-5' (see Figure 84 for numbering of the carbons).

4.3.5 Comparison of the phytochemical profile of roots and rhizomes

6 isoflavones, 2 benzophenones and one acetophenone derivative were isolated from the roots and the rhizomes of *Iris germanica* L., more precisely 5 isoflavones and one acetophenone derivative from the rhizome extract 1814A (EtOAc extract of the fresh rhizomes of *Iris germanica* L.; see Figure 54 or Table 15 in section 4.2.2.4) and 3 isoflavones and 2 benzophenones from the root extract 191A (EtOAc extract of the fresh roots of *Iris germanica* L.; see Figure 53 or Table 15 in section 4.2.2.4). But, as described before, some of them (irilone, 3'-methoxy-irilone and compound **1** (5,7-dihydroxy-6-methoxy-3-(4-methoxyphenyl)-4H-chromen-4-one), see Figure 74 for the structures) were already detected in the two extracts (see Figure S 29 of the Appendix). Therefore, all the investigated fractions were compared to the two extracts 1814A (EtOAc extract of the fresh rhizomes of *Iris germanica* L.) and 191A (EtOAc extract of the fresh roots of *Iris germanica* L.) with the analytical HPLC to determine if the isolated isoflavones, benzophenone and the acetophenone derivative were present only in the rhizomes or roots or in both. The comparison is shown in Figure 91. All compounds were present in the roots and the rhizomes except the two compounds **9** (iriflorentin) and **10** (iriflorentin isomer). They were detected only in the roots. A summary is shown in Table 28.



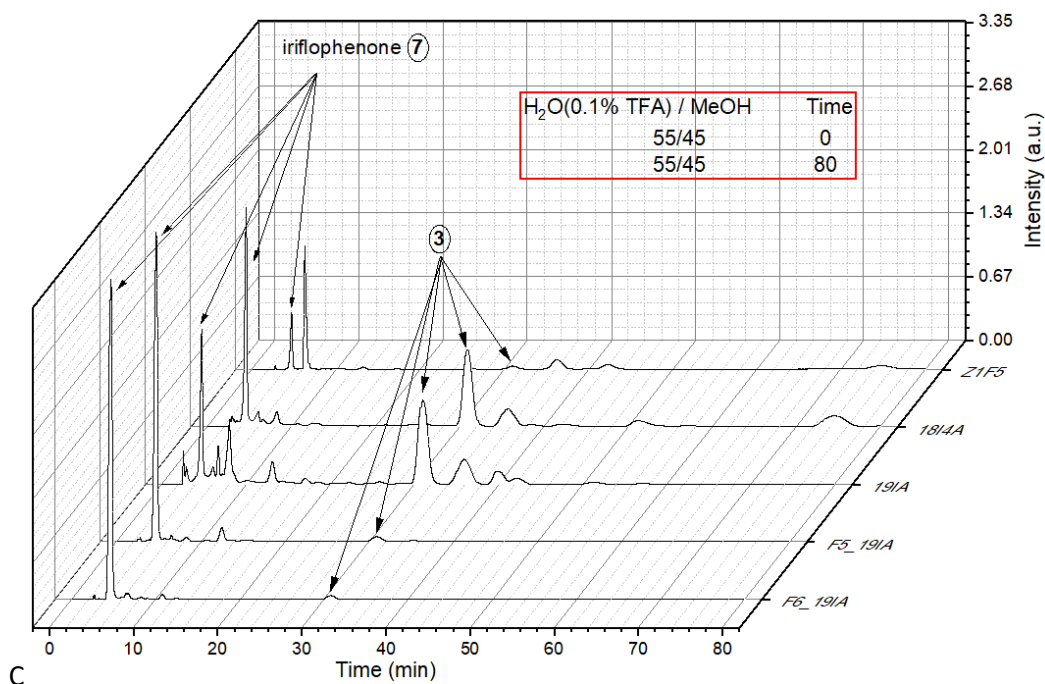


Figure 91: Analytical HPLC-chromatograms using a RP-18 column of the root extract 19IA (EtOAc extract of the fresh roots of *Iris germanica* L.), rhizome extract 18I4A (EtOAc extract of the fresh rhizomes of *Iris germanica* L.; see Figure 53, Figure 54, and Table 15 in section 4.2.2.4) and all investigated fractions: Z1F4 (A, fourth fraction of the elution of Z1, Z1 is the first main fraction of the elution of 18I4A, see Table 21 in section 4.3.3.2), F4F3 (B, third fraction of the elution of F4, F4 is the fourth fraction of the elution of 19IA, see Table 25 in section 4.3.4.2), Z1F5 (C, fifth fraction of the elution of Z1, Z1 is the first main fraction of the elution of 18I4A, see Table 21 in section 4.3.3.2), F5 (C, fifth fraction of the elution of 19IA, see Table 24 in section 4.3.4.1) and F6 (C, sixth fraction of the elution of 19IA, see Table 24 in section 4.3.4.1).

Table 28: Presence of the 10 isolated compounds (see Figure 74 in section 4.3.3.3 and Figure 84 in section 4.3.4.3 for the structures) in 18I4A (EtOAc extract of the fresh rhizomes of *Iris germanica* L.) or 19IA (EtOAc extract of the fresh roots of *Iris germanica* L.; see Figure 53, Figure 54, and Table 15 in section 4.2.2.4).

Name of the isolated compound		Present in	
		18I4A	19IA
1	5,7-dihydroxy-6-methoxy-3-(4-methoxyphenyl)-4H-chromen-4-one	x	x
2	4-hydroxy-3-methoxyacetophenone	x	x
3	irigenin	x	x
4	irigenin S	x	x
5	irilone	x	x
6	3'-methoxy-irilone	x	x
7	iriflophenone	x	x
8	4-O-methyl-iriflophenone	x	x
9	irisflorentin		x
10	isomer of irisflorentin		x

4.3.6 MTT and ICAM-1 assays

Isoflavones and benzophenones were isolated from the roots and the rhizomes of *Iris germanica* L. and some of them are already well-known in the literature as potential anti-inflammatory agent. Indeed, irilone, irigenin and irigenin S have already been tested as anti-inflammatory compounds using lab rats [185]. They were isolated from *Iris germanica* L. from Egypt and Ibrahim et al. found that they have potent anti-inflammatory properties. The induced paw oedema test was used with dexamethasone as positive control. The paw oedema of a rat was induced by a formalin solution (4%) injected in the left hind paw. After the intake of 10 mg isoflavonoids/kg and 24 hours, the paw oedema thickness was measured and compared to the untreated rat and the rat treated with the positive control. Irilone, irigenin and irigenin S showed a reduction of the paw thickness after 24 hours and therefore, had potent anti-inflammatory properties. The induced paw oedema test was first developed in 1962 by Winter et al. [186] and many flavonoids (flavones, flavanones and chalcones) were tested by Panthong et al. [187] in 1994 for anti-inflammatory activity.

Other anti-inflammatory assays using flavonoids and especially isoflavonoids are also described in the literature. A rapid anti-inflammatory assay was developed by Tan et al. [188] in 2000 using a tetrazolium salt (4-(3-(4-iodophenyl)-2-(4-nitrophenyl)-2H-tetrazol-3-ium-5-yl)-benzene-1,3-disulfonate, WST-1, see Figure S 30 of the Appendix for the structure) for quantification of the superoxide production by human peripherals blood neutrophils. Neutrophils are a type of granulocytes (the most abundant one) normally found in the bloodstream. They are part of the immune system and the first white blood cells which are recruited within minutes to a site of inflammation or injury. Superoxide radicals are produced by neutrophils to aiding in the killing of ingested microbes. But it is not the only function of superoxide, they are also used as attractor for neutrophils (that more neutrophils come to the site of injury) by reacting with chemotactic factors (substances that stimulate cellular migration) [189]. In the assay, superoxide radicals were produced by neutrophils stimulated with PMA (phorbol 12-myristate 13-acetate, tumour promoter, see Figure S 31 of the Appendix for the structure) and used to reduce WST-1 into formazan (see Figure S 30 of the Appendix for the structure), a dark red substance absorbing at 550 nm. By colorimetric measurements, the ability of a compound or extract to reduce the produced superoxide (meaning to have an anti-inflammatory effect) was measured. This assay was used by Rahman et al. [190] to screen the potent anti-inflammatory effect of some isoflavones from *Iris germanica* L.. They found that irigenin inhibits 50% of superoxide production at 93.52 μ M. Aspirin and indomethacine were used as positive controls.

The third types of anti-inflammatory assay reported in the literature using isoflavones is the lipopolysaccharide (LPS)-activated macrophages assay. LPS was used as macrophage stimulator, the

cells will then produce nitric oxide (NO), a signalling molecule that plays a key role in the inflammation process [191]. Indeed, NO are responsible for the inhibition of pathogen replication [192]. NO are also used for many others immunoregulatory functions such as inhibitor of T and B cells proliferation or of leukocyte recruitment [193]. Under normal physiological conditions, NO gives an anti-inflammatory effect. But its overproduction is also recognised as a pro-inflammatory factor and therefore, the use of compound which can decrease the NO production by the macrophages is of great interest. Wang et al. [194] have found that irigenin inhibited the production of NO in murine macrophages (decrease of the NO concentration from 0.8 μ M to 0.1 μ M if the murine (RAW 264.7) macrophages were pre-treated with 24.4 μ M of irigenin). Moreover, they found that irigenin inhibited also the production of pro-inflammatory mediators like TNF- α . Finally, irigenin had a potent anti-inflammatory effect by inhibiting the LPS-induced production of NO and TNF- α .

Taking these results into account, it was of interest to test the isolated isoflavones and benzophenones as well as the acetophenone derivative as potential anti-inflammatory agents using HMEC-1. The reduction of ICAM-1 protein was correlated with the anti-inflammatory effect. First, 7 compounds (**2** (4-hydroxy-3-methoxyacetophenone), **3(rh)** (irigenin isolated from the rhizomes), **3(rt)** (irigenin isolated from the roots), **4** (irigenin S), **5** (irilone), **7** (iriflophenone), **9** (irisflorentin), and **10** (irisflorentin isomer)) and the two extracts (18I4A (EtOAc extract of the fresh rhizomes of *Iris germanica* L.) and 19IA (EtOAc extract of the fresh roots of *Iris germanica* L.; see Figure 53, Figure 54, and Table 15 in section 4.2.2.4)) were tested (see Figure 74 in section 4.3.3.3 and Figure 84 in section 4.3.4.3 for the structures) with the MTT assay in order to see if the used concentrations were toxic for the HMEC-1 cells. Then they were tested in non-toxic concentrations in the ICAM-1 assay. The results of the MTT assay and ICAM-1 assay are shown in Figure 92 and Figure 93, respectively.

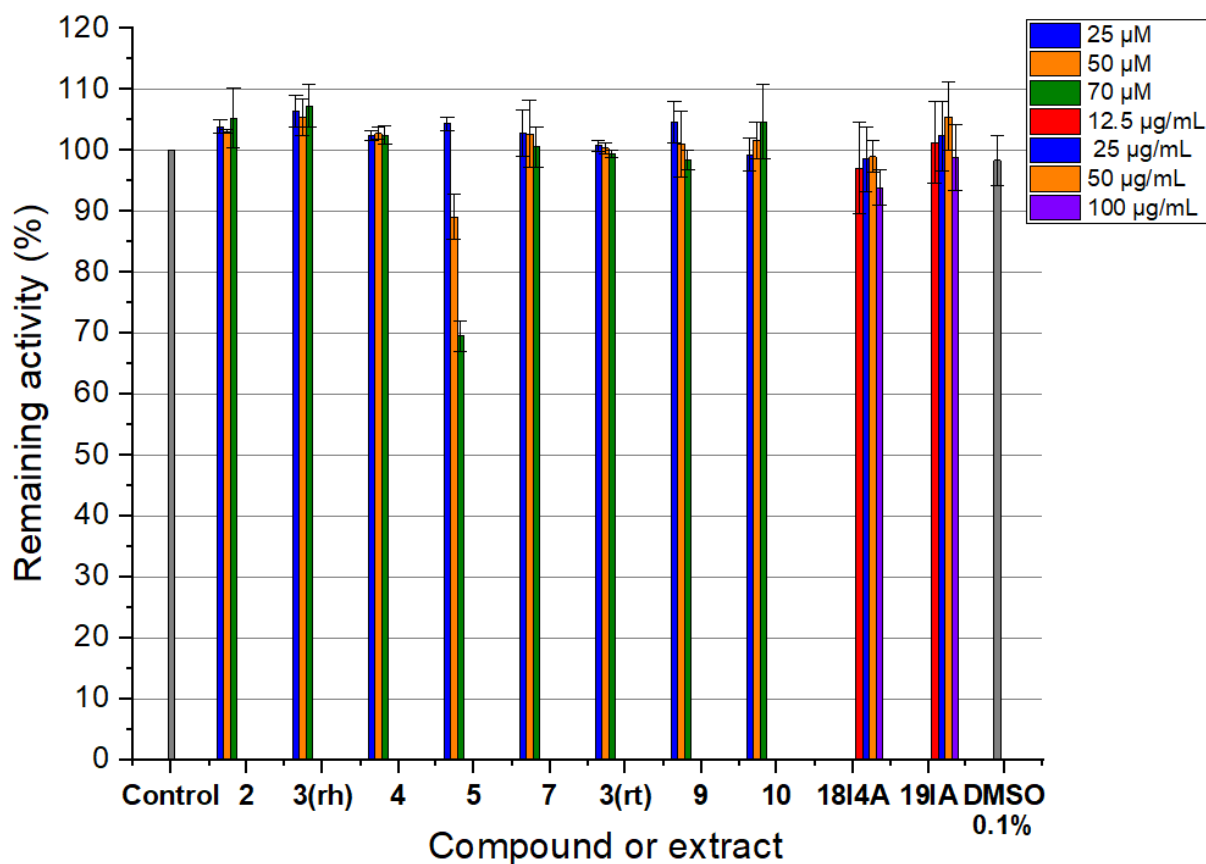


Figure 92: Remaining activity (correlated to the viability) of the HMEC-1 as function of the compound (see Figure 74 in section 4.3.3.3 and Figure 84 in section 4.3.4.3 for the structures) concentration (25 (blue), 50 (orange) and 70 μM (green)) or extract (18I4A (EtOAc extract of the fresh rhizomes of *Iris germanica* L.) or 19IA (EtOAc extract of the fresh roots of *Iris germanica* L.; see Figure 53, Figure 54, and Table 15 in section 4.2.2.4)) concentration (12.5 (red), 25 (blue), 50 (orange) and 100 $\mu\text{g/mL}$ (violet)). DMSO (grey) 0.1 % (V/V) was tested as solvent control. Three independent experiments were executed in hexaplicates. The data are shown as average \pm standard deviation. 3(rh) represent irigenin isolated from the rhizome of *Iris germanica* L. and 3(rt) irigenin isolated from the roots of *Iris germanica* L..

As can be seen, all compounds or extracts are non-toxic in the tested concentrations except irilone (compound 5). A concentration was considered non-toxic in the ICAM-1 assay if more than 90% cell viability (meaning 90% remaining activity) was still obtained with the MTT assay. Therefore, irilone was tested at a concentration of 12.5, 25 and 50 μM in the ICAM-1 assay. All other compounds were tested at 25, 50 and 70 μM .

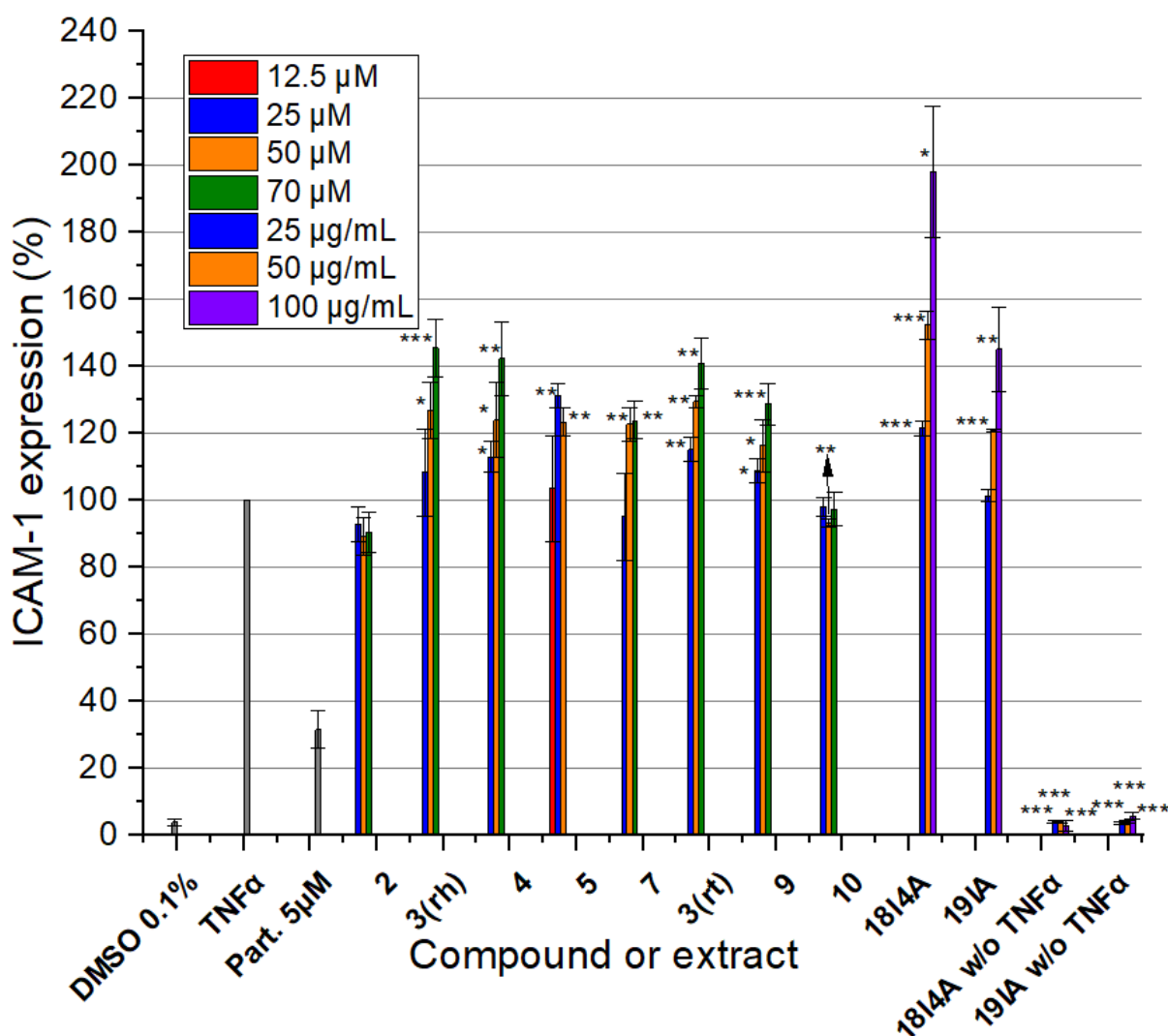


Figure 93: Impact of different compounds (see Figure 74 in section 4.3.3.3 and Figure 84 in section 4.3.4.3 for the structures) and extracts (1814A (EtOAc extract of the fresh rhizomes of *Iris germanica* L.) or 191A (EtOAc extract of the fresh roots of *Iris germanica* L.; see Figure 53, Figure 54, and Table 15 in section 4.2.2.4)) at different concentrations (12.5 (red), 25 (blue), 50 (orange) and 75 µM (green) and 12.5 (red), 25 (blue), 50 (orange) and 100 µg/mL (violet)) on the TNF-α-induced (10 ng/mL) ICAM-1 expression. DMSO (without TNF-α and untreated) 0.1 % (V/V) was tested as solvent control. Parthenolide (5 µM) was tested as positive control. The cells treated only with TNF-α was set as 100% ICAM-1 expression. Three independent experiments were executed in hexaplicates. The data are shown as average ± standard deviation. Level of significance: * $p < 0.05$, ** $p < 0.01$ and *** $p < 0.001$. **3(rh)** represent irigenin isolated from the rhizome of *Iris germanica* L. and **3(rt)** irigenin isolated from the roots of *Iris germanica* L..

Most of the compounds and the two extracts had unexpected pro-inflammatory properties. Compounds **2** (4-hydroxy-3-methoxyacetophenone) and **10** (irisflorentin isomer) showed no effect on the ICAM-1 expression (the TNF-α induced ICAM-1 expression was the same as for the untreated cells). On the contrary, the compounds **3(rh)**, **3(rt)**, **4**, **5**, **7** and **9** showed concentration dependent effects on a TNF-α induced ICAM-1 expression. Interestingly, isomers **9** and **10** showed different behaviour. Whereas **9** showed a concentration dependent increase of the TNF-α induced ICAM-1 expression, **10** had no effect.

For irilone (**5**), the concentration-dependent activity is somewhat unclear, as it showed a pro-inflammatory effect with an increase of ~30% of the ICAM-1 expression at 50 μ M. It is also good to notice that the highest irilone concentration used was at the limit of the toxicity, as seen with the MTT assay (only 90% cell viability). Compounds **3(rh/rt)** and **4** (irigenin S) showed the same concentration dependency on the TNF- α induced ICAM-1 expression. They were the isolates with the highest pro-inflammatory effect with an increase of ~40-50 % of the TNF- α induced ICAM-1 expression at concentrations of 70 μ M. It was surprising, because in other studies irigenin was found to have anti-inflammatory properties [185,190,194]. However, the system and the anti-inflammatory tests were completely different. In this study, human cells (HMEC-1) were used and not murine cells (RAW 264.7). The type of the test was also different: not the same stimulator was used (TNF- α with HMEC-1 cells and LPS with RAW 264.7 cells, although LPS can activate the same transcription pathway as TNF- α with another cytokine IL-1 with HMEC-1 cells (see Figure 52)) and not the same read out was measured (ICAM-1 for HMEC-1 cells and NO for RAW 264.7 cells). The extracts 18I4A and 19I1A showed as the isolates a concentration-dependent increase and thus pro-inflammatory effects on the TNF- α induced ICAM-1 expression with 18I4A doubling the ICAM-1 expression at 100 μ g/mL. The TNF- α induced ICAM-1 expression of cells treated with the extracts was also tested without stimulator to see if the extracts needed the stimulator to enhance the ICAM-1 expression. If not, it is possible that the extracts interacted with the TNF- α receptor and thus enhance the TNF- α induced ICAM-1 expression. As can be seen in Figure 93, no expression was detected without TNF- α (the ICAM-1 expression was the same as the solvent control). This means that the extracts and some isolates had an activating influence in the investigated transcription pathway if it is induced by TNF- α . The mode of action should be further investigated to exactly know and understand the mechanism and the pro-inflammatory effect.

To see if the extracts had exclusively an influence on the transcription pathway activated by TNF- α , another stimulator, IFN- γ , acting via another pathway was used. The results are shown in Figure 94. Here, NF- κ B is not involved and therefore, parthenolide should not demonstrate a pronounced anti-inflammatory effect.

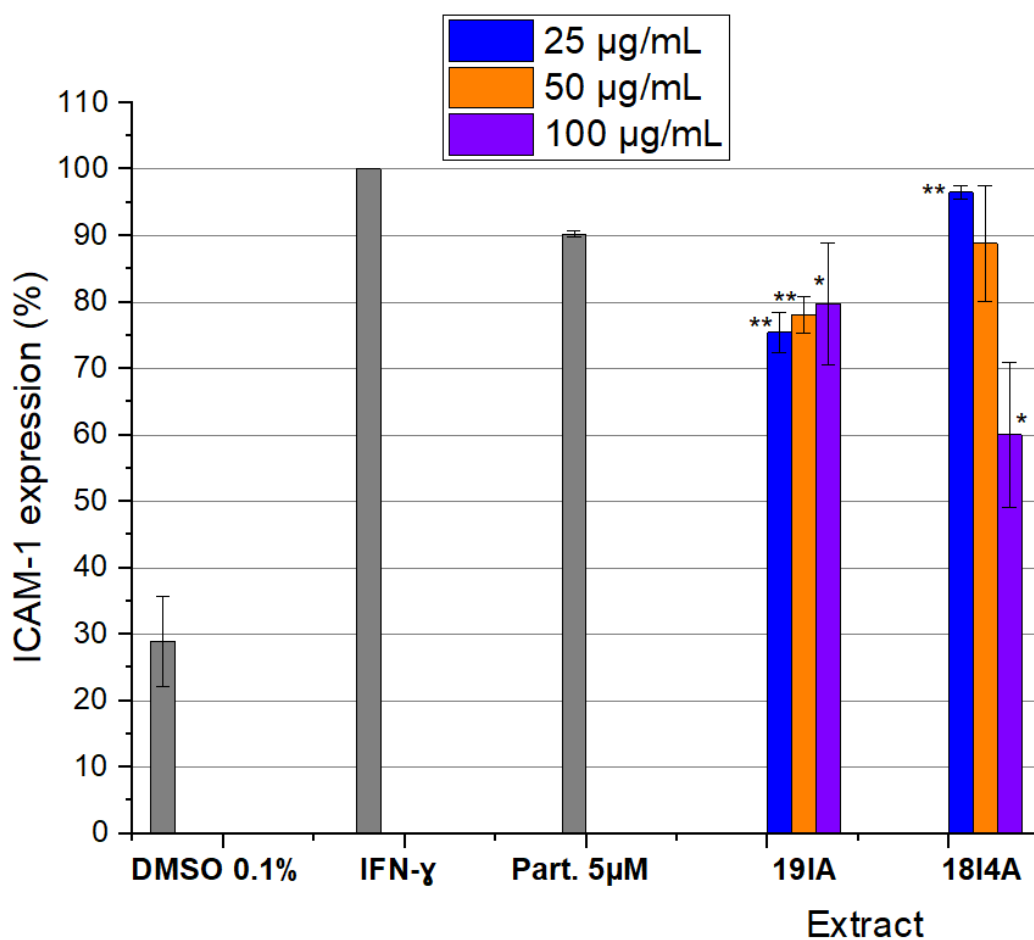


Figure 94: Impact of the extracts 1814A (EtOAc extract of the fresh rhizomes of *Iris germanica* L.) and 191A (EtOAc extract of the fresh roots of *Iris germanica* L.; see Figure 53, Figure 54, and Table 15 in section 4.2.2.4) at different concentrations (25 (blue), 50 (orange) and 100 μg/mL (violet)) on the IFN-γ induced (40 ng/mL) ICAM-1 expression. DMSO (without IFN-γ and untreated) 0.1 % (V/V) was tested as solvent control. Parthenolide (5 μM) was also tested. The cells treated only with IFN-γ was set as 100% ICAM-1 expression. Three independent experiments were executed in hexaplicates. The data are shown as average ± standard deviation. Level of significance: * $p < 0.05$, ** $p < 0.01$ and *** $p < 0.001$.

The ICAM-1 assay with IFN-γ as stimulator gave different results as both extracts do not exhibit a pro-inflammatory effect. Interestingly, 191A increased the IFN-γ induced ICAM-1 expression very slightly from lower to higher concentrations but did not really show a concentration dependent effect. 1814A showed a pronounced concentration dependent decrease compared to 191A meaning that in this set-up it showed an anti-inflammatory effect. Parthenolide demonstrated no anti-inflammatory effect with an insignificant decrease of the IFN-γ induced ICAM-1 expression compared to control. The results concerning the 100% value, negative and positive control are in line with the previously reported results [169].

The results of the anti-inflammatory assay with different stimulators showed two different effects for extract 1814A: on the one hand a slight anti-inflammatory effect with IFN-γ as stimulator and on the other hand a strong pro-inflammatory effect with TNF-α as stimulator. The reasons for this are still

unknown, but many different experiments could be realised to understand the action mechanism further. Especially the interaction between the isoflavones and benzophenones with NF- κ B should be deeply investigated. In fact, an anti-osteoporotic activity of some isoflavones from *Iris germanica* L. targeting the protein NF- κ B has been demonstrated in 2019 by Alam et al. [195]. Only five proteins are found in the NF- κ B family: p65/RelA, RelB, c-Rel, p105/p50 (NF- κ B1) and p100/p52 (NF- κ B2) [196]. These ones associate with each other forming distinct homo/heterodimeric complexes that share a common RHD (Rel homology domain of 300 amino acids length). They have found with *in silico* approach (meaning experimentation performed by computer) that some isoflavones had strong interactions with the NF- κ B p50 homodimer and therefore, demonstrated an anti-osteoporotic activity (*in silico* approach was supported with *in vivo* results using RAW 264.7 cells). Therefore, it could be possible that the extracts interfered in the transcription pathway of TNF- α , had an interaction with NF- κ B and strengthen the expression of the ICAM-1 molecule. Interesting was the fact, that the pro-inflammatory effect was observed only with TNF- α as stimulator. The expression of the ICAM-1 molecule was not affected without TNF- α . Therefore, it supported the fact, that the extracts and the isolates **3** (irigenin), **4** (irigenin S), **5** (irilone), and **7** (iriflophenone) interfered somewhere exclusively in the transcription pathway of TNF- α .

Finally, it could be also interesting to investigate the ICAM-1 assay with LPS as stimulator. Indeed, LPS activates both transcription pathways of TNF- α (with IL-1 as stimulator and not TNF- α) and IFN- γ (see Figure 52). The competition between the two transcription pathways could give more information concerning the preferential site of action of the isoflavones and if one transcription pathway is preferred.

4.3.7 Antimicrobial assay

The isolated isoflavones and benzophenones, as well as the different extracts and the iris butter, were tested for their potential antimicrobial activity. Indeed, some examples of isoflavones and extracts of *Iris germanica* L. were described in the literature to have the properties to kill many different bacteria like *S. aureus* [140,141,143,144,197,198]. Broth dilution method and agar diffusion were both found in the literature. Mostly, the agar diffusion test is used to determine the antimicrobial activity of an extract or compound, whereas the MIC is determined with a broth dilution method. In general, extracts of *Iris germanica* L. were more often tested than isolated compounds.

In this thesis, a broth dilution method was used (established by Julia Brunner, University of Regensburg). First, the CFU (colony-forming unit) for both bacteria was determined: 5×10^9 CFU/mL for *S. aureus* and 2.5×10^9 CFU/mL for *E. coli*. The results of the antimicrobial screening of the extracts

and isolates against *S. aureus* are shown in Figure 95 and Figure 96. Pictures were also taken of the plates. A picture of the plate containing 1819 is shown in Figure 97. It was defined, that an extract or an isolate showed an antimicrobial activity, if 70% of the bacteria were killed.

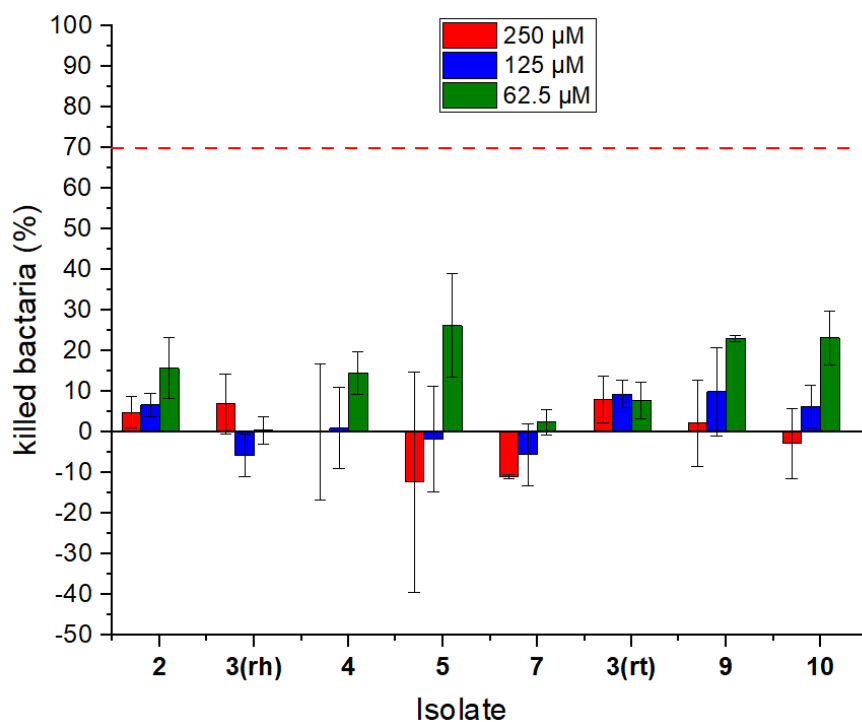


Figure 95: Results of the antimicrobial screening against *S. aureus*. Compounds **2** (4-hydroxy-3-methoxyacetophenone), **3(rh)** (irigenin isolated from the rhizomes of *Iris germanica* L.), **4** (irigenin S), **5** (irilone), **7** (iriflophenone), **3(rt)** (irigenin isolated from the roots of *Iris germanica* L.), **9** (irisfloreantin) and **10** (irisfloreantin isomer) were tested (see Figure 74 in section 4.3.3.3 and Figure 84 in section 4.3.4.3 for the structures) at three different concentrations (250 (red), 125 (blue) and 62.5 (green) μM). Three independent experiments were executed in triplicate. The data are shown as average ± standard deviation.

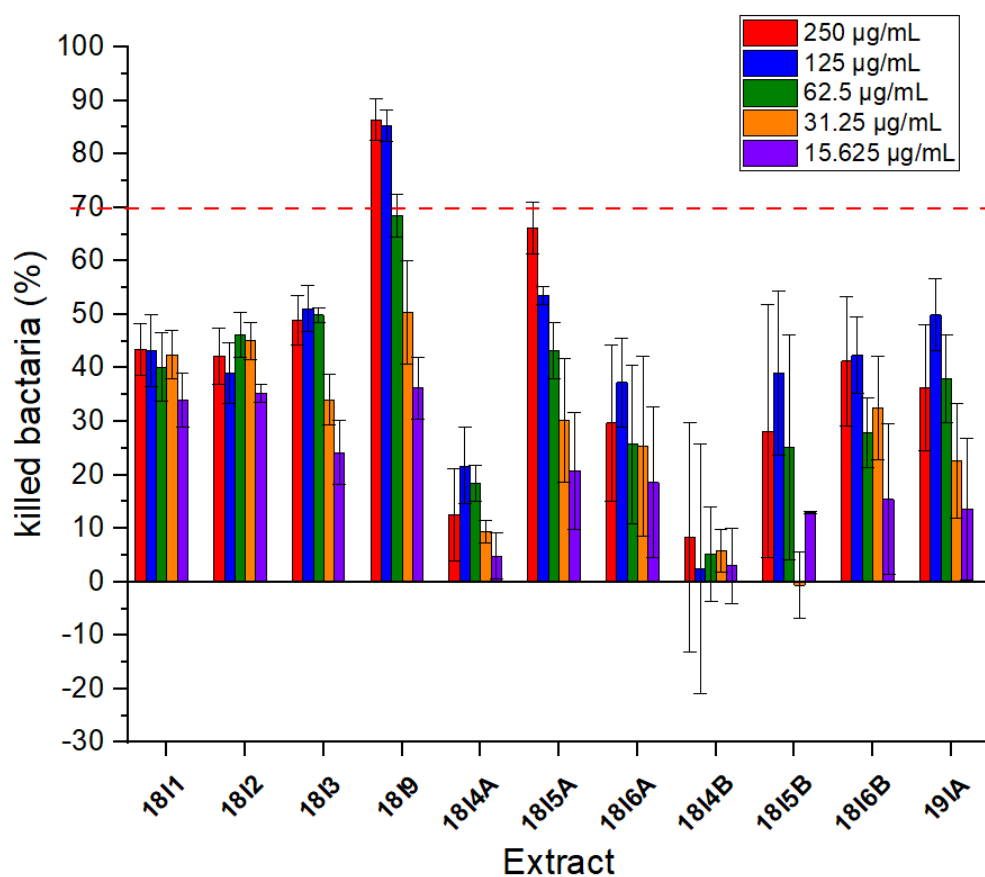


Figure 96: Results of the antimicrobial testing against *S. aureus*. The DCM extracts (1811 (fresh rhizomes), 1812 (aged rhizomes), 1813 (fresh roots)), EtOAc extracts (1814A (fresh rhizomes), 1815A (aged rhizomes), 186A (fresh roots)), and BuOH extracts (184B (fresh rhizomes), 185B (aged rhizomes), 186B (fresh roots); see Figure 54 or Table 15 in section 4.2.2.4) were tested at five different concentrations (250 (red), 125 (blue), 62.5 (green), 31.25 (orange) and 15.625 (violet) µg/mL). Three independent experiments were executed in triplicate. The data are shown as average ± standard deviation.

As can be seen, none of the isolated isoflavones and benzophenones showed an antimicrobial activity against *S. aureus*. This is quite surprising, because some isoflavones like genistein or biochanin A are known in the literature as antimicrobial agents. However, it seemed that the different substituents and the place of the substituents play an important role for the antimicrobial activity [141]. Irirogenin was found in one paper as active against *S. aureus* [143]. The major difference with the MIC determination in this thesis was the CFU used. Indeed, Dar et al. have used 2.10^5 CFU/mL in their work, which was very low compared to the CFU used in this thesis.

Unfortunately, none of the tested extracts showed an antimicrobial activity against *S. aureus*. Only the extract 1815A (EtOAc extract of the aged rhizome of *Iris germanica* L.; see Figure 54 or Table 15 in section 4.2.2.4) could show a potential antimicrobial activity, if the extract would be tested at a higher concentration (500 µg/mL for example). However, higher concentrations like 500 µg/mL were not tested because they are too high to have any potential for in vivo application. Moreover, solubilisation problems could occur.

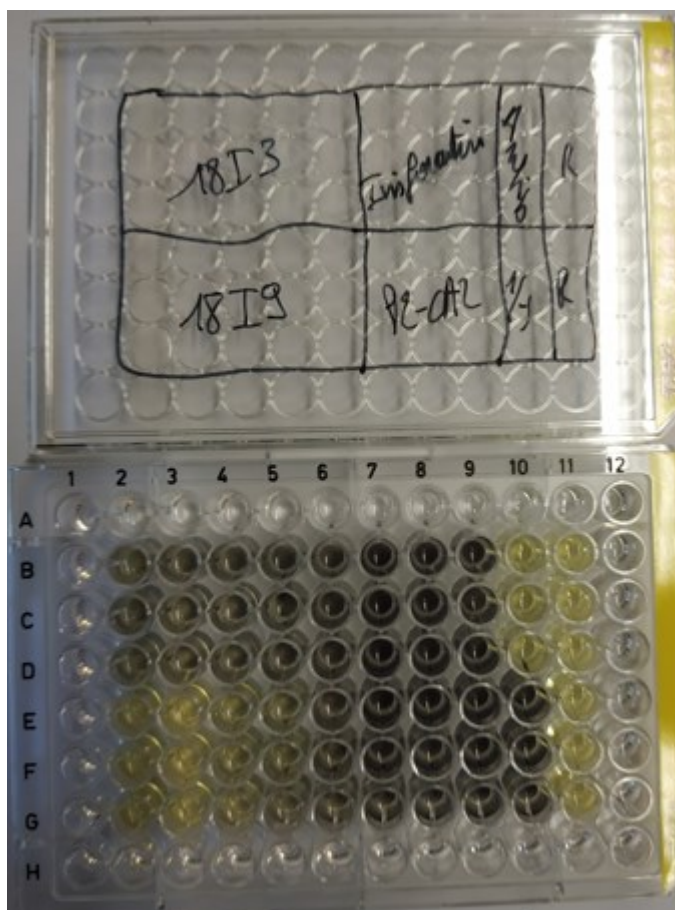


Figure 97: 96-wells plate containing 18I9 (iris butter from aged rhizomes from hydro distillation; Figure 53 or Table 15 in section 4.2.2.4) as test mixture against *S. aureus*. Chloramphenicol (positive control) was added in the wells B10, C10 and D10. In the wells E10, F10 and G10 only the bacterial solution was added. 18I9 is present in the wells E2 to G6 at different concentrations: 250 $\mu\text{g/mL}$ in E2 to G2, 125 $\mu\text{g/mL}$ in E3 to G3, 62.5 $\mu\text{g/mL}$ in E4 to G4, 32.25 $\mu\text{g/mL}$ in E5 to G5 and 16.625 $\mu\text{g/mL}$ in E6 to G6. The wells B11 to G11 are the negative control (wells with broth medium, DMSO and MTT solution only).

Only 18I9 (iris butter from aged rhizomes from hydro distillation; see Figure 53 or Table 15 in section 4.2.2.4) showed an antimicrobial activity. The MIC of 18I9 was $\sim 62.5 \mu\text{g/mL}$. The MIC of chloramphenicol was also determined: 9 $\mu\text{g/mL}$ (corresponding to 28 μM). 30 μL of the solution of chloramphenicol (3 mg/mL) was added to the wells B10, C10 and D10, corresponding to a final concentration of 1.2 mM in the wells (much higher than its MIC). The MIC value of the iris butter 18I9 is much higher than the MIC of chloramphenicol. Normally, an extract or a compound is said to be significantly active against a microorganism if the MIC is equal or less than 8 $\mu\text{g/mL}$ or 8 μM . The major constituents of the iris butter are fatty acids and especially myristic acid (47.7%, see Table 12). In the literature, fatty acids as antimicrobial agents are very often studied [199] and some MIC for myristic acid against *S. aureus* are given: 400 [200], 800 [201], 1000 [202] or 1600 $\mu\text{g/mL}$ [201] are typical MIC of myristic acid. Taking this into account, irones are the only constituents of the iris butter, which were potentially responsible for the determined antimicrobial activity. Therefore, α -irone was tested in the

same concentration range as 1819. The pictures of the plate with α -irone are shown in Figure 98. Unfortunately, the determination of the MIC was not possible because the maximum of absorbance of MTT was shifted. Indeed, α -irone built a violet complex with MTT, which is obviously kinetic.

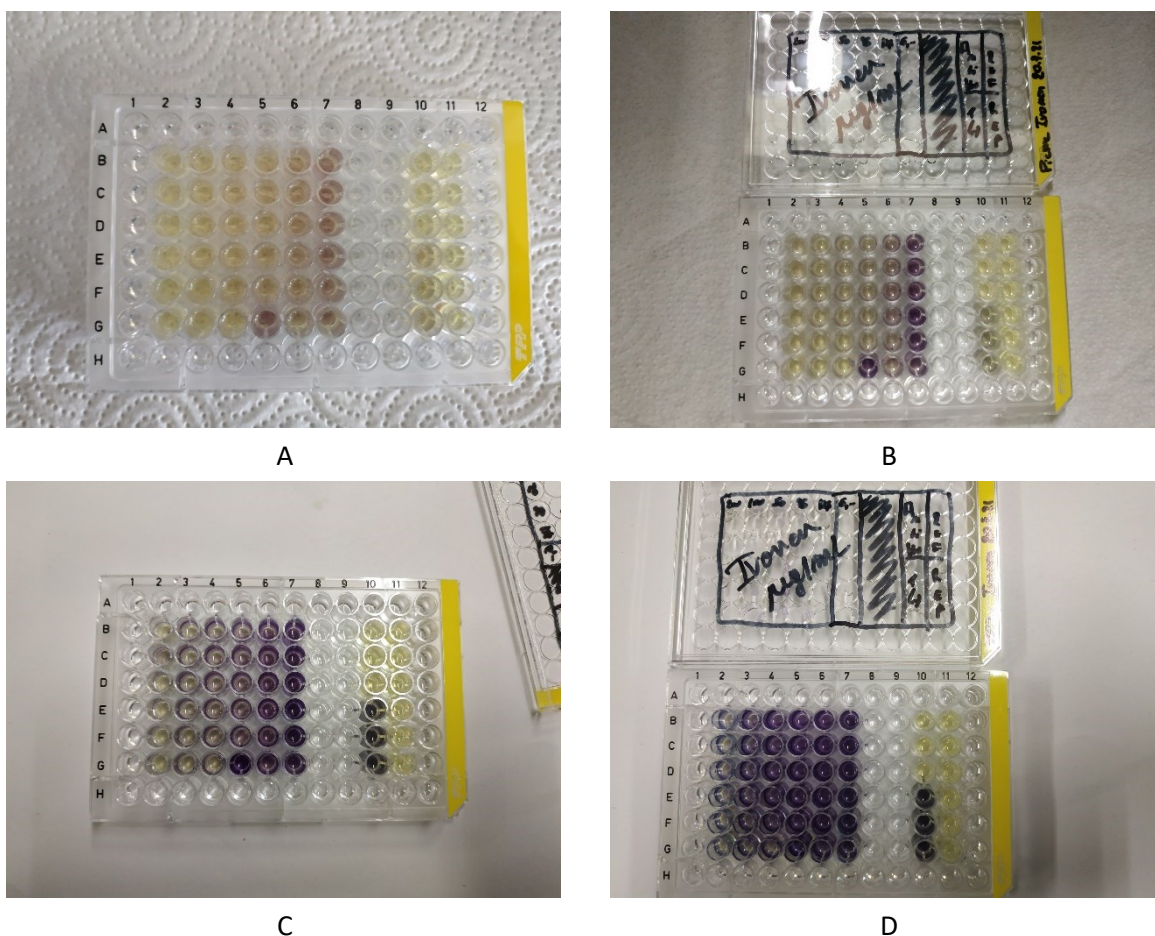


Figure 98: Pictures of the antimicrobial assay plates with α -irone: 30 min after MTT addition on the shaker at 37°C (A), 4 hours (30 min on the shaker and 210 min in the incubator at 37°C) after MTT addition (B), one day (stored overnight in darkness after the incubator) after the MTT addition (C) and 2 days (stored in the darkness) after the MTT addition (D).

Therefore, the agar diffusion assay was tried with α -irone to see if an antimicrobial activity can be detected. Some pictures of the agar-plate are shown in Figure 99.

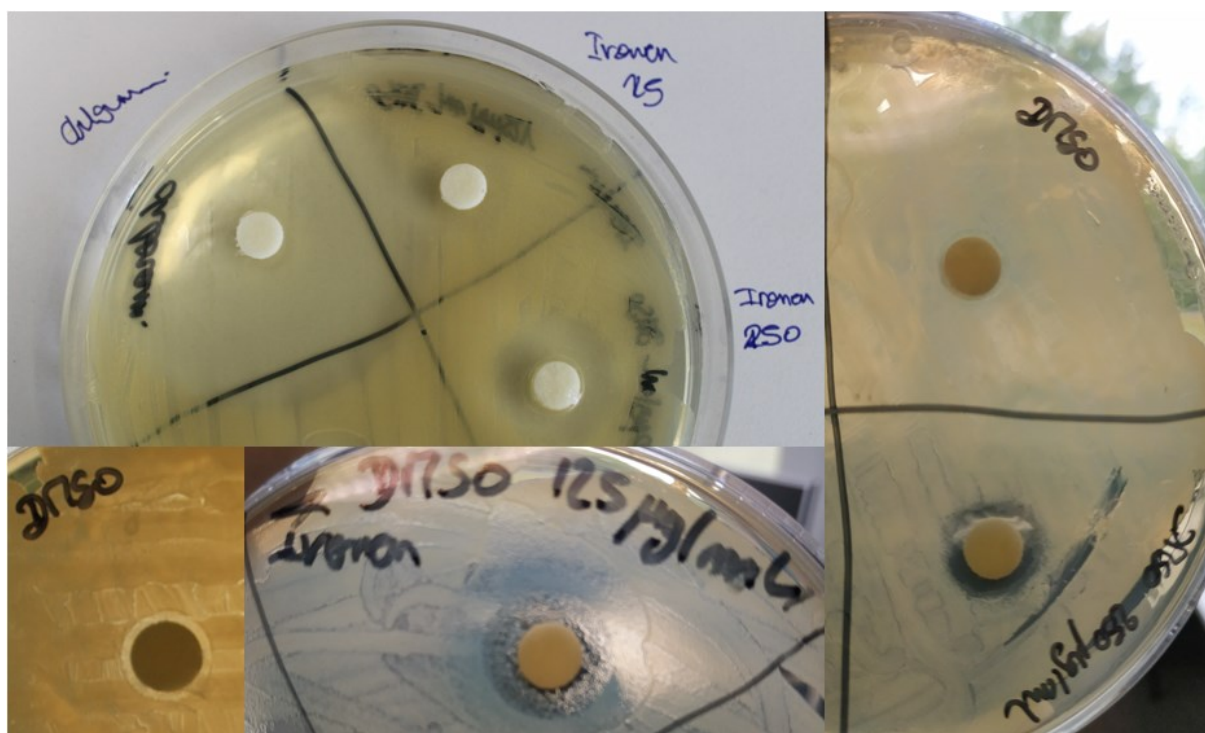


Figure 99: Pictures of the agar plate diffusion assay. Chloramphenicol, α -irone (dissolved in DMSO) as well as DMSO alone were tested against *S. aureus* as described in section 4.2.2.9.4..

Two high concentrations of α -irone in DMSO were tested (250 and 125 $\mu\text{g}/\text{mL}$). However, α -irone showed an antimicrobial activity against *S. aureus* although α -irone is not polar, and therefore should not easily diffuse through the agar. On the contrary, DMSO showed no antimicrobial activity in the used concentration. Two inhibition zones were measured: 14 ± 3 mm and 11.5 ± 0.5 mm for 250 and 125 μg α -irone/ mL DMSO, respectively. The agar diffusion test was only done to prove that α -irone possesses antimicrobial activity, but unfortunately no MIC could be determined.

As the iris butter showed an antimicrobial activity against *S. aureus*, it was also tested against *E. coli*. The other extracts were not tested. The broth dilution method was used and the results are shown in Figure 100. Pictures of the plate were taken and are shown in Figure 101. 8 $\mu\text{g}/\text{mL}$ is a typical MIC of chloramphenicol against *E. coli* [203,204]. An antimicrobial activity of the iris butter against *E. coli* was detected. Indeed, a yellow-green colouration of the wells at the highest concentration of the iris butter (250 μg α -irone/ mL DMSO) was obtained. The colouration was comparable in colour to the positive control. It became stronger and greener with the decrease of the iris butter concentration. The MIC was optically determined between 125 and 62.5 μg α -irone/ mL . The optical visualisation was supported by the results of the UV-vis measurements. Indeed, a concentration dependent effect was observed as against *S. aureus*. A MIC between 125 and 62.5 μg α -irone/ mL was determined. Here again, the MIC was quite high, but α -irone should be further investigated against *E. coli*.

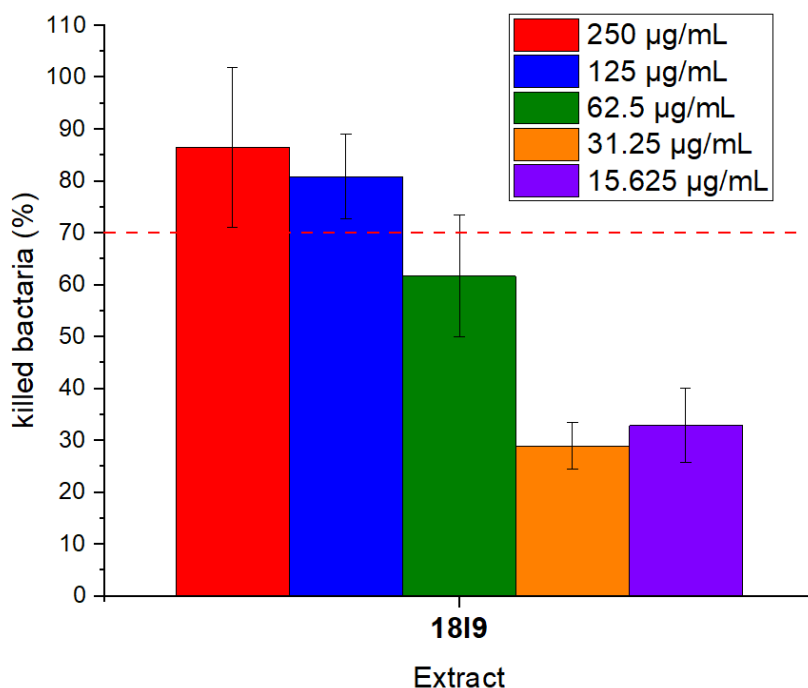


Figure 100: Results of the antimicrobial activity against *E. coli*. Only 1819 (iris butter from aged rhizomes from hydro distillation; Figure 53 or Table 15 in section 4.2.2.4) was tested at five different concentrations (250 (red), 125 (blue), 62.5 (green), 31.25 (orange) and 15.625 (violet) µg/mL). Three independent experiments were executed in hexaplicates. The data are shown as mean ± standard deviation.

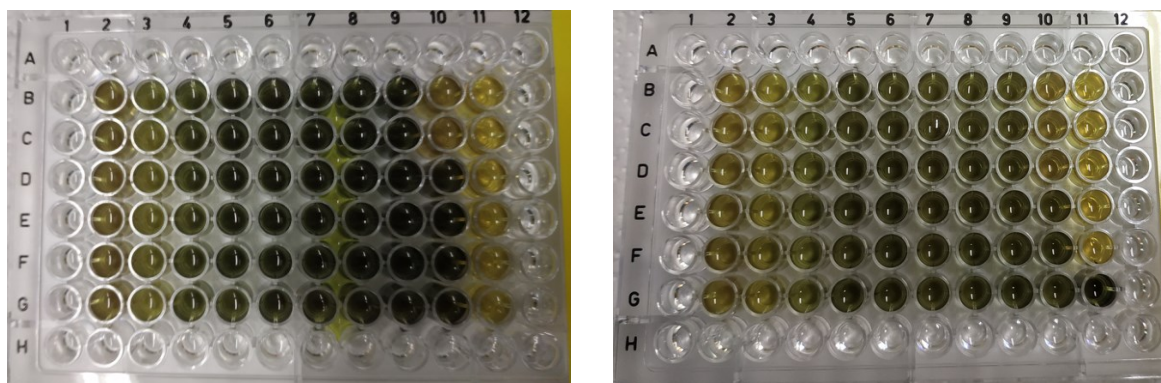


Figure 101: Picture of the 96-wells plate containing 1819 (iris butter from aged rhizomes from hydro distillation; Figure 53 or Table 15 in section 4.2.2.4) as test mixture against *E. coli*. Chloramphenicol (positive control) was added in the wells B10, C10 and D10. In the wells E10, F10 and G10 only the bacterial solution was added. The wells B11 to G11 are the negative control (wells with broth medium, DMSO and MTT solution only). Different concentrations were tested (from 250 µg/mL (wells B2 to G2) to 1.95 µg/mL (wells B9 to G9), a 1 to 1 dilution was done from the first six wells (B2 to G2) up to the six last wells (B9 to G9)).

As 1819 showed a significant antimicrobial activity against *S. aureus* and *E. coli*, the cytotoxicity was tested with HMEC-1 cells. The results are shown in Figure 102.

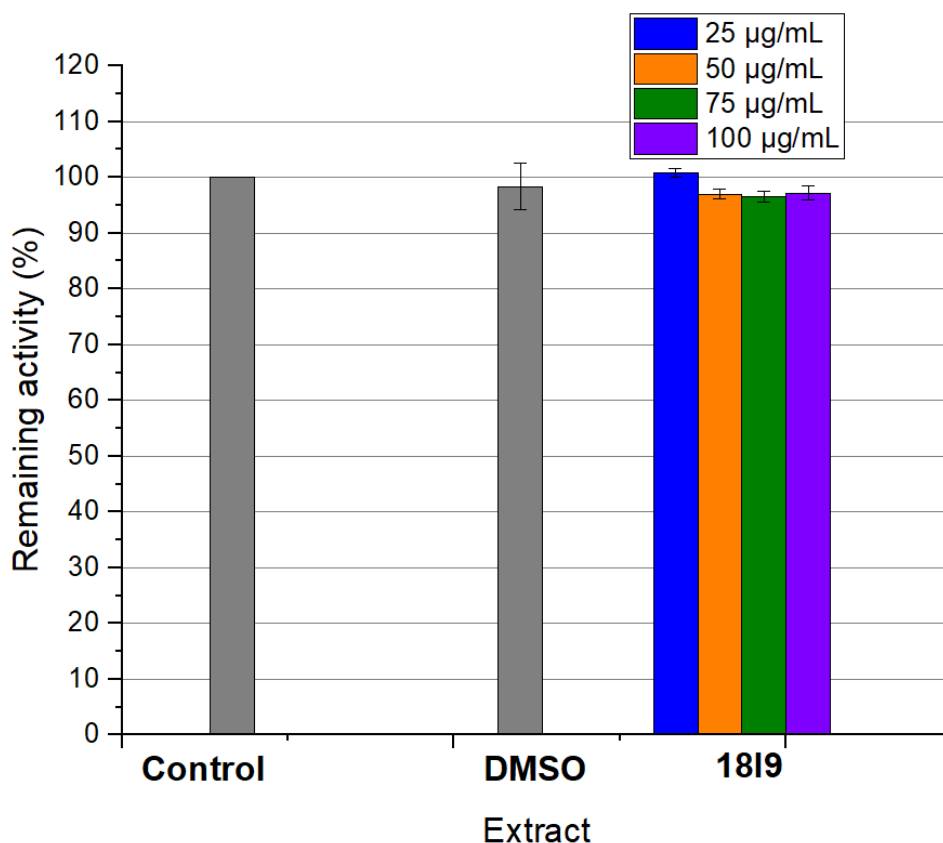


Figure 102: Remaining activity (correlated to the viability) of the HMEC-1 cells with 1819 (iris butter from aged rhizomes from hydro distillation; Figure 53 or Table 15 in section 4.2.2.4) as test mixture. 1819 was tested at different concentration: 25 (blue), 50 (orange), 75 (green) and 100 (violet) µg/mL. DMSO (grey) 0.1 % (V/V) was tested as solvent control. Three independent experiments were executed in hexaplates. The data are shown as average \pm standard deviation.

As can be seen, 1819 was not toxic for the HMEC-1 cells and thus it is selectively active against bacterial cells.

4.3.8 Utilisation of the roots and rhizomes as raw material for isolation of isoflavones and benzophenones

The main idea of the phytochemical investigation of iris rhizomes and roots was to screen the waste of the harvest (roots) and iris butter (remaining rhizomes and water in the distillation balloon) for valuable compounds. Three classes of compound were isolated from two iris extracts 1814A (EtOAc extract of the rhizomes of *Iris germanica* L.; the rhizomes were first extracted with DCM then with a binary mixture of water and EtOH (H₂O/EtOH 30/70 wt%) and after rotary evaporation of EtOH, the water remaining phase was shaken out with EtOAc; see Figure 54 in section 4.2.2.4) and 191A (EtOAc extract of the roots of *Iris germanica* L.; the roots were first extracted with n-hexane and then with EtOAc; see Figure 53 in section 4.2.2.4).

As depicted in Figure 65, the solvent extracts 201A (EtOAc) and 201B (BuOH) done with the residue of the hydro distillation (remaining rhizomes and water in the distillation balloon) were very similar to

18I5A (EtOAc extract of the aged rhizomes of *Iris germanica* L.) and 18I5B (BuOH extract of the aged rhizomes of *Iris germanica* L.; see Figure 54 or Table 15 in section 4.2.2.4), respectively. Qualitatively, it had been noticed that some secondary metabolites are more abundant in the solvent extract of aged rhizomes as extracting material. Moreover, the phytochemical compounds isolated from 18I4A are also present in 18I5A (three main spots of both extracts, see Figure 60 in 4.3.1 or Figure 67 in 4.3.2).

Taking all these results into account, it can be assumed that the residue of the hydro distillation (the waste of the hydro distillation) as well as the roots (they are co-harvested with the rhizomes, removed as far as possible and considered also as waste) can be used as raw material to isolate valuable compounds like isoflavones, benzophenones and acetophenone derivatives.

4.4 Conclusion

6 isoflavones, 2 benzophenones and one acetophenone derivative **1** (5,7-dihydroxy-6-methoxy-3-(4-methoxyphenyl)-4H-chromen-4-one), **2** (4-hydroxy-3-methoxyacetophenone), **3(rh)/3(rt)** (irigenin isolated from the rhizomes (rh) and roots (rt) of *Iris germanica* L.), **4** (irigenin S), **5** (irilone), **6** (3'-methoxy-irilone), **7** (iriflophenone), **8** (4-O-methyl- iriflophenone), **9** (irisfloreantin) and **10** (irisfloreantin isomer) were successfully extracted and isolated from the roots and the rhizomes of *Iris germanica* L. (see Figure 74 in section 4.3.3.3 and Figure 84 in section 4.3.4.3 for the structures). Their structures were elucidated with NMR and LC-MS data (sections 4.3.3.3 and 4.3.4.3). As the rhizomes have been used since centuries to treat several diseases, the extracts and the isolated compounds were tested for their ability as anti-inflammatory and antimicrobial agents. The obtained results showed unexpected concentration dependent pro-inflammatory properties for some extracts and test compounds if HMEC cells were stimulated with TNF- α . The pro-inflammatory effect was observed exclusively with TNF- α as stimulator. Indeed, if the cells were treated with the extracts and without stimulator, no effect on the ICAM-1 expression was detected. It reinforced the fact that the extracts and the isolates **3** (irigenin), **4** (irigenin S), **5** (irilone), and **7** (iriflophenone) interfered somewhere exclusively in the transcription pathway of TNF- α . The extracts were further studied using another stimulator, IFN- γ , and demonstrated some potential anti-inflammatory properties, especially 18I4A (EtOAc extract of the fresh rhizomes of *Iris germanica* L.; see Figure 54 or Table 15 in section 4.2.2.4). Therefore, the pro- and anti-inflammatory properties should be analysed further in order to understand the target of the isolated compounds and extracts.

Moreover, the isolated compounds and extracts were tested for antimicrobial activity. Only 18I9 (iris butter from aged rhizomes of *Iris germanica* L. from hydro distillation; Figure 53 or Table 15 in section 4.2.2.4) demonstrated a significant activity against *S. aureus* and *E. coli*. The major components of the

iris butter were fatty acids and did not show a strong activity against *S. aureus* and *E. coli* [112,114,200–202]. Therefore, one irone, α -irone, was tested as potential antimicrobial compound. It was not possible to determine a MIC with the broth method dilution, because α -irone formed a violet complex with MTT and consequently the determination of the MIC using UV-measurements was not possible. However, the agar diffusion method showed that α -irone had an antimicrobial activity, although the compound is lipophilic and should have diffusion problems to go through the agar. 18I9 should also be further investigated concerning its antimicrobial activity against other bacteria and fungi. It would also be interesting to test other iris butter of different iris species (*Iris pallida* Lam. or *Iris florentina* L.) in order to see if the different irones will have the same antimicrobial activity. Moreover, the 18I9 could be also tested as anti-inflammatory agent.

5 References

- [1] S. Sasidharan, Y. Chen, D. Saravanan, K.M. Sundram, L. Yoga Latha, Extraction, isolation and characterization of bioactive compounds from plants' extracts., *African J. Tradit. Complement. Altern. Med. AJTCAM*. 8 (2011) 1–10. <http://www.ncbi.nlm.nih.gov/pubmed/22238476>.
- [2] M. Palma, G.F. Barbero, Z. Piñeiro, A. Liazid, C.G. Barroso, M.A. Rostagno, J.M. Prado, M.A.A. Meireles, CHAPTER 2. Extraction of Natural Products: Principles and Fundamental Aspects, in: 2013: pp. 58–88. <https://doi.org/10.1039/9781849737579-00058>.
- [3] A. Gupta, M. Naraniwal, V. Kothari, Modern extraction methods for preparation of bioactive plant extracts, *Int. J. Appl. Nat. Sci.* 1 (2012) 8–26.
- [4] Q.-W. Zhang, L.-G. Lin, W.-C. Ye, Techniques for extraction and isolation of natural products: a comprehensive review, *Chin. Med.* 13 (2018) 20. <https://doi.org/10.1186/s13020-018-0177-x>.
- [5] F. Soxhlet, "Die gewichtsanalytische Bestimmung des Milchfettes," *Dingler's Polytech. J. Band* 232 (1879) 461–465. <http://dingler.culture.hu-berlin.de/article/pj232/ar232136>.
- [6] S.C. Mandal, V. Mandal, A.K. Das, Classification of Extraction Methods, in: *Essentials Bot. Extr.*, Elsevier, 2015: pp. 83–136. <https://doi.org/10.1016/B978-0-12-802325-9.00006-9>.
- [7] A. Nn, A Review on the Extraction Methods Use in Medicinal Plants, Principle, Strength and Limitation, *Med. Aromat. Plants.* 04 (2015) 3–8. <https://doi.org/10.4172/2167-0412.1000196>.
- [8] K.-G. Fahlbusch, F.-J. Hammerschmidt, J. Panten, W. Pickenhagen, D. Schatkowski, K. Bauer, D. Garbe, H. Surburg, *Flavors and Fragrances*, in: *Ullmann's Encycl. Ind. Chem.*, Wiley-VCH Verlag GmbH & Co. KGaA, Weinheim, Germany, 2003. https://doi.org/10.1002/14356007.a11_141.
- [9] F. Chemat, M.A. Vian, G. Cravotto, Green extraction of natural products: Concept and principles, *Int. J. Mol. Sci.* 13 (2012) 8615–8627. <https://doi.org/10.3390/ijms13078615>.
- [10] Paul Anastas and John Warner, *Green Chemistry: Theory and Practice*, Oxford University Press, New York, 1998.
- [11] T.G. McCloud, *Handbook of Thin Layer Chromatography*, Chromatographic Science Series, Vol 89, 3rd edition Edited by Joseph Sherma and Bernard Fried (Lafayette College). Marcel Decker, New York, NY. 2003. xvii + 1016 pp. 7 1 / 4 × 10 1 / 4 in. \$250.00. ISBN 0-8247-0895-4, *J. Nat. Prod.* 67 (2004) 1199–1199. <https://doi.org/10.1021/np030741o>.

- [12] D. Parriott, ed., *Practical guide to HPLC detection*, Academic Press, 1993.
- [13] V.R. Meyer, *CHROMATOGRAPHY | Principles*, in: *Ref. Modul. Chem. Mol. Sci. Chem. Eng.*, Elsevier, 2013. <https://doi.org/10.1016/B978-0-12-409547-2.00081-0>.
- [14] K.R.P.J.P. Haddad, *Principles and Practice of Modern Chromatographic Methods*, Academic Press, 1994.
- [15] C. Burgess, Chapter 1 The basics of spectrophotometric measurement, in: 2007: pp. 1–19. [https://doi.org/10.1016/S0167-9244\(07\)80003-5](https://doi.org/10.1016/S0167-9244(07)80003-5).
- [16] O. Thomas, V. Cerda, Chapter 2 From spectra to qualitative and quantitative results, in: 2007: pp. 21–45. [https://doi.org/10.1016/S0167-9244\(07\)80004-7](https://doi.org/10.1016/S0167-9244(07)80004-7).
- [17] R.P. Bruce J. Berne, *Dynamic Light Scattering: With Applications to Chemistry, Biology, and Physics*, John Wiley & Sons Inc, 1976.
- [18] M.L. Klossek, D. Touraud, T. Zemb, W. Kunz, Structure and Solubility in Surfactant-Free Microemulsions, *ChemPhysChem*. 13 (2012) 4116–4119. <https://doi.org/10.1002/cphc.201200667>.
- [19] T.N. Zemb, M. Klossek, T. Lopian, J. Marcus, S. Schöetl, D. Horinek, S.F. Prevost, D. Touraud, O. Diat, S. Marčelja, W. Kunz, How to explain microemulsions formed by solvent mixtures without conventional surfactants, *Proc. Natl. Acad. Sci.* 113 (2016) 4260–4265. <https://doi.org/10.1073/pnas.1515708113>.
- [20] W. Hou, J. Xu, Surfactant-free microemulsions, *Curr. Opin. Colloid Interface Sci.* 25 (2016) 67–74. <https://doi.org/10.1016/j.cocis.2016.06.013>.
- [21] S. Schöetl, N. Matubayasi, D. Horinek, Solubilization power of surfactant-free microemulsions, *Phys. Chem. Chem. Phys.* 22 (2020) 22185–22189. <https://doi.org/10.1039/D0CP02933E>.
- [22] J. Marcus, D. Touraud, S. Prévost, O. Diat, T. Zemb, W. Kunz, Influence of additives on the structure of surfactant-free microemulsions, *Phys. Chem. Chem. Phys.* 17 (2015) 32528–32538. <https://doi.org/10.1039/C5CP06364G>.
- [23] S. Prevost, T. Lopian, M. Pleines, O. Diat, T. Zemb, Small-angle scattering and morphologies of ultra-flexible microemulsions, *J. Appl. Crystallogr.* 49 (2016) 2063–2072. <https://doi.org/10.1107/S1600576716016150>.
- [24] T. Lopian, S. Schöetl, S. Prévost, S. Pellet-Rostaing, D. Horinek, W. Kunz, T. Zemb,

- Morphologies Observed in Ultraflexible Microemulsions with and without the Presence of a Strong Acid, *ACS Cent. Sci.* 2 (2016) 467–475. <https://doi.org/10.1021/acscentsci.6b00116>.
- [25] S.A. Vitale, J.L. Katz, Liquid Droplet Dispersions Formed by Homogeneous Liquid–Liquid Nucleation: “The Ouzo Effect,” *Langmuir*. 19 (2003) 4105–4110. <https://doi.org/10.1021/la026842o>.
- [26] P.J. Hore, *Nuclear Magnetic Resonance*, 1. Edition, Oxford University Press, 1995.
- [27] R.M. Silverstein, *Spectrometric Identification of Organic Compounds*, 7. Edition, Wiley, 2005.
- [28] T.D.W. Claridge, *High-Resolution NMR Techniques in Organic Chemistry*, 3. Edition, Elsevier Science, 2016.
- [29] R. Bärenwald, A. Achilles, F. Lange, T.M. Ferreira, K. Saalwächter, Applications of solid-state NMR spectroscopy for the study of lipid membranes with polyphilic guest (macro)molecules, 2016. <https://doi.org/10.3390/polym8120439>.
- [30] R.F. Tayyem, D.D. Heath, W.K. Al-Delaimy, C.L. Rock, Curcumin Content of Turmeric and Curry Powders, *Nutr. Cancer*. 55 (2006) 126–131. https://doi.org/10.1207/s15327914nc5502_2.
- [31] C.K. Mathai, Variability in turmeric (*curcuma* species) germplasm for essential oil and curcumin, *Qual. Plant. Plant Foods Hum. Nutr.* 25 (1976) 227–230. <https://doi.org/10.1007/BF02590300>.
- [32] I. Ali, A. Haque, K. Saleem, Separation and identification of curcuminoids in turmeric powder by HPLC using phenyl column, *Anal. Methods*. 6 (2014) 2526–2536. <https://doi.org/10.1039/C3AY41987H>.
- [33] A. Geethanjali, P. Lalitha, M.J. Firdhouse, Analysis of Curcumin Content of Turmeric Samples from Various States of India, *Int. J. Pharma Chem. Res.* 2 (2016) 55–62.
- [34] S.J. Taylor, I.J. McDowell, Determination of the Curcuminoid Pigments in Turmeric (*Curcuma domestica* Val) by Reversed-Phase High-Performance, *Chromatographia*. 34 (1992) 73–77.
- [35] C. Schneider, O.N. Gordon, R.L. Edwards, P.B. Luis, Degradation of Curcumin: From Mechanism to Biological Implications, *J. Agric. Food Chem.* 63 (2015) 7606–7614. <https://doi.org/10.1021/acs.jafc.5b00244>.
- [36] H.H. Tønnesen, J. Karlsen, Studies on curcumin and curcuminoids - V. Alkaline Degradation of Curcumin, *Z. Lebensm. Unters. Forsch.* 180 (1985) 132–134.

<https://doi.org/10.1007/BF01042637>.

- [37] K.M. Nelson, J.L. Dahlin, J. Bisson, J. Graham, G.F. Pauli, M.A. Walters, The Essential Medicinal Chemistry of Curcumin, *J. Med. Chem.* 60 (2017) 1620–1637.
<https://doi.org/10.1021/acs.jmedchem.6b00975>.
- [38] R. Wilken, M.S. Veena, M.B. Wang, E.S. Srivatsan, Curcumin: A review of anti-cancer properties and therapeutic activity in head and neck squamous cell carcinoma, *Mol. Cancer.* 10 (2011) 1–19. <https://doi.org/10.1186/1476-4598-10-12>.
- [39] B. Wilson, G. Abraham, V.S. Manju, M. Mathew, B. Vimala, S. Sundaresan, B. Nambisan, Antimicrobial activity of *Curcuma zedoaria* and *Curcuma malabarica* tubers, *J. Ethnopharmacol.* 99 (2005) 147–151. <https://doi.org/10.1016/j.jep.2005.02.004>.
- [40] K. Priyadarsini, The Chemistry of Curcumin: From Extraction to Therapeutic Agent, *Molecules.* 19 (2014) 20091–20112. <https://doi.org/10.3390/molecules191220091>.
- [41] M. Akram, A. Ahmed, K. Usmanghani, A. Hannan, E. Mohiuddin, M. Asif, *Curcuma Longa* and Curcumin: a Review Article, *Rom. J. Biol.* 55 (2010) 65–70. <http://ns.ibiol.ro/plant/volume55/art201.pdf>.
- [42] T. Esatbeyoglu, K. Ulbrich, C. Rehberg, S. Rohn, G. Rimbach, Thermal stability, antioxidant, and anti-inflammatory activity of curcumin and its degradation product 4-vinyl guaiacol, *Food Funct.* 6 (2015) 887–893. <https://doi.org/10.1039/c4fo00790e>.
- [43] N. Dosoky, P. Satyal, W. Setzer, Variations in the Volatile Compositions of *Curcuma* Species, *Foods.* 8 (2019) 53. <https://doi.org/10.3390/foods8020053>.
- [44] S.N. Garg, R.P. Bansal, M.M. Gupta, S. Kumar, Variation in the rhizome essential oil and curcumin contents and oil quality in the land races of turmeric *Curcuma longa* of North Indian plains, *Flavour Fragr. J.* 14 (1999) 315–318. [https://doi.org/10.1002/\(SICI\)1099-1026\(199909/10\)14:5<315::AID-FFJ838>3.0.CO;2-U](https://doi.org/10.1002/(SICI)1099-1026(199909/10)14:5<315::AID-FFJ838>3.0.CO;2-U).
- [45] A.C.C.M. Manzan, F.S. Toniolo, E. Bredow, N.P. Povh, Extraction of Essential Oil and Pigments from *Curcuma longa* [L.] by Steam Distillation and Extraction with Volatile Solvents, *J. Agric. Food Chem.* 51 (2003) 6802–6807. <https://doi.org/10.1021/jf030161x>.
- [46] R.K. Sharma, B.P. Misra, T.C. Sarma, A.K. Bordoloi, M.G. Pathak, P.A. Leclercq, Essential Oils of *Curcuma longa* L. from Bhutan, *J. Essent. Oil Res.* 9 (1997) 589–592.
<https://doi.org/10.1080/10412905.1997.9700783>.

- [47] W. Baumann, S. V. Rodrigues, L.M. Viana, Pigments and their solubility in and extractability by supercritical CO₂ - I: the case of curcumin, *Brazilian J. Chem. Eng.* 17 (2000) 323–328. <https://doi.org/10.1590/S0104-66322000000300008>.
- [48] A.L. Chassagnez-Méndez, N.C.F. Corrêa, L.F. França, N.T. Machado, M.E. Araújo, A mass transfer model applied to the supercritical extraction with CO₂ of curcumins from turmeric rhizomes (*Curcuma longa* L), *Brazilian J. Chem. Eng.* 17 (2000) 315–322. <https://doi.org/10.1590/S0104-66322000000300007>.
- [49] F. Chemat, N. Rombaut, A.G. Sicaire, A. Meullemiestre, A.S. Fabiano-Tixier, M. Abert-Vian, Ultrasound assisted extraction of food and natural products. Mechanisms, techniques, combinations, protocols and applications. A review, *Ultrason. Sonochem.* 34 (2017) 540–560. <https://doi.org/10.1016/j.ultsonch.2016.06.035>.
- [50] V. Mandal, Y. Mohan, S. Hemalatha, Microwave assisted extraction of curcumin by sample-solvent dual heating mechanism using Taguchi L9 orthogonal design, *J. Pharm. Biomed. Anal.* 46 (2008) 322–327. <https://doi.org/10.1016/j.jpba.2007.10.020>.
- [51] P. Amchova, H. Kotolova, J. Ruda-Kucerova, Health safety issues of synthetic food colorants, *Regul. Toxicol. Pharmacol.* 73 (2015) 914–922. <https://doi.org/10.1016/j.yrtph.2015.09.026>.
- [52] N.H. Choulis, Miscellaneous drugs, materials, medical devices, and techniques, *Side Eff. Drugs Annu.* 32 (2010) 891–902. [https://doi.org/10.1016/S0378-6080\(10\)32049-6](https://doi.org/10.1016/S0378-6080(10)32049-6).
- [53] Food Standards Agency, Guidelines on approaches to the replacement of Tartrazine , Allura Red , Ponceau 4R , Quinoline Yellow , Sunset Yellow and Carmoisine in food and beverages Summary, (2009). <http://www.food.gov.uk/multimedia/pdfs/publication/guidelinessotonsixcolours.pdf>.
- [54] V. Soleimani, A. Sahebkar, H. Hosseinzadeh, Turmeric (*Curcuma longa*) and its major constituent (curcumin) as nontoxic and safe substances: Review, *Phyther. Res.* 32 (2018) 985–995. <https://doi.org/10.1002/ptr.6054>.
- [55] M.I. Landim Neves, M.M. Strieder, R. Vardanega, E.K. Silva, M.A.A. Meireles, Biorefinery of turmeric (*Curcuma longa* L.) using non-thermal and clean emerging technologies: an update on the curcumin recovery step, *RSC Adv.* 10 (2020) 112–121. <https://doi.org/10.1039/C9RA08265D>.
- [56] A.L. Chassagnez-Méndez, N.T. Machado, M.E. Araujo, J.G. Maia, M.A.A. Meireles, Supercritical

- CO₂ Extraction of Curcumins and Essential Oil from the Rhizomes of Turmeric (*Curcuma longa* L.), *Ind. Eng. Chem. Res.* 39 (2000) 4729–4733. <https://doi.org/10.1021/ie000171c>.
- [57] W. Kunz, K. Holmberg, T. Zemb, Hydrotropes, *Curr. Opin. Colloid Interface Sci.* 22 (2016) 99–107. <https://doi.org/10.1016/j.cocis.2016.03.005>.
- [58] P. Bauduin, A. Renoncourt, A. Kopf, D. Touraud, W. Kunz, Unified Concept of Solubilization in Water by Hydrotropes and Cosolvents, *Langmuir.* 21 (2005) 6769–6775. <https://doi.org/10.1021/la050554l>.
- [59] D. V. Dandekar, V.G. Gaikar, Hydrotropic Extraction of Curcuminoids from Turmeric, *Sep. Sci. Technol.* 38 (2003) 1185–1215. <https://doi.org/10.1081/SS-120018130>.
- [60] P. Degot, V. Huber, E. Hofmann, M. Hahn, D. Touraud, W. Kunz, Solubilization and extraction of curcumin from *Curcuma Longa* using green, sustainable, and food-approved surfactant-free microemulsions, *Food Chem.* (2020) 127660. <https://doi.org/10.1016/j.foodchem.2020.127660>.
- [61] P. Degot, V. Huber, A. El Maangar, J. Gramüller, L. Rohr, D. Touraud, T. Zemb, R.M. Gschwind, W. Kunz, Triple role of sodium salicylate in solubilization, extraction, and stabilization of curcumin from *Curcuma longa*, *J. Mol. Liq.* 329 (2021). <https://doi.org/10.1016/j.molliq.2021.115538>.
- [62] C.F. Chignell, P. Bilskj, K.J. Reszka, A.G. Motten, R.H. Sik, T.A. Dahl, SPECTRAL AND PHOTOCHEMICAL PROPERTIES OF CURCUMIN, *Photochem. Photobiol.* 59 (1994) 295–302. <https://doi.org/10.1111/j.1751-1097.1994.tb05037.x>.
- [63] H.H. Tønnesen, J. Karlsen, G.B. Henegouwen, Studies on curcumin and curcuminoids VIII. Photochemical stability of curcumin, *Z. Lebensm. Unters. Forsch.* 183 (1986) 116–122. <https://doi.org/10.1007/BF01041928>.
- [64] M. Kharat, Z. Du, G. Zhang, D.J. McClements, Physical and Chemical Stability of Curcumin in Aqueous Solutions and Emulsions: Impact of pH, Temperature, and Molecular Environment, *J. Agric. Food Chem.* 65 (2017) 1525–1532. <https://doi.org/10.1021/acs.jafc.6b04815>.
- [65] S. Mondal, S. Ghosh, S.P. Moulik, Stability of curcumin in different solvent and solution media: UV–visible and steady-state fluorescence spectral study, *J. Photochem. Photobiol. B Biol.* 158 (2016) 212–218. <https://doi.org/10.1016/j.jphotobiol.2016.03.004>.
- [66] Z. Chen, Y. Xia, S. Liao, Y. Huang, Y. Li, Y. He, Z. Tong, B. Li, Thermal degradation kinetics study

- of curcumin with nonlinear methods, *Food Chem.* 155 (2014) 81–86.
<https://doi.org/10.1016/j.foodchem.2014.01.034>.
- [67] M. Griesser, V. Pistis, T. Suzuki, N. Tejera, D.A. Pratt, C. Schneider, Autoxidative and Cyclooxygenase-2 Catalyzed Transformation of the Dietary Chemopreventive Agent Curcumin, *J. Biol. Chem.* 286 (2011) 1114–1124. <https://doi.org/10.1074/jbc.M110.178806>.
- [68] V.P. Menon, A.R. Sudheer, ANTIOXIDANT AND ANTI-INFLAMMATORY PROPERTIES OF CURCUMIN, in: *Mol. Targets Ther. Uses Curcumin Heal. Dis.*, Springer US, Boston, MA, n.d.: pp. 105–125. https://doi.org/10.1007/978-0-387-46401-5_3.
- [69] G.K. Jayaprakasha, L. Jaganmohan Rao, K.K. Sakariah, Antioxidant activities of curcumin, demethoxycurcumin and bisdemethoxycurcumin, *Food Chem.* 98 (2006) 720–724.
<https://doi.org/10.1016/j.foodchem.2005.06.037>.
- [70] G. Litwinienko, K.U. Ingold, Abnormal Solvent Effects on Hydrogen Atom Abstraction. 2. Resolution of the Curcumin Antioxidant Controversy. The Role of Sequential Proton Loss Electron Transfer, *J. Org. Chem.* 69 (2004) 5888–5896. <https://doi.org/10.1021/jo049254j>.
- [71] P. Degot, D. Funkner, V. Huber, M. Köglmaier, D. Touraud, W. Kunz, Extraction of curcumin from *Curcuma longa* using meglumine and pyroglutamic acid, respectively, as solubilizer and hydrotrope, *J. Mol. Liq.* 334 (2021) 1–45. <https://doi.org/10.1016/j.molliq.2021.116478>.
- [72] C. Aloisio, A. G. de Oliveira, M. Longhi, Cyclodextrin and Meglumine-Based Microemulsions as a Poorly Water-Soluble Drug Delivery System, *J. Pharm. Sci.* 105 (2016) 2703–2711.
<https://doi.org/10.1016/j.xphs.2015.11.045>.
- [73] C. Aloisio, S.G. Antimisiaris, M.R. Longhi, Liposomes containing cyclodextrins or meglumine to solubilize and improve the bioavailability of poorly soluble drugs, *J. Mol. Liq.* 229 (2017) 106–113. <https://doi.org/10.1016/j.molliq.2016.12.035>.
- [74] C. Aloisio, A.G. de Oliveira, M. Longhi, Solubility and release modulation effect of sulfamerazine ternary complexes with cyclodextrins and meglumine, *J. Pharm. Biomed. Anal.* 100 (2014) 64–73. <https://doi.org/10.1016/j.jpba.2014.07.008>.
- [75] L.F. Gonçalves-Oliveira, F. Souza-Silva, L.M. de Castro Côrtes, L.B. Veloso, B.A. Santini Pereira, L. Cysne-Finkelstein, G.C. Lechuga, S.C. Bourguignon, F. Almeida-Souza, K. da Silva Calabrese, V.F. Ferreira, C.R. Alves, The combination therapy of meglumine antimoniate and oxiranes (epoxy- α -lapachone and epoxy-methyl-lawsone) enhance the leishmanicidal effect in mice

- infected by *Leishmania (Leishmania) amazonensis*, *Int. J. Parasitol. Drugs Drug Resist.* 10 (2019) 101–108. <https://doi.org/10.1016/j.ijpddr.2019.08.002>.
- [76] P. Baiocco, G. Colotti, S. Franceschini, A. Ilari, Molecular Basis of Antimony Treatment in Leishmaniasis, *J. Med. Chem.* 52 (2009) 2603–2612. <https://doi.org/10.1021/jm900185q>.
- [77] T. Ishiguchi, S. Takahashi, Safety of Gadoterate Meglumine (Gd-DOTA) as a Contrast Agent for Magnetic Resonance Imaging, *Drugs R. D.* 10 (2010) 133–145. <https://doi.org/10.2165/11539140-000000000-00000>.
- [78] F. Laerum, Cytotoxic Effects of Six Angiographic Contrast Media on Human Endothelium in Culture, *Acta Radiol.* 28 (1987) 99–105. <https://doi.org/10.1177/028418518702800121>.
- [79] S. Marstein, E. Jellum, L. Eldjarn, The concentration of pyroglutamic acid (2-pyrrolidone-5-carboxylic acid) in normal and psoriatic epidermis, determined on a microgram scale by gas chromatography, *Clin. Chim. Acta.* 49 (1973) 389–395. [https://doi.org/10.1016/0009-8981\(73\)90237-4](https://doi.org/10.1016/0009-8981(73)90237-4).
- [80] A. Kumar, A.K. Bachhawat, Pyroglutamic acid: Throwing light on a lightly studied metabolite, *Curr. Sci.* 102 (2012) 288–297.
- [81] A. El Maangar, P. Degot, V. Huber, J. Causse, P. Berthault, D. Touraud, W. Kunz, T. Zemb, Pre-nucleation cluster formation upon ethyl acetate addition to an aqueous solution of an anionic hydrotrope, *J. Mol. Liq.* 310 (2020) 113240. <https://doi.org/10.1016/j.molliq.2020.113240>.
- [82] V. Huber, Formulation and Extraction of Natural Dyes with Surfactant-Free Microemulsions, University of Regensburg, 2019.
- [83] T. Buchecker, S. Krickl, R. Winkler, I. Grillo, P. Bauduin, D. Touraud, A. Pfitzner, W. Kunz, The impact of the structuring of hydrotropes in water on the mesoscale solubilisation of a third hydrophobic component, *Phys. Chem. Chem. Phys.* 19 (2017) 1806–1816. <https://doi.org/10.1039/C6CP06696H>.
- [84] H.H. Tønnesen, M. Másson, T. Loftsson, Studies of curcumin and curcuminoids. XXVII. Cyclodextrin complexation: Solubility, chemical and photochemical stability, *Int. J. Pharm.* 244 (2002) 127–135. [https://doi.org/10.1016/S0378-5173\(02\)00323-X](https://doi.org/10.1016/S0378-5173(02)00323-X).
- [85] P. Degot, V. Huber, D. Touraud, W. Kunz, Curcumin extracts from *Curcuma Longa* – Improvement of concentration, purity, and stability in food-approved and water-soluble surfactant-free microemulsions, *Food Chem.* 339 (2021) 1–30.

<https://doi.org/10.1016/j.foodchem.2020.128140>.

- [86] M. Levitt, M.F. Perutz, Aromatic rings act as hydrogen bond acceptors, *J. Mol. Biol.* 201 (1988) 751–754. [https://doi.org/10.1016/0022-2836\(88\)90471-8](https://doi.org/10.1016/0022-2836(88)90471-8).
- [87] L. Jakobek, Interactions of polyphenols with carbohydrates, lipids and proteins, *Food Chem.* 175 (2015) 556–567. <https://doi.org/10.1016/j.foodchem.2014.12.013>.
- [88] Y. Cai, S.H. Gaffney, T.H. Lilley, E. Haslam, Carbohydrate — Polyphenol Complexation, in: *Chem. Significance Condens. Tann.*, Springer US, Boston, MA, 1989: pp. 307–322. https://doi.org/10.1007/978-1-4684-7511-1_19.
- [89] C. Krämer, Löslichkeit und Stabilisierung von Kurkumin in Wasser und ternären Mischungen Triacetin/Ethanol/Wasser mit Meglumine, University of Regensburg, 2021.
- [90] E. Yamasaki, THE SUCCESSIVE STAGES OF THE HYDROLYSIS OF TRIACETIN., *J. Am. Chem. Soc.* 42 (1920) 1455–1468. <https://doi.org/10.1021/ja01452a020>.
- [91] G.K. Jayaprakasha, L. Jagan Mohan Rao, K.K. Sakariah, Improved HPLC Method for the Determination of Curcumin, Demethoxycurcumin, and Bisdemethoxycurcumin, *J. Agric. Food Chem.* 50 (2002) 3668–3672. <https://doi.org/10.1021/jf025506a>.
- [92] S. Revathy, S. Elumalai, M. Benny, B. Antony, Isolation , Purification and Identification of Curcuminoids from Turmeric (*Curcuma longa* L .) by Column Chromatography, *J. Exp. Sci.* 2 (2011) 21–25. jexpsciences.com/article/download/7767/3965..
- [93] A.M. Navarro, B. García, F.J. Hoyuelos, I.A. Peñacoba, J.M. Leal, Preferential Solvation in Alkan-1-ol/Alkylbenzoate Binary Mixtures by Solvatochromic Probes, *J. Phys. Chem. B.* 115 (2011) 10259–10269. <https://doi.org/10.1021/jp202019x>.
- [94] M. T. Baltazar, R. J. Dinis-Oliveira, J. A. Duarte, M. L. Bastos, F. Carvalho, Antioxidant Properties and Associated Mechanisms of Salicylates, *Curr. Med. Chem.* 18 (2011) 3252–3264. <https://doi.org/10.2174/092986711796391552>.
- [95] N.A. Shaath, Ultraviolet filters, *Photochem. Photobiol. Sci.* 9 (2010) 464. <https://doi.org/10.1039/b9pp00174c>.
- [96] I. Sathisaran, S.V. Dalvi, Crystal Engineering of Curcumin with Salicylic Acid and Hydroxyquinol as Coformers, *Cryst. Growth Des.* 17 (2017) 3974–3988. <https://doi.org/10.1021/acs.cgd.7b00599>.

- [97] F. Kerkel, D. Brock, D. Touraud, W. Kunz, Stabilisation of biofuels with hydrophilic, natural antioxidants solubilised by glycerol derivatives, *Fuel*. 284 (2021) 119055. <https://doi.org/10.1016/j.fuel.2020.119055>.
- [98] K. Roguz, M.K. Gallagher, E. Senden, Y. Bar-Lev, M. Lebel, R. Heliczzer, Y. Sapir, All the Colors of the Rainbow: Diversification of Flower Color and Intraspecific Color Variation in the Genus *Iris*, *Front. Plant Sci.* 11 (2020). <https://doi.org/10.3389/fpls.2020.569811>.
- [99] A.W. Meerow, Taxonomy and Phylogeny, in: R. Kamenetsky, H. Okubo (Eds.), *Ornam. Geophytes*, CRC Press, 2012: pp. 17–42.
- [100] C. Linnaeus, *Species Plantarum*, 1753.
- [101] W.R. Dykes, *The genus iris*, Cambridge University Press, 1913.
- [102] G.H.M. Lawrence, A reclassification of the genus *Iris*, s.n, 1953.
- [103] G.I. Rodionenko, *The genus iris L*, Academy of Sciences of the USSR, 1961.
- [104] B. Mathew, *The Iris*, B.T. Batsford Ltd, 1981.
- [105] R. Phillips, M. Rix, B. Mathew, *Bulbs*, Pan Books, 1989.
- [106] T. Weber, J. Jakše, B. Sladonja, D. Hruševar, N. Landeka, S. Brana, B. Bohanec, M. Milović, D. Vladović, B. Mitić, D. Poljuha, Molecular Study of Selected Taxonomically Critical Taxa of the Genus *Iris L.* from the Broader Alpine-Dinaric Area, *Plants*. 9 (2020) 1229. <https://doi.org/10.3390/plants9091229>.
- [107] M.M. Okba, P.M. Abdel Baki, A.E. Khaleel, M.M. El-Sherei, M.A. Salem, Discrimination of common *Iris* species from Egypt based on their genetic and metabolic profiling, *Phytochem. Anal.* 32 (2021) 172–182. <https://doi.org/10.1002/pca.2945>.
- [108] S. Jozghasemi, V. Rabiei, A. Soleymani, A. Khalighi, Karyotype analysis of seven *Iris* species native to Iran, *Caryologia*. (2016) 1–11. <https://doi.org/10.1080/00087114.2016.1239162>.
- [109] C.A. Wilson, Subgeneric classification in *Iris* re-examined using chloroplast sequence data, *Taxon*. 60 (2011) 27–35. <https://doi.org/10.1002/tax.601004>.
- [110] J.J. Taylor, A reclassification of *Iris* species bearing arillate seeds, in: *Proc. Biol. Soc. Washingt.* Vol. 89, Biological Society of Washington, 1976: pp. 411–420.
- [111] C. Linnæus, *Triandria monogynia Iris*, in: *Species Plantarum*, 1753: p. 38.

- [112] B. Roger, V. Jeannot, X. Fernandez, S. Cerantola, J. Chahboun, Characterisation and Quantification of Flavonoids in *Iris germanica* L. and *Iris pallida* Lam. Resinoids from Morocco, *Phytochem. Anal.* 23 (2012) 450–455. <https://doi.org/10.1002/pca.1379>.
- [113] J.B. Sharmeen, F.M. Mahomoodally, G. Zengin, F. Maggi, Essential Oils as Natural Sources of Fragrance Compounds for Cosmetics and Cosmeceuticals, *Molecules.* 26 (2021) 666. <https://doi.org/10.3390/molecules26030666>.
- [114] T. Höß, *Alternative Green Extraction Methods for Natural Products*, University of Regensburg, 2018.
- [115] B.S. Yousefsani, M. Boozari, K. Shirani, A. Jamshidi, M. Dadmehr, A review on phytochemical and therapeutic potential of *Iris germanica*, *J. Pharm. Pharmacol.* 73 (2021) 611–625. <https://doi.org/10.1093/jpp/rgab008>.
- [116] O. Mykhailenko, V. Kovalyov, T. Orlova, Chemical composition of the essential oil of several *Iris* species, *Thai J. Pharm. Sci.* 44 (2020) 179–185.
- [117] M. Flemming, METHOD FOR ARTIFICIAL AGEING OF IRIS RHIZOMES FOR ACCELERATED FORMATION OF IRON ISOMERS, EP 3 127 994 B1, 2018.
- [118] W. Kukula-Koch, E. Sieniawska, J. Widelski, O. Urjin, P. Głowniak, K. Skalicka-Woźniak, Major secondary metabolites of *Iris* spp., *Phytochem. Rev.* 14 (2015) 51–80. <https://doi.org/10.1007/s11101-013-9333-1>.
- [119] H. Wang, Y. Cui, C. Zhao, Flavonoids of the Genus *Iris* (Iridaceae), *Mini-Reviews Med. Chem.* 10 (2010) 643–661. <https://doi.org/10.2174/138955710791384027>.
- [120] J. Buckingham, V.R.N. Munasinghe, *Dictionary of Flavonoids with CD-ROM*, 2015. <https://doi.org/10.1201/b18170>.
- [121] Ø.M. Andersen, K.R. Markham, eds., *Chemistry, Biochemistry and Applications*, Taylor & F, CRC Press, 2006.
- [122] T. Iwashina, Contribution to Flower Colors of Flavonoids Including Anthocyanins: A Review, *Nat. Prod. Commun.* 10 (2015) 1934578X1501000. <https://doi.org/10.1177/1934578X1501000335>.
- [123] C.J. van der Kooij, J. Ollerton, The origins of flowering plants and pollinators, *Science* (80-.). 368 (2020) 1306–1308. <https://doi.org/10.1126/science.aay3662>.

- [124] H.M. Schaefer, G.D. Ruxton, Fatal attraction: Carnivorous plants roll out the red carpet to lure insects, *Biol. Lett.* 4 (2008) 153–155. <https://doi.org/10.1098/rsbl.2007.0607>.
- [125] Y. Manetas, Why some leaves are anthocyanic and why most anthocyanic leaves are red?, *Flora Morphol. Distrib. Funct. Ecol. Plants.* 201 (2006) 163–177. <https://doi.org/10.1016/j.flora.2005.06.010>.
- [126] E. Grotewold, The genetics and biochemistry of floral pigments, *Annu. Rev. Plant Biol.* 57 (2006) 761–780. <https://doi.org/10.1146/annurev.arplant.57.032905.105248>.
- [127] M.L. Falcone Ferreyra, S.P. Rius, P. Casati, Flavonoids: Biosynthesis, biological functions, and biotechnological applications, *Front. Plant Sci.* 3 (2012) 1–16. <https://doi.org/10.3389/fpls.2012.00222>.
- [128] L. Chalker-Scott, Environmental significance of anthocyanins in plant stress responses, *Photochem. Photobiol.* 70 (1999) 1–9. <https://doi.org/10.1111/j.1751-1097.1999.tb01944.x>.
- [129] B.A. Bohm, Intraspecific flavonoid variation, *Bot. Rev.* 53 (1987) 197–279. <https://doi.org/10.1007/BF02858524>.
- [130] P. Kaššák, Secondary metabolites of the chosen Genus *Iris* species, *Acta Univ. Agric. Silv. Mendeliana Brun.* 60 (2012) 269–280. <https://doi.org/10.11118/actaun201260080269>.
- [131] O. Mykhailenko, Z. Gudžinskas, V. Kovalyov, V. Desenko, L. Ivanauskas, I. Bezruk, V. Georgiyants, Effect of ecological factors on the accumulation of phenolic compounds in *Iris* species from Latvia, Lithuania and Ukraine, *Phytochem. Anal.* 31 (2020) 545–563. <https://doi.org/10.1002/pca.2918>.
- [132] K.L. Dhar, A.K. Kalla, A new isoflavone from *Iris germanica*, *Phytochemistry.* 12 (1973) 734–735. [https://doi.org/10.1016/S0031-9422\(00\)84481-7](https://doi.org/10.1016/S0031-9422(00)84481-7).
- [133] C. Schütz, M. Quitschau, M. Hamburger, O. Potterat, Profiling of isoflavonoids in *Iris germanica* rhizome extracts by microprobe NMR and HPLC-PDA-MS analysis, *Fitoterapia.* 82 (2011) 1021–1026. <https://doi.org/10.1016/j.fitote.2011.06.005>.
- [134] A.I. Foudah, M.S. Abdel-Kader, Isoflavonoids, *Flavonoids - From Biosynth. to Hum. Heal.* (2017). <https://doi.org/10.5772/intechopen.68701>.
- [135] T. Iwashina, T. Mizuno, Flavonoids and Xanthones From the Genus *Iris*: Phytochemistry, Relationships with Flower Colors and Taxonomy, and Activities and Function, *Nat. Prod.*

- Commun. 15 (2020). <https://doi.org/10.1177/1934578X20937151>.
- [136] T.K. Lim, *Iris x germanica*, in: *Edible Med. Non-Medicinal Plants*, Springer International Publishing, Cham, 2016: pp. 27–40. https://doi.org/10.1007/978-3-319-26062-4_2.
- [137] L. Hoang, F. Beneš, M. Fenclová, O. Kronusová, V. Švarcová, K. Řehořová, E. Baldassarre Švecová, M. Vosátka, J. Hajšlová, P. Kaštánek, J. Viktorová, T. Ruml, Phytochemical composition and in vitro biological activity of *iris* spp. (iridaceae): A new source of bioactive constituents for the inhibition of oral bacterial biofilms, *Antibiotics*. 9 (2020) 1–24. <https://doi.org/10.3390/antibiotics9070403>.
- [138] M. Albulescu, M. Popovici, Isoflavones - Biochemistry, pharmacology and therapeutic USE, *Rev. Roum. Chim.* 52 (2007) 537–550.
- [139] S.R.M. Ibrahim, G.A. Mohamed, M.F. Zayed, S.A. Ross, 8-Hydroxyirilone 5-methyl ether and 8-hydroxyirilone, new antioxidant and α -amylase inhibitors isoflavonoids from *Iris germanica* rhizomes, *Bioorg. Chem.* 70 (2017) 192–198. <https://doi.org/10.1016/j.bioorg.2016.12.010>.
- [140] J. Hummelova, J. Rondevaldova, A. Balastikova, O. Lapcik, L. Kokoska, The relationship between structure and in vitro antibacterial activity of selected isoflavones and their metabolites with special focus on antistaphylococcal effect of demethyltexasin, *Lett. Appl. Microbiol.* 60 (2015) 242–247. <https://doi.org/10.1111/lam.12361>.
- [141] A.P. Mukne, V. Viswanathan, A.G. Phadatare, Structure pre-requisites for isoflavones as effective antibacterial agents, *Pharmacogn. Rev.* 5 (2011) 13–18. <https://doi.org/10.4103/0973-7847.79095>.
- [142] L. Qiu, B. Lin, Z. Lin, Y. Lin, M. Lin, X. Yang, Biochanin A ameliorates the cytokine secretion profile of lipopolysaccharide-stimulated macrophages by a PPAR γ -dependent pathway, *Mol. Med. Rep.* 5 (2012) 217–222. <https://doi.org/10.3892/mmr.2011.599>.
- [143] B.A. Dar, S.H. Lone, W.A. Shah, K.A. Bhat, LC-MS Guided Isolation of Bioactive Principles from *Iris hookeriana* and Bioevaluation of Isolates for Antimicrobial and Antioxidant Activities, *Drug Res. (Stuttg)*. 66 (2016) 427–431. <https://doi.org/10.1055/s-0042-108337>.
- [144] R. Pereira, A.L. Pereira, M.M. Ferreira, R.O.S. Fontenelle, S. Saker-Sampaio, H.S. Santos, P.N. Bandeira, M.A. Vasconcelos, J.A.N. Queiroz, R. Braz-Filho, E.H. Teixeira, Evaluation of the antimicrobial and antioxidant activity of 7-hydroxy-4', 6-dimethoxy-isoflavone and essential oil from *myroxylon peruiferum* l.f, *An. Acad. Bras. Cienc.* 91 (2019) 1–13.

<https://doi.org/10.1590/0001-3765201920180204>.

- [145] D.C.G.A. Pinto, M.A.M. Simões, A.M.S. Silva, *Genista tridentata* L.: A Rich Source of Flavonoids with Anti-Inflammatory Activity, *Medicines*. 7 (2020) 31.
<https://doi.org/10.3390/medicines7060031>.
- [146] A. García-Lafuente, E. Guillamón, A. Villares, M.A. Rostagno, J.A. Martínez, Flavonoids as anti-inflammatory agents: Implications in cancer and cardiovascular disease, *Inflamm. Res.* 58 (2009) 537–552. <https://doi.org/10.1007/s00011-009-0037-3>.
- [147] K. Zaheer, M. Humayoun Akhtar, An updated review of dietary isoflavones: Nutrition, processing, bioavailability and impacts on human health, *Crit. Rev. Food Sci. Nutr.* 57 (2017) 1280–1293. <https://doi.org/10.1080/10408398.2014.989958>.
- [148] O.H. Franco, R. Chowdhury, J. Troup, T. Voortman, S. Kunutsor, M. Kavousi, C. Oliver-Williams, T. Muka, Use of Plant-Based Therapies and Menopausal Symptoms, *JAMA*. 315 (2016) 2554. <https://doi.org/10.1001/jama.2016.8012>.
- [149] P. Bedi, R. Gupta, R. Gupta, T. Pramanik, T. Pramanik, Synthesis and biological properties of pharmaceutically important xanthenes and benzoxanthone analogs: brief review, *Asian J. Pharm. Clin. Res.* 11 (2018) 12. <https://doi.org/10.22159/ajpcr.2018.v11i2.22426>.
- [150] L.M.M. Vieira, A. Kijjoa, Naturally-Occurring Xanthenes: Recent Developments, *Curr. Med. Chem.* 12 (2005) 2413–2446. <https://doi.org/10.2174/092986705774370682>.
- [151] V. Silano, C. Bolognesi, L. Castle, K. Chipman, J. Cravedi, K. Engel, P. Fowler, R. Franz, K. Grob, R. Gürtler, T. Husøy, S. Kärenlampi, M.R. Milana, K. Pfaff, G. Riviere, J. Srinivasan, M. de F. Tavares Poças, C. Tlustos, D. Wölfle, H. Zorn, R. Benigni, M. Binderup, L. Brimer, F. Marcon, D. Marzin, P. Mosesso, G. Mulder, A. Oskarsson, C. Svendsen, M. Anastassiadou, M. Carfi, S. Saarma, W. Mennes, Safety of benzophenone to be used as flavouring, *EFSA J.* 15 (2017). <https://doi.org/10.2903/j.efsa.2017.5013>.
- [152] F. Stenbäck, P. Shubik, Lack of toxicity and carcinogenicity of some commonly used cutaneous agents, *Toxicol. Appl. Pharmacol.* 30 (1974) 7–13. [https://doi.org/10.1016/0041-008X\(74\)90242-7](https://doi.org/10.1016/0041-008X(74)90242-7).
- [153] M.C. Rhodes, J.R. Bucher, J.C. Peckham, G.E. Kissling, M.R. Hejtmancik, R.S. Chhabra, Carcinogenesis studies of benzophenone in rats and mice, *Food Chem. Toxicol.* 45 (2007) 843–851. <https://doi.org/10.1016/j.fct.2006.11.003>.

- [154] D. NAKAJIMA, S. ASADA, S. KAGEYAMA, T. YAMAMOTO, H. KURAMOCHI, N. TANAKA, K. TAKEDA, S. GOTO, Activity Related to the Carcinogenicity of Plastic Additives in the Benzophenone Group, *J. UOEH.* 28 (2006) 143–156. <https://doi.org/10.7888/juoeh.28.143>.
- [155] EFSA, Scientific Opinion of EFSA prepared by the Panel on food contact materials, enzymes, flavourings and processing aids (CEF) on Toxicological evaluation of benzophenone, 2009. <https://doi.org/10.2903/j.efsa.2008.888>.
- [156] G. Bhat, A.S. Shahl, Z. Shah, M. Tantry, HPLC-DAD-ESI-MS/MS Identification and Characterization of Major Constituents of *Iris crocea*, *Iris germanica* and *Iris spuria* Growing in Kashmir Himalayas, India, *J. Anal. Bioanal. Tech.* 5 (2014). <https://doi.org/10.4172/2155-9872.1000223>.
- [157] C.A. Williams, J.B. Harborne, M. Colasante, Flavonoid and xanthone patterns in bearded *Iris* species and the pathway of chemical evolution in the genus, *Biochem. Syst. Ecol.* 25 (1997) 309–325. [https://doi.org/10.1016/S0305-1978\(97\)00008-2](https://doi.org/10.1016/S0305-1978(97)00008-2).
- [158] R.M.M. Crawford, D.A. Lindsay, J.C. Walton, B. Wollenweber-Ratzer, Towards the characterization of radicals formed in rhizomes of *Iris germanica*, *Phytochemistry.* 37 (1994) 979–985. [https://doi.org/10.1016/S0031-9422\(00\)89513-8](https://doi.org/10.1016/S0031-9422(00)89513-8).
- [159] A.Ž. Kostić, U.M. Gašić, M.B. Pešić, S.P. Stanojević, M.B. Barać, M.P. Mačukanović-Jocić, S.N. Avramov, Ž.L. Tešić, Phytochemical Analysis and Total Antioxidant Capacity of Rhizome, Above-Ground Vegetative Parts and Flower of Three *Iris* Species, *Chem. Biodivers.* 16 (2019) e1800565. <https://doi.org/10.1002/cbdv.201800565>.
- [160] E.W. Ades, F.J. Candal, R.A. Swerlick, V.G. George, S. Summers, D.C. Bosse, T.J. Lawley, HMEC-1: Establishment of an Immortalized Human Microvascular Endothelial Cell Line, *J. Invest. Dermatol.* 99 (1992) 683–690. <https://doi.org/10.1111/1523-1747.ep12613748>.
- [161] T. Mosmann, Rapid colorimetric assay for cellular growth and survival: Application to proliferation and cytotoxicity assays, *J. Immunol. Methods.* 65 (1983) 55–63. [https://doi.org/10.1016/0022-1759\(83\)90303-4](https://doi.org/10.1016/0022-1759(83)90303-4).
- [162] T. Thorburn, M. Aali, C. Lehmann, Immune response to systemic inflammation in the intestinal microcirculation, *Front. Biosci. - Landmark.* 23 (2018) 782–795. <https://doi.org/10.2741/4616>.
- [163] K. Ley, C. Laudanna, M.I. Cybulsky, S. Nourshargh, Getting to the site of inflammation: the leukocyte adhesion cascade updated, *Nat. Rev. Immunol.* 7 (2007) 678–689.

<https://doi.org/10.1038/nri2156>.

- [164] R.P. McEver, R.D. Cummings, Perspectives series: cell adhesion in vascular biology. Role of PSGL-1 binding to selectins in leukocyte recruitment., *J. Clin. Invest.* 100 (1997) 485–491. <https://doi.org/10.1172/JCI119556>.
- [165] E. Chavakis, E. Choi, T. Chavakis, Novel aspects in the regulation of the leukocyte adhesion cascade, *Thromb. Haemost.* 102 (2009) 191–197. <https://doi.org/10.1160/TH08-12-0844>.
- [166] A. van de Stolpe, P.T. van der Saag, Intercellular adhesion molecule-1, *J. Mol. Med.* 74 (1996) 13–33. <https://doi.org/10.1007/BF00202069>.
- [167] L. Rink, A. Kruse, H. Haase, *Immunologie für Einsteiger*, Spektrum Akademischer Verlag, Heidelberg, 2012. <https://doi.org/10.1007/978-3-8274-2440-2>.
- [168] K.A. Roebuck, A. Finnegan, Regulation of intercellular adhesion molecule-1 (CD54) gene expression, *J. Leukoc. Biol.* 66 (1999) 876–888. <https://doi.org/10.1002/jlb.66.6.876>.
- [169] M. Flemming, *Phytochemische, pharmakologische und chemoökologische Untersuchungen zu Sesquiterpenlactonen aus Kamille, Schafgarbe und Arnika*, (2014).
- [170] J.L. Luo, H. Kamata, M. Karin, IKK/NF- κ B signaling: Balancing life and death - A new approach to cancer therapy, *J. Clin. Invest.* 115 (2005) 2625–2632. <https://doi.org/10.1172/JCI26322>.
- [171] A.A. Beg, S.M. Ruben, R.I. Scheinman, S. Haskill, C.A. Rosen, A.S. Baldwin, I kappa B interacts with the nuclear localization sequences of the subunits of NF-kappa B: a mechanism for cytoplasmic retention., *Genes Dev.* 6 (1992) 1899–1913. <https://doi.org/10.1101/gad.6.10.1899>.
- [172] A.A. Beg, T.S. Finco, P. V Nantermet, A.S. Baldwin, Tumor necrosis factor and interleukin-1 lead to phosphorylation and loss of I kappa B alpha: a mechanism for NF-kappa B activation., *Mol. Cell. Biol.* 13 (1993) 3301–3310. <https://doi.org/10.1128/MCB.13.6.3301>.
- [173] A.A. Beg, A.S. Baldwin, The I kappa B proteins: multifunctional regulators of Rel/NF-kappa B transcription factors., *Genes Dev.* 7 (1993) 2064–2070. <https://doi.org/10.1101/gad.7.11.2064>.
- [174] S.P. Hehner, T.G. Hofmann, W. Dröge, M.L. Schmitz, The antiinflammatory sesquiterpene lactone parthenolide inhibits NF-kappa B by targeting the I kappa B kinase complex., *J. Immunol.* 163 (1999) 5617–23. <https://www.jimmunol.org/content/163/10/5617>.

- [175] A.. García-Piñeres, M.. Lindenmeyer, I. Merfort, Role of cysteine residues of p65/NF- κ B on the inhibition by the sesquiterpene lactone parthenolide and N-ethyl maleimide, and on its transactivating potential, *Life Sci.* 75 (2004) 841–856.
<https://doi.org/10.1016/j.lfs.2004.01.024>.
- [176] J. Iredell, Antimicrobial resistance, *Microbiol. Aust.* 40 (2019) 55–56.
<https://doi.org/10.1071/MA19016>.
- [177] H.D. Marston, D.M. Dixon, J.M. Knisely, T.N. Palmore, A.S. Fauci, Antimicrobial resistance, *JAMA - J. Am. Med. Assoc.* 316 (2016) 1193–1204. <https://doi.org/10.1001/jama.2016.11764>.
- [178] M. Balouiri, M. Sadiki, S.K. Ibensouda, Methods for in vitro evaluating antimicrobial activity: A review, *J. Pharm. Anal.* 6 (2016) 71–79. <https://doi.org/10.1016/j.jpha.2015.11.005>.
- [179] B.A. Byrne, Laboratory Diagnosis of Bacterial Infections, in: *Equine Infect. Dis.*, Elsevier, 2014: pp. 257-265.e1. <https://doi.org/10.1016/B978-1-4557-0891-8.00027-0>.
- [180] N.G. Heatley, A method for the assay of penicillin, *Biochem. J.* 38 (1944) 61–65.
<https://doi.org/10.1042/bj0380061>.
- [181] A.G. Al-Bakri, F.U. Afifi, Evaluation of antimicrobial activity of selected plant extracts by rapid XTT colorimetry and bacterial enumeration, *J. Microbiol. Methods.* 68 (2007) 19–25.
<https://doi.org/10.1016/j.mimet.2006.05.013>.
- [182] K. Winkelmann, J. Heilmann, O. Zerbe, T. Rali, O. Sticher, New phloroglucinol derivatives from *Hypericum papuanum*, *J. Nat. Prod.* 63 (2000) 104–108. <https://doi.org/10.1021/np990417m>.
- [183] H.C.J. Gram, C. Friedlaender, Ueber die isolirte Färbung der Schizomyceten : in Schnitt-und Trockenpräparaten, *Fortschritte der Medizin*, 2: 185-189, 1884.
- [184] M.J. Osborn, Structure and Biosynthesis of the Bacterial Cell Wall, *Annu. Rev. Biochem.* 38 (1969) 501–538. <https://doi.org/10.1146/annurev.bi.38.070169.002441>.
- [185] S.R.M. Ibrahim, G.A. Mohamed, N.M. Al-Musayeib, New constituents from the rhizomes of *Egyptian Iris germanica L.*, *Molecules.* 17 (2012) 2587–2598.
<https://doi.org/10.3390/molecules17032587>.
- [186] C.A. Winter, E.A. Risley, G.W. Nuss, Carrageenin-Induced Edema in Hind Paw of the Rat as an Assay for Antiinflammatory Drugs, *Exp. Biol. Med.* 111 (1962) 544–547.
<https://doi.org/10.3181/00379727-111-27849>.

- [187] A. Panthong, D. Kanjanapothi, P. Tuntiwachwuttikul, O. Pancharoen, V. Reutrakul, Antiinflammatory activity of flavonoids, *Phytomedicine*. 1 (1994) 141–144.
[https://doi.org/10.1016/S0944-7113\(11\)80032-2](https://doi.org/10.1016/S0944-7113(11)80032-2).
- [188] A.S. Tan, M. V. Berridge, Superoxide produced by activated neutrophils efficiently reduces the tetrazolium salt, WST-1 to produce a soluble formazan: A simple colorimetric assay for measuring respiratory burst activation and for screening anti-inflammatory agents, *J. Immunol. Methods*. 238 (2000) 59–68. [https://doi.org/10.1016/S0022-1759\(00\)00156-3](https://doi.org/10.1016/S0022-1759(00)00156-3).
- [189] J.M. McCord, R.S. Roy, The pathophysiology of superoxide: roles in inflammation and ischemia, *Can. J. Physiol. Pharmacol.* 60 (1982) 1346–1352. <https://doi.org/10.1139/y82-201>.
- [190] A.- Rahman, S. Nasim, I. Baig, S. Jalil, I. Orhan, B. Sener, M.I. Choudhary, Anti-inflammatory isoflavonoids from the rhizomes of *Iris germanica*, *J. Ethnopharmacol.* 86 (2003) 177–180.
[https://doi.org/10.1016/S0378-8741\(03\)00055-2](https://doi.org/10.1016/S0378-8741(03)00055-2).
- [191] R.C. Blantz, K. Munger, Role of Nitric Oxide in Inflammatory Conditions, *Nephron*. 90 (2002) 373–378. <https://doi.org/10.1159/000054723>.
- [192] P. Tripathi, P. Tripathi, L. Kashyap, V. Singh, The role of nitric oxide in inflammatory reactions, *FEMS Immunol. Med. Microbiol.* 51 (2007) 443–452. <https://doi.org/10.1111/j.1574-695X.2007.00329.x>.
- [193] C. Bogdan, Nitric oxide and the immune response, *Nat. Immunol.* 2 (2001) 907–916.
<https://doi.org/10.1038/ni1001-907>.
- [194] G.H. Wang, G.X. Zou, X.M. You, Y. Zhang, H. Jiang, F. Li, G.X. Li, Tectorigenin and irigenin inhibit lipopolysaccharide-induced nitric oxide synthase expression in murine macrophages, *Biomed. Res.* 28 (2017) 5412–5417.
- [195] A. Alam, M. Verma, K.K. Naik, D. Choudhary, S. Kumar, Anti - osteoporotic activity of isoflavones from *Iris germanica* targeting NF - kappaB, (2019).
<https://doi.org/10.4103/jphi.JPHI>.
- [196] A. Oeckinghaus, S. Ghosh, The NF- B Family of Transcription Factors and Its Regulation, *Cold Spring Harb. Perspect. Biol.* 1 (2009) a000034–a000034.
<https://doi.org/10.1101/cshperspect.a000034>.
- [197] A. Uzair, J. Bakht, A. Iqbal, K. Naveed, N. Ali, In vitro antimicrobial activities of different solvent extracted samples from *Iris germinica*., *Pak. J. Pharm. Sci.* 29 (2016) 145–50.

<http://www.ncbi.nlm.nih.gov/pubmed/26826828>.

- [198] S.H. Wani, A. Amin, M.A. Rather, J.A. Parray, Q. Parvaiz, R.A. Qadri, Antibacterial And Phytochemical Screening of Different Extracts of Five Iris Species Growing in Kashmir, *Phytochemistry*. 5 (2012) 3376–3378.
- [199] A.P. Desbois, V.J. Smith, Antibacterial free fatty acids: activities, mechanisms of action and biotechnological potential, *Appl. Microbiol. Biotechnol.* 85 (2010) 1629–1642. <https://doi.org/10.1007/s00253-009-2355-3>.
- [200] T. Watanabe, Y. Yamamoto, M. Miura, H. Konno, S. Yano, Y. Nonomura, Systematic analysis of selective bactericidal activity of fatty acids against staphylococcus aureus with minimum inhibitory concentration and minimum bactericidal concentration, *J. Oleo Sci.* 68 (2019) 291–296. <https://doi.org/10.5650/jos.ess18220>.
- [201] T. Kitahara, N. Koyama, J. Matsuda, Y. Aoyama, Y. Hirakata, S. Kamihira, S. Kohno, M. Nakashima, H. Sasaki, Antimicrobial activity of saturated fatty acids and fatty amines against methicillin-resistant Staphylococcus aureus, *Biol. Pharm. Bull.* 27 (2004) 1321–1326. <https://doi.org/10.1248/bpb.27.1321>.
- [202] J.J. Kabara, D.M. Swieczkowski, A.J. Conley, J.P. Truant, Fatty acids and derivatives as antimicrobial agents., *Antimicrob. Agents Chemother.* 2 (1972) 23–28. <https://doi.org/10.1128/AAC.2.1.23>.
- [203] K.F. Devienne, M.S.G. Raddi, Screening for antimicrobial activity of natural products using a microplate photometer, *Brazilian J. Microbiol.* 33 (2002) 166–168. <https://doi.org/10.1590/S1517-83822002000200014>.
- [204] Y.P. Chen, M.Y. Tsao, S.H. Lee, C.H. Chou, H.J. Tsai, Prevalence and molecular characterization of chloramphenicol resistance in *Riemerella anatipestifer* isolated from ducks and geese in Taiwan, *Avian Pathol.* 39 (2010) 333–338. <https://doi.org/10.1080/03079457.2010.507761>.
- [205] C. Bruckschlegel, Characterization of various aqueous extracts of the rhizomes and roots of *Iris germanica* L., University of Regensburg, 2019.

6 Appendix

6.1 Compositions used for the DLS experiment with H₂O/EtOH or DiA/TriA

Table S 1: Different compositions used for the DLS experiment.

H ₂ O (wt%)	EtOH (wt%)	TriA (wt%)	DiA (wt%)
0	40	60	0
5	38	57	0
15	34	51	0
30	28	42	0
40	24	36	0
0	0	40	60
5	0	38	57
15	0	34	51
25	0	30	45

6.2 Calibration curves of the three curcuminoids

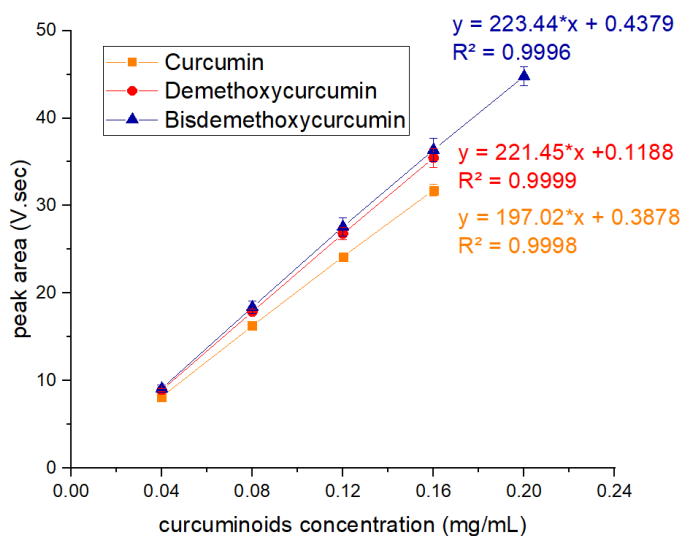


Figure S 1: Calibration curves of the three different curcuminoids in acetonitrile (curcumin: orange square, demethoxycurcumin: red circle, bisdemethoxycurcumin: blue triangle) obtained via HPLC [60].

6.3 Compositions used for the extraction procedure with H₂O/EtOH or DiA/TriA

Table S 2: Compositions used for the extraction experiments with H₂O/EtOH or DiA/TriA.

H2O (wt%)	EtOH (wt%)	TriA (wt%)	DiA (wt%)
0	100	0	0
0	0	100	0
0	0	0	100
20	80	0	0
0	40	60	0
5	38	57	0
15	34	51	0
30	28	42	0
40	24	36	0
0	0	40	60
5	0	38	57
15	0	34	51
25	0	30	45

6.4 Second calibration curves of the three curcuminoids

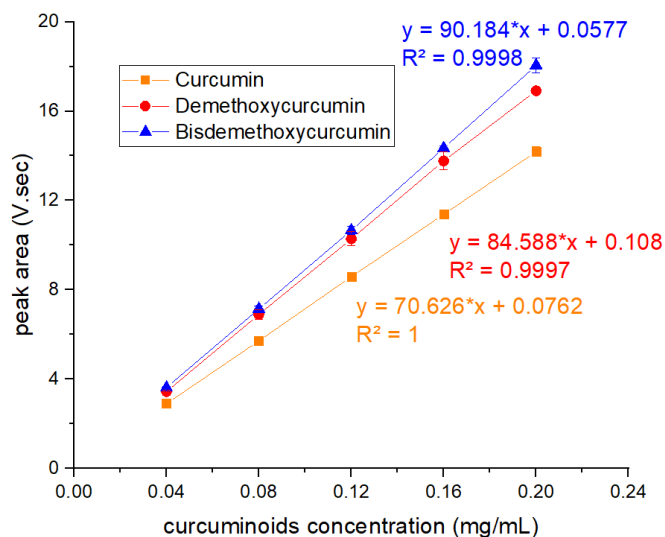


Figure S 2: New calibration curves of the three different curcuminoids in acetonitrile (curcumin: orange square, demethoxycurcumin: red circle, bisdemethoxycurcumin: blue triangle) obtained via HPLC [71].

6.5 Compositions for the extraction experiments with meglumine

Table S 3: Compositions of the extraction mixtures with different concentrations of meglumine in water at different pH.

The water used in the ternary extraction mixture contained 5 wt% of meglumine (water/meglumine 95/5). The pH of the water/meglumine mixture is regulated with addition of PCA. $R_{pH\ 7}$ and $R_{pH\ 9}$ are the mole ratio PCA/meglumine for the pH 7 and 9 respectively.			
H ₂ O with additives (wt%)	EtOH (wt%)	TriA (wt%)	pH of the water with additives
5	38	57	7 with meglumine and PCA, $R_{pH\ 7} = 0.88$
15	34	51	
30	28	42	
40	24	36	
5	38	57	9 with meglumine and PCA, $R_{pH\ 9} = 0.92$
15	34	51	
30	28	42	
40	24	36	
5	38	57	11.3 with only meglumine
15	34	51	
30	28	42	
40	24	36	
The water used in the ternary extraction mixture contained 15 wt% of meglumine (water/meglumine 85/15). The pH of the water/meglumine mixture is regulated with addition of PCA. $R_{pH\ 7}$ and $R_{pH\ 9}$ are the mole ratio PCA/meglumine for the pH 7 and 9 respectively.			
0	65	35	7 with meglumine and PCA, $R_{pH\ 7} = 0.82$
5	61	34	
15	51	34	
30	38	32	
40	30	30	
0	65	35	9 with meglumine and PCA, $R_{pH\ 9} = 0.85$
5	61	34	
15	51	34	
30	38	32	
40	30	30	
5	38	57	11.5 with only meglumine
15	34	51	
30	28	42	
40	24	36	

6.6 Compositions for the stability of curcumin in the phase diagram with meglumine with and without PCA

Table S 4: Compositions of the investigated solutions for the stability of curcumin in the ternary phase diagram H₂O/EtOH/TriA containing meglumine with and without PCA in the water phase.

H ₂ O with additives (wt%)	EtOH (wt%)	TriA (wt%)	Additives: wt% of meglumine	pH of the water with additives
15	51	34	15 wt%	9 R _{pH 9} = 0.85
15	51	34	without additives	5.5
40	24	36	15 wt%	11.5
40	24	36	5 wt%	11.3
40	24	36	5 wt%	9 R _{pH 9} = 0.92
40	24	36	without additives	5.5
40	24	36	0 wt%	11.5 with NaOH

6.7 Compositions for all experiments in the ternary phase diagram H₂O/NaSal/EtOAc

Table S 5: Investigated compositions for the determination of the curcumin solubility map, the extraction procedure, the stability experiments and the determination of the oxygen content in the phase diagram H₂O/NaSal/EtOAc. The parameters that were examined at the specific compositions are marked with X.

EtOAc(wt%)	NaSal (wt%)	H ₂ O (wt%)	Solubility	Extraction	Stability	Oxygen content
27	40	33	X			
20	30	50	X			
17	25	58	X			
14	20	66	X			
10	15	75	X			
3.5	5	91.5	X			
38	37	25	X			
33	37	30	X			
25	37	38	X			
13	37	50	X			
8	37	55	X			
3	37	60	X			
0	37	63	X			
0	50	50	X	X	X	X
10	45	45	X	X	X	X
30	35	35	X	X	X	X

49	26	24	X	X	X	X
70	15	15	X		X	X
100	0	0	X	X	X	X
60	20	20	X			
63	19	18	X			
66	17	17	X			
70	15	15	X			
73	13	14	X			
76	12	12	X		X	X
80	10	10	X			
83	8	9	X		X	X
88	6	6	X		X	X
90	5	5	X			
92	4	4	X		X	X
96	2	2	X		X	X
0	0	100	X			
58	21	21	X			
55	22.5	22.5	X			
52.5	23.5	24	X			
47.5	26.5	26	X			
45	27.5	27.5	X			
42.5	28.5	29	X			
40	30	30	X			
71	12	17	X	X		
60	26	14	X	X		
70	19.5	10.5	X	X		
80	13	7	X	X		
96	0	4			X	
96	2	2			X	
99.9	0.05	0.05			X	

6.8 Curcuminoid extraction yields

Table S 6: Curcuminoid extraction yields with varying *C. longa* to extraction mixture ratio and of the investigated SFME compositions, extraction solvents, and the reference extraction mixture EtOH/H₂O 80/20 (in weight). All the given ratios are in weight percent.

<i>C. longa</i> to extraction mixture ratios/Extraction mixtures or solvents	Curcumin (mg/g)	Demethoxycurcumin (mg/g)	Bisdemethoxycurcumin (mg/g)
1:2	6.44 ± 0.22	2.06 ± 0.07	1.54 ± 0.05
1:3	6.59 ± 0.78	2.07 ± 0.26	1.54 ± 0.26
1:4	8.54 ± 0.14	2.69 ± 0.06	2.11 ± 0.05
1:5	8.89 ± 0.14	2.78 ± 0.03	2.19 ± 0.05
1:6	9.24 ± 0.03	2.91 ± 0.03	2.30 ± 0.02
1:7	9.26 ± 0.13	2.91 ± 0.06	2.04 ± 0.02
Soxhlet	11.64 ± 0.70	3.82 ± 0.21	1.67 ± 0.26
TriA/EtOH 60/40	8.82 ± 0.11	2.78 ± 0.04	2.19 ± 0.04
TriA/EtOH/H ₂ O 57/38/5	8.98 ± 0.16	2.85 ± 0.04	2.29 ± 0.04
TriA/EtOH/ H ₂ O 51/34/15	8.97 ± 0.21	2.97 ± 0.07	2.58 ± 0.10
TriA/EtOH/ H ₂ O 42/28/30	8.96 ± 0.25	3.07 ± 0.09	2.83 ± 0.06
TriA/EtOH/ H ₂ O 36/24/40	9.21 ± 0.32	3.18 ± 0.23	2.89 ± 0.38
TriA/DiA 40/60	7.19 ± 0.13	2.25 ± 0.04	1.67 ± 0.06
TriA/DiA/ H ₂ O 38/57/5	7.54 ± 0.06	2.36 ± 0.02	1.81 ± 0.01
TriA/DiA/ H ₂ O 34/51/15	6.97 ± 0.28	2.42 ± 0.11	2.15 ± 0.10
TriA/DiA/ H ₂ O 30/45/25	7.1 ± 0.34	2.42 ± 0.11	2.32 ± 0.14
EtOH	4.34 ± 0.08	1.34 ± 0.05	0.92 ± 0.04
DiA	7.41 ± 0.04	2.28 ± 0.02	1.61 ± 0.01
TriA	3.13 ± 0.21	0.94 ± 0.06	0.51 ± 0.06
EtOH/H ₂ O 80/20	4.36 ± 0.14	1.43 ± 0.05	1.03 ± 0.10

6.9 Preliminary test for the enrichment procedure

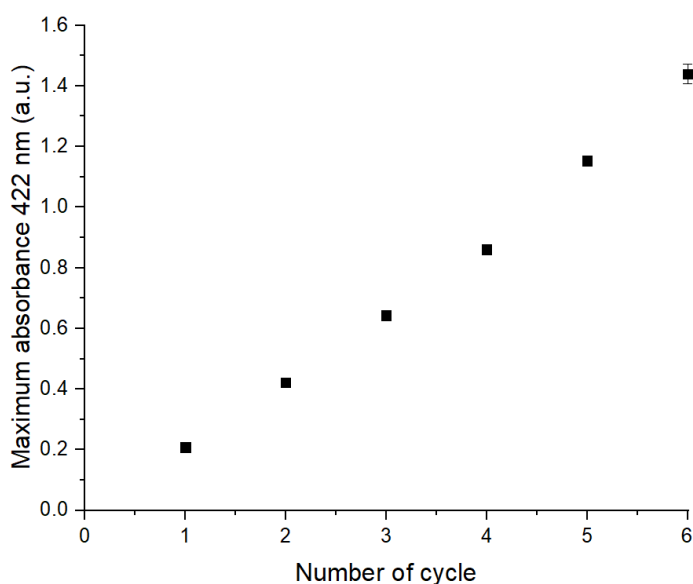


Figure S 3: Proof of concept for the cycle extraction of the curcuminoids from *C. longa* examined via UV/Vis [82].

6.10 Detailed curcuminoid content after each extraction cycle

Table S 7: Detailed curcuminoid content for different water contents for both weight ratios after each extraction cycle.

<i>C. longa</i> to binary or SFME extraction system/cycle number	Water content in the SFME extraction system (wt%)	Curcumin (mg in the SFME extraction system)	Demethoxycurcumin (mg in the SFME extraction system)	Bisdemethoxycurcumin (mg in the SFME extraction system)
<i>Extraction cycle</i>	1 to 16			
1	0	17.97 ± 0.56	5.74 ± 0.18	3.16 ± 0.15
	5	20.80 ± 0.19	7.10 ± 0.06	5.06 ± 0.04
	15	21.75 ± 0.46	6.69 ± 1.22	5.72 ± 0.20
	30	21.85 ± 1.39	7.69 ± 0.46	6.30 ± 0.48
	40	21.82 ± 0.53	7.70 ± 0.20	6.42 ± 0.18
2	0	38.28 ± 0.44	12.44 ± 0.16	9.06 ± 0.17
	5	38.27 ± 0.51	12.27 ± 0.21	8.57 ± 0.05
	15	41.82 ± 2.58	14.36 ± 0.98	12.33 ± 0.86
	30	51.20 ± 3.91	17.95 ± 1.40	16.64 ± 1.49
	40	40.27 ± 0.64	14.29 ± 0.38	13.28 ± 0.37
3	0	57.9 ± 0.5	18.91 ± 0.11	14.54 ± 0.20
	5	58.36 ± 2.36	18.77 ± 0.64	14.09 ± 0.47
	15	62.48 ± 0.72	21.34 ± 0.18	19.11 ± 0.36
	30	59.18 ± 1.62	20.75 ± 0.36	20.1 ± 0.59
	40	53.86 ± 4.48	19.02 ± 1.66	18.39 ± 1.67
4	0	72.72 ± 0.71	23.52 ± 0.24	18.14 ± 0.11
	5	74.06 ± 0.53	24.31 ± 0.38	19.31 ± 0.16
	15	77.72 ± 1.22	26.38 ± 0.45	24.19 ± 0.41
	30	68.38 ± 1.56	24.23 ± 0.67	23.25 ± 0.23
	40	52.47 ± 5.64	18.53 ± 1.97	17.9 ± 2.11
<i>Extraction cycle</i>	1 to 24			
1	0	19.27 ± 0.19	6.15 ± 0.08	3.42 ± 0.04
	5	22.99 ± 0.52	8 ± 0.22	6.3 ± 0.29
	15	23.26 ± 0.21	8.24 ± 0.09	6.45 ± 0.08
	30	24.45 ± 0.5	8.69 ± 0.23	7.22 ± 0.22
	40	24.54 ± 0.22	8.82 ± 0.06	7.4 ± 0.12
2	0	39.86 ± 0.1	12.84 ± 0.01	9.03 ± 0.05
	5	44.31 ± 0.85	14.87 ± 0.36	12.45 ± 0.63
	15	46.22 ± 0.54	15.94 ± 0.22	13.73 ± 0.34
	30	48.07 ± 0.77	17.05 ± 0.32	15.65 ± 0.33

	40	47.89 ± 1.31	17.00 ± 0.39	15.86 ± 0.53
3	0	59.1 ± 0.11	18.97 ± 0.11	14.5 ± 0.14
	5	65.11 ± 0.44	21.66 ± 0.18	18.37 ± 0.23
	15	68.8 ± 0.44	23.66 ± 0.16	20.97 ± 0.13
	30	69.14 ± 0.76	24.57 ± 0.32	23.66 ± 0.3
	40	68.69 ± 0.96	24.35 ± 0.35	23.75 ± 0.28
4	0	79.47 ± 0.27	25.5 ± 0.11	20.55 ± 0.03
	5	82.7 ± 0.69	27.5 ± 0.24	23.42 ± 0.53
	15	88.52 ± 0.64	30.28 ± 0.19	27.5 ± 0.31
	30	86.63 ± 0.98	30.81 ± 0.5	30.57 ± 0.39
	40	87.21 ± 2.28	30.96 ± 0.87	30.25 ± 0.85

6.11 Average loss of extraction system after each extraction cycle

Table S 8: Average loss of extraction system for every water content for both ratios after each extraction cycle [85].

<i>C. longa</i> to binary or SFME extraction system	Average loss of extraction system after each extraction cycle (g)				
	0 wt% H ₂ O	5 wt% H ₂ O	15 wt% H ₂ O	30 wt% H ₂ O	40 wt% H ₂ O
1 to 16	2.0	2.0	3.1	4.4	5.2
1 to 24	2.1	2.8	3.1	4.0	4.3

6.12 Detailed curcuminoid content after different purification processes

Table S 9: Detailed curcuminoid content of the different extracts (TriA/EtOH/ H₂O 36/24/40 in weight and TriA/EtOH/ H₂O 17.5/32.5/50 in weight as SFME extraction system) without and after the different purification processes: steam distillation, vacuum distillation, and lyophilisation.

SFME composition (w/w/w)	Purification process	Curcumin (mg/g)	Demethoxycurcumin (mg/g)	Bisdemethoxycurcumin (mg/g)
TriA/EtOH/ H ₂ O 36/24/40	Steam distillation	5.92 ± 0.23	2.14 ± 0.05	1.32 ± 0.06
TriA/EtOH/ H ₂ O 36/24/40	Without steam distillation	11.50 ± 0.45	4.04 ± 0.17	3.32 ± 0.20
TriA/EtOH/ H ₂ O 36/24/40	Vacuum distillation	9.5 ± 0.72	3.38 ± 0.24	1.65 ± 0.28

TriA/EtOH/ H ₂ O 36/24/40	Without vacuum distillation	10.68 ± 0.39	3.83 ± 0.11	2.25 ± 0.19
TriA/EtOH/ H ₂ O 17.5/32.5/50	Vacuum distillation	8.94 ± 0.67	3.30 ± 0.25	1.53 ± 0.21
TriA/EtOH/ H ₂ O 17.5/32.5/50	Without vacuum distillation	10.85 ± 0.36	3.93 ± 0.16	2.42 ± 0.16
TriA/EtOH/ H ₂ O 36/24/40	Without lyophilisation	9.23 ± 0.49	3.24 ± 0.19	2.96
	Lyophilisation/ 3 times freeze drying	9.35 ± 0.13	3.28 ± 0.03	2.97
	Lyophilisation/ 4 times freeze drying	9.1 ± 0.27	3.22 ± 0.10	2.94
	Lyophilisation/ 5 times freeze drying	7.92 ± 0.09	2.71 ± 0.03	2.37
	Lyophilisation/ 7 times freeze drying	7.84 ± 0.25	2.73 ± 0.08	2.28
TriA/EtOH/ H ₂ O 17.5/32.5/50	Without lyophilisation	9.46 ± 0.09	3.32 ± 0.02	3.03 ± 0.02
	Lyophilisation/ 3 times freeze drying	9.28 ± 0.31	3.24 ± 0.11	2.93 ± 0.12
	Lyophilisation/ 5 times freeze drying	7.58 ± 0.34	2.65 ± 0.09	2.28 ± 0.08
	Lyophilisation/ 7 times freeze drying	8.18 ± 0.55	2.82 ± 0.19	2.49 ± 0.20

6.13 Pictures of the precipitate after dilution of the extract solution with water



Figure S 4: Pictures of the precipitate of the three different diluted extracts after three days at day light. The turmeric powder *C. longa* was freeze dried 4, 5 and 6 times (from the left to the right) before extraction [85].



Figure S 5: Pictures of the precipitate of the three different extracts after thirty days at day light. The turmeric powder *C. longa* was freeze dried 4, 5 and 6 times (from the left to the right) before extraction [85].

6.14 Kinetic measurement

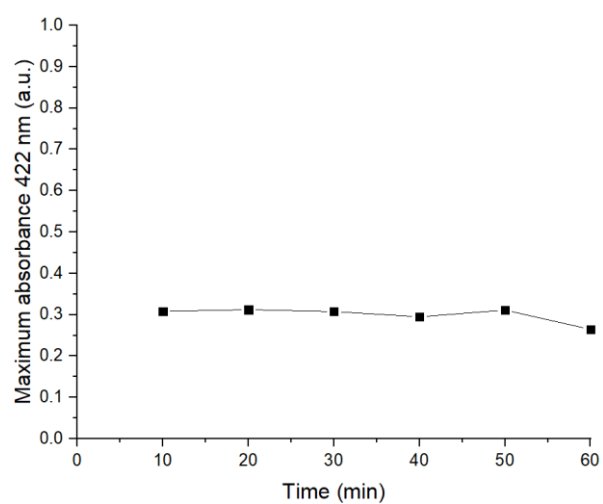


Figure S 6: Maximum absorbance at 422 nm after a defined agitation time of a solution containing 5 wt% of meglumine in water (95 wt%) with 150 mg of curcumin [89].

6.15 Detailed $^1\text{H-NMR}$ spectra of curcumin and meglumine

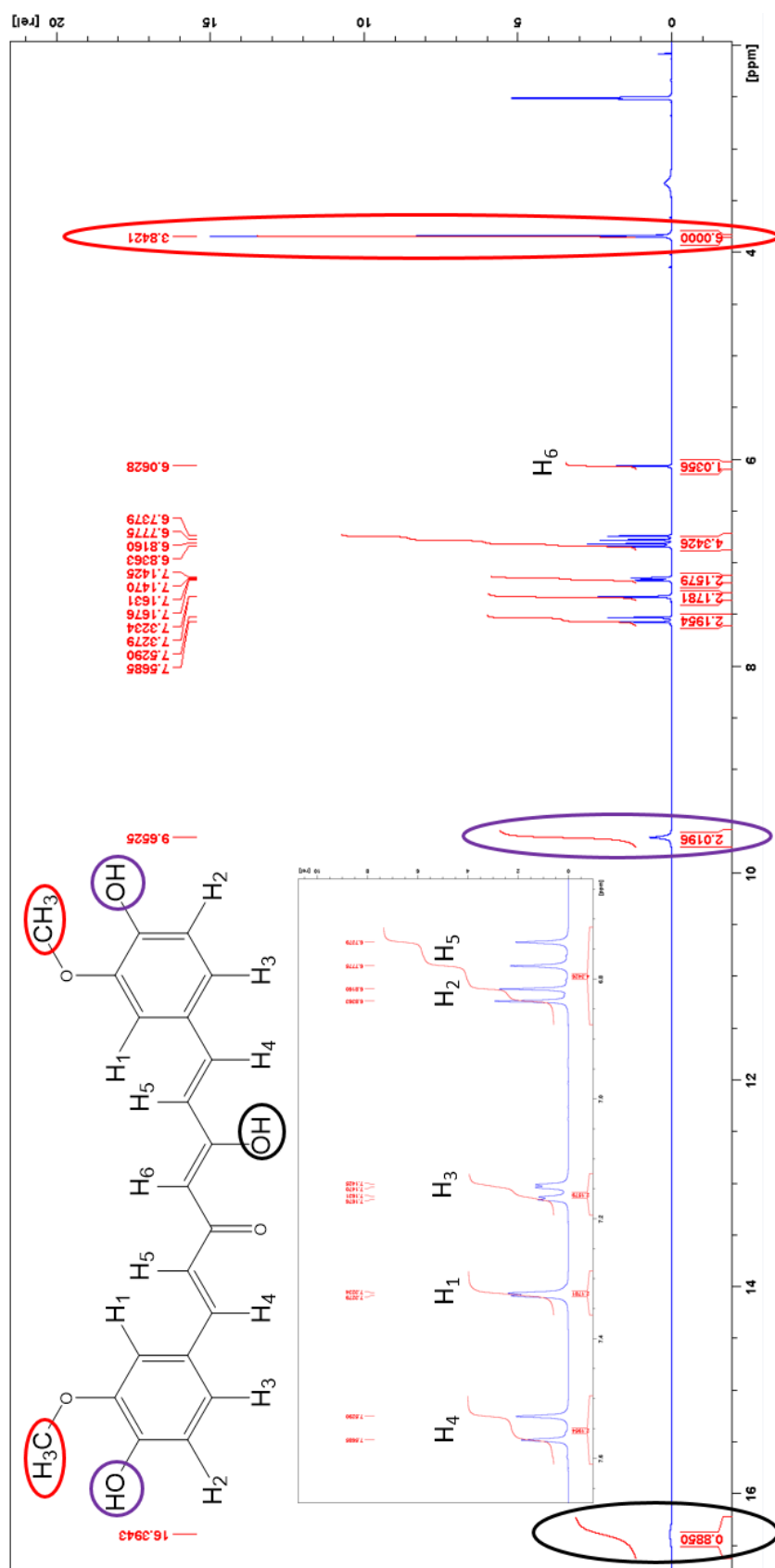


Figure S 7: Detailed $^1\text{H-NMR}$ spectrum of curcumin in DMSO-d_6 . The area between 7.6 and 6.8 ppm has been zoomed.

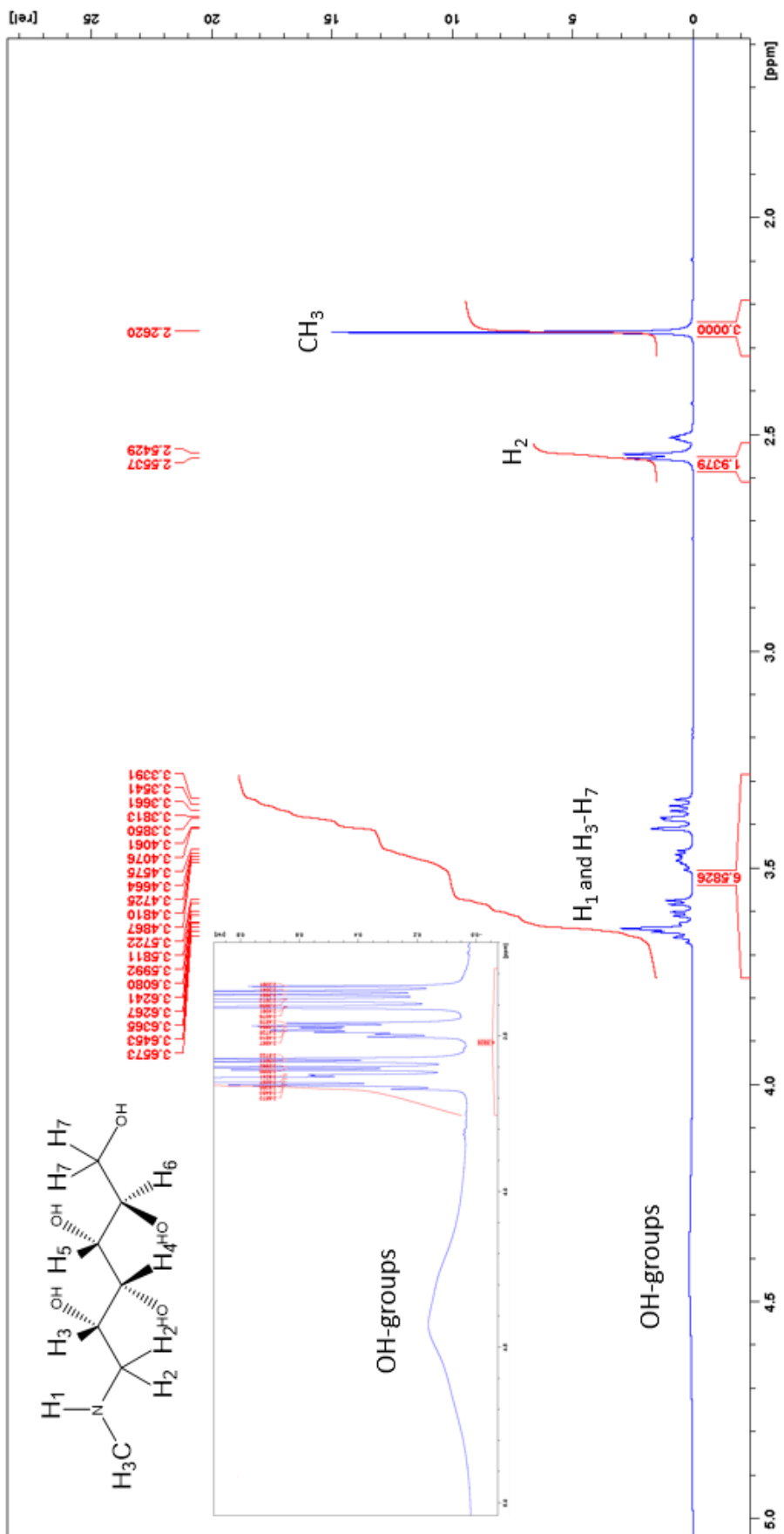


Figure S 8: Detailed ^1H -NMR spectrum of meglumine in DMSO-d_6 . The area between 5.0 and 4.0 ppm has been zoomed.

6.16 ROESY meglumine/curcumin 1/2

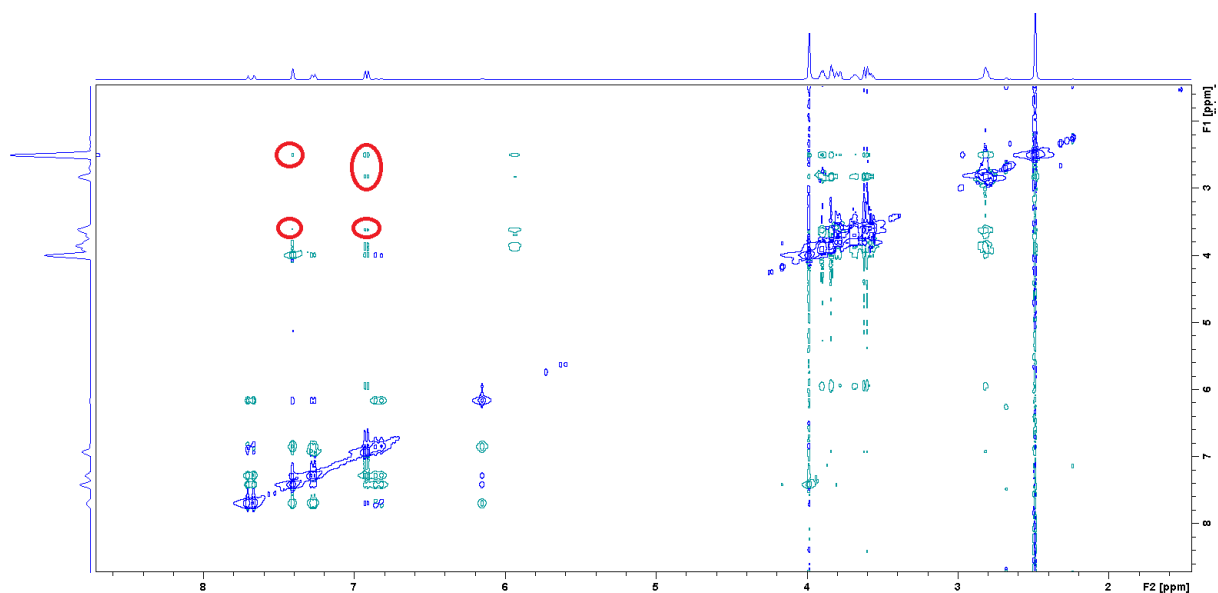


Figure S 9: 2D- ROESY-spectrum of the mixture meglumine/curcumin 2/1 in mol in DMSO- d_6 . The red circles show the cross peaks between the aromatic proton of curcumin and the proton of the sugar-chain and of the methyl group of meglumine.

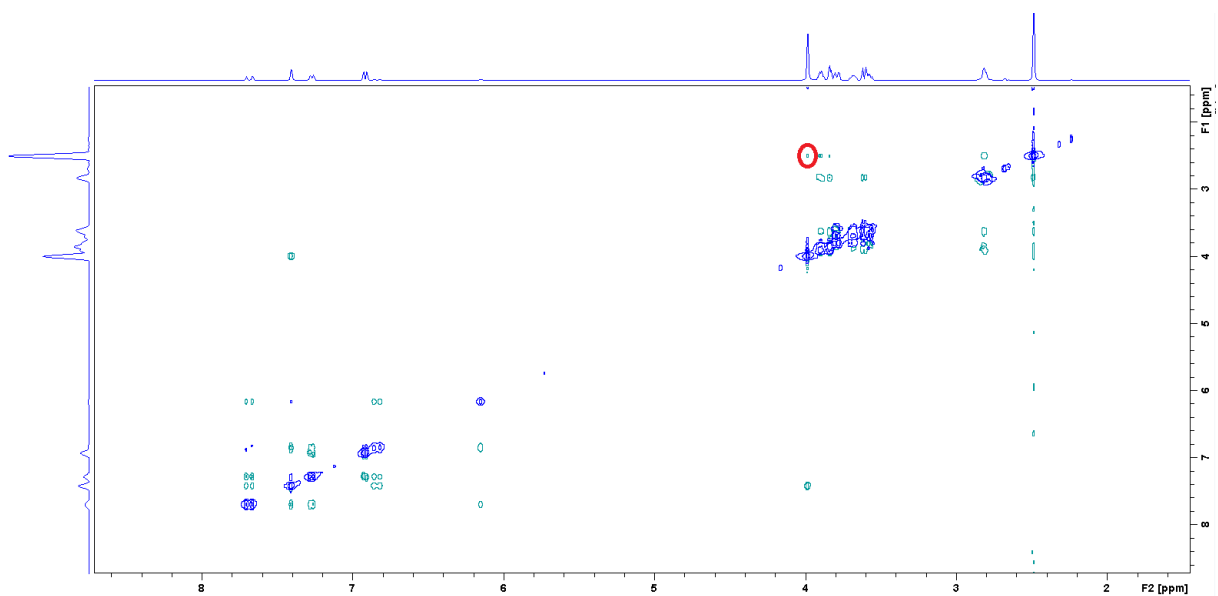


Figure S 10: 2D- ROESY-spectrum of the mixture meglumine/curcumin 2/1 in mol in DMSO- d_6 . The red circle shows the cross peak between the methoxy group of curcumin and the methyl group of meglumine.

6.17 Determination of the pK_a of meglumine

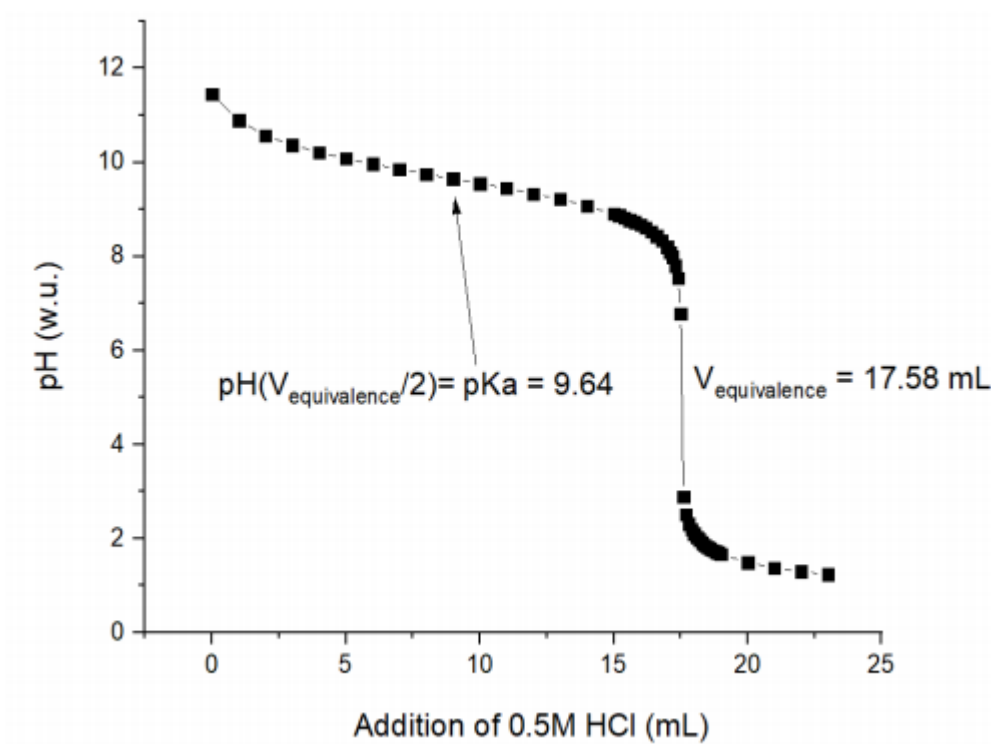


Figure S 11: Titration curve of an aqueous solution of meglumine (15 wt% of meglumine) with a hydrogen chloride solution (0.5 mol/L) to determine the pK_a of meglumine [71].

6.18 Viscosity measurement

Table S 10: Viscosity of different extraction systems with water with and without meglumine and PCA at different pH [71].

Extraction system			Viscosity η (mPa.s)
Composition TriA/EtOH/H ₂ O (w/w/w)	Additives in water	pH	
0/0/100	15 wt% meglumine	11.5	1.55
0/0/100	5 wt% meglumine	11.3	1.05
60/40/0	without additives	n.a.	2.21
36/24/40	without additives	5.5	2.90
36/24/40	15 wt% meglumine	11.5	3.87
30/30/40	15 wt% meglumine with PCA ($R_{pH\ 9} = 0.85$)	9	3.88
30/30/40	15 wt% meglumine with PCA ($R_{pH\ 7} = 0.91$)	7	4.10
36/24/40	5 wt% meglumine	11.3	3.19
36/24/40	5 wt% meglumine with PCA ($R_{pH\ 9} = 0.82$)	9	3.32
36/24/40	5 wt% meglumine with PCA ($R_{pH\ 7} = 0.88$)	7	3.38

6.19 Precipitation of curcumin



Figure S 12: Precipitation of curcumin in the samples 4 and 5 after two days (samples with the SFME composition with 5 wt% of meglumine as additive in water, on the left) and in the sample 5 after one day (sample with the SFME composition with 15 wt% of meglumine as additive in water, on the right) [89].

6.20 Precipitation of curcumin and bisdemethoxycurcumin

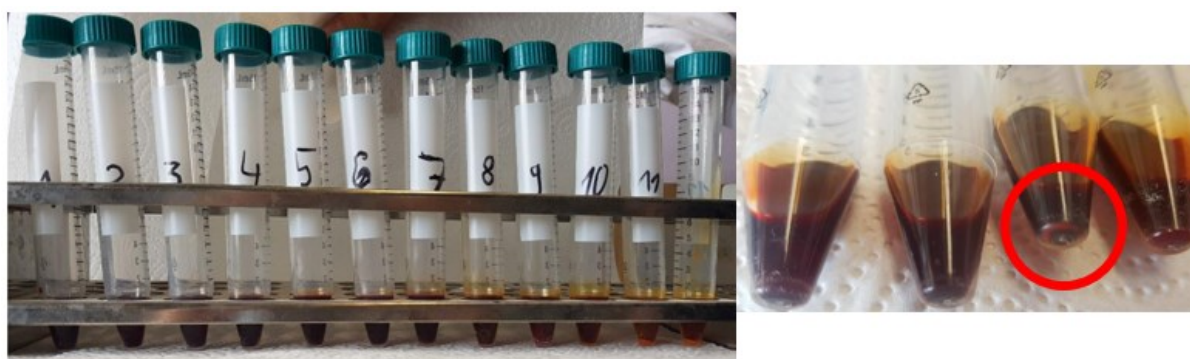


Figure S 13: Picture of the centrifuge tubes for the investigation of the pH of precipitation of curcumin (left). On the right is a precise picture of the tubes 5, 6, 7, and 8 (from the left to the right). The red circle indicates the tube where the precipitation of curcumin has started (here tube 7) [89].

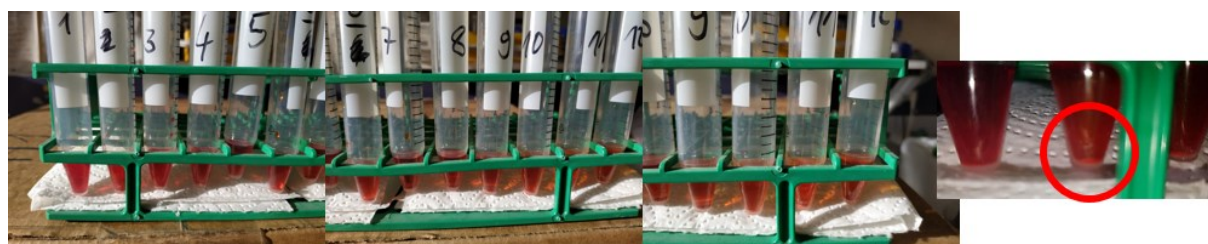


Figure S 14: Picture of the centrifuge tubes for the investigation of the pH of precipitation of bisdemethoxycurcumin (left). On the right is a precise picture of the tubes 1, 2, and 3 (from the left to the right). The red circle indicates the tube where the precipitation of curcumin has started (hear tube 2) [89].

6.21 Total of curcuminoids extracted with different additives in water

[71]

Table S 11: Total of the different curcuminoids extracted from *C. longa* with varying amount of water in the SFME extraction system with 5 and 15 wt% of meglumine in pure water at different pH (7, 9, 11.3 and 11.5) and with NaOH at pH 11.2.

The water used in the ternary extraction mixture contained 5 wt% of meglumine (water/meglumine 95/5). The pH of the water/meglumine mixture is regulated with addition of PCA. $R_{pH 7}$ and $R_{pH 9}$ are the mole ratio PCA/meglumine for the pH 7 and 9 respectively.				
Water content (with additives) in the extraction mixture (wt%)	Curcumin (mg/g <i>C. longa</i>)	Demethoxycurcumin (mg/g <i>C. longa</i>)	Bisdemethoxycurcumin (mg/g <i>C. longa</i>)	pH of the water with additives (meglumine, PCA)
5	8.98 ± 0.16	2.85 ± 0.04	2.29 ± 0.04	< 7 without meglumine and PCA, reference system [60]
15	8.97 ± 0.21	2.97 ± 0.07	2.58 ± 0.10	
30	8.96 ± 0.25	3.07 ± 0.09	2.83 ± 0.06	
40	9.21 ± 0.32	3.18 ± 0.34	2.89 ± 0.38	
5	8.95 ± 0.06	2.67 ± 0.02	2.21 ± 0.02	7 with meglumine and PCA, $R_{pH 7} = 0.88$
15	9.25 ± 0.23	2.91 ± 0.07	2.69 ± 0.07	
30	7.88 ± 0.26	2.57 ± 0.09	2.58 ± 0.09	
40	5.54 ± 0.98	1.77 ± 0.34	1.81 ± 0.34	
5	10.84 ± 0.07	3.26 ± 0.03	2.7 ± 0.03	9 with meglumine and PCA, $R_{pH 9} = 0.92$
15	11.12 ± 0.21	3.50 ± 0.07	3.18 ± 0.06	
30	10.44 ± 0.35	3.42 ± 0.12	3.38 ± 0.11	
40	9.31 ± 0.07	3.04 ± 0.03	3.03 ± 0.02	
5	10.23 ± 0.48	3.08 ± 0.15	2.59 ± 0.12	11.3 with only meglumine
15	10.16 ± 0.20	3.17 ± 0.07	2.87 ± 0.05	
30	9.74 ± 0.60	3.20 ± 0.20	3.17 ± 0.19	
40	8.55 ± 0.15	2.79 ± 0.06	2.8 ± 0.06	
The water used in the ternary extraction mixture contained 15 wt% of meglumine (water/meglumine 85/15). The pH of the water/meglumine mixture is regulated with addition of PCA. $R_{pH 7}$ and $R_{pH 9}$ are the mole ratio PCA/meglumine for the pH 7 and 9 respectively.				
Water content (with additives) in the extraction mixture (wt%)	Curcumin (mg/g <i>C. longa</i>)	Demethoxycurcumin (mg/g <i>C. longa</i>)	Bisdemethoxycurcumin (mg/g <i>C. longa</i>)	pH of the water with additives (meglumine, PCA)
5	8.98 ± 0.16	2.85 ± 0.04	2.29 ± 0.04	< 7 without meglumine and PCA,
15	8.97 ± 0.21	2.97 ± 0.07	2.58 ± 0.10	
30	8.96 ± 0.25	3.07 ± 0.09	2.83 ± 0.06	

40	9.21 ± 0.32	3.18 ± 0.34	2.89 ± 0.38	reference system [60]
5	9.69 ± 0.33	2.9 ± 0.1	2.38 ± 0.09	7 with meglumine and PCA, R _{pH} ₇ = 0.82
15	10.06 ± 0.18	3.12 ± 0.06	2.77 ± 0.05	
30	8.53 ± 0.15	2.77 ± 0.05	2.76 ± 0.05	
40	6.01 ± 0.63	1.92 ± 0.22	1.96 ± 0.21	
5	11.19 ± 0.21	3.38 ± 0.08	2.81 ± 0.07	9 with meglumine and PCA, R _{pH} ₉ = 0.85
15	10.94 ± 0.20	3.4 ± 0.07	3.01 ± 0.07	
30	9.39 ± 0.21	3.04 ± 0.08	3.01 ± 0.07	
40	8.04 ± 0.63	2.60 ± 0.22	2.60 ± 0.22	
5	11.7 ± 0.19	3.58 ± 0.06	3.02 ± 0.05	11.5 with only meglumine
15	11.09 ± 0.17	3.52 ± 0.06	3.22 ± 0.05	
30	9.72 ± 0.54	3.21 ± 0.19	3.22 ± 0.18	
40	8.07 ± 0.15	2.64 ± 0.05	2.66 ± 0.04	
The water used in the ternary extraction mixture contains NaOH as additive at pH 11.2				
Water content (with additive) in the extraction mixture (wt%)	Curcumin (mg/g <i>C. longa</i>)	Demethoxycurcumin (mg/g <i>C. longa</i>)	Bisdemethoxycurcumin (mg/g <i>C. longa</i>)	pH of the water with additive
5	10.03 ± 0.37	2.89 ± 0.11	2.47 ± 0.08	11.2 with NaOH
15	10.55 ± 0.10	3.07 ± 0.03	2.69 ± 0.17	
30	10.05 ± 0.03	3.04 ± 0.01	3.06 ± 0.01	
40	8.03 ± 0.18	2.41 ± 0.06	2.46 ± 0.05	

6.22 Detailed curcuminoid extraction efficiencies for the SFME H₂O/NaSal/EtOAc

Table S 12: Detailed curcuminoid extraction efficiencies for the investigation of the best *C. longa* to SFME extraction system weight ratio at the composition of the critical point and for the extraction at different SFME composition [61].

<i>C. longa</i> to SFME extraction system (in weight)	Curcumin (mg/g <i>C. longa</i>)	Demethoxycurcumin (mg/g <i>C. longa</i>)	Bisdemethoxycurcumin (mg/g <i>C. longa</i>)
1 to 3	1.17 ± 0.28	0.14 ± 0.09	0.28 ± 0.09
1 to 4	5.16 ± 0.13	1.42 ± 0.04	1.57 ± 0.04
1 to 5	5.60 ± 0.49	1.56 ± 0.16	1.72 ± 0.15
1 to 6	7.01 ± 0.51	2.00 ± 0.16	2.18 ± 0.16
1 to 10	9.34 ± 0.66	2.75 ± 0.21	2.91 ± 0.22
1 to 15	11.56 ± 0.22	3.15 ± 0.08	3.52 ± 0.09
1 to 20	11.48 ± 0.85	3.15 ± 0.30	3.56 ± 0.32
Soxhlet	11.64 ± 0.70	3.82 ± 0.21	1.67 ± 0.26
SFME extraction system H ₂ O/NaSal/EtOAc (w/w/w)	Curcumin (mg/g <i>C. longa</i>)	Demethoxycurcumin (mg/g <i>C. longa</i>)	Bisdemethoxycurcumin (mg/g <i>C. longa</i>)
50/50/0	n.d.	n.d.	n.d.
35/35/30	6.87 ± 0.77	2.00 ± 0.25	2.17 ± 0.25
25/25/50	9.02 ± 0.58	2.69 ± 0.19	2.87 ± 0.19
17/12/71	9.38 ± 0.51	2.80 ± 0.17	2.97 ± 0.17
0/0/100	10.45 ± 0.04	2.77 ± 0.04	2.35 ± 0.06
14/26/60	9.08 ± 0.16	2.59 ± 0.05	2.57 ± 0.05
10.5/19.5/70	9.25 ± 0.71	2.83 ± 0.47	2.50 ± 0.15
7/13/80	9.93 ± 0.87	2.82 ± 0.27	2.73 ± 0.25

6.23 Free energy of extraction and excess chemical potential

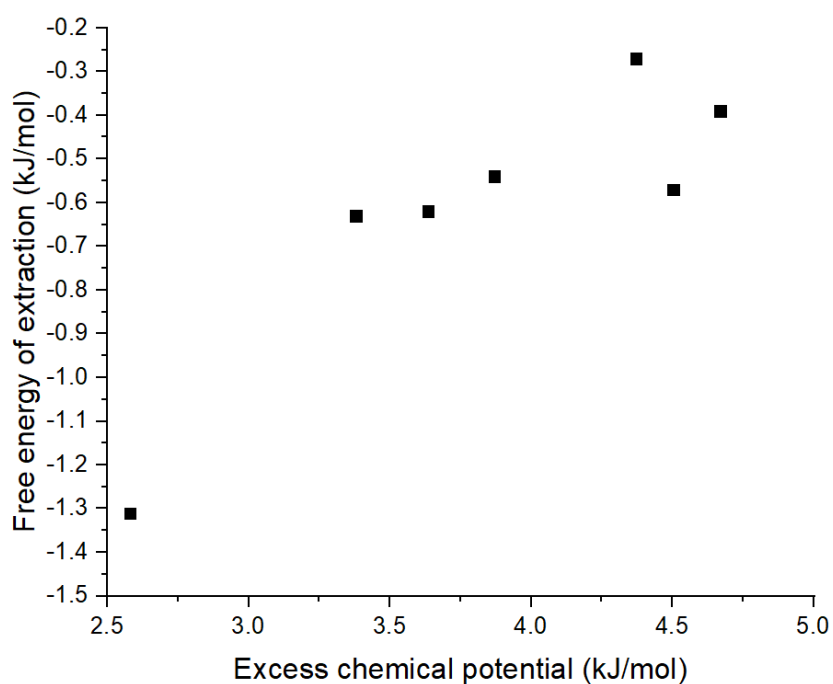


Figure S 15: Correlation between the free energy of extraction and the excess of chemical potential (both in kJ/mol) [61].

6.24 DOSY and SAXS experiments

Table S 13: Self-diffusion coefficients of water, EtOAc, and NaSal at the end of the three different tie-lines with and without curcumin. W indicates the water-rich phase at the left end of the tie-lines and O indicates the oil-rich phase at the right end of the tie-lines [61].

Without Curcumin				With Curcumin			
Self-diffusion coefficient D_i [m^2/s]							
Sample	H ₂ O	EtOAc	NaSal	H ₂ O	EtOAc	NaSal	Curcumin
A8C1 W	$1.17 \cdot 10^{-9}$	$5.81 \cdot 10^{-10} \pm 7.25 \cdot 10^{-12}$	$3.48 \cdot 10^{-10} \pm 4.16 \cdot 10^{-12}$	$1.14 \cdot 10^{-9}$	$5.68 \cdot 10^{-10} \pm 9.39 \cdot 10^{-13}$	$3.32 \cdot 10^{-10} \pm 1.01 \cdot 10^{-12}$	n.d.
A8C2 W	$1.39 \cdot 10^{-9}$	$5.68 \cdot 10^{-10} \pm 2.76 \cdot 10^{-12}$	$4.00 \cdot 10^{-10} \pm 7.44 \cdot 10^{-12}$	$1.48 \cdot 10^{-9}$	$5.88 \cdot 10^{-10} \pm 2.96 \cdot 10^{-12}$	$4.13 \cdot 10^{-10} \pm 1.00 \cdot 10^{-11}$	n.d.
A8C3 W	$1.66 \cdot 10^{-9}$	$5.91 \cdot 10^{-10} \pm 1.83 \cdot 10^{-12}$	$4.62 \cdot 10^{-10} \pm 2.63 \cdot 10^{-11}$	$1.53 \cdot 10^{-9}$	$6.05 \cdot 10^{-10} \pm 4.68 \cdot 10^{-12}$	$4.54 \cdot 10^{-10} \pm 1.74 \cdot 10^{-13}$	n.d.
A8C1 O	$3.17 \cdot 10^{-9}$	$2.85 \cdot 10^{-9} \pm 6.77 \cdot 10^{-11}$	$9.33 \cdot 10^{-10} \pm 1.05 \cdot 10^{-11}$	$3.45 \cdot 10^{-9}$	$2.71 \cdot 10^{-9} \pm 5.24 \cdot 10^{-11}$	$9.05 \cdot 10^{-10} \pm 5.59 \cdot 10^{-12}$	$8.69 \cdot 10^{-10} \pm 2.38 \cdot 10^{-12}$
A8C2 O	$3.39 \cdot 10^{-9}$	$2.81 \cdot 10^{-9} \pm 5.68 \cdot 10^{-11}$	$1.03 \cdot 10^{-9} \pm 1.73 \cdot 10^{-11}$	$3.22 \cdot 10^{-9}$	$2.73 \cdot 10^{-9} \pm 5.36 \cdot 10^{-11}$	$1.07 \cdot 10^{-9} \pm 1.57 \cdot 10^{-11}$	$8.97 \cdot 10^{-10} \pm 4.08 \cdot 10^{-12}$
A8C3 O	$3.41 \cdot 10^{-9}$	$2.87 \cdot 10^{-9} \pm 7.73 \cdot 10^{-11}$	$1.20 \cdot 10^{-9} \pm 2.64 \cdot 10^{-11}$	$3.33 \cdot 10^{-9}$	$2.70 \cdot 10^{-9} \pm 4.64 \cdot 10^{-11}$	$1.03 \cdot 10^{-9} \pm 4.87 \cdot 10^{-12}$	$8.63 \cdot 10^{-10} \pm 3.08 \cdot 10^{-12}$

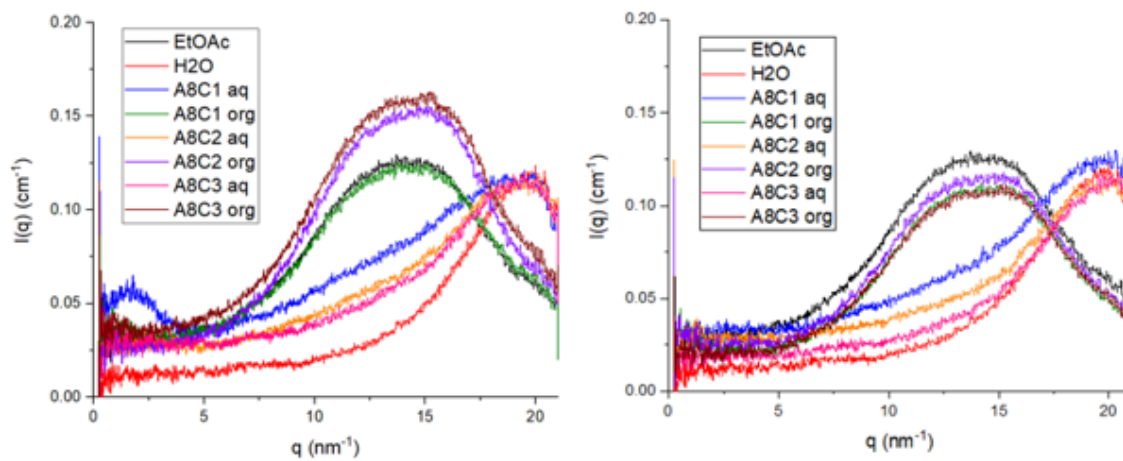


Figure S 16: SAXS measurements at the end of the three different tie-lines with (right) and without (left) curcumin [61].

6.25 GC-MS chromatograms

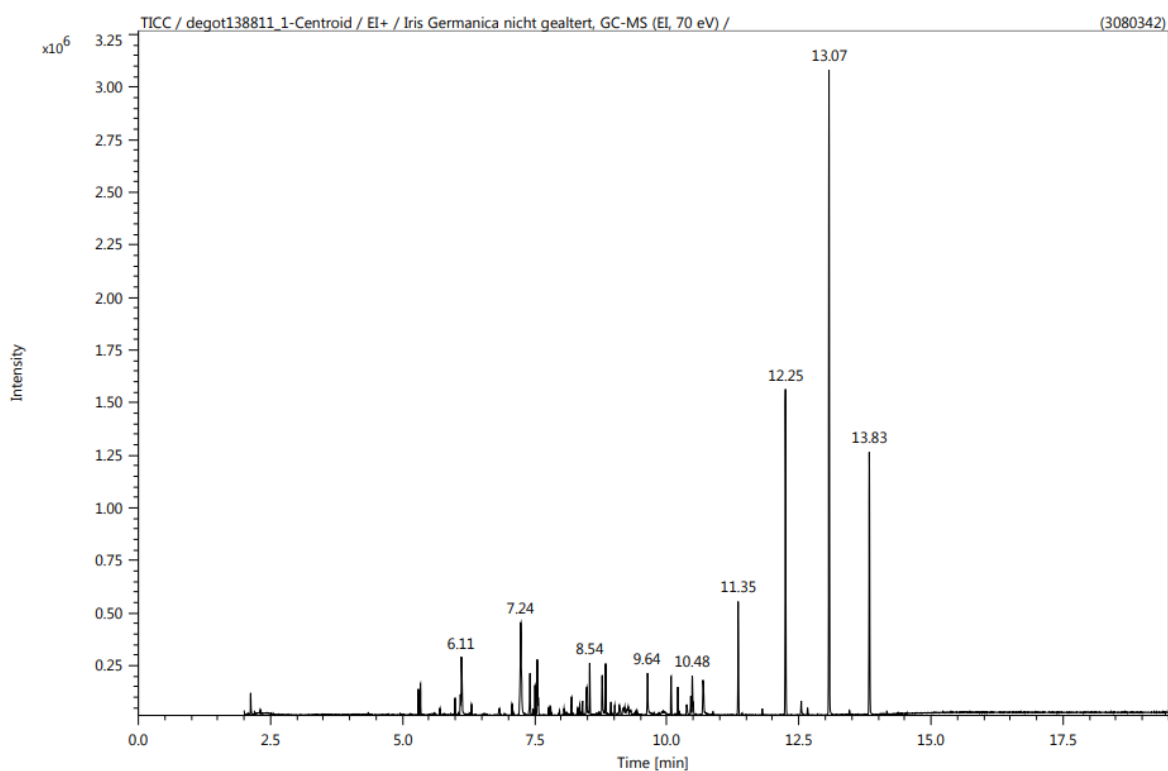
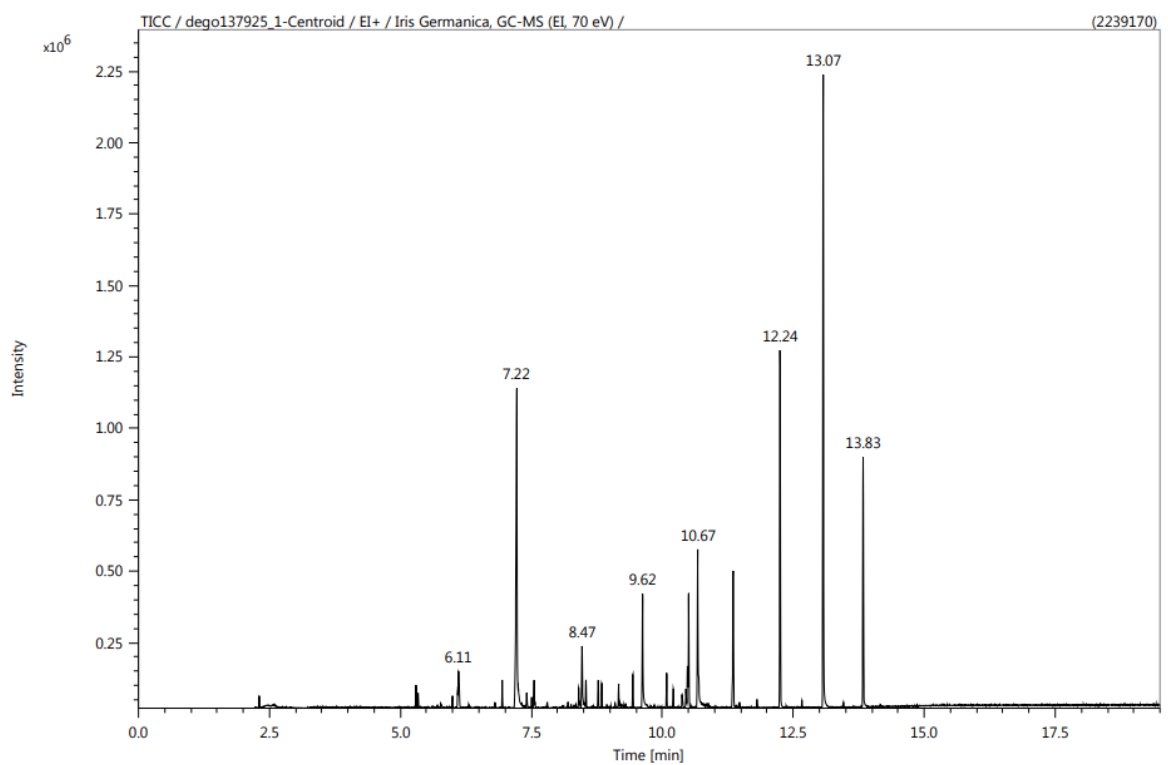


Figure S 17: GC-chromatograms of the aged root's butter (1919a (see Figure 53 in section 4.2.2.4), top) and the fresh root's butter (1919 (see Figure 53 in section 4.2.2.4), bottom) of *Iris germanica* L..

6.26 TLC plates of 18I1, 18I2, and 18I3

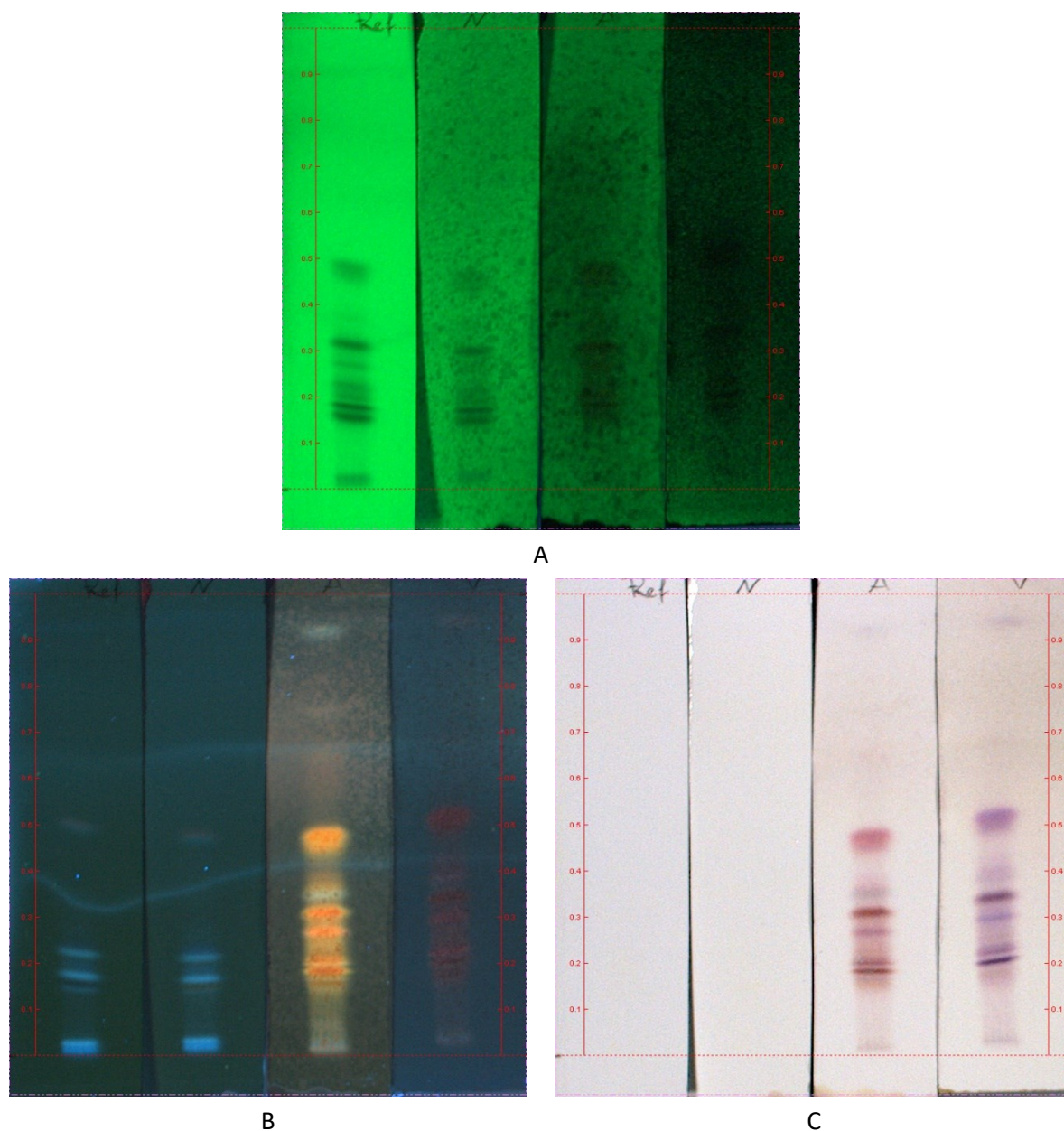


Figure S 18: TLC plates of 18I1 (DCM extract of the fresh rhizomes of *Iris germanica* L.; see Figure 54 in section 4.2.2.4) after derivatisation with N, AA and V (see section 2.2.2) under UV-light at 254 nm (A), at 366 nm (B) and white light (C). The four spots from the left to the right for every plate correspond to: 18I1 without derivatisation, 18I1 derivatised with N, with AA and with V. Mobile phase for every plate: TLC_1 (see Table 16 in section 4.2.2.5).

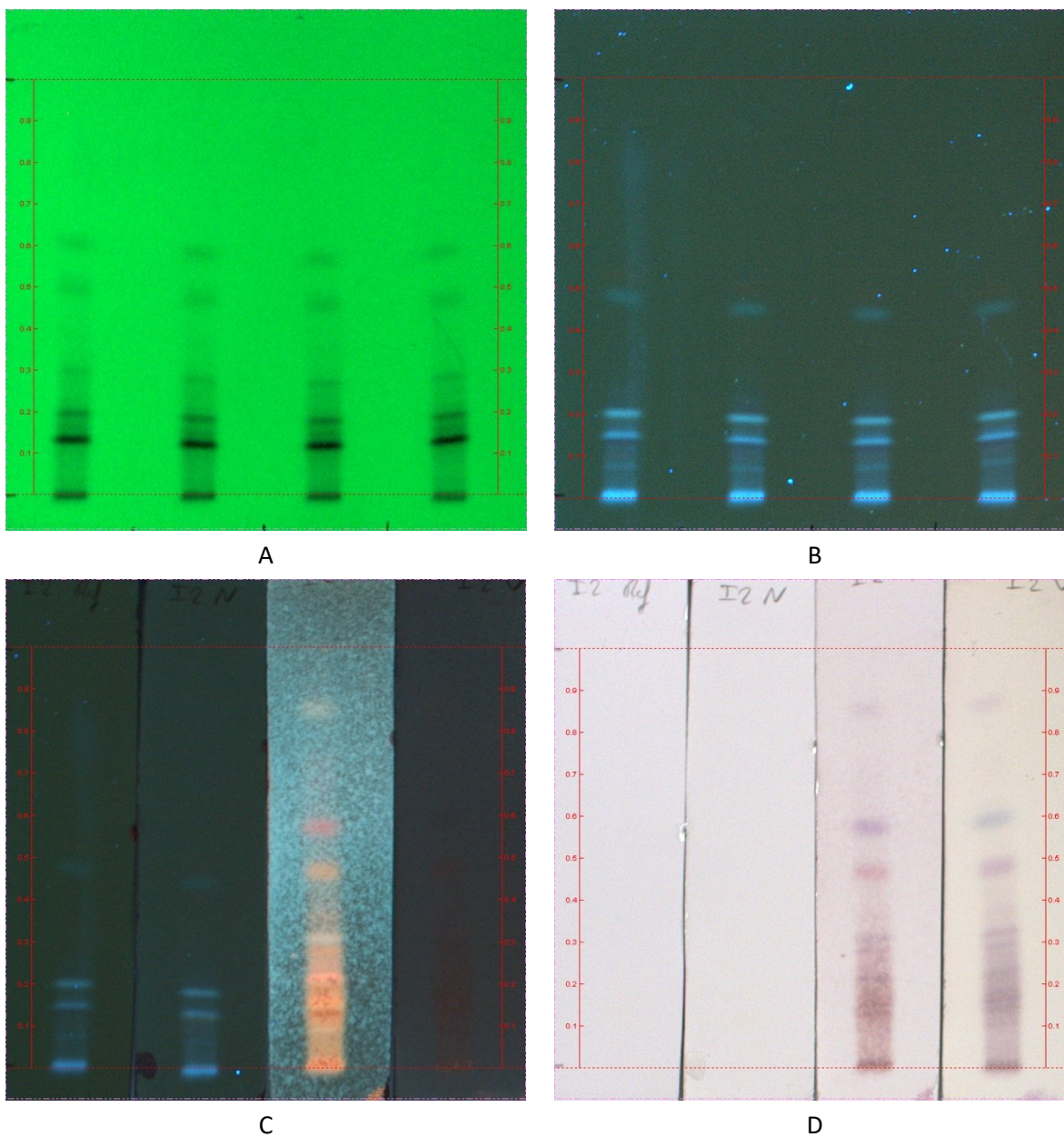


Figure S 19: TLC plates of 18I2 (DCM extract of the aged rhizomes of *Iris germanica* L.; see Figure 54 in section 4.2.2.4) without derivatisation under UV-light at 254 nm (A) and 366 nm (B). TLC plates of 18I2 after derivatisation with N, AA and V (see section 2.2.2) under UV-light at 366 nm (C) and under white light (D). The four spots from the left to the right for every plate correspond to: 18I2 without derivatisation, 18I2 derivatised with N, with AA and with V. Mobile phase for every plate: TLC_1 (see Table 16 in section 4.2.2.5).

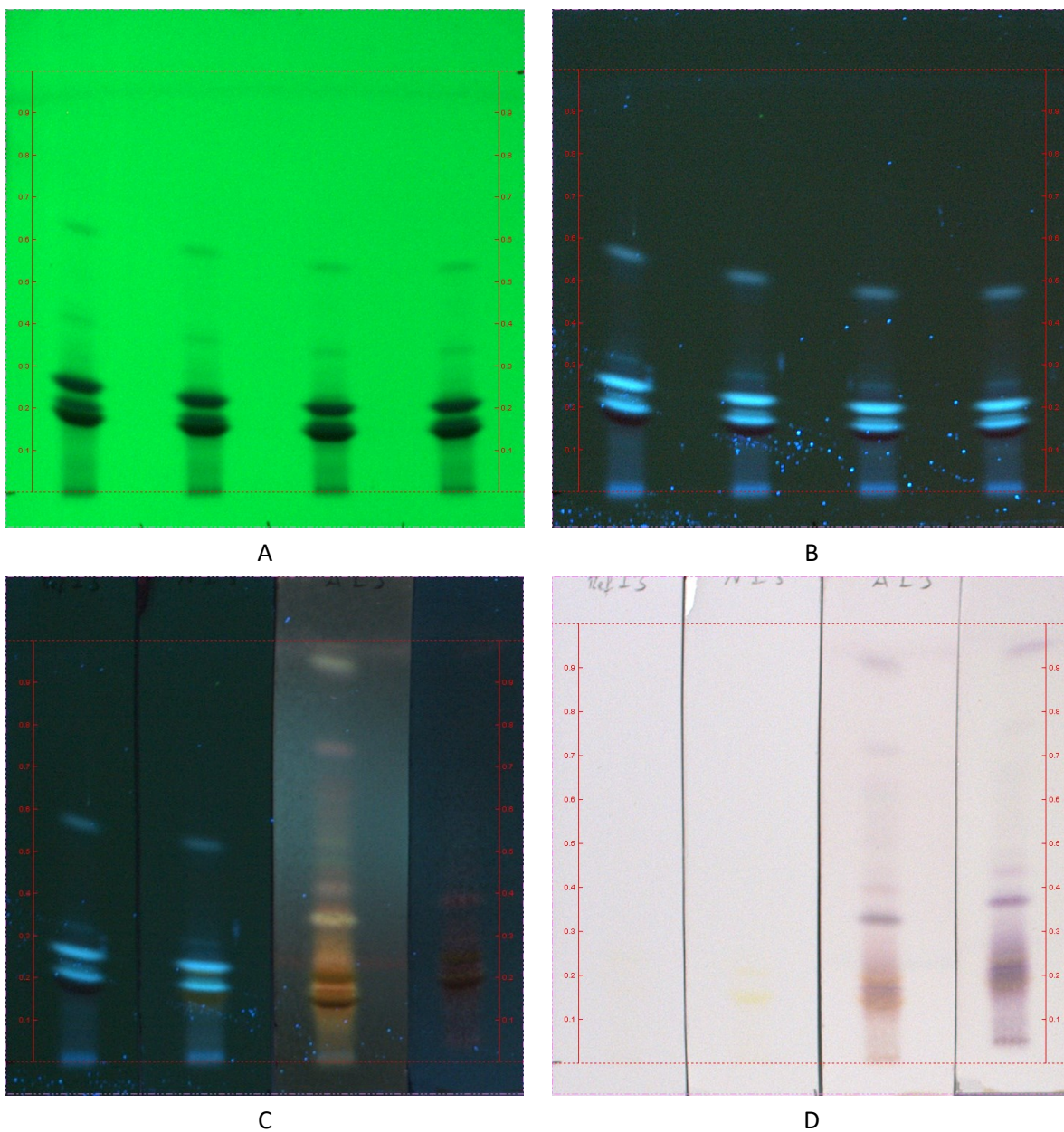


Figure S 20: TLC plates of 1813 (DCM extract of the fresh roots of *Iris germanica* L.; see Figure 54 in section 4.2.2.4) without derivatisation under UV-light at 254 nm (A) and 366 nm (B). TLC plates of 1813 after derivatisation with N, AA and V (see section 2.2.2) under UV-light at 366 nm (C) and under white light (D). The four spots from the left to the right for every plate correspond to: 1813 without derivatisation, 1813 derivatised with N, with AA and with V. Mobile phase for every plate: TLC_1 (see Table 16 in section 4.2.2.5).

6.27 TLC plates of the comparison between 18I4B, 18I5B and 18I6B

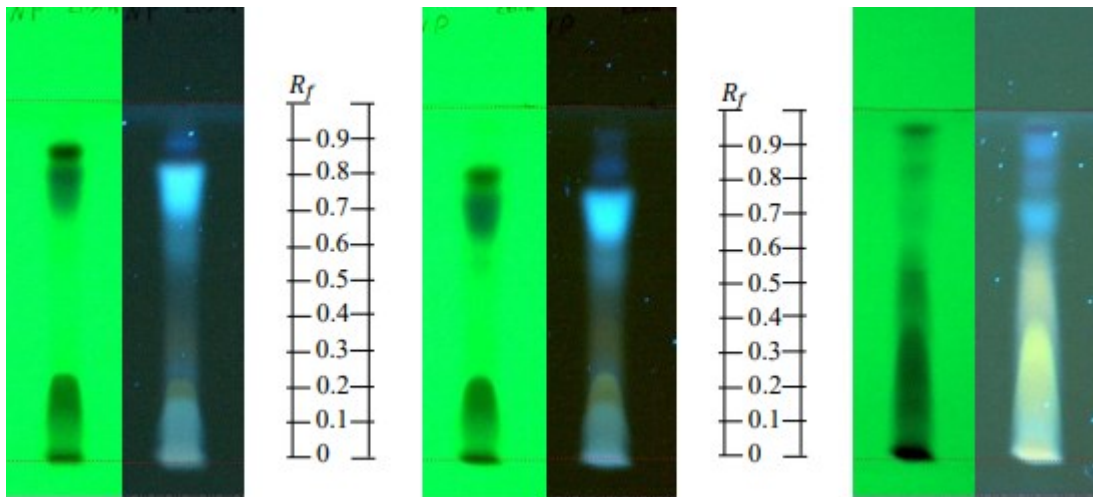
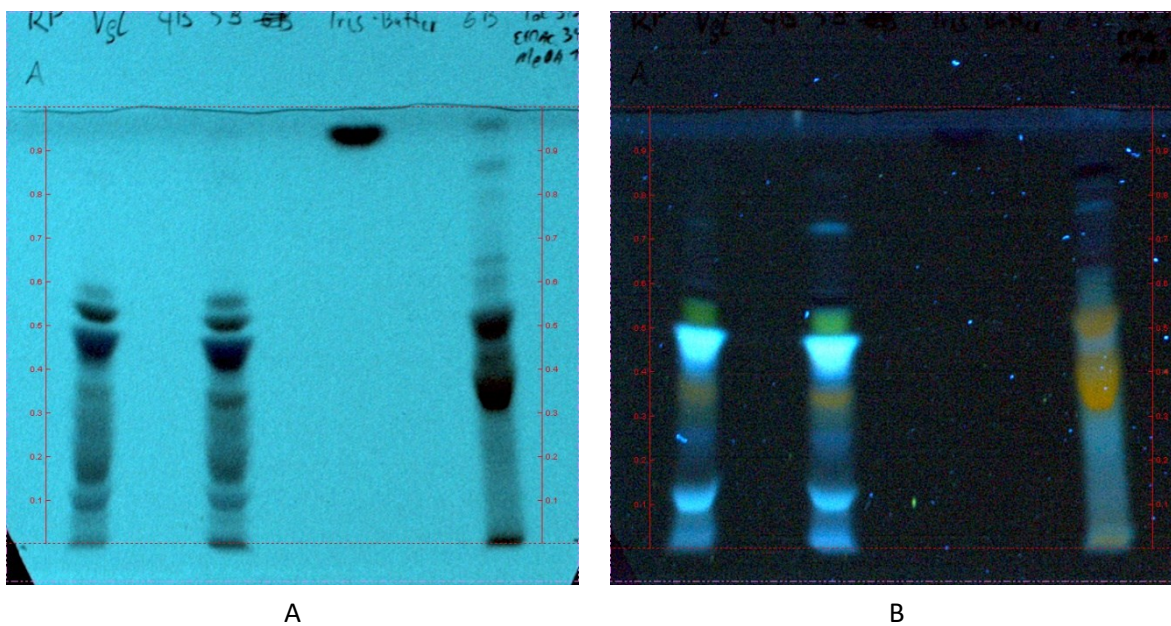
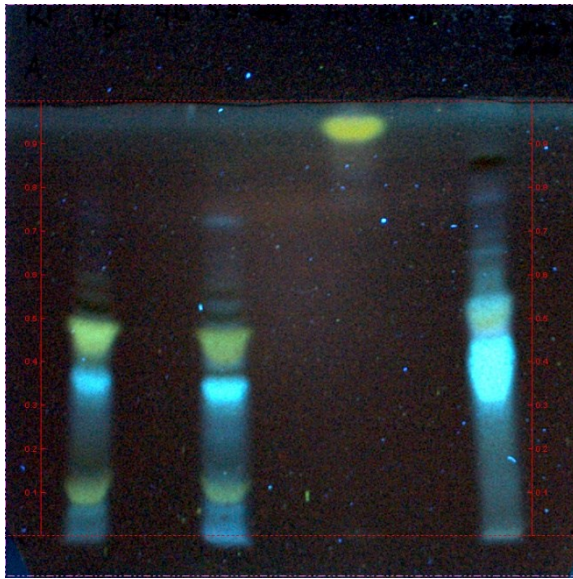


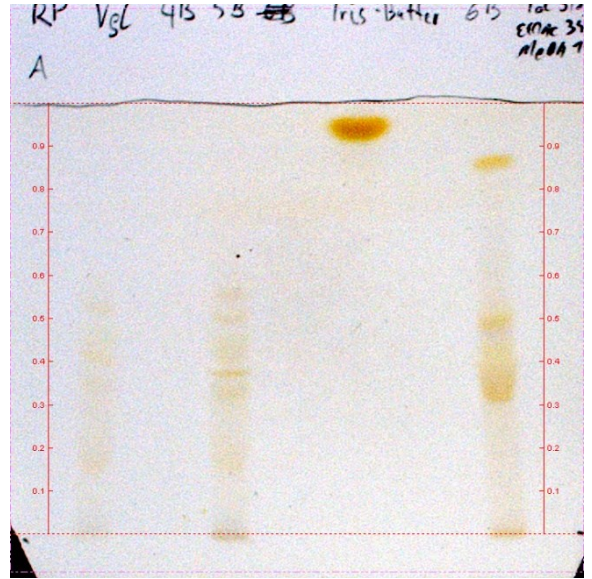
Figure S 21: From the left to the right: TLC plates of the BuOH extracts 18I4B (fresh rhizomes), 18I5B (aged rhizomes) and 18I6B (fresh roots; see Figure 54 in section 4.2.2.4) without derivatisation under UV-light at 254 nm (left part of the plate) and 366 nm (right part of the plate). Eluent: TLC_3 (see Table 16 in section 4.2.2.5) [205].

6.28 Comparison between BuOH-extracts and 18I9





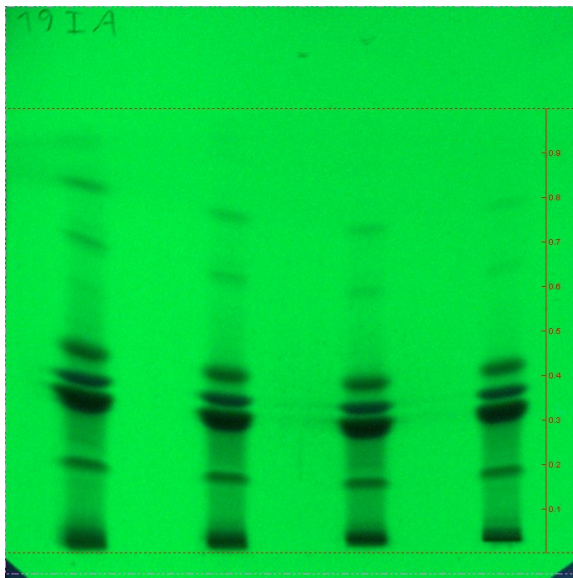
C



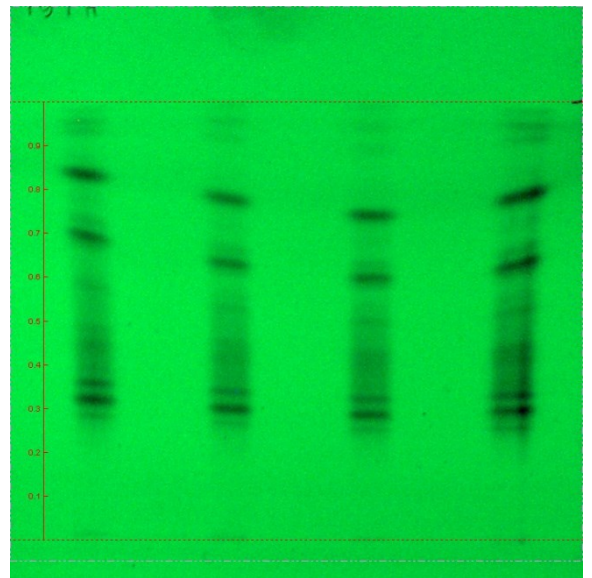
D

Figure S 22: TLC comparison plates between the BuOH extracts 1814B (fresh rhizomes), 1815B (aged rhizomes), 1816B (fresh roots), and 1819 (iris rhizome's butter from aged rhizome won by hydro distillation); see Figure 54 in section 4.2.2.4). The four spots on every plate correspond from the left to the right to 1814B, 1815B, 1819 and 1816B. A/B: TLC plate without derivatisation under UV-light at 254 nm (A) and 366 nm (B). C/D: TLC plate derivatised with AA under UV-light at 366 nm (C) and under white light (D). Mobile phase for every plate: TLC_4 (see Table 16 in section 4.2.2.5).

6.29 19IA and 19IH



A



B

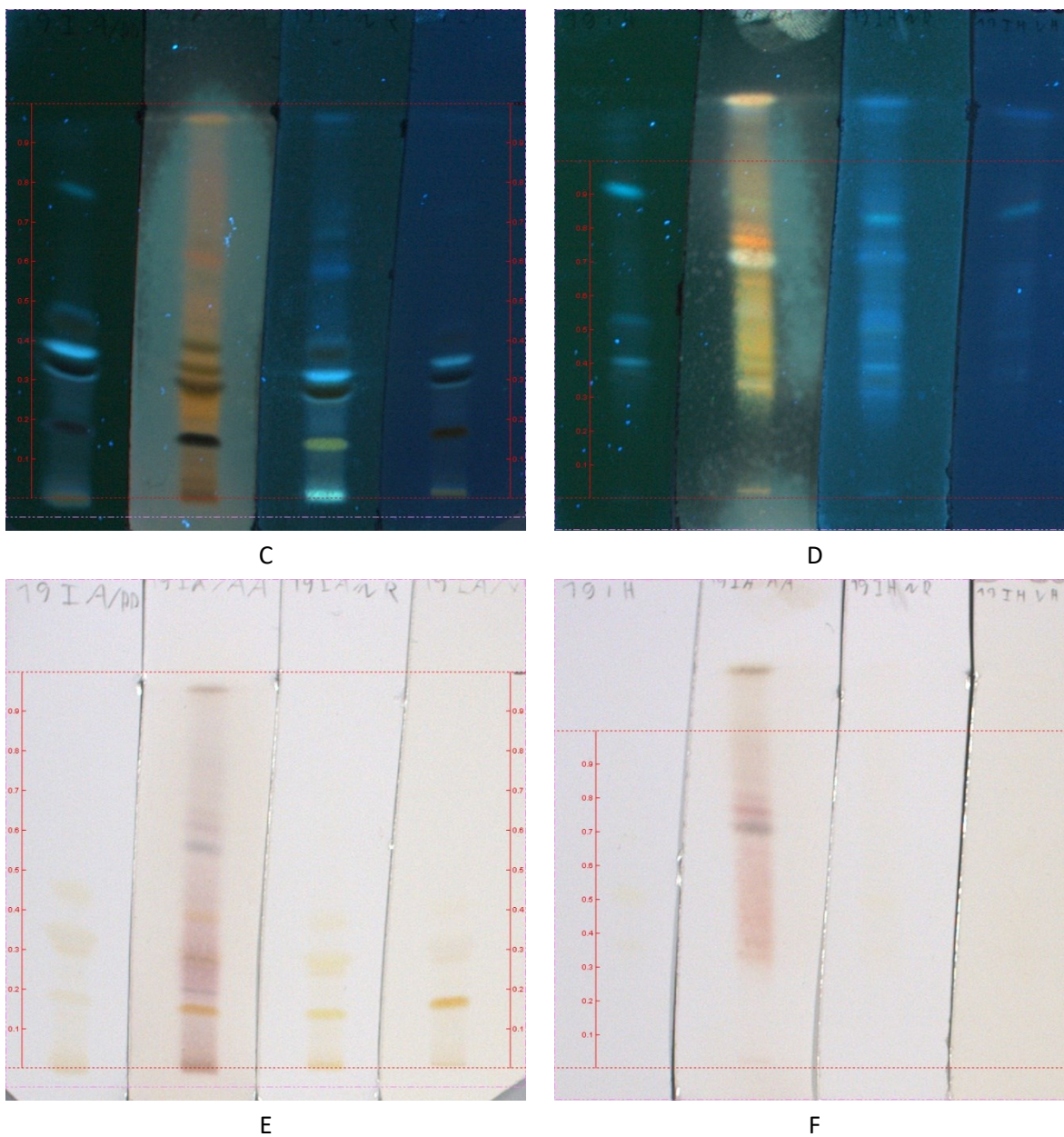


Figure S 23: TLC plate of 19IA (on the right, EtOAc extract of the fresh roots of *Iris germanica* L.; see Figure 53 in section 4.2.2.4) and 19IH (on the left, *n*-hexane extract of the fresh roots of *Iris germanica* L.; see Figure 53 in section 4.2.2.4) without derivatisation under UV-light at 254 nm (A/B), at 366 nm without derivatisation, derivatised with AA, N and V (C/D) and under white light without derivatisation, derivatised with AA, N and V (E/F). Mobile phase for every plate: TLC_6 (see Table 16 in section 4.2.2.5).

6.30 Comparison DCM-extracts and 19IH

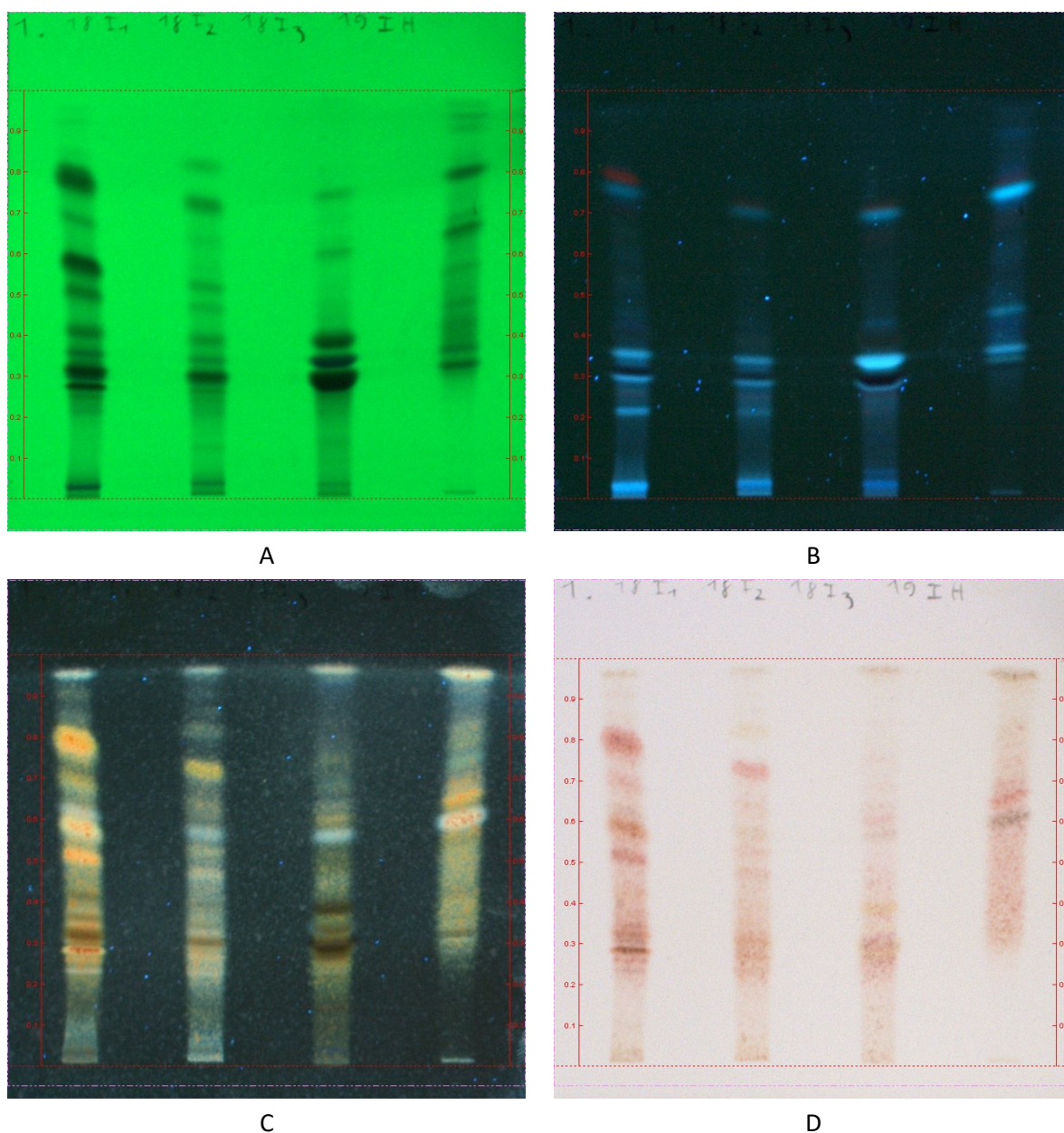
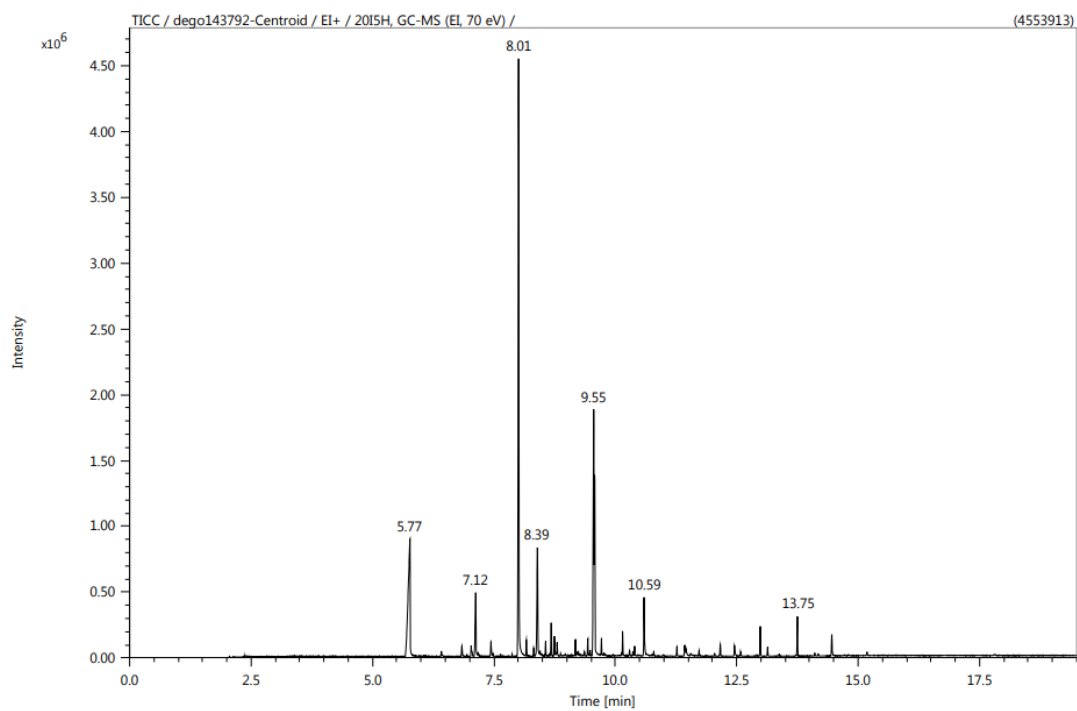
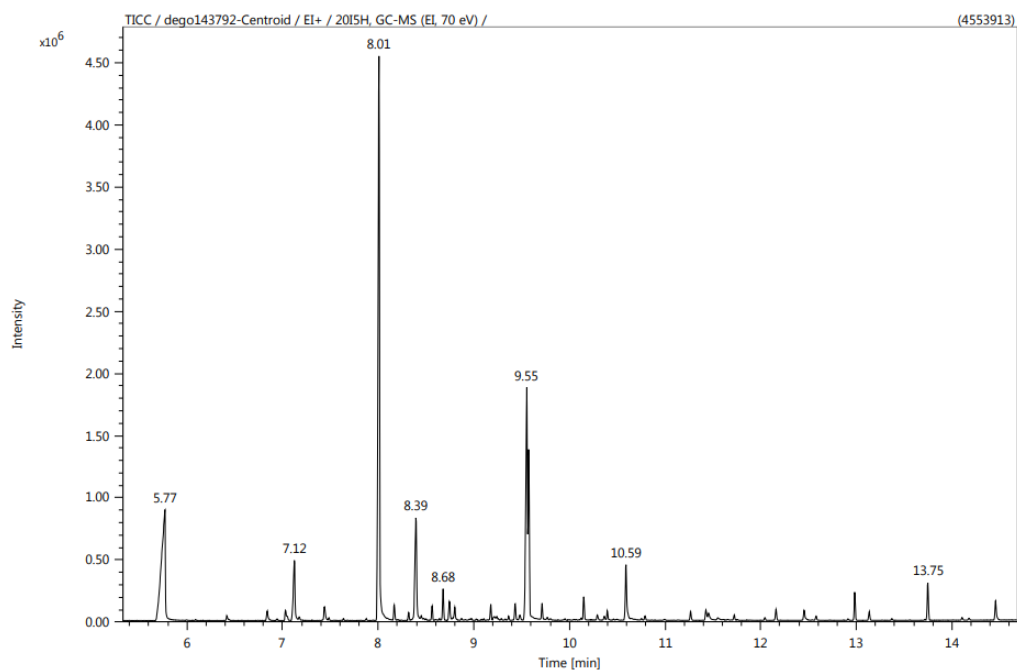


Figure S 24: TLC comparison plates between the DCM extracts 18I1 (fresh rhizomes), 18I2 (aged rhizomes), and 18I3 (fresh roots; see Figure 54 in section 4.2.2.4) and 19IH (n-hexane extract of the fresh roots of *Iris germanica* L.; see Figure 53 in section 4.2.2.4). The four spots on every plate correspond from the left to the right to 18I1, 18I2, 18I3 and 19IH. A/B: TLC plate without derivatisation under UV-light at 254 nm (A) and 366 nm (B). C/D: TLC plate derivatised with AA under UV-light at 366 nm (C) and under white light (D). Mobile phase for every plate: TLC_5 (see Table 16 in section 4.2.2.5).

6.31 GC-MC of 20IH



A



B

Figure S 25: GC-MS chromatograms of 20IH (*n*-hexane extract of the residue of the hydro distillation of the aged rhizomes of *Iris germanica* L.; see Figure 53 in section 4.2.2.4). A: complete GC-chromatogram. B: GC-chromatogram between 5 and 15 min.

6.32 Cytotoxicity of the BuOH-extracts on HeLa and SK-MEL-28 cells

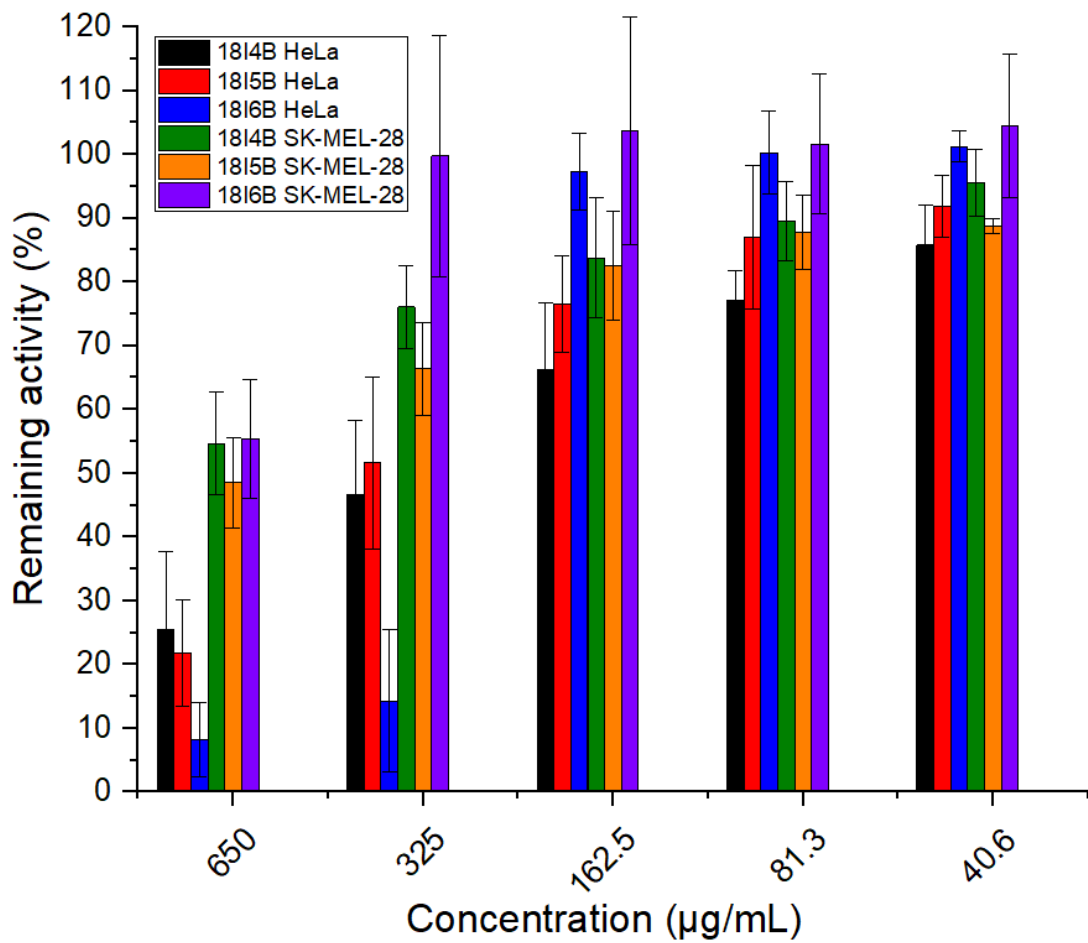


Figure S 26: Remaining activity in % (correlated to the cell viability) of BuOH extracts 1814B (fresh rhizomes), 1815B (aged rhizomes) and 1816B (fresh roots; see Figure 54 in section 4.2.2.4) on HeLa and SK-MEL-28 cells. The given remaining activity with the calculated standard deviation is the average of 3 to 5 tested plates. The results are used to determine the IC_{50} .

6.33 Overview of the 25 fractions obtained from the elution of 18I4A

Table S 14: Overview of the obtained amounts of each fractions from the separation of 18I4A (EtOAc extracts of the fresh rhizomes of *Iris germanica* L.; see Figure 54 in section 4.2.2.4) and the combination of the fractions (Mobile phase for separation of 18I4A: SGC_1, see Table 18 in section 4.2.2.7.1).

Fraction name	Mass (mg)	Fraction name	Mass (mg)
F1	120	F14	20
F2	230	F15	420
F3	20	F16	40
F4	30	F17	150
F5	580	F18	89
F6	110	F19	59
F7	90	F20	61
F8	240	F21	38
F9	50	F22	36
F10	100	F23	500
F11	50	F24	28
F12	20	F25	19
F13	180	Total F1 to F25	3280
Combination			
Fraction name	Used fractions		Mass (mg)
Z1	F5, F8, F15, F16, F23		1722
Z2	F3, F7, F13, F14, F20, F21, F22		500
Z3	F1, F6, F10, F18		380

6.34 Z3 and 1819

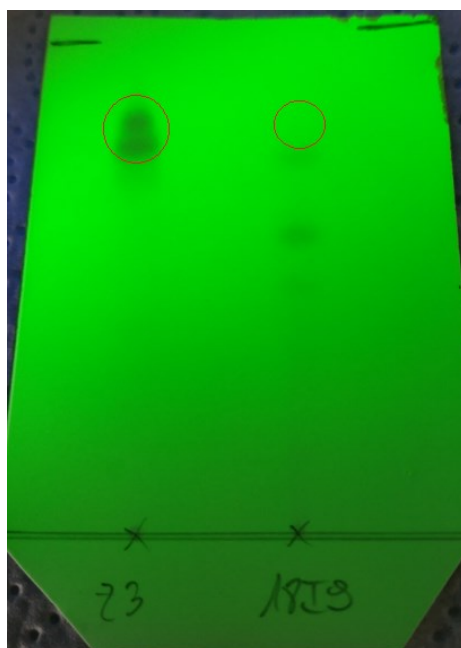


Figure S 27: TLC comparison of 1819 (iris butter from aged rhizomes of *Iris germanica* L. from hydro distillation; see Figure 53 in section 4.2.2.4) and Z3 (third fraction from the separation of 1814A (EtOAc extracts of the fresh rhizomes of *Iris germanica* L.; see Figure 54 in section 4.2.2.4). Mobile phase for the separation of 1814A: SGC_1, see Table 18 in section 4.2.2.7.1). Z3 and 1819 were both dissolved in EtOAc. The red circles show that the two spots of Z3 are not present in 1819. The highest spot of 1819 possesses a lowest R_f -value than the lowest spot of Z3. Mobile phase for every plate: TLC_7 (see Table 16 in section 4.2.2.5).

6.35 F4_18I4A and Z2

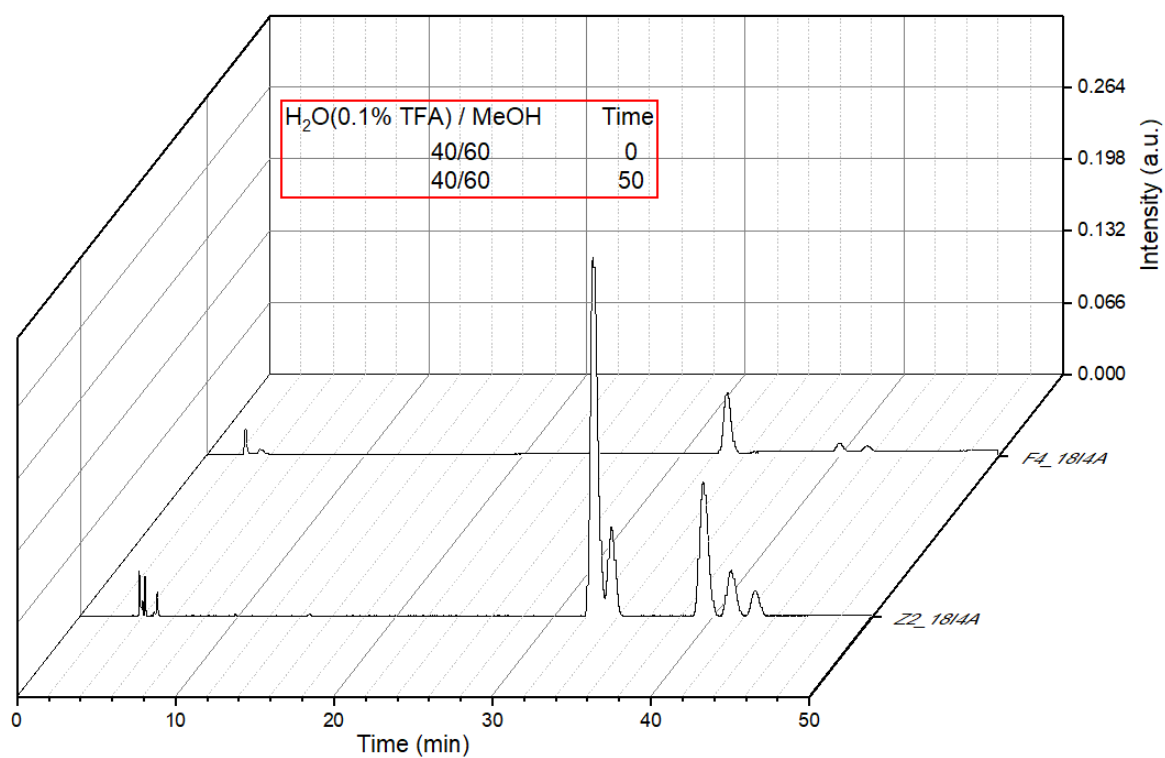


Figure S 28: Analytical HPLC-chromatograms (biphenyl column) of F4_18I4A (spot with a R_f -value of 0.45 on A in Figure 68 of the fourth applied spot (corresponding to the fraction F4, see Table S 14 of the Appendix) and fraction Z2 from 18I4A (EtOAc extract of the fresh rhizomes of *Iris germanica* L.; see Figure 54 or Table 15 in section 4.2.2.4).

6.36 F4F1_19IA and Z2_18IA

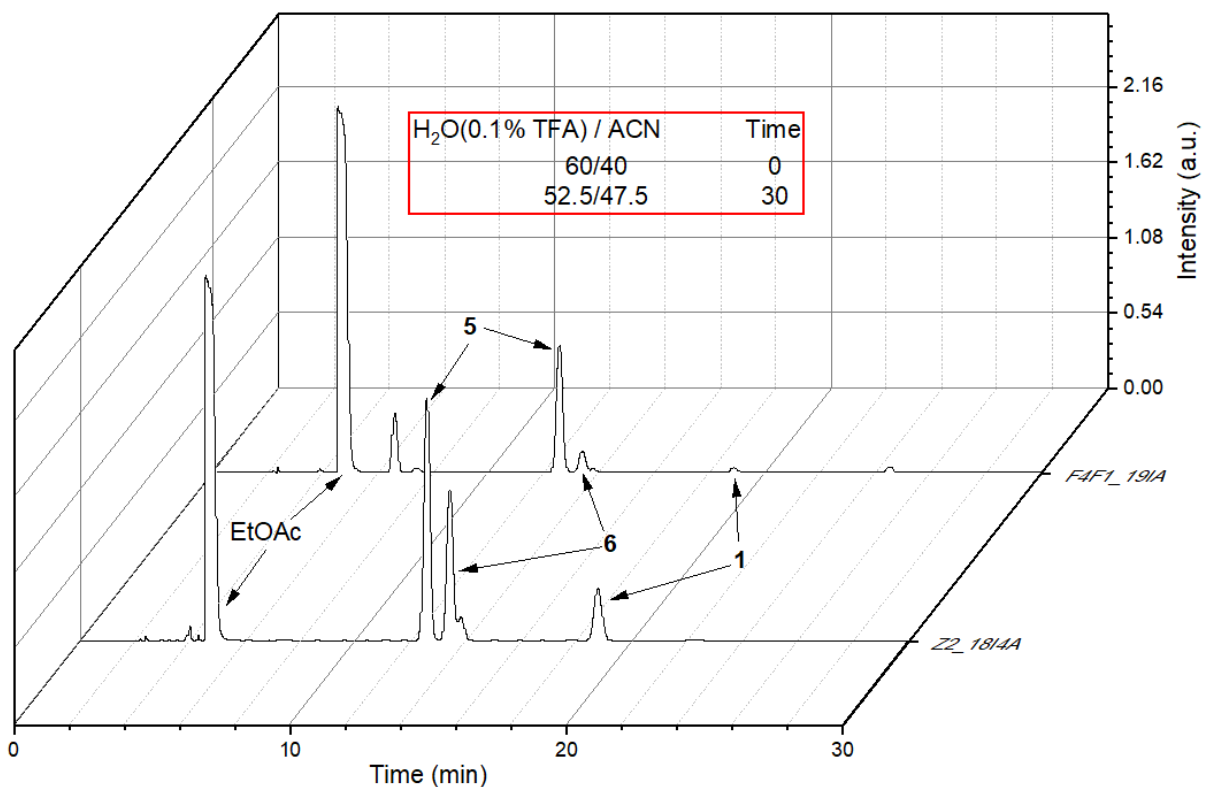
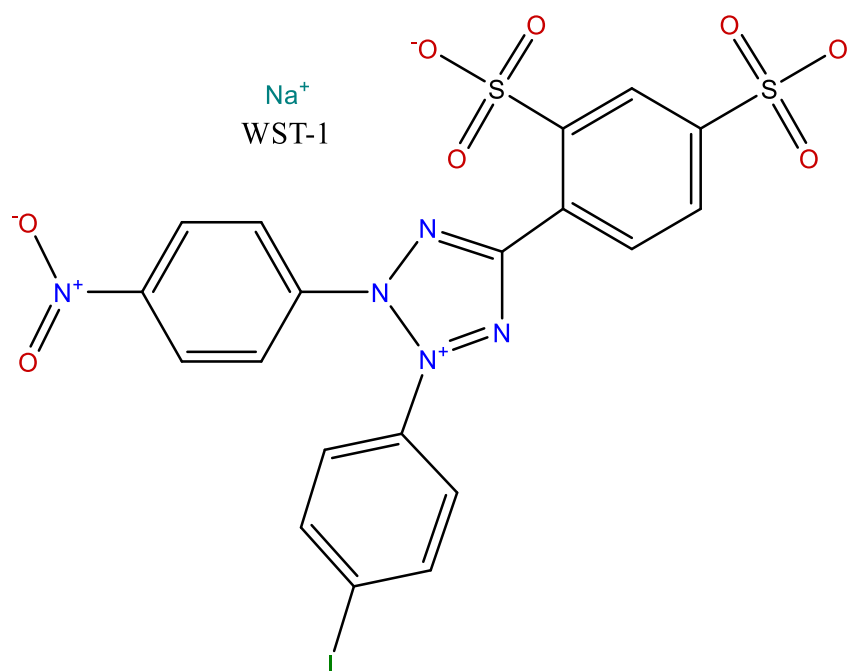
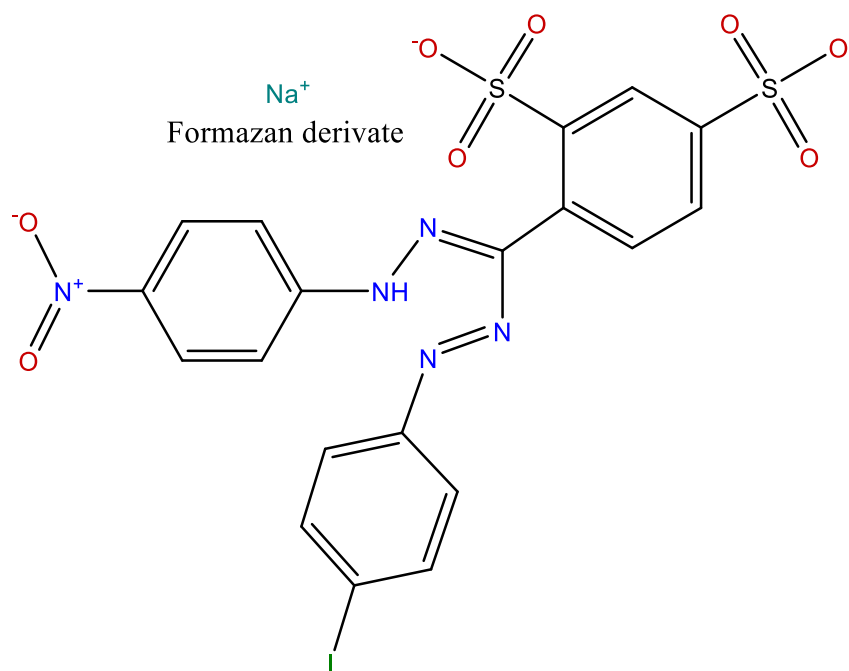


Figure S 29: Analytical HPLC-chromatograms (RP-18 column) of F4F1_19IA (first fraction of the elution of F4 (fourth fraction obtained from the elution of 19IA (EtOAc extract of the fresh roots of *Iris germanica* L.; see Figure 53 in section 4.2.2.4) using the mobile phase SGC_3, see Table 18 in section 4.2.2.7.1), see Table 25 in section 4.3.4.2) and fraction Z2 from 18IA (EtOAc extract of the fresh rhizomes of *Iris germanica* L.; see Figure 54 in section 4.2.2.4. Eluent solvent: SGC_1, see Table 18 in section 4.2.2.7.1).

6.37 WST-1



4-(3-(4-iodophenyl)-2-(4-nitrophenyl)-2*H*-tetrazol-3-ium-5-yl)benzene-1,3-disulfonate



4-((*Z*)-((*E*)-(4-iodophenyl)diazenyl)(2-(4-nitrophenyl)hydrazineylidene)methyl)benzene-1,3-disulfonate

Figure S 30: Structure of WST-1 salt and the formazan salt produced from the reduction of WST-1 salt

7 Eidesstattliche Erklärung

Ich erkläre hiermit an Eides statt, dass ich die vorliegende Arbeit ohne zulässige Hilfe Dritter und ohne Benutzung anderer als der angegebenen Hilfsmittel angefertigt habe; die aus anderen Quellen direkt oder indirekt übernommenen Daten und Konzepte sind unter Angabe des Literaturzitats gekennzeichnet.

Weitere Personen waren an der inhaltlich-materiellen Herstellung der vorliegenden Arbeit nicht beteiligt. Insbesondere habe ich hierfür nicht die entgeltliche Hilfe eines Promotionsberaters oder anderer Personen in Anspruch genommen. Niemand hat von mir weder unmittelbar noch mittelbar geldwerte Leistungen für Arbeiten erhalten, die im Zusammenhang mit dem Inhalt der vorgelegten Dissertation stehen.

Die Arbeit wurde bisher weder im In- noch im Ausland in gleicher oder ähnlicher Form einer anderen Prüfungsbehörde vorgelegt.

Regensburg, den 09.02.2022

Ort und Datum

Unterschrift